Biology and function of the *OsALMT1* gene in rice (*Oryza sativa* L.)

by

Jie Liu

Submitted in fulfilment of the requirement for the

Degree of Doctor of Philosophy

University of Tasmania

December 2015

DECLARATION

The thesis contains no material, which has been accepted for the award of any other degree or diploma in any tertiary institution, and to the best of my knowledge, contains no material previously published or written by any other person, except where due reference is made in the text of this thesis.

Jie Liu

This thesis may be made available for loan and limited copying in accordance with the *Copyright Act* 1968.

Jie Liu
University of Tasmania

ACKNOWLEDGEMENTS

Four year is not a long term for one's whole life, but the last four years will be the most precious time along my life. Looking back, I still remember the first day when I arrived at this special place, but the completion of my thesis and subsequent Ph.D. has been a long journey. I could not have succeeded without the invaluable support of my supervisors, colleagues, friends and family. Without these supporters, especially the select few I'm about to mention, I may not have gotten to where I am today, at least not sanely.

First and foremost I would like to express my special appreciation and thanks to my supervisors Associate Professor Meixue Zhou, Dr. Peter Ryan, Dr. Emmanual Delhaize and Professor Sergey Shabala, for giving me the chance to study with them and supporting me during these past four years. I would like to thank all of you for encouraging my research and for helping on my life. Your advices on both research as well as on my career have been priceless. I would especially like to thank Dr. Peter Ryan who entirely guide my research throughout my Ph.D. with his wide knowledge and deep intuitions. I appreciate all his contributions of time, patience, ideas and funding to make my Ph.D. experience productive and stimulating. Without his guidance and constant feedback this Ph.D. would not have been achievable.

I offer my sincerest gratitude to people who provided help and advises during my experiment. Many thanks to Professor Jianfeng Ma who gave the advises on plant inner manganese measurement, to Dr. Sergio Moroni who shared the knowledge on physiological leaf spots, to Greg Cawthray who helped on the organic acids measurement by HPLC, to Miguel Pineros who attempted to measure OsALMT1 malate efflux by using oocytes experiments, to Richard James who helped on osmotic potential calculation of salt and mannitol, to Gonzalo Estavillo who performed the photosynthesis measurements, to Rosemary White who helped a lot with microscopy and to Tina Rathjen, Kumara Weligama and David Lewis who assisted with technique support.

I gratefully acknowledge the living allowance funding received towards my PhD from the China Scholarship Council (CSC). I am also grateful to the funding received through the University of Tasmania for offering me with the tuition fee scholarship. My deep

appreciation goes out to Professor Youliang Zheng, Professor Yuming Wei and Associate Professor Yaxi Liu for their supporting and encouraging to apply for the CSC scholarship and restart my Ph.D. at the University of Tasmania.

The years spent in Australia would not have been as wonderful without my Chinese friends, including Dr. Qing Liu, Dr. Zhongyi Li, Dr. Ming Luo, Yao Zhi, Lijun Tian, Gaofeng Zhou, Muyun Xu, Ting Tang and Feiyi Wang. Also thanks to my friends outside Australia, including Shihang Liu, Zehou Liu, Ma Yu and Junyan Feng for their valuable friendship these years and forever.

Last, but certainly not least, I must acknowledge with tremendous and deep thanks to my family who support me throughout my study overseas. I appreciate both my parents and my parents-in-law always who always believing in me and encouraging me to follow my dreams. And finally to Liang Zhang, who has been by my side throughout this Ph.D., accompanying every single minute of it, and without whom, I would not have had the courage to embark on this journey in the first place.

Jie Liu

December, 2015

PUBLICATIONS

Liu J, Delhaize E, Zhou M, Shabala S, Ryan PR (2014) Functional Characterisation of *OsALMT1* in Rice. ComBio2014, 28 September - 02 October

Liu J, Delhaize E, Zhou M, Shabala S, Ryan PR (2015) Characterisation of the malate-permeable anion channel in rice, OsALMT1. The 9th Symposium of the International Society of Root Research (ISRR9), 06-09 October

Liu J, Zhou M, Delhaize E, Shabala S, Ryan PR (2016) *OsALMT1* encodes a malate permeable anion channel in rice (*Oryza sativa* L.) which is required for normal growth in conditions of low light and chloride deficiency. Plant Physiology (in preparation)

Liu J, Zhou M, Delhaize E, Shabala S, Ryan PR (2016) Over-expression of the anion channel OsALMT1 in transgenic rice (*Oryza sativa* L.) increases sensitivity to manganese and enhances tolerance to boron toxicity. New Phytologist (in preparation)

Table of Contents

DECLARATION I

ACKNOWLEDGEMENTS II

PUBLICATIONS V

Table of Contents V

List of Figures XII

List of Tables XVI

List of Abbreviations XVII

Abstract XIXX

CHAPTER 1 General Introduction 1

1.1 The ALMT gene family 1

1.2 Functions of the ALMT family 2

1.2.1 The first member of the ALMT gene family was identified in wheat 2

1.2.2 *ALMT* genes contributing to Al resistance 4

1.2.3 *ALMT* genes involved in guard cell function 11

1.2.4 *ALMT* genes involved with mineral nutrition 14

1.2.5 *ALMT* genes contributing to fruit and berry acidity 14

1.3 Structural analysis and evolution of the ALMT family 16

1.3.1 Phylogeny of the ALMT family 16

1.3.2 Secondary structure 19

1.3.3 The structure-function relationship of ALMT proteins 20

1.4 Objectives 26

1.5 References 28

CHAPTER 2 General materials and methods 35

2.1 Plant material and growth conditions 35

2.1.1 Plant material and seed germination 35
2.1.2 Plant growth conditions 35
2.2 Online sequence resources 35
2.3 Primer design 36
2.4 DNA and RNA extractions 36
2.4.1 Standard genomic DNA (gDNA) extraction 36
2.4.2 High throughput DNA isolation for genotype test 37
2.4.3 RNA extraction and 1st strand cDNA synthesis 42
2.5 PCR reactions 43
2.5.1 Standard PCR 43
2.5.2 Proof-reading PCR 43
2.5.3 Quantitative reverse transcription PCR (qRT-PCR) 44
2.5.4 PCR products and gel purification 44
2.5.5 Fusion PCR 45
2.6 Cloning 46
2.6.1 Preparation of *E. coli* cells for electroporation 46
2.6.2 Electroporation 46
2.6.3 Plasmid isolation 47
2.6.4 Enzyme digestion reaction 48
2.6.5 Ligation reaction 48
2.7 Sequencing and sequence analysis 49
2.7.1 Sequencing 49
2.7.2 Sequence alignment and vector maps construction 49
2.8 Rice transformation 49
2.8.1 Callus inducement 49
2.8.2 Growth of Agrobacterium 50

2.8.3 Inoculation of the callus 50

2.8.4 Regeneration of plantlets 50

2.9 Statistical analyses 51

2.10 References 52

CHAPTER 3 Cloning of the *OsALMT1* coding and promoter regions and initial characterisation with on-line resources 55

3.1 Introduction 55

3.2 Materials and Methods 56

3.2.1 Cloning the *OsALMT1* coding region 56

3.2.2 *OsALMT1* promoter cloning 59

3.2.3 Investigating gene function using on-line resources 59

3.2.4 On-line resources investigating the gene promoters 62

3.3 Results 62

3.3.1 Expression of *ALMT* genes in roots and shoots and structure of the *OsALMT1* coding region and promoter 62

3.3.2 On-line resources investigating *OsALMT1* biology 63

3.3.3 Analysis of the *OsALMT1* promoter 64

3.4 Discussion 75

3.5 References 76

CHAPTER 4 Sub-cellular localisation of OsALMT1 80

4.1 Introduction 80

4.2 Materials and Methods 82

4.2.1 Plant materials 82

4.2.2 Vector construction 82

4.2.3 Leek bombardment 83

4.2.4 Tobacco leaf infiltration 84

4.2.5 Co-localization system 87
4.3 Results 88
4.3.1 Sub-cellular localization in leek 88
4.3.2 Sub-cellular localization in tobacco 88
4.4 Discussion 89
4.5 References 94
CHAPTER 5 Tissue-specific expression of *OsALMT1* 97
5.1 Introduction 97
5.2 Materials and methods 99
5.2.1 Vector construction 99
5.2.2 Tissue collection time and method 100
5.3 Results 101
5.3.1 Distribution of *OsALMT1* expression in rice roots 101
5.3.2 Distribution of *OsALMT1* expression in rice leaves 101
5.3.3 Distribution of *OsALMT1* expression in flower parts 108
5.3.4 Fluorescent images in developing rice grain 108
5.3.5 Fluorescent images in developing rice grain 108
5.4 Discussion 111
5.5 References 114
CHAPTER 6 Changes in *OsALMT1* expression in response to different stress and hormone treatments 117
6.1 Introduction 117
6.2 Materials and methods 120
6.2.1 Treatments and gene expression 120
6.3 Results 120

6.3.1 Effect of osmotic stress, light and low Cl^- treatments on *OsALMT1* expression 120

6.3.2 Changes in *OsALMT1* expression with hormone treatments 121

6.3.3 *OsALMT1* expression pattern under other stress conditions 122

6.4 Discussion 122

6.5 References 129

CHAPTER 7 Generation of transgenic rice plants with altered levels of *OsALMT1* expression 132

7.1 Introduction 132

7.2 Materials and Methods 134

7.2.1 Vector construction 134

7.2.2 System for naming transgenic materials 142

7.2.3 Identifying homozygous and null lines 142

7.2.4 Examining appearance of the leaf phenotype on transgenic lines 144

7.2.5 Oxidative determination of the transgenic rice leaf 144

7.2.6 Growth experiments for biomass measurements 145

7.2.7 Mineral analysis in leaf tissue 145

7.2.8 Weight of the T3 generation seed 146

7.3 Results 146

7.3.1 *OsALMT1* expression in T0 plants 146

7.3.2 Identifying homozygous and null lines 146

7.3.3 General phenotypes of the transgenic lines 147

7.4 Discussion 153

7.5 References 161

CHAPTER 8 Characterisation of transgenic plants with altered *OsALMT1* expression 165

8.1 Introduction 165

8.2 Materials and methods 167

8.2.1 Measuring organic anion efflux from rice plants. 167

8.2.2 Measurements of Al^{3+} resistance in hydroponic culture 169

8.2.3 Effect of different treatments on malate efflux from roots 169

8.2.4 Measuring malate concentrations in xylem sap 170

8.2.5 Mineral analysis in grain 170

8.2.6 Qualitative estimates of endosperm pH 171

8.3 Results 171

8.3.1 Organic anion release from the root of transgenic rice plants over-expressing OsALMT1 171

8.3.2 Greater malate release from transgenic rice over-expressing *OsALMT1* increases their tolerance to Al toxicity 172

8.3.3 Effect of different treatments on malate efflux from transgenic rice 173

8.3.4 Overexpression of *OsALMT1* increases malate concentration in the xylem sap 180

8.3.5 Effect of altered *OsALMT1* expression on grain mineral content 180

8.3.6 Pattern of starchy endosperm acidification in transgenic grains following germination 183

8.4 Discussion 183

8.5 References 190

CHAPTER 9 Growth experiments to investigate OsALMT1 function 195

9.1 Introduction 195

9.2 Materials and methods 197

9.2.1 Stress conditions 197

9.2.2 Biomass measurement 198

9.3 Results 198

9.3.1 Biomass accumulation under a high salt treatment 198

9.3.2 Biomass accumulation under a high mannitol treatment 199

9.3.3 Biomass accumulation under a low Cl^- treatment 199

9.3.4 Biomass under low light conditions 203

9.3.5 Biomass accumulation during H_3BO_3 stress 203

9.3.6 Biomass under $MnCl_2$ stress 205

9.4 Discussion 206

9.5 References 212

Chapter 10 General discussion and conclusions 213

10.1 General information on OsALMT1 213

10.2 Responses of *OsALMT1* expression to hormone treatments 215

10.3 OsALMT1 and manganese 216

10.4 OsALMT1 and boron 220

10.5 OsALMT1 and water relations 223

10.6 OsALMT1 and electroneutrality 225

10.7 OsALMT1 and light 226

10.8 Conclusion 227

10.9 Future directions 227

10.10 References 229

Appendix 233

List of Figures

Figure 1.1 The major Al resistance mechanism in wheat 5

Figure 1.2 Promoter patterns of *TaALMT1* associated with Al resistance in wheat..... 6

Figure 1.3 ALMT members involved with Al resistance 8

Figure 1.4 Members of the ALMT family involved in stomatal function 15

Figure 1.5 ALMTs contributing to fruit and berry acidity 18

Figure 1.6 Unrooted phylogenetic tree of the ALMT family 21

Figure 1.7 Different predictions for the secondary structure of TaALMT1 23

Figure 1.8 Structures of some members of the ALMT protein family 24

Figure 1.9 Hydropathy plots showing the domain structure and transmembrane regions of ALMT proteins in grape (VvALMT5) and *Perkinsus marinus* 25

Figure 1.10 Hypothetical model for TaALMT1 showing residues and domains potentially important for function 27

Figure 3.1 Phylogenetic tree of ALMT proteins from Arabidopsis and rice and some characterised members 58

Figure 3.2 Vector map of pOsALMT1 GEM-T Easy 60

Figure 3.3 Vector map of pOsALMT1 promoter GEM-T Easy 61

Figure 3.4 Predicted structure of the *OsALMT1* gene 63

Figure 3.5 Significant Pfam-A matches of OsALMT1 to the family of ALMTs 64

Figure 3.6 Predictions for the secondary structure of OsALMT1 65

Figure 3.7 Prediction for the sub-cellular localisation of OsALMT1 66

Figure 3.8 Pattern of *OsALMT1* expression as predicted by the on-line resource RiceXPro 67

Figure 3.9 Pattern of *OsALMT1* expression as predicted by the online resource PLEXdb 68

Figure 3.10 Predicted OsALMT1 network interactions with on-line resources 69

Figure 3.11 Predicted transcription start sites for *OsALMT1* 70

Figure 4.1 Vector maps of pART7-OsALMT1::GFP and pART7-GFP::OsALMT1 85

Figure 4.2 Vector maps used for sub-cellular localisation of OsALMT1..... 86

Figure 4.3 Vector map of the plasma-membrane localising control protein pm-rk fused with the mCherry fluorophore..... 90

Figure 4.4 OsALMT1 protein localises to the periphery of leek cells..... 91

Figure 4.5 OsALMT1 localises to the plasma membrane of tobacco cells..... 92

Figure 4.6 Co-localisation of OsALMT1 with the plasma membrane marker. 93

Figure 5.1 Vector maps of pS1a-OsALMT1 Promoter::GFP 102

Figure 5.2 Rice roots expressing *GFP* with the *OsALMT1* promoter 103

Figure 5.3 Detailed images of GFP fluorescence in root tissue 104

Figure 5.4 Fluorescence in leaves of rice expressing *GFP* with the *OsALMT1* promoter 105

Figure 5.5 Fluorescence in the whole flower of rice plants expressing *GFP* with the *OsALMT1* promoter 106

Figure 5.6 Fluorescence in different parts of the flower of rice plants expressing *GFP* with the *OsALMT1* promoter 107

Figure 5.7 GFP fluorescence in developing grain 109

Figure 5.8 GFP fluorescence in germinating grain, coleoptiles and shoots..... 110

Figure 6.1 Changes in *OsALMT1* expression with osmotic treatments..... 125

Figure 6.2 Changes in *OsALMT1* expression with hormone treatments..... 126

Figure 6.3 Changes in *OsALMT1* expression with different abiotic stresses..... 127

Figure 7.1 Construction of the pWBVec8-Ubi-OsALMT1 plasmid vector..... 140

Figure 7.2 Construction of the pWBVec8-Starling(a)-OsALMT1 RNAi plasmid vector..... 141

Figure 7.3 Nomenclature of transgenic plants and likely ratios for a single transgene insert..... 143

Figure 7.4 Relative expression of *OsALMT1* in T0 plants..... 148

Figure 7.5 Relative expression of *OsALMT1* in transgenic T2 lines 150

Figure 7.6 Leaf phenotype on rice plants showing increased *OsALMT1* expression 152

Figure 7.7 Mineral composition of leaves 154

Figure 7.8 Weight of 100 grains from different transgenic lines 158

Figure 8.1 Malate efflux from transgenic lines over-expressing *OsALMT1* and nulls ... 174

Figure 8.2 Citrate efflux from transgenic lines over-expressing *OsALMT1* and nulls ... 175

Figure 8.3 Relationship between malate and citrate efflux from homozygous T2 lines over-expressing *OsALMT1* and nulls 176

Figure 8.4 Relative Al tolerance of the transgenic rice over-expressing OsALMT1 178

Figure 8.5 Effect of different treatments on the efflux of malate from homozygous rice over-expressing *OsALMT1* 179

Figure 8.6 Malate concentrations in the xylem sap of transgenic rice lines with altered *OsALMT1* expression 181

Figure 8.7 Mineral composition of rice grain 182

Figure 8.8 pH staining of grain endosperm three days after germination 184

Figure 8.9 pH staining of the transgenic grain following germination 185

Figure 9.1 Total plant biomass and relative biomass under a salt treatment 200

Figure 9.2 Total plant biomass and relative biomass under a high mannitol treatment . 201

Figure 9.3 Total plant biomass and relative biomass in low Cl^- 202

Figure 9.4 Shoot biomass and relative shoot biomass under low light 204

Figure 9.5 Shoot, root, total biomass and relative biomass of transgenic lines under a high H_3BO_3 treatment 207

Figure 9.6 Shoot, root, total biomass and relative biomass of transgenic lines under a higher $MnCl_2$ treatments 208

Figure 9.7 Leaf symptoms on rice lines in high Mn treatments 209

Figure 10.1 Model for the increased accumulation of Mn in transgenic lines overexpressing *OsALMT1* 218

Figure 10.2 Model for how increased expression of *OsALMT1* improves the tolerance of rice plants to toxic concentrations of B..... 222

List of Tables

Table 1.1 Functions and characteristics of members of the ALMT family 3

Table 2.1 Primers used in the experiments 38

Table 2.2 All the culture media used in the rice transformation 53

Table 3.1 Sequence information of the ALMT members of rice 57

Table 3.2 Cis-element prediction by PlantCARE 73

Table 6.1 Treatments for measuring changes in OsALMT1 expression in WT rice 124

Table 7.1 Homologous and heterologous expression of ALMT members 135

Table 7.2 Initial characterisation of the transgenic rice plants 149

Table 7.3 Leaf phenotype appearance time line 155

Table 7.4 Concentration of Mn in the leaves of lines overexpressing *OsALMT1* and their nulls from different experiments and different ages. 156

Table 7.5 Dry weight of transgenic lines grown in hydroponic and flooded soil conditions. 157

Table 8.1 Organic anion efflux measured from transgenic rice by HPLC 177

Table S1 Physical Properties of NaCl 233

Table S2 Physical Properties of Mannitol 234

Table S3 Nutrient solution for low Cl^- treatment 235

Table S4 Elemental analysis of T2 rice leaf 236

Table S5 Elemental analysis of T3 rice seed 237

List of Abbreviations

2,4-D	2,4-dichlorophenoxyacetic acid
ABA	Abscisic acid
Al	aluminium
ALMT	aluminium-activated malate transporter
Amp	ampicillin
AS	Acetosyringone
BAC	bacteria artificial chromosome
BAP	6-Benzylaminopurine
bp	base pair
BSA	bovine serum albumin
cDNA	complementary DNA
CDS	Coding DNA sequence
CL	confidence limit
d	day
ddH_2O	didistilled water
DNA	deoxyribonucleic acid
DTT	dithiothreitol
E. Coli	*Escherichia coli*
EDTA	ethylene dinitrilotetracetic acid
ER	Endoplasmic reticulum
g	gram
GA	Gibberellic acid
GABA	gamma-Aminobutyric acid
GFP	green fluorescent protein
GMO	Genetically modified organism
GOI	Gene of interest
GUS	β-Glucuronidase
h	hour
HMM	Hidden Markov Models
IAA	Indole-3-acetic acid
ICP	Inductively coupled plasma mass spectrometry
Kb	kilobase

L	litre
LB	Lysogeny broth medium
Mb	Megabase
MeJA	Methyl jasmonate
min	minute
mg	milligram
ml	millilitre
mRNA	messenger RNA
MS	Murashige and Skoog medium
NAA	1-Naphthaleneacetic acid
NAD	nicotinamide adenine dinucleotide
NADH	nicotinamide adenine dinucleotide (NAD) + hydrogen (H)
ng	nanogram
OD	optical density
Oligo（dT）	oligodeoxythymidylic acid
ORF	Open reading frame
PCD	Programmed cell death
PCR	polymerase chain reaction
qRT-PCR	Quantitative reverse transcription polymerase chain reaction
rpm	rounds per minute
RNA	ribonucleic acid
RNAi	RNA interference
s	second
SA	Salicylic acid
SDW	sterile distilled water
SE	standard error
SOC	super optimal broth with Catabolite repression
Spec	spectinomycine
U	enzyme unit
WT	wild type
µg	microgram
µl	microlitre
V	volt

Abstract

Members of the *aluminium (Al)-activated malate transporter (ALMT)* gene family encode transmembrane proteins which function as anion channels and perform multiple functions involving anion transport. The *TaALMT1* gene from wheat was the first member identified in plants because it controlled the major mechanism of aluminium (Al) resistance in that species. TaALMT1 mediates the Al-activated efflux of malate from roots which chelates the toxic Al^{3+} and prevents it from inhibiting root growth. Other ALMTs characterised to date show a range of functions related to Al resistance, guard cell function, mineral nutrition, grain development and germination, vacuolar malate balance and fruit acidity. The rice (*Oryza sativa* L.) genome contains nine members of the *ALMT* family but no functional information is available for any of these genes. This study characterised *OsALMT1* and provides the first detailed analysis of an *ALMT* gene in rice.

OsALMT1 expression in roots and leaves was examined by qRT-PCR under various treatments and results showed it was responsive to salt and osmotic stress, dehydration, low Cl^-, various light treatments, as well as several hormones (abscisic acid, indol-3 acetic acid, and salicylic acid). The cDNA of *OsALMT1* was predicted to encode a protein with a typical ALMT structure of six trans-membrane regions and a long hydrophilic C-terminus end. The cDNA was fused with the green fluorescence protein (GFP) and transient expression in leek (*Allium ampeloprasum*) tissues and tobacco (*Nicotiana benthamiana*) leaves demonstrated that OsALMT1 localised to the plasma membrane.

Tissue specific expression of *OsALMT1* was examined by using 2496 bp of sequence upstream of the coding region to drive GFP expression in transgenic rice plants. OsALMT1 was widely expressed in roots and shoots. Expression was prominent in vascular tissues (stele of roots and vascular bundles of leaves), in the root apices, in emerging lateral roots and root hairs, the collar of the leaf, regions of the rachillas, the nucellar projection of developing grain and embryo and in various flower parts.

Rice cultivar "*Nipponbare*" was transformed with the *OsALMT1* gene using the *Agrobacterium* method and several independent T2 or T3 rice homozygous lines

showing approximately 40-fold higher *OsALMT1* expression were. Transgenic lines with reduced *OsALMT1* expression were also generated with RNAi and two independent homozygous lines with expression levels 10 to 20% of wild type plants were used to investigate gene function. Transgenic rice plants over-expressing OsALMT1 tended to have smaller roots and shoots than null lines and develop brown spots on the leaves which were consistent with manganese toxicity. Those transgenic plants also showed a constitutive release of malate and fumarate from their roots and had higher concentrations of malate in the xylem sap. The malate efflux was increased by high light intensity and inhibited by niflumic acid, salicylic acid and high concentrations of GABA. The transgenic plants showed greater tolerance to Al toxicity than null lines and sometimes accumulated higher concentrations of boron, manganese and other elements in the leaves and grain. In longer-term growth studies transgenic lines with increased *OsALMT1* expression tended to be more sensitive to osmotic stress, low light and manganese toxicity and they tended to be more resistant to low Cl^- treatments and to B toxicity. Transgenic lines with reduced *OsALMT1* expression tended to be more sensitive to low Cl^- conditions and to low light.

In conclusion, OsALMT1 is a plasma membrane-localised ion channel that is widely expressed throughout rice plants. It is permeable to the organic anions malate and fumarate and it is predicted to be permeable to borate anions as well. *OsALMT1* expression in roots and shoots is responsive to several abiotic stresses and hormone treatments which indicates a central role in plant metabolism. We conclude that OsALMT1 is primarily a malate transporter that performs multiple functions including osmotic adjustment and the maintenance of electroneutrality.

CHAPTER 1
General Introduction

1.1 The ALMT gene family

The *aluminium activated malate transporter* (*ALMT*) gene family is named after the first member of the family identified in wheat (*Triticum aestivum* L.) (Sasaki *et al.*, 2004). The product of this gene controls resistance to aluminium (Al) toxicity. *TaALMT1* was the first member of this novel family of genes encoding anion channels. Although widely spread in plants, relatively little information is available on the roles performed by other members of this family. However those that have been characterised show a range of functions including Al resistance (Sasaki *et al.*, 2004; Hoekenga *et al.*, 2006; Ligaba *et al.*, 2006; Collins *et al.*, 2008), stomatal function (Kovermann *et al.*, 2007; Gruber *et al.*, 2010; Meyer *et al.*, 2010; Sasaki *et al.*, 2010; Gruber *et al.*, 2011; Meyer *et al.*, 2011; De Angeli *et al.*, 2013), mineral nutrition (Pineros *et al.*, 2008; Ligaba *et al.*, 2012) and fruit acidity (Bai *et al.*, 2012; De Angeli *et al.*, 2013) (**Table 1.1**).

ALMT genes encode transmembrane proteins that function as anion channels (see below) and perform multiple functions involving the transport of organic anions (e.g. carboxylates) and inorganic anions in cells (Delhaize *et al.*, 2007; Barbier-Brygoo *et al.*, 2011; Dreyer *et al.*, 2012). Carboxylic acids such as malic and citric acids are important metabolites in plant cells due to their involvement in photosynthesis, the tricaboxylic acid pathway, carbohydrate metabolism, cytosolic pH regulation, contribution to the maintenance of electroneutrality and nutrition (Ryan and Delhaize, 2001; Mariano *et al*., 2005; Maurino and Engqvist, 2015). These organic anions also confer resistance to Al toxicity in acid soils because when released from roots their carboxyl groups chelate the trivalent Al cations (Al^{3+}) rendering them less toxic (Ryan *et al.*, 2001; Ma *et al.*, 2001). Carboxylic anions can also bind with other multivalent metal ions (Barbier-Brygoo *et al.*, 2011).

Anion channels are integral membrane proteins that form aqueous pores to selectively allow the rapid transport of anions across membranes down their electrochemical gradients (Roberts, 2006). Therefore anion channels are passive transporters located on many plant membranes including the plasma membrane, tonoplast, endoplasmic reticulum,

mitochondrial and chloroplast membranes. Some also perform signalling roles and function as master switches in stress responses (Roberts, 2006; Isayenkov *et al.*, 2010; Roelfsema *et al.*, 2012). The development of the patch-clamping technique provided a method for detailed research on the functioning of ion channels. Other useful methods for studying ion channels also include the analysis of substrate concentrations in native and heterologous expression systems. In plants, the guard cells that regulate stomatal aperture have become a popular model system for characterising membrane transport and signal transduction. For instance, in *Vicia faba* guard cells, researchers have identified two types of anion channel considered important for stomatal closure: the rapid-type (R-type) and the slow-type (S-type) (see below) (Schroeder and Keller, 1992). The patch-clamp technique has been used to investigate the function of some members of the ALMT family. Some are permeable to malate anions while others are also permeable to other organic inions (such as fumarate) or inorganic inions (such as Cl^-, NO_3^- and less so SO_4^{2-}) (**Table 1.1**).

1.2 Functions of the ALMT family

1.2.1 The first member of the ALMT gene family was identified in wheat

In acid soils the soluble Al ions exist mainly in the trivalent (Al^{3+}) form which damages membranes and rapidly inhibits root growth (Ryan *et al.*, 1992). A widespread mechanism for Al resistance in many plant species relies on the release of organic anions from roots apices (the sensitive region of the root for Al toxicity). The organic anions, such as malate, citrate and oxalate, are able to chelate Al^{3+} to prevent it from binding in the cell wall and membranes and from entering the cytosol. This chelation reduces harmful interactions from occurring in the apoplast and in the cytosol of the root apex (Ryan *et al*., 2001; Kinraide *et al*., 2005; Kopittke et al., 2015).

The first gene identified in this family was *TaALMT1* in wheat because it controlled the major mechanism of aluminium (Al) resistance. By using a cDNA subtractive hybridization technique, Sasaki *et al.* (2004) cloned a cDNA which was more highly expressed in the root apices of an Al-resistant wheat line (ET8) than in a near-isogenic but Al-sensitive line (ES8). Furthermore, the *ALMT-1* allele from ET8 co-segregated with Al

Table 1.1 Functions and characteristics of members of the ALMT family

Function	Gene	Species	Sub-cellular Localization	Permeability	References
Al Resistance	*TaALMT1*	Wheat	Plasma membrane	$malate^{2-}$, Cl^-, NO_3^-, SO_4^{2-}	(Yamaguchi *et al.*, 2005)
	AtALMT1	Arabidopsis	Plasma membrane	$malate^{2-}$	(Sasaki *et al.*, 2004)
	BnALMT1	Rape	Plasma membrane	$malate^{2-}$	(Ligaba *et al.*, 2006)
	BnALMT2	Rape	Plasma membrane	$malate^{2-}$	(Ligaba *et al.*, 2006)
	ScALMT1	Rye	ND*	ND	(Collins *et al.*, 2008)
	AetALMT1	Aegilops tauschii	ND	At least malate	(Ryan *et al.*, 2010)
	MsALMT1	*Alfalfa*	ND	ND	(Chen *et al.*, 2013)
	GmALMT1	Soybean	Plasma membrane	ND	(Liang *et al.*, 2013)
	HlALMT1	Yorkshire fog	Plasma membrane	$malate^{2-}$	(Chen *et al.*, 2013)
	CsALMT1/CgALMT1	*Citrus*	ND	ND	(Yang *et al.*, 2012)
Stomatal Functions	*HvALMT1*	Barley	PM, motile vesicles	fumarate, $malate^{2-}$, citrate, Cl^-, MES	(Gruber *et al.*, 2010; Gruber *et al.*, 2011)
	AtALMT12	Arabidopsis	Plasma membrane	Cl^-, NO_3^-, $malate^{2-}$	(Meyer *et al.*, 2010)
	AtALMT6	Arabidopsis	Tonoplast	Fumarate, $malate^{2-}$	(Meyer *et al.*, 2011)
	AtALMT9	Arabidopsis	Tonoplast	$malate^{2-}$	(De Angeli *et al.*, 2013)
Mineral Nutrition	*ZmALMT1*	Maize	Plasma membrane	$malate^{2-}$, citrate, Cl^-	(Pineros *et al.*, 2008)
	ZmALMT2	Maize	Plasma membrane	$malate^{2-}$, Cl^-, NO_3^-	(Ligaba *et al.*, 2012)
Fruit acidity	*Ma1/Ma2*	Apple	ND	ND	(Bai *et al.*, 2012)
	VvALMT9	Grape	Vacuolar membrane	Malate, succinate, tartrate	(De Angeli *et al.*, 2013)

*ND: No data

resistance which confirmed that *TaALMT1* was linked with Al resistance (Sasaki *et al.*, 2004). *TaALMT1* was mapped to chromosome 4DL by using Chinese Spring deletion lines and the relative expression of this gene among various genotypes of wheat was strongly correlated with Al-activated malate efflux capacity and Al resistance (Raman *et al.*, 2005). Electrophysiological characterization in *Xenopus laevis* oocytes indicated that *TaALMT1* encodes an Al-activated transporter that can mediate both inward and outward currents. The malate transport permeability is enhanced by external Al but it is also permeable to a lesser degree to other physiologically relevant anions such as Cl^- and NO_3^- (Sasaki *et al.*, 2004; Pineros *et al.*, 2008). Patch-clamping studies in transgenic tobacco (*Nicotiana tabacum*) cell lines showed that *TaALMT1* was ~18-fold more permeable to malate than Cl^- and provided direct evidence that TaALMT1 functioned as an anion channel (Zhang *et al.*, 2008). Therefore, TaALMT1 is an anion channel located in the plasma membrane that mediates the Al-activated malate efflux from roots (**Figure 1.1**). Transgenic rice (*Oryza sativa*), Arabidopsis, barley (*Hordeum vulgare*) and tobacco cultured cell lines expressing *TaALMT1* all showed an Al-activated malate efflux. In the later three cases, TaALMT1 also increased Al resistance (Delhaize *et al.*, 2004; Sasaki *et al.*, 2004).

The higher expression of *TaALMT1* in resistant than sensitive wheat genotypes is due to a series of mutations in the promoter (Sasaki *et al.*, 2006). Six main patterns were identified in the sequence immediately upstream of the *TaALMT1* coding region. Repeated blocks of sequence in different patterns could be found and the number of repeats in this region was positively correlated with the *TaALMT1* expression levels and Al resistance (Sasaki *et al.*, 2006) (**Figure 1.2**). Transgenic rice with different promoter alleles driving GFP demonstrated that promoters with multiple repeats can generate more fluorescence and accumulate higher levels of GFP transcript in callus and root apices (Ryan *et al.*, 2010).

1.2.2 *ALMT* genes contributing to Al resistance

Until recently, the *TaALMT1* homologous from *Arabidopsis thaliana*, rape (*Brassica napus*), rye (*Secale cereale*), goat grass (*Aegilops tauschii*), alfalfa (*Medicago sativa*), soybean (*Glycine max*), Yorkshire fog (*Holcus lanatus*) and citrus species were the only ones identified (see **Table 1.1**). All these genes encode transmembrane proteins which likely function as anion channels to mediate malate efflux from roots to provide

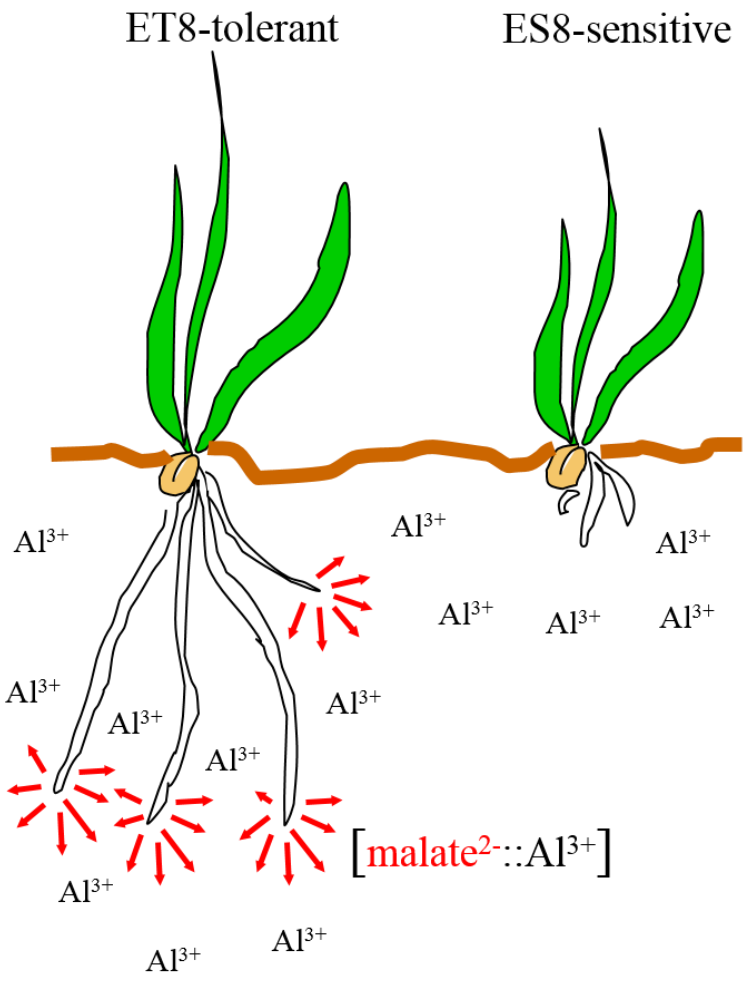

Figure 1.1 The major Al resistance mechanism in wheat

The expression of *TaALMT1* in Al^{3+}-resistant wheat genotypes encodes malate permeable anion channels in the plasma membrane which release $malate^{2-}$ from root apices when activated by Al^{3+}. Malate binds to Al^{3+} and reduces its toxicity to the sensitive growing region of the root apices.

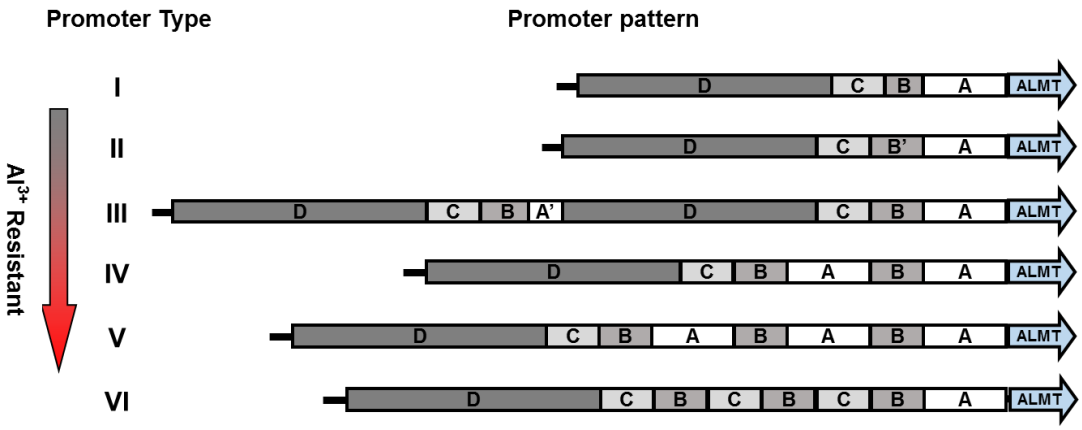

Figure 1.2 Promoter patterns of *TaALMT1* associated with Al resistance in wheat

The figure shows six sequence patterns upstream of *TaALMT1* but others also exist. The promoter types are based on different patterns of repeated blocks of sequence (A-D). Block A' is the 70 bp region from the 5' of block A. Block B' is mostly same as the block B with 31 bp repeat near the 5' end. The type I^a promoter allele (not shown) is similar to type I but with 11 additional SNPs or indels. Figure was modified from Sasaki *et al.*, (2006) and Ryan *et al.*, (2010).

protection from Al^{3+} (Hoekenga *et al*., 2006; Ligaba *et al*., 2006; Collins *et al*., 2008; Ryan *et al*., 2010; Yang *et al*., 2012; Chen *et al*., 2013; Chen *et al*., 2013; Liang *et al*., 2013) (**Figure 1.3**). The Arabidopsis *ALMT* gene family contains 14 members and *AtALMT8* shares the highest similarity (64%) with *TaALMT1*. However this gene is widely expressed throughout the plant and is not involved with Al resistance. The first homolog of *TaALMT1* with a similar function to *TaALMT1* was *AtALMT1*. Interestingly, AtALMT1, which is only 44% identical to TaALMT1, is mostly expressed in Arabidopsis roots and knock-out mutants are more sensitive to Al stress (Hoekenga *et al.*, 2006). Expression studies showed that *AtALMT1* expression is induced by Al treatment and low pH (Hoekenga *et al.*, 2006). Electrophysiological characterization in *Xenopus* oocytes indicated that *AtALMT1* functions as a malate-permeable channel (Hoekenga *et al.*, 2006; Kobayashi *et al.*, 2007). However other researchers could not demonstrate AtALMT1 function in oocytes (Sasaki *et al.*, 2014).

The Al-dependent release of organic anions from roots show one of two general patterns based on the response time to Al. For pattern I, the organic acid release begins immediately after the addition of Al. For pattern II, secretion of organic acids is delayed after applying Al for several hours or even days (Ma *et al*., 2001). The *TaALMT1* gene in wheat encodes a protein that belongs to pattern I because it is constitutively expressed in root tissues and the protein responds rapidly to Al treatment to release malate. By contrast, *AtALMT1* in Arabidopsis follows the pattern II response. Expression in roots increases over 12 hours after Al exposure and malate release is therefore delayed for many hours before reaching a maximum rate (Kobayashi *et al.*, 2007). Interestingly, *AtALMT1* expression is not only induced by external Al but also by low pH, hydrogen peroxide and phytohormones such as ABA and IAA (Kobayashi *et al.*, 2013). Furthermore *AtALMT1* might also be involved in biotic interactions. A transgenic Arabidopsis line in which GUS expression was driven by the promoter of *AtALMT1* showed increase GUS expression in the roots when the leaves were treated with the foliar pathogen *Pseudomonas syringae* pv *tomato* (Pst DC3000). This same treatment also induced malate release from the roots. The authors found that the malate release helped recruit the beneficial bacterium *Bacillus* FB17 around the roots (Rudrappa *et al*., 2008; Kobayashi *et al*., 2013). Furthermore, *AtALMT1* expression was induced by *flg22*, a kind of MAMP (microbe-associated molecular pattern) in a manner that was independent of the salicylic acid and jasmonic acid pathways (Lakshmanan *et al.*, 2012). These results indicate that *AtALMT1* expression could contribute to plant-pathogen

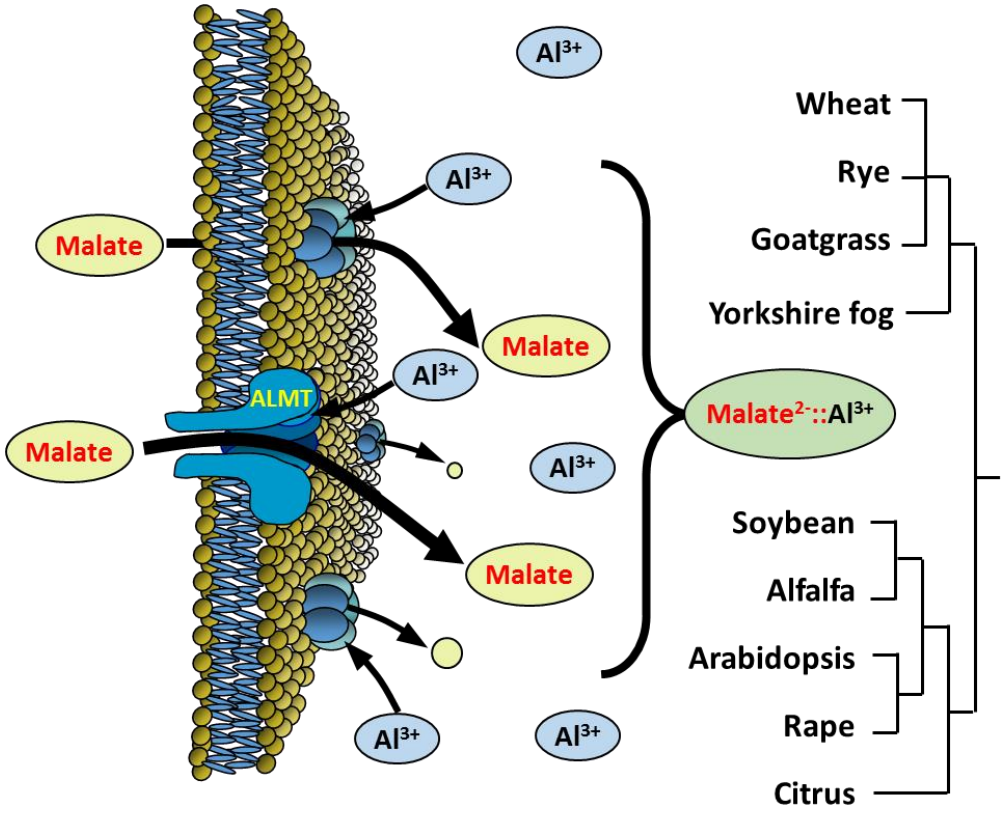

Figure 1.3 ALMT members involved with Al resistance

These genes encode transmembrane proteins located on the plasma membrane which function as anion channels to mediate malate efflux. The malate efflux from root tissues chelates the toxic Al^{3+} and prevents it from inhibiting root growth. The tree shows the relatedness of those ALMT proteins from different species that are known to be involved in Al resistance. Species listed include both monocotyledons like wheat (*Triticum aestivum*), rye (*Secale cereale*), goatgrass (*Aegilops tauschii*) and Yorkshire fog (*Holcus lanatus*) and eudicots like soybean (*Glycine max*), alfalfa (*Medicago sativa*), Arabidopsis, rape (*Brassica napus*) and citrus species. The species tree was collected from Pfam database based on the ALMT family (PF11744) (http://pfam.xfam.org/family/almt#tabview=tab7).

interactions (Rudrappa *et al.*, 2008) and that a single *ALMT* gene can perform multiple functions.

Unlike other plant species, rape releases both malate and citrate when exposed to Al (Ligaba *et al.*, 2004). In 2006, Ligaba *et al.* (2006) cloned two *TaALMT1* homologs from rape. These proteins only have 40% similarity with the wheat gene, but they still proved to be related to Al resistance (Ligaba *et al.*, 2006). Similar to other Al related members, BnALMT1 is localized in the plasma membrane (Ligaba *et al.*, 2006). The expression of *BnALMT1* and *BnALMT2* was detected mainly in root but not shoots and their expression can be enhanced by Al treatment and to a lesser degree by other multivalent cations (such as lanthanum, ytterbium, and erbium). Transgenic tobacco culture cells expressing these genes showed increased malate efflux when exposed to Al and some other cations such as ytterbium and erbium (Ligaba *et al.*, 2006).

Among cereal crops, rye is among the most Al resistant species. Researchers have mapped Al-resistance loci on chromosomes 3R (*Alt2*), 4RL (*Alt3*), 6RS (*Alt1*) and 7RS (*Alt4*) by using segregating populations and wheat-rye addition lines (Gallego and Benito, 1997; Gallego *et al.*, 1998; Gallego *et al.*, 1998; Ma *et al.*, 2000; Matos *et al.*, 2005). Using primers to the *TaALMT1* gene, Fontecha *et al.* (2007) cloned a 1359 bp cDNA called *ScALMT1* from rye and showed that it co-segregated with the Al resistance locus *Alt4*. *ScALMT1* is mainly expressed in roots and expression is upregulated by exogenous Al treatment (Fontecha *et al.*, 2007). Collins *et al.* (2008) showed that the *Alt4* resistance locus contains a cluster of *ALMT* genes. This locus in a tolerant haplotype, *M39A-1-6*, contained five genes whereas a sensitive haplotype, *M77A-1*, contained only two genes. Three of the genes in the resistant haplotype (*ScALMT1-M39.1*, *ScALMT1-M39.2* and *ScALMT1-M77.1*) were highly expressed in root tips and expression was enhanced by Al. Although there are some mRNA splice variations that might affect protein function, the *M77.1* promoter and *ScALMT1-M39.1* gene are sufficient to explain most of the Al resistance in that line (Collins *et al.*, 2008).

As the ancestor of the wheat D genome, *Aegilops tauschii* contains more genetic variation than bread wheat perhaps because it experienced less artificial selection. Ryan *et al.* (2010) screened 760 accessions in a total of seven progenitor species of hexaploid wheat and other early relatives. These included *Triticum monococcum* A^mA^m, *Triticum dicoccoides* BBAA, *Triticum zhukovskyi* AAAABB, *Triticum timopheevii* A^tA^tGG, *Triticum uratu* A^uA^u,

Triticum turgidum BBAA and *Aegilops tauschii* DD). Of these only five of 29 *Aegilops tauschii* tested showed a moderate level of resistance to Al. The coding sequences of the *AetALMT1* genes in the five resistant genotypes were identical to *TaALMT1* and resistance was correlated with *AetALMT1* expression level and with Al-activated malate efflux. Unlike *TaALMT1*, all the *Aegilops tauschii* genes lacked any of the tandem repeats in the promoter region - even the moderately resistant ones. Most of their promoter alleles belong to type I and Ia promoters which are usually associated with Al-sensitive hexaploid wheats (**Figure 1.2**) (Ryan *et al.*, 2010).

Medicago sativa (lucerne or alfalfa) is an Al-sensitive pasture legume species. Nevertheless transcript analysis using a cDNA library from cultivar YM1 SSH indicated that *MsALMT1* expression was up-regulated by a 24 h treatment with 5 μM Al (Chen *et al.*, 2011). Transgenic tobacco expressing *MsALMT1* showed malate efflux and the rate correlated with *MsALMT1* transcription level. Under Al stress, these transgenic tobacco plants also had better root growth than control lines which suggests that this gene could be involved with Al resistance in *Medicago* even though it was cloned from a sensitive genotype (Chen *et al.*, 2013).

Liao *et al.* (2013) cloned *GmALMT1* from soybean. Sub-cellular localisation of the protein indicated that it is located in the plasma membrane. Heterologous expression in *Xenopus laevis* cells shows that this gene encodes a protein that mediates inward and outward currents. *GmALMT1* is mainly expressed on root tips with expression and malate efflux altered by both low pH and Al treatments. Arabidopsis plants overexpressing *GmALMT1* show better malate efflux and higher Al resistance. Additionally, increasing and decreasing the expression of this gene in transgenic hairy roots of soybean indicated that accumulation of Al in the root tissues was inversely correlated with relative *GmALMT1* expression level. Together these results demonstrate that *GmALMT1* is also likely to function as an Al resistance gene in soybean (Liang *et al.*, 2013).

Yorkshire fog (*Holcus lanatus*) is a grass that shows a large genotypic variation in acid soil tolerance. Resistant and sensitive accessions of *Holcus lanatus* were collected from acidic (soil pH 3.6, HL-A) and neutral plots (pH 7.1, HL-N) from the Rothamsted Long-Term Park Grass experiment. Chen *et al.* (2013) cloned the *HlALMT1* gene and compared expression of this gene in the two populations. Plants from plots with acidic soil (HL-A) had significantly higher *HlALMT1* expression levels in their roots than plants from plots

with neutral pH soil (HL-N). The higher expression in HL-A plants was linked with a greater number of the *cis*-acting elements which recognise an Al-responsive transcription factor (HlART1) (Chen *et al.*, 2013). Furthermore the HL-A roots secreted approximately twice as much malate as the HL-N roots, but there was no difference in citrate secretion. These results indicated that *cis* elements in the promoter of the *HvALMT1* gene generated higher expression of *HlALMT1* leading to higher malate efflux and greater Al resistance.

In many acid soils it is common for Al toxicity to be linked with phosphorus (P) deficiency. This is because the soluble P is likely to be in a complex with iron or Al or fixed in other less soluble forms. Indeed some plants very efficient at taking up P from highly P-fixing soils, such white lupin (*Lupinus albus*), rely on organic anion release from roots (especially citrate release) to access more P (Ryan *et al.*, 2001). Research indicates that members of the ALMT family might also contribute to greater P-use efficiency. For instance, the Al resistant species of citrus 'Xuegan' (*Citrus sinensis*, *CsALMT1*) displayed more resistance to P-deficiency than a sensitive species 'Sour pummelo' (*Citrus grandis*, *CgALMT1*). Evidence was presented that *ALMT* genes in these species might contribute to the resistance of citrus to Al and/or P-deficiency (Yang *et al.*, 2012).

1.2.3 *ALMT* genes involved in guard cell function

Plants control gas exchange (CO_2 uptake and O_2 release) and water loss through the stomata on the leaf epidermis by regulating the turgor of the two guard cells. Guard cells change their osmotic potentials to draw water in or out. This deforms their shape and leads to opening or closing of the stomatal aperture (Misra *et al.*, 2015). It has been shown that the accumulation of K^+ is related to stomatal opening and the loss of K^+ to stomatal closing (Fischer, 1971). Chloride and malate are the main anions that balance cation movement to maintain electroneutrality during these process (Bowling, 1976). These ions need to exchange between the vacuole and cytosol over the tonoplast and between the symplast and apoplast over the plasma membrane. Malate plays another important role in this process both as a substrate and by acting as a signalling molecule and gating modifier to regulate the activity of anion channels (Dreyer *et al.*, 2012). ALMT members were shown to be involved in facilitating anion efflux from guard cells during stomatal closure (**Figure 1.4**).

The Arabidopsis *ALMT12* gene was the first member of the family to be implicated in stomatal function. Mutant analysis demonstrated that AtALMT12 is involved in regulating stomatal closure but not opening. *AtALMT12* is predominantly expressed in guard cells. The expression level of *AtALMT12* in shoots is 10 times higher than in roots and it is mainly expressed in guard cells (Sasaki *et al.*, 2010). Electrophysiological studies of guard cells during stomatal closure divided the inward currents (which by convention involves anion efflux) into those mediated by a rapid anion channel (R-type) also known as quick-activating anion channels (QUAC), and a slow anion channels (S-type) also known as the slow-activating anion channels (SLAC). The R-type anion channels can be activated rapidly within 50 ms by depolarization and activates potassium release when the membrane potential falls below the equilibrium potential for K^+ while S-type channels showed a much slower (seconds) voltage-dependent activation and deactivation (Schroeder and Keller, 1992; Dreyer *et al.*, 2012). Initial reports disagreed as to the sub-cellular localisation and function of AtALMT12. Sasaki *et al.* (2010) localized this protein to endomembranes and plasma membrane and predicted that AtALMT12 can mediate Cl^- and NO_3^- fluxes but not malate. They also concluded that this protein was not responsible for either the R-type not S-type anion currents. Meyer *et al.* (2010) by contrast, found that the protein did localise to the plasma membrane and concluded that AtALMT12 can mediate malate transport and likely functions as the R-type anion channel (Meyer *et al.*, 2010; Sasaki *et al.*, 2010). Further studies confirmed that AtALMT12 is a malate-dependent R-type channel in guard cells and interacts with the kinase Open Stomata 1 to regulate stomatal closure (Meyer *et al.*, 2010; Hedrich, 2012; Imes *et al.*, 2013).

Barley *HvALMT1* is also involved in stomatal function. Gruber *et al.* (2010) cloned the *HvALMT1* gene by screening a bacteria artificial chromosome (BAC) library. They subsequently showed that *HvALMT1* is located on chromosome 2H. Tissue localization showed that this protein was expressed in guard cells and in emerging lateral roots, the nucellar projection, aleurone layer and the scutellum of developing barley grain (Gruber *et al.*, 2010; Xu *et al.*, 2015). Unlike AtALMT12, intracellular localisation of HvALMT1 included the plasma membrane and small motile vesicles in the cytosol but the identity and function of those vesicles is unknown. Heterologous expression in *Xenopus* oocytes showed that this protein could mediate both inward and outward currents. HvALMT1 is permeable to malate and its activity is sensitive to pH (Gruber *et al.*, 2010). The transgenic plants over-expressing HvALMT1 released more malate from roots than the control plants

and they took significantly longer to close their stomata under low light than null controls. They also tended to reach a lower stomatal conductance at low light but the results were not significant. Combined with the finding that *HvALMT1* is highly expressed in guard cells these results provided evidence that this channel contributes to stomatal function (Gruber *et al.*, 2011). Interestingly, overexpressing *HvALMT1* to high levels with a constitutive promoter affected plant growth and grain formation. Further experiments showed that malate release measured from isolated aleurone layers of grain was significantly lower in transgenic lines in which *HvALMT1* expression was reduced by RNAi compared to control plants (Xu *et al*., 2015). Therefore HvALMT1 function affects stomatal aperture, grain development and plant growth. This shows that a single *ALMT* gene may perform multiple functions (Gruber *et al.*, 2010; Gruber *et al.*, 2011; Xu *et al.*, 2015).

Malate movement can also be important to balance the accumulation of cations in the vacuole such as potassium during stomatal opening. Therefore, ALMTs probably contribute to balancing anion movement across the tonoplast as well. For instance, in Arabidopsis the AtALMT6 and AtALMT9 proteins localise to the tonoplast. *AtALMT6* is expressed in guard cells of leaf, stem and flower tissues. Transient and stable expression of AtALMT6::GFP fusion protein show localization to the tonoplast. Meyer *et al.* (2011) concluded that AtALMT6 is a Ca^{2+}-activated malate channel as its transport activity was significantly altered by cytosolic Ca^{2+}. Moreover, AtALMT6 activity can be regulated by vacuolar pH and cytosolic malate. The *atalmt6* T-DNA knockout mutant showed reduced malate current density across the tonoplast membrane (Meyer *et al.*, 2011). Kovermann *et al.* (2007) cloned the *AtALMT9* gene and 1785 bp upstream of the coding region. Subcellular localization in both Arabidopsis and onion epidermal tissue showed localisation to the tonoplast. Tissue-specific localization using the promoter to drive *GUS* expression showed the gene is expressed in many organs including leaves (mesophyll tissue), roots and flower tissues. Malate currents were inhibited across the tonoplast of *AtALMT9* knock-out lines compared to WT controls but enhanced in tobacco lines expressing *AtALMT9*. AtALMT9 appears to function primarily as a malate channel although it exhibits weak conductance to fumarate and chloride (Kovermann *et al.*, 2007). More recently, De Angeli *et al.* (2013) confirmed that *AtALMT9* is an anion channel located on the tonoplast and is involved with stomatal opening. Unlike AtALMT6, AtALMT9 is not sensitive to cytosolic Ca^{2+} but can be activated by malate in the cytosol

but not by malate in the vacuole (De Angeli *et al.*, 2013). Further research also demonstrated that AtALMT9 transport can be modulated by cytosolic nucleotides and other vacuolar anions (Zhang *et al.*, 2014).

1.2.4 *ALMT* genes involved with mineral nutrition

In maize (*Zea mays*), *ZmALMT1* was considered a candidate for an Al resistance gene due to its sequence homology with *TaALMT1* (Pineros *et al.*, 2008). Although ZmALMT1 localises to the plasma membrane, is mainly expressed in root tissue, and shows increased expression with Al treatment, other results indicated that this gene was not involved with the mechanism of Al resistance. Firstly, electrophysiological characterization in *Xenopus* oocytes showed that ZmALMT1 had greater permeability to NO_3^- and Cl^- than malate and these anions would not bind with Al^{3+} to reduce its activity in the apoplast. Furthermore, *ZmALMT1* expression was low in the root tips where protection from Al^{3+} stress by organic anions is crucial. Lastly, transport activity of ZmALMT1 was independent of exogenous Al. The researchers concluded that ZmALMT1 is more likely to be related to mineral nutrition rather than to Al resistance (Pineros *et al.*, 2008).

Linkage analysis of Al resistance genes in maize identified another *ALMT* gene, *ZmALMT2*, that is associated with net root growth under Al stress (Krill *et al.*, 2010). However, once again, ZmALMT2 is more permeable to inorganic anions (NO_3^-, SO_4^{2-} and Cl^-) than organic anions such as malate. Furthermore, *ZmALMT2* is mainly expressed in mature roots and not root apices, expression levels are similar in Al-sensitive and resistant genotypes. Therefore this gene is also unlikely to be involved with Al resistance despite its genetic linkage with that trait. Instead the authors suggested ZmALMT2 is involved with mineral nutrition (Ligaba *et al.*, 2012).

1.2.5 *ALMT* genes contributing to fruit and berry acidity

Organic acids such as malate, citrate and tartrate exist in many fruits and their concentration in the pulp plays a critical role in fruit acidity (Etienne *et al.*, 2013). Malate

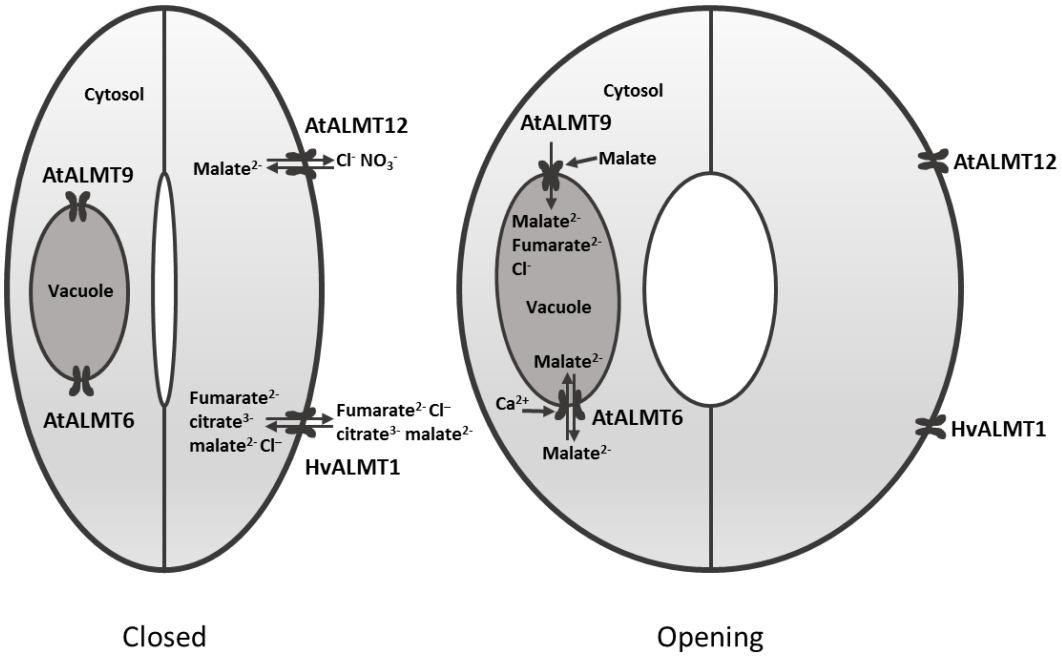

Figure 1.4 Members of the ALMT family involved in stomatal function

This cartoon depicts ALMTs from various species. During stomatal closing, AtALMT12 from Arabidopsis and HvALMT1 from barley mediate the efflux of anions across the plasma membrane to balance the loss of K^+. These processes lead to increased water potential in the symplast, loss of water to the apoplast and shrinkage of guard cells. During stomatal opening, the AtALMT9 and AtALMT6 that are located on the tonoplast, mediate anion influx to the vacuole. Solutes accumulating in the vacuole of guard cells decrease the water potential (more negative) which encourages water uptake, leading to increased turgor and stomatal opening. AtALMT9 is activated by cytosolic malate while AtALMT6 is regulated by Ca^{2+} concentrations. Arrows for fluxes are show in both directions since studies in *Xenopus* oocytes demonstrate this is possible. However it is expected that the ALMTs mostly facilitate substrate efflux. This figure is modified from Wikipedia (https://en.wikipedia.org/wiki/Guard_cell).

mainly accumulates in the vacuole which occupies 90% of the volume of most mature fruit cells. The storage of organic acids in the vacuole helps to regulate the cytosolic concentration of malate and thus plays a fundamental role in the regulation of cytosolic pH (Etxeberria *et al.*, 2012). In apple and grape fruit, *ALMT* genes play a role in adjusting fruit and berry acidity (**Figure 1.5**).Some ALMT proteins appear to affect fruit acidity by transporting malate across the tonoplast membrane. This was revealed when Bai *et al.* (2012) narrowed down the *Ma* locus to a 65-82 kb region on chromosome 16 of the apple cultivar Golden Delicious (Xu *et al.*, 2012). The *Ma* locus is associated with fruit acidity in apple and the genomic region contains 12-19 predicted genes. By aligning these genes with two BACs covering different haplotypes of the *Ma* locus (high and low acidity), they identified two *ALMT* homologues and named them *Ma1* and *Ma2*. Phylogenetic analysis using these two apple ALMT members against the Arabidopsis proteins indicated that these two members from apple were most similar to AtALMT6 and AtALMT9 which mediate anion transport across the tonoplast (Bai *et al.*, 2012). Ma1 was shown to localise on the tonoplast and heterologous expression in yeast increased malate influx into yeast cells. Quantitative RT-PCR experiments predicted that expression of *Ma1,* but not *Ma2,* is significantly linked with fruit acidity (high *Ma1* expression was correlated with more acidic fruit). Moreover, a natural mutation in *Ma1* leading to a truncation of the gene was also associated with low fruit acidity. The *Ma1* genotype is closely related to apple fruit acidity suggesting *Ma1* is associated with the accumulation of malic acid in apple fruits (Ma *et al*., 2015).

Similarly, De Angeli *et al.* (2013) cloned an *AtALMT9* homolog from grape (*Vitis vinifera*) called *VvALMT9*. *VvALMT9* expression increased as the berry matured. The VvALMT9 protein has 64% identity with AtALMT9 and also localises to the tonoplast. VvALMT9 is not only permeable to malate, but also displays a low permeability to tartrate. The authors predicted that VvALMT9 is a tonoplast channel that contributes to malate and tartrate accumulation in grape berries (De Angeli *et al.*, 2013).

1.3 Structural analysis and evolution of the ALMT family

1.3.1 Phylogeny of the ALMT family

Identification of *TaALMT1* in wheat stimulated further interest in this novel family of

genes as described above. When Delhaize *et al.* (2007) analysed the phylogeny of the ALMT family they used the UPF0005 (uncharacterised protein family five domain) for identifying other members. Using UPF0005 as the search sequence they concluded that the ALMT family was restricted to the seed-forming plants (Spermatophyta). The possible inclusion of ALMT in other phylogenetic groups other than the plants was largely unexplored. With the continual update of the Pfam database, the UPF0005 domain has been renamed to Bax1-I (Inhibitor of apoptosis-promoting Bax1, PF01027, http://pfam.sanger.ac.uk/family/PF01027) which is a member of the Apoptosis-Inhib Clan (CL0453, http://pfam.sanger.ac.uk/clan/CL0453). The ALMTs have been removed from that group to its own category (aluminium activated malate transporter, PF11744, http://pfam.sanger.ac.uk/family/PF11744) which falls within the FUSC Clan (Fusaric acid resistance protein-like superfamily, CL0307, http://pfam.sanger.ac.uk/clan/FUSC) (Punta *et al.*, 2012). The PF11744 domain contains the WEP fingerprint motif (Trp-Glu-Pro) present in all ALMTs (Dreyer *et al.*, 2012). Until recently, the ALMT family has been generally regarded as specific to plant species (Zhang *et al*., 2013) and largely angiosperms. Dreyer *et al.* (2012) showed that the distribution of ALMTs included the Bryophyta (mosses) and Lycophyta (vascular moss or club moss, e.g. *Selaginella sp*.) (Delhaize *et al*., 2007; Barbier-Brygoo *et al*., 2011; Dreyer *et al*., 2012; De Angeli *et al*., 2013). Before the first ALMT member was identified, Harley and Saier (2000) defined a PET (Putative Efflux Transporter) family which included efflux transporters and proteins from bacteria, plants, yeast and protozoans (Harley and Saier, 2000). By aligning the plant proteins in that group with proteins from Arabidopsis, we confirmed that the plant sequences analyzed by Harley and Saier (2000) are all ALMTs providing further insights into the phylogeny of the ALMTs. With the new classification, those bacterial sequences that were grouped with the ALMTs in the PET family (Harley and Saier 2000) are now included in the same FUSC Clan as the ALMT family. Therefore the PF11744 domain is present in bacterial proteins indicating an ancient common ancestry. Recent phylogeny on ALMT protein evolution either have a small sampling size or do not include fungi and bacterial sequences. With the development of genome-scale sequencing technologies, more information is available on the *ALMT* genes that extends this family beyond plants. This is demonstrated by combining the latest Pfam database and NCBI website and searching for the PF11744 Pfam domain (**Figure 1.6**). Among the new sequences included in the ALMT family by using the

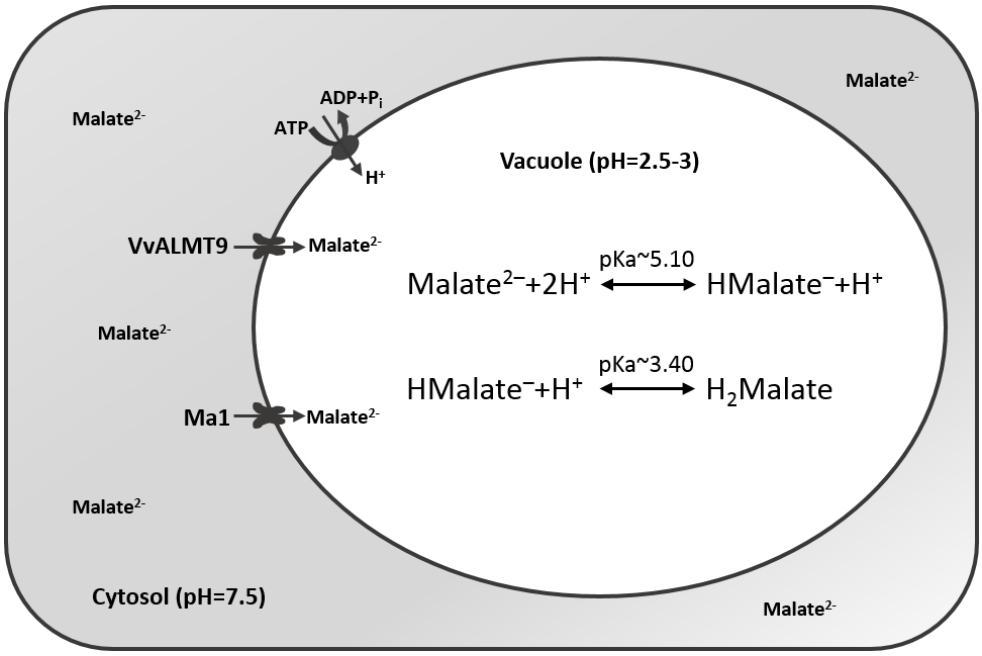

Figure 1.5 ALMTs contributing to fruit and berry acidity

The pH of the cytosol is neutral or slightly alkaline so malate exists mainly in the malate^{2-} form. In the vacuole, where the pH is acidic, a larger proportion of malate exists either as the protonated malic acid or the mono-valent anion (malate^{-}). Once malate^{2-} is transported from the cytosol to the vacuole across the tonoplast, a proportion will be protonated which partly helps to maintain the electrochemical potential gradient for malate^{2-} influx into the vacuole (Etienne *et al.*, 2013). Also shown is a H^+ pump which transports H^+ into the vacuole. This figure is modified from De Angeli *et al.* (2013).

PF11744 domain are proteins of various lengths and structures. The PF11744 domain in these proteins range from 150 to 950 residues in different species and phylogenetic analysis shows approximately 30% similarity among 564 protein sequences. The conserved regions are mainly found in the trans-membrane domains at the N-terminal ends and less frequently at the C-terminal ends. Some other members only contain part of the ALMT domain and these were excluded from the analysis. We constructed a phylogenetic tree and found that ALMT-like protein sequences are present in the bacteria, Alveolata (single-celled Eukaryotes), Stramenopiles (brown algae, oomycetes), Amoebozoa, fungi, and Viridiplantae. Within the Viridiplantae, ALMTs occur in non-vascular plants (mosses), spore-forming vascular plants (club mosses) and seed-forming vascular plants which is consistent with Dreyer *et al.* (2012) (**Figure 1.6**). The phylogenetic analysis shows that the ALMT family is far more ancient than the plant kingdom but appears to be absent from animal genomes.

1.3.2 Secondary structure

Most algorithms for secondary structure predict that plant members of the ALMT protein family have five to seven transmembrane regions in the N-terminal half and a long hydrophilic "tail" in the C-terminal half (Delhaize *et al.*, 2007). However even for the same protein sequence different programmes can predict different transmembrane arrangements. For instance **Figure 1.7** shows three contrasting predictions for the secondary structure of TaALMT1. The first experimental examination of the topology of an ALMT protein was performed on TaALMT1. In that immunocytochemical approach antibodies were generated to target different regions of the TaALMT1 protein. It was concluded that both the C-terminal and N-terminal tails were orientated extracellularly (Motoda *et al.*, 2007). More recent studies have questioned this structure and instead have suggested that the C-terminal end is oriented toward the intracellular space (Meyer *et al.*, 2010; Ryan and Delhaize, 2010; Dreyer *et al.*, 2012; Ligaba *et al.*, 2013; Mumm *et al.*, 2013). Secondary structures of ALMT proteins with the ALMT domain (PF11744) vary. Most of the ALMT proteins contain five to six transmembrane regions (TMRs). Although some of these proteins only contain a part of the PF11744 domain, they still have the typical structure of transmembrane regions in the N-terminal half of the protein (three to

seven transmembrane regions) and a hydrophilic C-terminal 'tail'. Within this group there are various protein arrangements where some have a single PF11744 (ALMT) domain while others contain more than one PF11744 domain (**Figure 1.8**). For example, a grape ALMT protein comprising of 1070 amino acid residues has a repetitive structure with two almost complete ALMT domains with six transmembrane regions in each domain (**Figure 1.9a**). Other examples include the S3 and S4 structures which contain two or three incomplete ALMT domains all connected to each other (**Figure 1.8**).

The S5, S6, S7 and S8 are composite structures with one or two ALMT domains combined with other domains (**Figure 1.8**). Some of those other domains also belong to the FUSC clan along with the ALMT domain (such as the FUSC_2, ArAE_2_N) or they belong to other clans with no relationship with ALMTs. These other domains include the EF hand which has a helix-loop-helix motif found in a large family of calcium-binding proteins, the glycoside hydrolase family 43 or domains with uncharacterised functions (such as TLD). The ALMT-like protein in *Perkinsus marinus* (single-celled pathogen of oysters) has a more complex structure with two ALMT domains, a FUSC_2 domain and a total of 24 predicted transmembrane regions among its 2287 residues (**Figure 1.9b**). Most of the complex structures exist in species with an ancient history such as fungi, green algae and Alveolata. Based on these patterns we would predict that the more recent members of ALMT might not function as single subunits but function as dimers or multimers. For instance, the Arabidopsis AtALMT9 appears to forms a multimeric channel of four subunits (Zhang *et al.*, 2013). By contrast, evidence collected with bimolecular fluorescence complementation (BiFC) indicates that TaALMT1 functions as a homodimer (Pineros MA, Ligaba A, Kochian LV, personal communication).

1.3.3 The structure-function relationship of ALMT proteins

As discussed above, the ALMT family members have a conserved secondary structure with an N-terminus region containing transmembrane domains and a hydrophilic C-terminus sometimes comprising up to half of the length of the entire protein. Recent studies have started to examine aspects of the structure-function and especially the amino acid residues critical for activation of transport activity by Al^{3+} and for its permeability to anions (**Figure 1.10**).

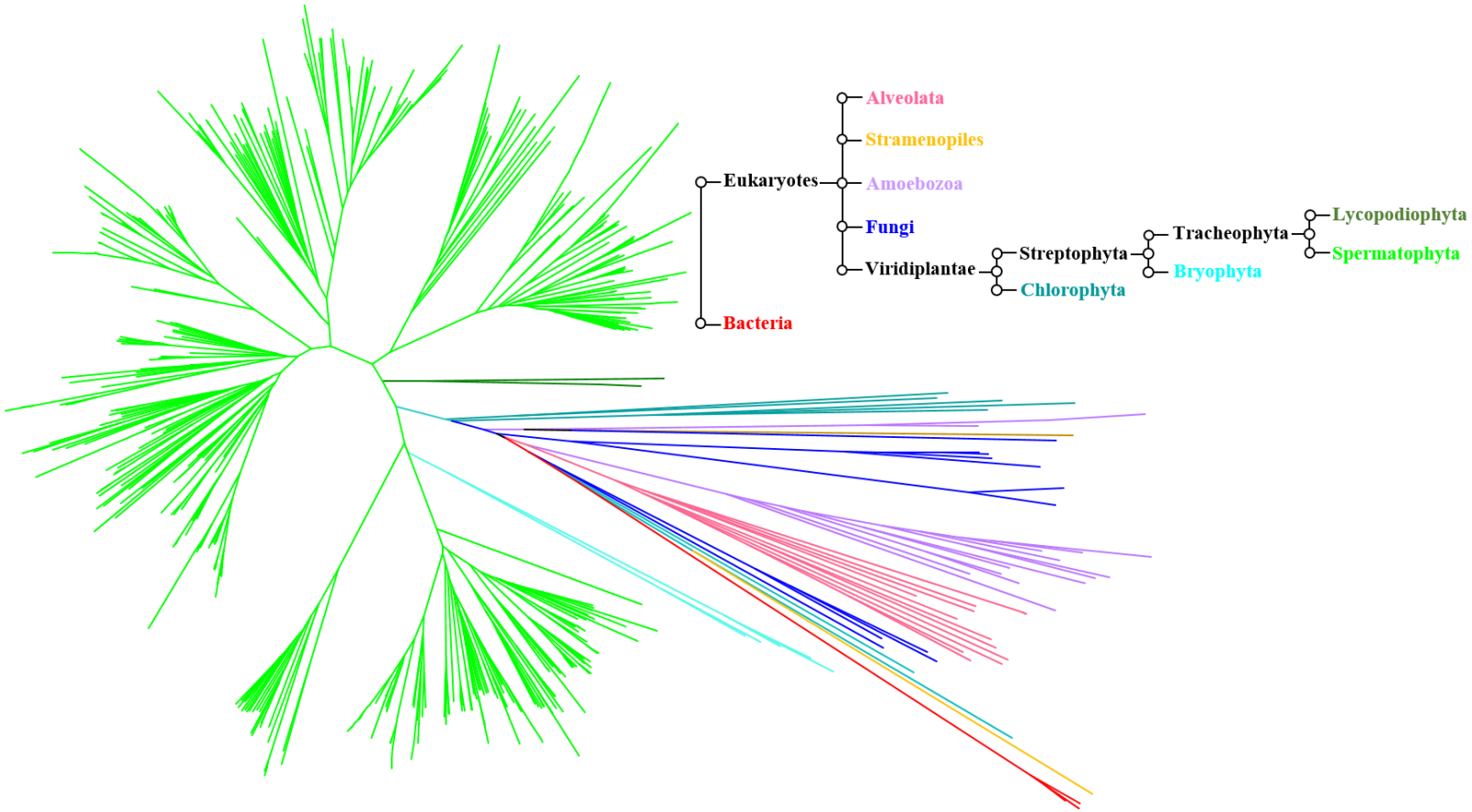

Figure 1.6 Unrooted phylogenetic tree of the ALMT family

The phylogenetic tree was constructed using the PF11744 domain sequences of ALMT proteins. These were obtained from the Pfam website (Punta *et al.*, 2012). ALMT sequences were aligned with ClustalW in the MEGA 5.0 software (Tamura *et al.*, 2011) phylogenetic tree was constructed using the neighbour-joining method. Each line represents an individual phenotype. Species are represented by various colours with 5 bacteria, 2 Alveolata, 3 Stramenopiles, 4 Amoebozoa, 19 Fungi, 3 Chlorophyta, 1 Bryophyta, 1 Lycopodiophyta and 53 species of Spermatophyta.

Studies using protein kinase and phosphatase inhibitors first indicated that reversible protein phosphorylation may be involved in activating malate efflux via ALMTs from wheat and Arabidopsis roots (Osawa and Matsumoto, 2001; Kobayashi *et al.*, 2007). Whether responses to these inhibitors were caused by direct modifications to the ALMT proteins or due to upstream signalling cascades that later lead to malate efflux is unclear. By systematically modifying candidate amino acids in the TaALMT1 protein that could be involved in phosphorylation, it was concluded that S384 is an essential residue regulating TaALMT1 activity via direct protein phosphorylation and that this process precedes Al^{3+} enhancement of transport activity (Ligaba *et al.*, 2009). In oocytes expressing the S384A mutated protein, TaALMT1-dependent basal currents and the Al-enhanced currents were significantly reduced. Furthermore, the currents were insensitive to protein kinase inhibitor staurosporine and the protein kinase C (PKC) activator, phorbol 12-myristate 13-acetate (PMA). Using a similar mutational approach, Furuichi *et al.*, (2010) concluded that three acidic residues, E274Q, D275N and E284Q, located on the hydrophilic C-terminal region of TaALMT1 are important for the Al^{3+}-activated transport activity because mutations at these sites decreased the Al-dependent responses without affecting basal transport activity (Furuichi *et al.*, 2010). A comparable mutation in AtALMT1, E284Q, has the same effect (Furuichi *et al.*, 2010) and the mutations E256Q in AtALMT1 and E276Q in AtALMT12 are comparable to E274Q in TaALMT1 and show the same decreases to Al-dependent transport function (Mumm *et al.*, 2013). However subsequent studies demonstrated that those three residues in TaALMT1 (E274, D275 and E284) are highly conserved throughout the entire ALMT family, even in ALMTs that are not activated by Al. Therefore the residues might be more important to tertiary protein structure rather than specifically involved with the activation by Al (Ligaba *et al.*, 2013). This was confirmed when Ligaba *et al.*, (2013) who showed that mutations in 43 additional acidic (negatively charged) residues of TaALMT1 also affected protein function. Indeed the residue E284 is part of a WEP fingerprint motif (Trp-Glu-Pro) which is in all ALMTs (Dreyer *et al.*, 2012). Rather than targeting specific residues to investigate the structure-function of ALMTs, other researchers have focussed on large domains of the protein. For instance, when the entire hydrophilic C-terminal region was removed from TaALMT1 or AtALMT12 the resulting proteins lost both basal and Al-dependent transport activity when expressed in *Xenopus* oocytes (Furuichi *et al.*, 2010). The Al^{3+}-dependent activity could be recovered in TaALMT1 by adding the C-terminal region from the Arabidopsis protein AtALMT1

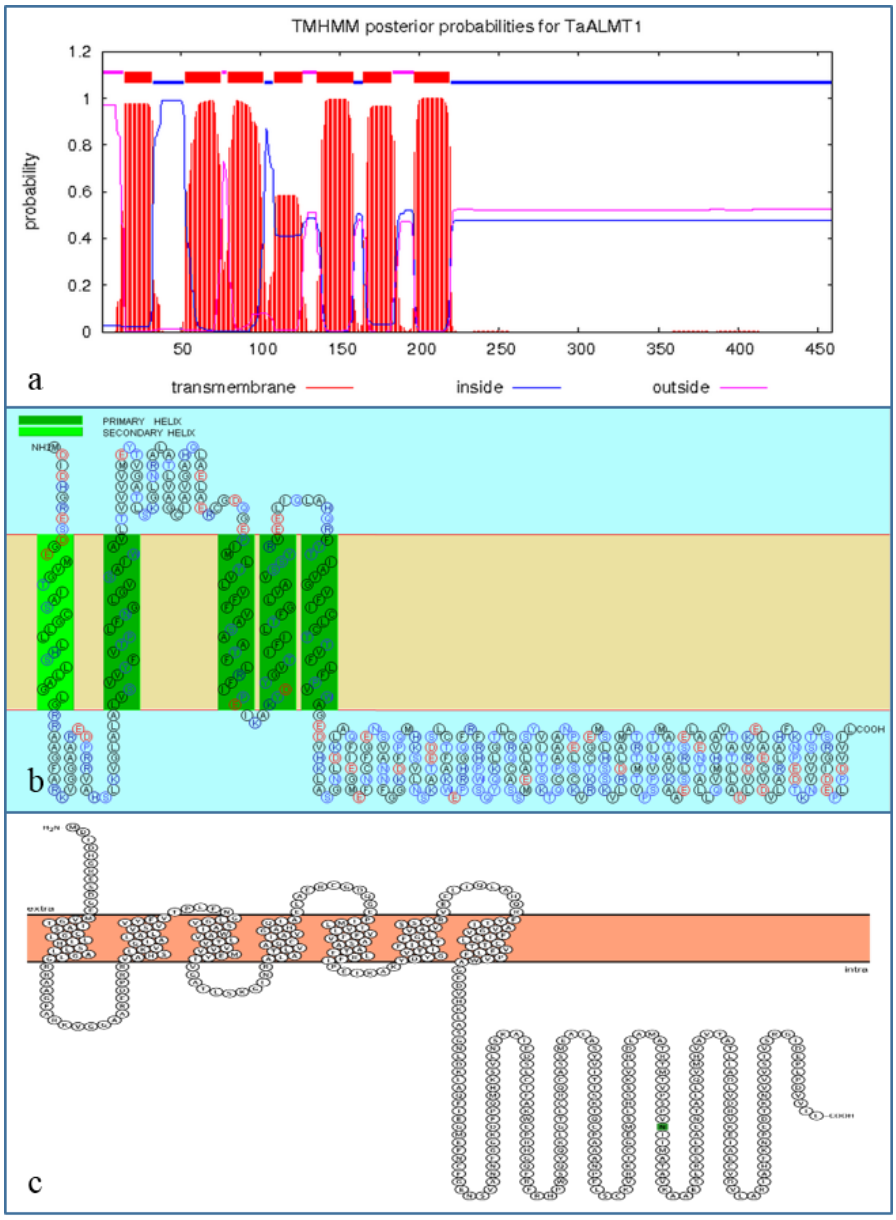

Figure 1.7 Different predictions for the secondary structure of TaALMT1

Secondary structure of TaALMT1 from wheat was predicted by TMHMM (a), SOSUI (b) and Protter (c). In (a) the number of transmembrane helices is seven. The N-terminal end is predicted to face the apoplast while the C-terminal end is predicted to be intracellular. In (b) five transmembrane helices are predicted. The N-terminal end is predicted to face the apoplast while the C-terminal end is predicted to be intracellular. In (c) the TaALMT1 is predicted to have seven transmembrane regions. The N-terminal end is predicted to face the apoplast while the C-terminal end is predicted to be intracellular. Chapter 3 provides the websites for these algorithms.

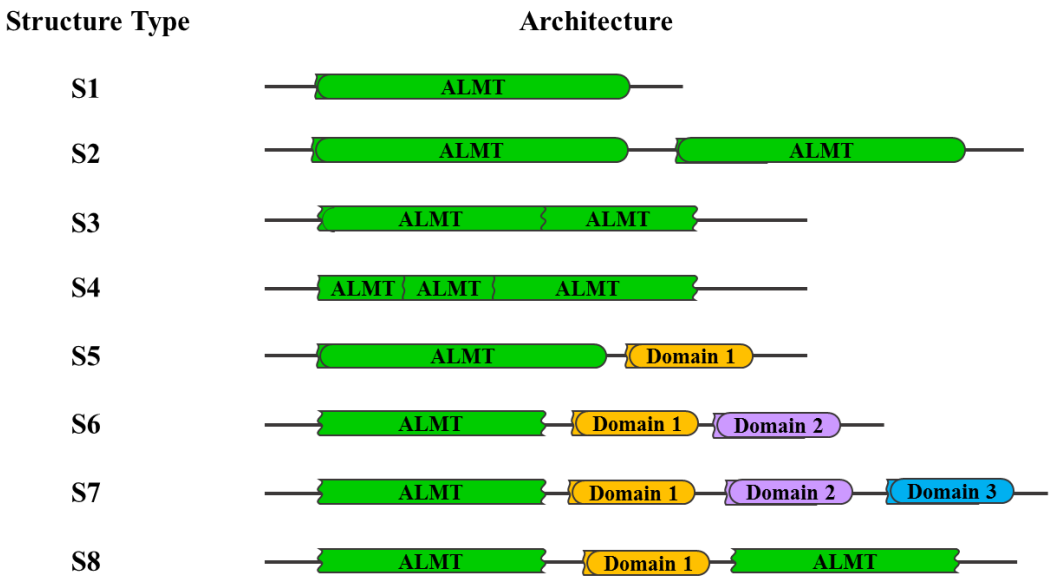

Figure 1.8 Structures of some members of the ALMT protein family

Members of the ALMT family of proteins may contain one or more PF11744 domains. S1 architecture is the simplest and most widespread structure and contains only one complete (or incomplete) ALMT domain. For other structures, the ALMT protein may contain more than one PF11744 domains with or without other domains. These domains may or may not be complete but maintain the same general structure. For instance, proteins with structures S5 to S8 contain domain(s) other than the ALMT domain and these are represented by Domains 1, 2, 3 etc. (Note that these Domains do not represent a specific domain in each case but just indicate domains that are different from PF11744). (See http://pfam.xfam.org/family/ALMT for more details).

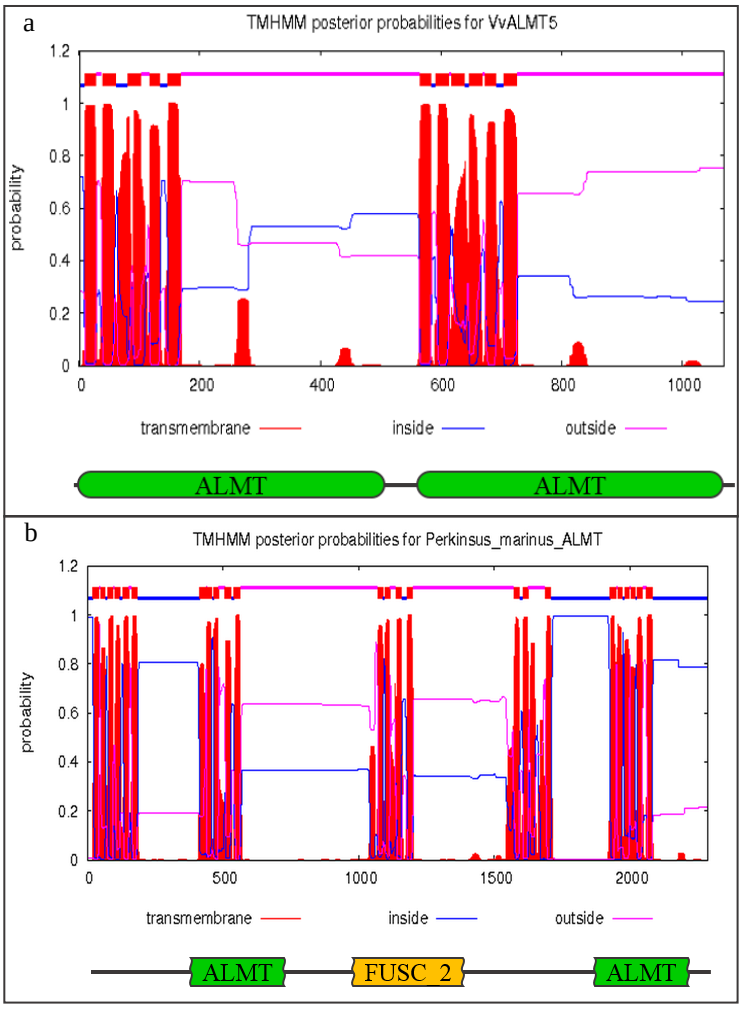

Figure 1.9 Hydropathy plots showing the domain structure and transmembrane regions of ALMT proteins in grape (VvALMT5) and *Perkinsus marinus*

(a) The grape VvALMT5 protein which contains 1070 amino acids displays a repetitive structure and forms two nearly complete ALMT domains with six transmembrane regions each. (b) The *Perkinsus marinus* (an alveolate protozoan) ALMT protein contains 2287 residues with 24 predicted transmembrane regions, two ALMT domains and a FUSC_2 domain.

(Furuichi *et al.*, 2010). Further experiments demonstrated that both the N- and C-domains are involved in Al-mediated enhancement of TaALMT1 transport activity. Ligaba *et al.* (2013) proposed that a motif on the N-terminus denoted by [D,E]-[H,K,R]-x-[K,R]-[D,E]-x-x-x-[D,E] is required for this response observed in a subset of ALMTs (Ligaba *et al.*, 2013). Similar conclusions were reported by Sasaki *et al.*, (2014) who generated chimeric proteins from TaALMT1 of wheat and AtALMT1 of Arabidopsis and examined their transport function in *Xenopus* oocytes. Firstly they detected transport activity only for TaALMT1 but not for AtALMT1. However where the N- and C-terminal halves of TaALMT1 and AtALMT1 were swapped (Ta::At and At::Ta) they found transport activity whenever the N-terminal half of TaALMT1 was present (Sasaki *et al.*, 2014). Moreover, they identified a putative helical domain on the N-terminal and another on the C-terminal ends of TaALMT1 which are important for its transport activity (Sasaki *et al.*, 2014).

In conclusion, the topology of ALMT transporters remains unclear and doubt still remains whether the N and the C-terminal ends are intracellular or extracellular (Motoda *et al.*, 2007; Meyer *et al.*, 2010; Meyer *et al.*, 2011; Ryan *et al.*, 2011; Dreyer *et al.*, 2012; Mumm *et al.*, 2013). Recently Ramesh *et al.* (2015) showed that the transport activity of several ALMTs expressed in *Xenopus* oocytes is very sensitive to inhibition by gamma-aminobutyric acid (GABA) and muscimol, an agonist of $GABA_A$ receptor (Ramesh *et al.*, 2015). Subsequent studies suggest that ALMT proteins may be GABA receptors in plants and underlay novel signalling pathways associated with stress responses. Although the ALMTs have a low overall sequence similarity with the $GABA_A$ receptors in animal cells, ALMTs contain a conserved motif that is similar to the GABA binding site on $GABA_A$ receptors. This intriguing result suggests that ALMTs may perform many other functions in plants which are still to be discovered.

1.4 Objectives

The aluminium-activated malate transporter (*ALMT*) gene family encode transmembrane proteins that function as anion channels and perform multiple functions related to plant anion transport. Relatively few members of this family have been characterised but those that have been characterised show a wide range of functions related to Al resistance,

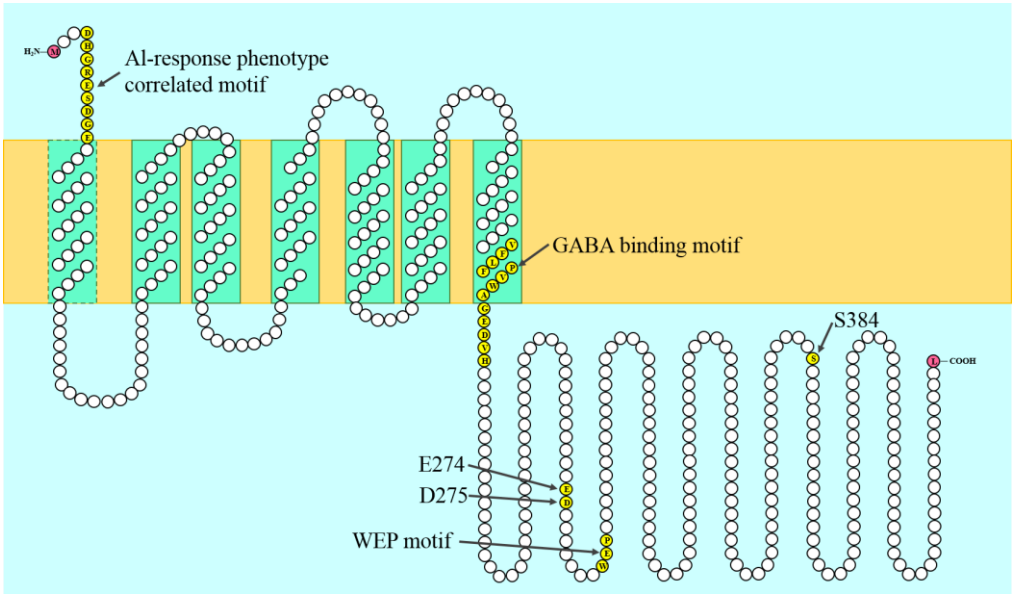

Figure 1.10 Hypothetical model for TaALMT1 showing residues and domains potentially important for function

TaALMT1 most likely has six transmembrane regions (green boxes with solid line border) based on a consensus of several different predictive programs for secondary structure. Another transmembrane region (green boxes with dashed line border) is also predicted by some programmes. The direction of the C-terminals ends are uncertain and will depend on the number of transmembrane regions. The "DHGRESDGE" motif within the N-terminus prior to transmembrane regions is correlated with the Al-response phenotype according to Ligaba *et al*., (2013), and the "FLFPVWAGEDVH" motif residing near the end of the sixth transmembrane domain is the binding site for GABA. The WEP motif is highly conserved in all ALMTs. E274, D275 and S384 initially predicted to be essential for ALMT function are instead likely to be important for overall protein structural.

stomatal function, mineral nutrition and ion balance. There are nine ALMT members in rice but no information has been published on any of these genes. The aim of this study is to provide the first detailed examination of the molecular biology and physiology of an *ALMT* gene and the protein it encodes in rice. The specific objectives of this study are to:

- clone small diagnostic regions of each *ALMT* gene in rice to enable expression of the genes in shoot and root tissues to be examined. Based on this analysis, one gene will be selected for detailed characterisation.
- clone the coding and promoter regions of the selected gene (ie. *OsALMT1*).
- determine the subcellular localisation of the selected gene product by transient expression of gene::GFP fusion constructs in leek and tobacco tissues.
- determine the tissue-specific localisation of the selected gene by using its promoter region to drive GFP expression in stably transformed rice plants .
- examine changes in gene expression in WT rice plants under different stresses and hormones.
- generate transgenic lines with increased and reduced levels of gene expression for detailed characterisation of gene and protein function.
- establish a likely function for the protein encoded by the gene.

1.5 References

Bai Y, Dougherty L, Li MJ, Fazio G, Cheng LL, Xu KN (2012) A natural mutation-led truncation in one of the two aluminum-activated malate transporter-like genes at the *Ma* locus is associated with low fruit acidity in apple. Mol Genet Genomics 287: 663-678

Barbier-Brygoo H, De Angeli A, Filleur S, Frachisse JM, Gambale F, Thomine S, Wege S (2011) Anion channels/transporters in plants: from molecular bases to regulatory networks. Annu Rev Plant Biol 62: 25-51

Barbier-Brygoo H, Vinauger M, Colcombet J, Ephritikhine G, Frachisse J-M, Maurel C (2000) Anion channels in higher plants: functional characterization, molecular structure and physiological role. BBA - Biomembranes 1465: 199-218

Bowling DJF (1976) Malate-switch hypothesis to explain the action of stomata. Nature 262: 393-394

Chen Q, Wu KH, Wang P, Yi J, Li KZ, Yu YX, Chen LM (2013) Overexpression of *MsALMT1*, from the aluminum-sensitive *Medicago sativa*, enhances malate exudation and aluminum resistance in Tobacco. Plant Mol Biol Rep 31: 769-774

Chen Q, Zhang XD, Wang SS, Wang QF, Wang GQ, Nian HJ, Li KZ, Yu YX, Chen LM (2011) Transcriptional and physiological changes of alfalfa in response to aluminium stress. J Agr Sci 149: 737-751

Chen ZC, Yokosho K, Kashino M, Zhao FJ, Yamaji N, Ma JF (2013) Adaptation to acidic soil is achieved by increased numbers of cis-acting elements regulating *ALMT1* expression in *Holcus lanatus*. Plant J 76: 10-23

Collins NC, Shirley NJ, Saeed M, Pallotta M, Gustafson JP (2008) An *ALMT1* gene cluster controlling aluminum tolerance at the *Alt4* locus of rye (*Secale cereale* L.). Genetics 179: 669-682

De Angeli A, Baetz U, Francisco R, Zhang J, Chaves MM, Regalado A (2013a) The vacuolar channel VvALMT9 mediates malate and tartrate accumulation in berries of *Vitis vinifera*. Planta 238: 283-291

De Angeli A, Zhang JB, Meyer S, Martinoia E (2013b) AtALMT9 is a malate-activated vacuolar chloride channel required for stomatal opening in *Arabidopsis*. Nat. Commun 4: 1804

Delhaize E, Gruber BD, Ryan PR (2007) The roles of organic anion permeases in aluminium resistance and mineral nutrition. FEBS Lett 581: 2255-2262

Delhaize E, Ryan PR, Hebb DM, Yamamoto Y, Sasaki T, Matsumoto H (2004) Engineering high-level aluminum tolerance in barley with the *ALMT1* gene. PNAS 101: 15249-15254

Dreyer I, Gomez-Porras JL, Riano-Pachon DM, Hedrich R, Geiger D (2012) Molecular evolution of slow and quick anion channels (SLACs and QUACs/ALMTs). Front Plant Sci 3: 263

Etienne A, Genard M, Lobit P, Mbeguie AMD, Bugaud C (2013) What controls fleshy fruit acidity? A review of malate and citrate accumulation in fruit cells. J Exp Bot 64: 1451-1469

Etxeberria E, Pozueta-Romero J, Gonzalez P (2012) In and out of the plant storage vacuole. Plant Sci 190: 52-61

Fischer RA (1971) Role of potassium in stomatal opening in the leaf of *Vicia faba*. Plant Physiol 47: 555-558

Fontecha G, Silva-Navas J, Benito C, Mestres MA, Espino FJ, Hernandez-Riquer MV, Gallego FJ (2007) Candidate gene identification of an aluminum-activated organic acid transporter gene at the *Alt4* locus for aluminum tolerance in rye (*Secale cereale* L.). Thero Appl Genet 114: 249-260

Furuichi T, Sasaki T, Tsuchiya Y, Ryan PR, Delhaize E, Yamamoto Y (2010) An extracellular hydrophilic carboxy-terminal domain regulates the activity of TaALMT1, the aluminum-activated malate transport protein of wheat. Plant J 64: 47-55

Gallego FJ, Benito C (1997) Genetic control of aluminium tolerance in rye (*Secale cereale* L.). TAG 95: 393-399

Gallego FJ, Calles B, Benito C (1998) Molecular markers linked to the aluminium tolerance gene Alt1 in rye (*Secale cereale* L.). TAG 97: 1104-1109

Gallego FJ, Lopez-Solanilla E, Figueiras AM, Benito C (1998) Chromosomal location of PCR fragments as a source of DNA markers linked to aluminium tolerance genes in rye. TAG 96: 426-434

Gruber BD, Delhaize E, Richardson AE, Roessner U, James RA, Howitt SM, Ryan PR (2011) Characterisation of *HvALMT1* function in transgenic barley plants. Funct Plant Biol 38: 163-175

Gruber BD, Ryan PR, Richardson AE, Tyerman SD, Ramesh S, Hebb DM, Howitt SM, Delhaize E (2010) HvALMT1 from barley is involved in the transport of organic anions. J Exp Bot 61: 1455-1467

Harley KT, Saier MH (2000) A Novel Ubiquitous Family of Putative Efflux Transporters. J Mol Microbiol Biotechnol 2: 195-198

Hedrich R (2012) Ion Channels in Plants. Physiol Rev 92: 1777-1811

Hoekenga OA, Maron LG, Pineros MA, Cancado GMA, Shaff J, Kobayashi Y, Ryan PR, Dong B, Delhaize E, Sasaki T, Matsumoto H, Yamamoto Y, Koyama H, Kochian LV (2006) *AtALMT1*, which encodes a malate transporter, is identified as one of several genes critical for aluminum tolerance in *Arabidopsis*. PNAS 103: 9738-9743

Imes D, Mumm P, Bohm J, Al-Rasheid KA, Marten I, Geiger D, Hedrich R (2013) Open stomata 1 (OST1) kinase controls R-type anion channel QUAC1 in Arabidopsis guard cells. Plant J 74: 372-382

Isayenkov S, Isner JC, Maathuis FJ (2010) Vacuolar ion channels: Roles in plant nutrition and signalling. FEBS Lett 584: 1982-1988

Kinraide TB, Parker DR, Zobel RW (2005) Organic acid secretion as a mechanism of aluminium resistance: a model incorporating the root cortex, epidermis, and the external unstirred layer. J Exp Bot 56: 1853-1865

Kobayashi M, Ohura I, Kawakita K, Yokota N, Fujiwara M, Shimamoto K, Doke N, Yoshioka H (2007) Calcium-dependent protein kinases regulate the production of reactive oxygen species by potato NADPH oxidase. Plant Cell 19: 1065-1080

Kobayashi Y, Hoekenga OA, Itoh H, Nakashima M, Saito S, Shaff JE, Maron LG, Pineros MA, Kochian LV, Koyama H (2007) Characterization of *AtALMT1* expression in aluminum-inducible malate release and its role for rhizotoxic stress tolerance in arabidopsis. Plant Physiol145: 843-852

Kobayashi Y, Kobayashi Y, Sugimoto M, Lakshmanan V, Iuchi S, Kobayashi M, Bais HP, Koyama H (2013a) Characterization of the Complex Regulation of *AtALMT1* Expression in Response to Phytohormones and Other Inducers. Plant Physiol 162: 732-740

Kobayashi Y, Lakshmanan V, Kobayashi Y, Asai M, Iuchi S, Kobayashi M, Bais HP, Koyama H (2013b) Overexpression of AtALMT1 in the Arabidopsis thaliana ecotype Columbia results in enhanced Al-activated malate excretion and beneficial bacterium recruitment. Plant Signal Behav 8: 25561-25564

Kopittke PM, Moore KL, Lombi E, Gianoncelli A, Ferguson BJ, Blamey FP, Menzies NW, Nicholson TM, McKenna BA, Wang P, Gresshoff PM, Kourousias G, Webb RI, Green

K, Tollenaere A (2015) Identification of the primary lesion of toxic aluminum in plant roots. Plant Physiol 167:1402-1411

Kovermann P, Meyer S, Hortensteiner S, Picco C, Scholz-Starke J, Ravera S, Lee Y, Martinoia E (2007) The Arabidopsis vacuolar malate channel is a member of the ALMT family. Plant J 52: 1169-1180

Krill AM, Kirst M, Kochian LV, Buckler ES, Hoekenga OA (2010) Association and linkage analysis of aluminum tolerance genes in maize. PLoS One 5: e9958

Lakshmanan V, Kitto SL, Caplan JL, Hsueh YH, Kearns DB, Wu YS, Bais HP (2012) Microbe-associated molecular patterns-triggered root responses mediate beneficial rhizobacterial recruitment in Arabidopsis. Plant Physiol 160: 1642-1661

Liang CY, Pineros MA, Tian J, Yao ZF, Sun LL, Liu JP, Shaff J, Coluccio A, Kochian LV, Liao H (2013) Low pH, aluminum, and phosphorus coordinately regulate malate exudation through *GmALMT1* to improve soybean adaptation to acid soils. Plant Physiol 161: 1347-1361

Ligaba A, Dreyer I, Margaryan A, Schneider DJ, Kochian L, Piñeros M (2013) Functional, structural and phylogenetic analysis of domains underlying the Al-sensitivity of the aluminium-activated malate/anion transporter, TaALMT1. Plant J 76: 766-780

Ligaba A, Katsuhara M, Ryan PR, Shibasaka M, Matsumoto H (2006) The *BnALMT1* and *BnALMT2* genes from rape encode aluminum-activated malate transporters that enhance the aluminum resistance of plant cells. Plant Physiol 142: 1294-1303

Ligaba A, Kochian L, Pineros M (2009) Phosphorylation at S384 regulates the activity of the TaALMT1 malate transporter that underlies aluminum resistance in wheat. Plant J 60: 411-423

Ligaba A, Maron L, Shaff J, Kochian L, Pineros M (2012) Maize ZmALMT2 is a root anion transporter that mediates constitutive root malate efflux. Plant Cell Environ 35: 1185-1200

Ligaba A, Shen H, Shibata K, Yamamoto Y, Tanakamaru S, Matsumoto H (2004) The role of phosphorus in aluminium-induced citrate and malate exudation from rape (*Brassica napus*). Physiol Plant 120: 575-584

Ma B, Liao L, Zheng H, Chen J, Wu B, Ogutu C, Li S, Korban SS, Han Y (2015) Genes encoding aluminum-activated malate transporter II and their association with fruit acidity in apple. The Plant Genome 8:3

Ma JF, Ryan PR, Delhaize E (2001) Aluminium tolerance in plants and the complexing role of organic acids. Trends Plant Sci 6: 273-278

Ma JF, Taketa S, Yang ZM (2000) Aluminum tolerance genes on the short arm of chromosome 3R are linked to organic acid release in triticale. Plant Physiol 122: 687-694

Mariano ED, Jorge RA, Keltjens WG, Menossi M (2005) Metabolism and root exudation of organic acid anions under aluminium stress. Brazilian Journal of Plant Physiology 17: 157-172

Matos M, Camacho MV, Perez-Flores V, Pernaute B, Pinto-Carnide O, Benito C (2005) A new aluminum tolerance gene located on rye chromosome arm 7RS. TAG 111: 360-369

Maurino VG, Engqvist MKM (2015) 2-Hydroxy acids in plant metabolism. The Arabidopsis Book / American Society of Plant Biologists 13: e0182

Meyer S, De Angeli A, Fernie AR, Martinoia E (2010) Intra- and extra-cellular excretion of carboxylates. Trends Plant Sci15: 40-47

Meyer S, Mumm P, Imes D, Endler A, Weder B, Al-Rasheid KAS, Geiger D, Marten I, Martinoia E, Hedrich R (2010) AtALMT12 represents an R-type anion channel required for stomatal movement in Arabidopsis guard cells. Plant J 63: 1054-1062

Meyer S, Scholz-Starke J, De Angeli A, Kovermann P, Burla B, Gambale F, Martinoia E (2011) Malate transport by the vacuolar AtALMT6 channel in guard cells is subject to multiple regulation. Plant J 67: 247-257

Misra BB, Acharya BR, Granot D, Assmann SM, Chen S (2015) The guard cell metabolome: functions in stomatal movement and global food security. Front Plant Sci 6: 334

Motoda H, Sasaki T, Kano Y, Ryan PR, Delhaize E, Matsumoto H, Yamamoto Y (2007) The membrane topology of ALMT1, an aluminum-activated malate transport protein in wheat (*Triticum aestivum*). Plant Signal Behav 2: 467-472

Mumm P, Imes D, Martinoia E, Al-Rasheid KA, Geiger D, Marten I, Hedrich R (2013) C-terminus-mediated voltage gating of Arabidopsis guard cell anion channel QUAC1. Mol Plant 6: 1550-1563

Osawa H, Matsumoto H (2001) Possible involvement of protein phosphorylation in aluminum-responsive malate efflux from wheat root apex. Plant Physiol 126: 411-420

Pineros MA, Cancado GMA, Kochian LV (2008a) Novel properties of the wheat aluminum tolerance organic acid transporter (TaALMT1) revealed by electrophysiological characterization in *Xenopus* oocytes: functional and structural implications. Plant Physiol 147: 2131-2146

Pineros MA, Cancado GMA, Maron LG, Lyi SM, Menossi M, Kochian LV (2008b) Not all ALMT1-type transporters mediate aluminum-activated organic acid responses: the case of *ZmALMT1* - an anion-selective transporter. Plant J 53: 352-367

Punta M, Coggill PC, Eberhardt RY, Mistry J, Tate J, Boursnell C, Pang N, Forslund K, Ceric G, Clements J, Heger A, Holm L, Sonnhammer EL, Eddy SR, Bateman A, Finn RD (2012) The Pfam protein families database. Nucl Acids Res 40: 290-301

Raman H, Zhang KR, Cakir M, Appels R, Garvin DF, Maron LG, Kochian LV, Moroni JS, Raman R, Imtiaz M, Drake-Brockman F, Waters I, Martin P, Sasaki T, Yamamoto Y, Matsumoto H, Hebb DM, Delhaize E, Ryan PR (2005) Molecular characterization and mapping of *ALMT1*, the aluminium-tolerance gene of bread wheat (*Triticum aestivum* L.). Genome 48: 781-791

Ramesh SA, Tyerman SD, Xu B, Bose J, Kaur S, Conn V, Domingos P, Ullah S, Wege S, Shabala S, Feijo JA, Ryan PR, Gillham M (2015) GABA signalling modulates plant growth by directly regulating the activity of plant-specific anion transporters. Nature Communications 6: 7879

Roberts SK (2006) Plasma membrane anion channels in higher plants and their putative functions in roots. New phytol 169: 647–666

Roelfsema MR, Hedrich R, Geiger D (2012) Anion channels: master switches of stress responses. Trends Plant Sci 17: 221-229

Rudrappa T, Czymmek KJ, Pare PW, Bais HP (2008) Root-secreted malic acid recruits beneficial soil bacteria. Plant Physiol 148: 1547-1556

Ryan PR, Delhaize E (2001) Function and mechanism of organic anion exudation from plant roots. Annu Rev Plant Physiol 52: 527-560

Ryan PR, Delhaize E (2010) The convergent evolution of aluminium resistance in plants exploits a convenient currency. Funct Plant Biol 37: 275-284

Ryan PR, Delhaize E, Jones DL (2001) Function and mechanism of organic anion exudation from plant roots. Annu Rev Plant Physiol 52: 527-560

Ryan PR, Raman H, Gupta S, Sasaki T, Yamamoto Y, Delhaize E (2010) The multiple origins of aluminium resistance in hexaploid wheat include *Aegilops tauschii* and more recent *cis* mutations to *TaALMT1*. Plant J 64: 446-455

Ryan PR, Shaff JE, Kochian LV (1992) Aluminum toxicity in roots: correlation among ionic currents, ion fluxes, and root elongation in aluminum-sensitive and aluminum-tolerant wheat cultivars. Plant Physiol 99: 1193-1200

Ryan PR, Tyerman SD, Sasaki T, Furuichi T, Yamamoto Y, Zhang WH, Delhaize E (2011) The identification of aluminium-resistance genes provides opportunities for enhancing crop production on acid soils. J Exp Bot 62: 9-20

Sasaki T, Mori IC, Furuichi T, Munemasa S, Toyooka K, Matsuoka K, Murata Y, Yamamoto Y (2010) Closing plant stomata requires a homolog of an aluminum-activated malate transporter. Plant Cell Physiol 51: 354-365

Sasaki T, Ryan PR, Delhaize E, Hebb DM, Ogihara Y, Kawaura K, Noda K, Kojima T, Toyoda A, Matsumoto H, Yamamoto Y (2006) Sequence upstream of the wheat (*Triticum aestivum* L.) *ALMT1* gene and its relationship to aluminum resistance. Plant Cell Physiol 47: 1343-1354

Sasaki T, Tsuchiya Y, Ariyoshi M, Ryan PR, Furuichi T, Yamamoto Y (2014) A domain-based approach for analyzing the function of aluminum-activated malate transporters from wheat (*Triticum aestivum*) and *Arabidopsis thaliana* in *Xenopus* oocytes. Plant Cell Physiol 55: 2126-2138

Sasaki T, Yamamoto Y, Ezaki B, Katsuhara M, Ahn SJ, Ryan PR, Delhaize E, Matsumoto H (2004) A wheat gene encoding an aluminum-activated malate transporter. Plant J 37: 645-653

Schroeder JI, Keller BU (1992) Two types of anion channel currents in guard cells with distinct voltage regulation. PNAS 89: 5025-5029

Tamura K, Peterson D, Peterson N, Stecher G, Nei M, Kumar S (2011) MEGA5: molecular evolutionary genetics analysis using maximum likelihood, evolutionary distance, and maximum parsimony methods. Mol Bio and Evo 28: 2731-2739

Xu KN, Wang AD, Brown S (2012) Genetic characterization of the *Ma* locus with pH and titratable acidity in apple. Molecular Breeding 30: 899-912

Xu M, Gruber BD, Delhaize E, White RG, James RA, You J, Yang Z, Ryan PR (2015) The barley anion channel, HvALMT1, has multiple roles in guard cell physiology and grain metabolism. Physiol Plant 153: 183-193

Yamaguchi M, Sasaki T, Sivaguru M, Yamamoto Y, Osawa H, Ahn SJ, Matsumoto H (2005) Evidence for the plasma membrane localization of Al-activated malate transporter (ALMT1). Plant Cell Physiol 46: 812-816

Yang LT, Jiang HX, Qi YP, Chen LS (2012) Differential expression of genes involved in alternative glycolytic pathways, phosphorus scavenging and recycling in response to aluminum and phosphorus interactions in Citrus roots. Mol Bio Rep 39: 6353-6366

Zhang J, Baetz U, Krugel U, Martinoia E, De Angeli A (2013) Identification of a probable pore-forming domain in the multimeric vacuolar anion channel AtALMT9. Plant Physiol 163: 830-843

Zhang J, Martinoia E, De Angeli A (2014) Cytosolic nucleotides block and regulate the Arabidopsis vacuolar anion channel AtALMT9. J Biol Chem 289: 25581-25589

Zhang WH, Ryan PR, Sasaki T, Yamamoto Y, Sullivan W, Tyerman SD (2008) Characterization of the TaALMT1 protein as an Al^{3+}-activated anion channel in transformed tobacco (*Nicotiana tabacum* L.) cells. Plant Cell Physiol 49: 1316-1330

CHAPTER 2
General materials and methods

2.1 Plant material and growth conditions

2.1.1 Plant material and seed germination

The plant material used in this thesis is rice (*Oryza sativa*) cultivar *Nipponbare*. The rice seeds were obtained from the collection at CSIRO (Commonwealth Scientific and Industrial Research Organization) Agricultural Flagship in Canberra, Australia.

Rice seeds were surface sterilized by 50% bleach (White King^{TM}) for 15 min, rinsed thoroughly in water and pre-germinated under dark on ½ MS media for two days in the 28 ℃ growth room. Germinated seedlings then grown under continuous light for five days and moved into hydroponic tanks or soil.

2.1.2 Plant growth conditions

Hydroponic experiments werewere performed in 10 L tanks with ½ strength Kimura B nutrient solution, with pH adjusted to 5.6. The nutrient solution contains a final concentration of 250 μM KNO_3, 250 μM $CaCl_2$, 250 μM NH_4NO_3, 75 μM $MgSO_4$, 10 μM KH_2PO_4, 0.4 μM EDTA:Fe, 5.5 μM H_3BO_3, 1 μM $MnCl_2$, 0.175 μM $ZnCl_2$ and 0.1 μM $CuCl_2$. The pH was adjusted to 5.6-5.7 and the solution was changed every three days. Soil experiments were performed with Φ8.5 cm ×20 cm pots with “rice soil” (standard mix from CSIRO potting sheds) under water-flooded conditions. Plants were maintained in a 28/22 ℃ glasshouse under normal day/night cycle.

2.2 Online sequence resources

The ALMT gene sequences in rice were obtained from The National Centre for Biotechnology Information (NCBI, http://www.ncbi.nlm.nih.gov/). Nine members of the

rice ALMT gene family were gathered with the references NM_001048968.1 (*OsALMT1*), NM_001050715.1 (*OsALMT2*), NM_001054246.1 (*OsALMT3*), XM_467616.1 (*OsALMT4*), NM_001059303.1 (*OsALMT5*), NM_001060121.1 (*OsALMT6*), NM_001063889.1 (*OsALMT7*), NM_001064078.1 (*OsALMT8*) and NM_001071993.1 (*OsALMT9*). These sequences were further confirmed from the Rice Genome Annotation Project (http://rice.plantbiology.msu.edu/index.shtml) with the reference of LOC_Os01g12210 (*OsALMT1*), LOC_Os01g53570 (*OsALMT2*), LOC_Os02g45160 (*OsALMT3*), LOC_Os02g49790 (*OsALMT4*), LOC_Os04g34010 (*OsALMT5*), LOC_Os04g47930 (*OsALMT6*), LOC_Os06g15779 (*OsALMT7*), LOC_Os06g22600 (*OsALMT8*) and LOC_Os10g42180 (*OsALMT9*).

The 4000 bp OsALMT1 upstream sequence was also found form NCBI database and the 2496 bp OsALMT1 promoter region which is next to the OsALMT1 initiation codon was selected for further experiment.

2.3 Primer design

The primers used in this thesis were designed by Vector NTI® 11.5 programme and further confirmed by OligoAnalyzer 3.1 (http://sg.idtdna.com/calc/analyzer). All the primers used in this thesis are listed in **Table 2.1**.

2.4 DNA and RNA extractions

2.4.1 Standard genomic DNA (gDNA) extraction

Genomic DNA was isolated from 20 days old soil grown wild type rice (cv. *Nipponbare*) by DNeasy® Plant Mini Kit, QIAGEN. Leaf tissue (~100 mg) was placed in 1.5 ml Eppendorf tube and frozen in liquid nitrogen. The sample was grounded into powder with a sterile plastic stick. Extraction buffer (400 µl Buffer AP1 and 4 µl RNase A stock solution) was added at 100 mg/ml to the sample and vortexed vigorously. The mixture was incubated at 65 ℃ for 10 min by inverting the tube. Buffer AP2 (130 µl) was added to the lysate, mixed and incubated for 5 min on ice. The lysate was centrifuged for 5 min at

14,000 rpm. The filtrate was pipetted into the QIAshredder Mini spin column placed in a 2 ml collection tube and centrifuged for 2 min at 14,000 rpm. The flow-through fraction was transferred into a new tube without disturbing the cell-debris pellet and 1.5 volumes of Buffer AP3/E was added to the cleared lysate. The lysate mixture (650 µl including any precipitate that may have formed) was pipetted into the DNeasy Mini spin column placed in a 2 ml collection tube and centrifuged for 1 min at 8,000 rpm. The DNeasy Mini spin column was placed into a new 2 ml collection tube, washed by added 500 µl Buffer AW and centrifuged for 1 min at 8,000 rpm twice. The DNeasy Mini spin column was transferred to a 1.5 ml microcentrifuge tube and 100 µl Buffer AE was pipetted directly onto the DNeasy membrane. The column was incubated for 5 min at room temperature (15-25 ℃), and then centrifuged for 1 min at 8,000 rpm. The DNA was to use.

2.4.2 High throughput DNA isolation for genotype test

High throughput DNA was isolated by a Nimbus liquid handing robot. Leaf tissue (5 cm lengths) was collected and placed into a deep-well microtiter plate. The plate was frozen at -80 ℃ for 30 min and frozen dry overnight. One SDS and ethanol washed stainless steel ball bearing was added to each well. The plate was sealed with 8-lid strips and shaken on the QIAGEN shaker at a frequency of 23/second for 2 min each side. The plate was spun by a centrifuge for 15 min at 3,000 rpm to settle contents before opening the lids, then 375 µl extraction buffer (0.1 M Tris-HCl, pH 8.0; 0.05 M EDTA, pH 8.0 and 1.25% SDS, pre-warmed to 65 ℃) was added to each well and incubated at 65 ℃ for one hour in an oven. The plate was cooled in a fridge to room temperature and 187 µl 6 M ammonium acetate (stored at 4 ℃) was added to each well. The lysate was mixed by inverting the plate and left in the fridge for 30 min. The plate was centrifuged for 30 min at 3000 rpm and 340 µl supernatant was recovered into a new deep well microtiter plant containing 220 µl isopropanol. DNA was allowed to precipitate for 5 min at room temperature. The plate was centrifuged for 30 min at 3,000 rpm and the supernatant was poured off. Then 70% ethanol (320 µl) was added to the plate and centrifuged for 30 min at 3,000 rpm. Supernatant was poured off and DNA was resuspended in 225 µl dH_2O and left overnight at 4 ℃ for the DNA pellet to dissolve. The plate was centrifuged for 20 min at 3,000 rpm and 150 µl of supernatant was transferred to a new microtiter plate. The DNA was ready to use.

Table 2.1 Primers used in the experiments

Primer No.	Details	Sequence
PRR-101	Fwd: Amplify PCR fragment for expression of OsALMT1	5’-GTATAAGGATTGACATTTGCC-3’
PRR-102	Rev: Amplify PCR fragment for expression of OsALMT1	5’-GCCACCTGAATAACAACTAC-3’
PRR-103	Fwd: Amplify PCR fragment for expression of OsALMT1	5’-GTTCTTCGCCACTGTGCCT-3’
PRR-104	Rev: Amplify PCR fragment for expression of OsALMT1	5’-GAATGTTGCAGACGCTCG-3’
PRR-105	Fwd: Amplify PCR fragment for expression of OsALMT2	5’-GAGGCGATGACCGAAGCGAGC-3’
PRR-106	Rev: Amplify PCR fragment for expression of OsALMT2	5’-CAACTCCGGCCACCATGCTC-3’
PRR-107	Fwd: Amplify PCR fragment for expression of OsALMT6	5’-TCGCGGGAGAGGAGGAGG-3’
PRR-108	Rev: Amplify PCR fragment for expression of OsALMT6	5’-GATCGCTCACGGTTTGCAG-3’
PRR-109	Fwd: Amplify PCR fragment for expression of OsALMT3	5’-CGTCATCAGAGGCAGAGCAGC-3’
PRR-110	Rev: Amplify PCR fragment for expression of OsALMT3	5’-GTTGGAGTTGGGTACGGGCA-3’
PRR-111	Fwd: Amplify PCR fragment for expression of OsALMT8	5’-GGTGGGACAGCTGGTGAAG-3’
PRR-112	Rev: Amplify PCR fragment for expression of OsALMT8	5’- GCGTGGGCCGTGAAGTCC-3’
PRR-113	Fwd: Amplify PCR fragment for expression of OsALMT7	5’- GGTGGGTGGAAGGAGGGC-3’
PRR-114	Rev: Amplify PCR fragment for expression of OsALMT7	5’- CTTCCTCCAGCTTTCCCAG-3’
PRR-115	Fwd: Amplify PCR fragment for expression of OsALMT4	5’-GGCAAGCTCTCATCAGGCG-3’

Primer No.	Details	Sequence
PRR-116	Rev: Amplify PCR fragment for expression of OsALMT4	5’- GCTCTCGTAGGTTCTCGCC-3’
PRR-117	Fwd: Amplify whole length cDNA for OsALMT1	5’-GCGGATCCATGAATGGAAAGAAGGGT-3’
PRR-118	Fwd: Amplify whole length cDNA for OsALMT1	5’-GGGGTACCATGAATGGAAAGAAGGG-3’
PRR-119	Rev: Amplify whole length cDNA for OsALMT1	5’-CCGGAATTCTTAGTTTGCAATCTGCTG-3’
PRR-120	pUC/M13 Forward Primer	5 ´-CGCCAGGGTTTTCCCAGTCACGAC-3 ´
PRR-121	pUC/M13 Reverse Primer	5 ´-TCACACAGGAAACAGCTATGAC-3 ´
PRR-122	Fwd: Amplify OsALMT1 Promoter	5’-TGCCCGGGACCTGTTACTACTTGTTATGC-3’
PRR-123	Rev: Amplify OsALMT1 Promoter	5’-CTGGGTACCTCTCTAACTTGCGGTCTCTT-3’
PRR124	Middle primer for OsALMT1 promoter sequencing	5’-GTTCCTACTTTGGGTGCGACAT-3’
PRR125	Middle primer for OsALMT1 promoter sequencing	5’AGTTTTGTGATTCCTCTGGT-3’
PRR-128	Fwd: primer for OsALMT1 Pro location	5’-CCTTAATTAAACCTGTTACTACTTGTTATGC-3’
PRR-129	Rev: primer for OsALMT1 Pro location	5’-TTGGCGCGCCTCTCTAACTTGCGGTCTCTT-3’
PRR-130	Reverse primer for ALMT1::GFP	5’-GGTGAACAGCTCCTCGCCCTTGCTCACCAT GTTTGCAATCTGCTGCTTGAAC-3’
PRR-131	Forward primer for ALMT1::GFP	5’- TGGCAAGGTTCAAGCAGCAGATTGCAAAC ATGGTGAGCAAGGGCGAGGAGCTGTTCACC-3’
PRR-132	Reverse primer for GFP	5’-CGGAATTCTTACTTGTACAGCTCGTC-3’
PRR-133	Forward primer for GFP	5’-GCGGATCCATGGTGAGCAAGGGCGAGG-3’

Primer No.	Details	Sequence
PRR-134	Reverse primer for GFP::ALMT1	5’-TCCTTATACTACCCTTCTTTCCATTCAT CTTGTACAGCTCGTCCATGCCG-3’
PRR-135	Forward primer for GFP::ALMT1	5’-ATCACTCACGGCATGGACGAGCTGTACAAG ATGAATGGAAAGAAGGGTAGT-3’
PRR-136	Forward primer for OsALMT1 RNAi	5’-GGATCCGGTACCCAAACTAGCTTAC-3’
PRR-137	Reverse primer for OsALMT1 RNAi	5'- CCCGGGACTAGTCATCATCTCATGG -3'
PRR-138	Forward primer for pART-OsALMT1::GFP	5’-GAATTCATGAATGGAAAGAAGGGT-3’
PRR-139	Reverse primer for pART-OsALMT1::GFP	5’-GGATCCTTACTTGTACAGCTCGTC-3’
PRR-140	Forward primer for pART-GFP::OsALMT1	5’-GAATTCATGGTGAGCAAGGGCGAG-3’
PRR-141	Reverse primer for pART-GFP::OsALMT1	5’-GGATCCTTAGTTTGCAATCTGCT-3’
PRR-142	Forward primer for OsALMT1 qRT-PCR	5’-CCTTAGAAGAGTGTGTCAAGAAG-3’
PRR-143	Reverse primer for OsALMT1 qRT-PCR	5’-CCATTTAGCAGAGTTCGCCAG-3’
PRR-80F	Forward primer for genotype identification	5’-TGCAGCATCTATTCATATGCTCT-3’
PRR-80R	Reverse primer for genotype identification	5’-AACACCAAACAACAGGGTGAG-3’
UbiP	Forward primer for sequencing pUbi-OsALMT1	5’-CTTGATATACTTGGATGATGG-3’
TM/pWUbi	Reverse primer for sequencing pUbi-OsALMT1	5’-GTGTTCTAAGCTAGCCTGG-3’
35SP	Forward primer on 35S promoter	5’-TATCCTTCGCAAGACCCTTCCT-3’
TM ocs	Reverse primer on ocs terminator	5’- GGATCTGAGCTACACATGCTC-3’

Primer No.	Details	Sequence
OsGAPDHF	Forward primer for qRT-PCR as a reference	5'-GTTGAGGGTTTGATGACCAC-3'
OsGAPDHR	Reverse primer for qRT-PCR as a reference	5'-TCAGACTCCTCCTTGATAGC-3'
OseEF-1α F	Forward primer for qRT-PCR as a reference	5'-TTTCACTCTTGGTGTGAAGCAGAT-3'
OseEF-1α R	Reverse primer for qRT-PCR as a reference	5'-GACTTCCTTCACGATTTCATCGTAA-3'
Oligo dT	Primer for cDNA synthesis	5'-TTTTTTTTTTTTTTTTTTTTVN-3'

2.4.3 RNA extraction and 1st strand cDNA synthesis

Total RNA from leaf and root tissues were extracted by using the RNeasy® Plant Mini Kit, QIAGEN. Residual DNA was removed by on column DNase digestion by using the RNase-Free DNase Set, QIAGEN. Leaf tissue (~100 mg) was put into 1.5 ml Eppendorf tube and frozen in liquid nitrogen. The sample was grounded into a powder with a sterile plastic stick. Buffer RLT (450 µl with 40 µl/mL 1 M Dithiothreitol (DTT)) was added to the powdered tissue and vortexed vigorously. The lysate was transferred to a QIAshredder spin column placed in a 2 ml collection tube, and centrifuged for 2 min at full speed. The supernatant of the flow-through was carefully transferred to a new microcentrifuge tube without disturbing the cell-debris pellet in the collection tube. Ethanol (96–100%) of 0.5 volume of the flow-through was added to the cleared lysate and mixed immediately by pipetting. The sample, including any precipitate that may have formed, was transferred to an RNeasy spin column placed in a 2 ml collection tube. The lid was gently closed, and centrifuged for 15 s at 10,000 rpm with the flow-through discarded. Buffer RW1 (350 µl) was added to the RNeasy spin column. The lid was gently closed, and centrifuged for 15 s at 10,000 rpm to wash the spin column membrane with the flow-through discarded. The DNase I incubation mix (10 µl DNase I stock solution to 70 µl Buffer RDD) was directly added to the RNeasy spin column membrane, and placed on the benchtop for 15 min at room temperature. Buffer RW1 (350 µl) was added to the RNeasy spin column. The lid was gently closed, and centrifuged for 15 s at 10,000 rpm with the flow-through discarded. Buffer RPE (500 µl) was added to the RNeasy spin column. The lid was gently closed, and centrifuged for 15 s at 10,000 rpm to wash the spin column membrane with the flow-through discarded. Another 500 µl Buffer RPE was added to the RNeasy spin column and repeat the centrifuge steps. The RNeasy spin column was placed in a new 2 ml collection tube, and the old collection tube was discarded with the flow-through. The lid was gently closed, and centrifuged at full speed for 1 min. The RNeasy spin column was placed in a new 1.5 ml collection tube and 50 µl RNase-free water was directly added to the spin column membrane. The lid was gently closed, and centrifuged for 1 min at 10,000 rpm to elute the RNA. The RNA was ready for next step.

First strand cDNA was synthesised by SuperScript® III Reverse Transcriptase, Invitrogen™. Total RNA (1 µg) and oligo$(dT)_{20}$ (1 µl, 0.5 µg/µl) were added to a nuclease-free microcentrifuge tube, vortexed and spun briefly. The sample was incubated at 70 ℃ for 10

min and incubated on ice for at least 1 minute. The content was collected by brief centrifugation and 4 µl 5X First-Strand Buffer, 2 µl 0.1 M DTT, 1 µl 10 mM dNTP Mix (10 mM each dATP, dGTP, dCTP and dTTP at neutral pH) and 0.5 µl of SuperScript™ III RT (200 units/µl) were added. The content was immediately incubated at 42 ℃ for one hour in a PCR machine. RNase H (0.25 µl, 4 U/µl) was added to the tube and incubated at 37 ℃ for 30 min to remove the redundant RNA.

2.5 PCR reactions

2.5.1 Standard PCR

Standard PCR was performed by the flowing system by using HotStarTaq®, QIAGEN and C1000 Touch™ Thermal Cycler, BIO-RAD. The reaction was as follows: PCR template (50 ng/µl) 1µl, HotStarTaq Master Mix (2x, 1 kb/min) 10 µl, Forward primer (10 mM) 1 µl, Reverse primer (10 mM) 1 µl, and they were made up to 20 µl by adding miliQ water. The PCR program was as follows: 95 ℃ for 15min, 35 cycles of 95 ℃ for 30 s, annealing temperature for 10 s and 72 ℃ for X min (X based on the length of PCR product), 72 ℃ for 10 min.

2.5.2 Proof-reading PCR

Proof-reading PCR was performed by using Phusion High-Fidelity DNA Polymerase, Thermo Scientific and C1000 Touch™ Thermal Cycler, BIO-RAD. The reaction was as follows: PCR template (50 ng/µl) 2 µl, Phusion GC buffer (5X) 10 µl, 10 mM dNTP 1 µl, Forward primer (10 mM) 1 µl, Reverse primer (10 mM) 1 µl, Phusion DNA Polymerase 0.5 µl (15-30 s/kb), DMSO 1.5 µl and they were made up to 50 µl by adding miliQ water. The PCR program was as follows: 98 ℃ for 30 s, 30 cycles of 98 ℃ for 30 s, annealing temperature for 10 s and 72 ℃ for X min (X based on the length of PCR product), 72 ℃ for 10 min.

If the PCR product required a ligation step to the pGEM®-T Easy Vector, an adenine needed to be added to the end before the ligation. denine reaction was added as follows:

Pure PCR product 30 µl, 10 mM dNTP 1 µl, Taq DNA Polymerase Buffer (10X) 3.5 µl and Taq DNA Polymerase 0.5 µl. The mixture was incubated on a PCR machine at 72 ℃ for 15 min.

2.5.3 Quantitative reverse transcription PCR (qRT-PCR)

qRT-PCR was performed by using SsoAdvanced™ SYBR® Green Supermix, BIO-RAD and CFX96 Touch™ Real-Time PCR Detection System, BIO-RAD. The reaction was as follows: PCR template (20 ng/µl) 1 µl, SsoAdvanced™ SYBR® Green Supermix 5 µl, Forward primer (10 mM) 0.5 µl, Reverse primer (10 mM) 0.5 µl, they were made up to 10 µl by adding miliQ water. The PCR program was as follows: 95 ℃ for 3 min, 40 cycles of 95 ℃ for 10 s, annealing temperature for 20 s and 68 ℃ for 10 s (+ plate read), 60 -95 ℃ (with increment 0.5 ℃) for 5 s (+plate read).

The final result was analysed by CFX Manager™ Software, BIO-RAD. Multiple reference genes expression was normalized by BIO-RAD CFX Manager™ Software as described by the user manual. Relative gene expression was calculated by the $2^{-\Delta\Delta CT}$ method as described by Livak and Schmittgen (2001).

2.5.4 PCR products and gel purification

PCR product and gel were purified by ISOLATE II PCR and Gel Kit, Bioline. For isolation of PCR products, the final volume was adjusted to 100 µl with water and one volume of sample was mixed with two volumes of Binding Buffer CB. The ISOLATE II PCR and Gel Column was placed in a 2 ml Collection Tube and the sample was loaded on to the membrane. The column was centrifuged 30 s at 10,000 rpm and the flow-through was discarded. Wash Buffer CW (700 µl) was added to the ISOLATE II PCR and Gel Column and centrifuged 30 s at 10,000 rpm. The flow-through was discarded and the column was put back into collection tube, centrifuged 1 min at 10,000 rpm to remove residual ethanol. The ISOLATE II PCR and Gel Column was placed in a 1.5 ml microcentrifuge tube and 30 µl Elution Buffer C was directly added onto the silica

membrane. This was then incubated at room temperature for 1 min and centrifuged 1min at 10,000 rpm to elute DNA.

To extract DNA from an agarose gel, the DNA fragment was excised from the gel by using a clean scalpel. Binding Buffer CB (200 µl) was added per 100 mg of 2 % agarose gel and the sample was incubated at 50 ℃ for 5-10 min. The sample was vortexed briefly every two to three minutes until the gel slice was completely dissolved. An ISOLATE II PCR and Gel Column was placed in a 2 ml Collection Tube and the sample was loaded onto the membrane. The column was centrifuged 30 s at 10,000 rpm and the flow-through was discarded. Wash Buffer CW (700 µl) was added to ISOLATE II PCR and Gel Column and centrifuged 30 s at 10,000 rpm. The column was centrifuged 1 min at 10,000 rpm to remove residual ethanol. The ISOLATE II PCR and Gel Column was placed in a new 1.5 ml microcentrifuge tube and 30 µl Elution Buffer C was added directly onto the silica membrane. The column was incubated at room temperature for 1 min and centrifuged 1 min at 10,000 rpm to elute DNA.

2.5.5 Fusion PCR

Fusion PCRs were used to overlap two primary PCR products with two set of primers. In step one, the GOI and GFP was amplified separately with primers with long tails (about 20 bp) at the fusion side. These PCR steps were the same as proof-reading PCR described above. Gel DNAs from each PCR were isolated by ISOLATE II PCR and Gel Kit, Bioline (as above).

The GOI and GFP were fused together by two steps by PCR: GOI (20 ng/µl) 2.5 µl, GFP (20 ng/µl) 2.5 µl, Phusion GC buffer (5X) 10 µl, 5 mM dNTP 2.5 µl, DMSO 1.5 µl, Phusion DNA Polymerase (15-30 s/kb) 0.5 µl and they were made up to 50 µl by adding miliQ water. The PCR program was as follows: 98 ℃ for 1 min, five cycles of 98 ℃ for 20 s, annealing temperature for 30 s and 72 ℃ for X min (X based on the length of PCR product), 72 ℃ for 10 min. After five cycles, forward primer of the front fragment and reverse primer of the back fragment (10 mM, 2 µl each) were added into the reaction for 30 more cycles. The PCR program was as follows: 98 ℃ for 1 min, 30 cycles of 98 ℃ for 20

s, annealing temperature for 30 s and 72 ℃ for X min (X based on the length of PCR product), 72 ℃ for 10 min.

2.6 Cloning

2.6.1 Preparation of *E. coli* cells for electroporation

A fresh colony of DH5α was inoculated in 5 ml of L-broth medium (LB, 1% Peptone 140, 0.5% Yeast Extract, 0.5% sodium chloride) in a 50 ml sterile Falcon tube. They were vigorously shaken at 180 rpm overnight at 37 ℃. Cells from above (2.5 ml) were applied into 250 ml of LB medium in a 1 L flask. The cells were grown at 37 ℃ shaking at 300 rpm to an OD_{600} of approximately 0.5-0.7. The cells were chilled on ice for about 20 min. For all subsequent steps, the cells were kept as close to 0 ℃ as possible (in an ice/water bath) and all containers were chilled in ice before adding cells. To harvest, the cells were transferred to a cold centrifuge bottle and spun at 3,000 rpm for 15 min at 4 ℃. The pellet was gently resuspended in 250 ml of ice-cold 10% glycerol and centrifuge at 3000 rpm for 15 min at 4 ℃. The pellet was gently resuspended in another 250 ml of ice-cold 10% glycerol and centrifuged at 3,000 rpm for 15 min at 4 ℃. The pellet was resuspended in 10 ml of ice-cold 10% glycerol, transferred to a 50 ml sterile Falcon tube and centrifuged at 3,000 rpm for 15 min at 4 ℃. The cell pellet was resuspended in a final volume of 1-2 ml of ice-cold 10% glycerol. The cell concentration was about 1-3 x 10^{10} cells/ml. This suspension was frozen in aliquots of 50 µl on dry ice and stored at -70 ℃.

2.6.2 Electroporation

An aliquot of competent cells was thawed on ice and then 1 µl of ligation reaction was added to the competent cells. They were mixed quickly and placed on ice for 10 min. The MicroPulser ((MicropulserTM BioRad, USA) was set to “Ec1”. The mixture of cells and DNA was transferred to a cold electroporation cuvette and the suspension was tapped to the bottom. The cuvette was placed in the chamber slide and the slide was pushed into the chamber until the cuvette was seated between the contacts in the base of the chamber. The cuvette was pulsed once and the sample was electroporated at a 2.4 kV discharge voltage.

The cuvette was removed from the chamber and 1 ml of SOC medium (2% tryptone, 0.5% yeast extract, 10 mM NaCl, 2.5 mM KCl, 10 mM $MgCl_2$, 10 mM $MgSO_4$, and 20 mM glucose) was immediately added to the cuvette. The cells were resuspended with a pipette quickly but gently and transferred to a 1.5 ml microcentrifuge tube and incubated at 37 ℃ (for bacteria) or 28 ℃ (for agro-bacteria) for one hour at 225 rpm. The cells were transferred to plate with selective LB medium for further growth.

2.6.3 Plasmid isolation

Plasmid was extracted by using the Isolate Plasmid Mini Kit, BIOLINE. A saturated high copy E. *coli* LB culture (2 ml) or low copy E. *coli* or agro-bacteria LB culture cells (5 ml) were pelleted by centrifuging at 12,000 rpm for 30 s. The supernatant was discarded and the liquid was removed as much as possible. Resuspension Buffer P1 (250 μl) was added to the cell pellet and resuspended completely by vortexing. Lysis Buffer P2 (250 μl) was added to the suspension and mixed gently by inverting the tube six to eight times. The lysate was incubated at room temperature until it appeared clear and 300 μl Neutralization Buffer P3 was added. The lysate was mixed thoroughly by inverting the tube six to eight times and centrifuged for five minute at 12,000 rpm. For each preparation, 750 μl of the clarified sample was transferred on to the ISOLATE II Plasmid Mini Spin Column which was placed in a Collection Tube. The column was centrifuged for one minute at 12,000 rpm and the follow-through was discarded. This was repeated with the remaining clarified sample supernatant. Wash Buffer PW1 (500 μl) was added to the column and centrifuged for one minute at 12,000 rpm. Wash Buffer PW2 (600 μl) was added to the column and centrifuged for one minute at 12,000 rpm. The flow-through was discarded and the column was centrifuged for two minutes at 12,000 rpm to remove residual ethanol. The ISOLATE II Plasmid Mini Spin Column was placed in a 1.5 ml microcentrifuge tube and 50 μl Elution Buffer P was added directly on to the silica membrane. The column was incubated at room temperature for one minute and the plasmid DNA was eluted by centrifugation for one minute at 12,000 rpm.

2.6.4 Enzyme digestion reaction

Plasmid was digested by different restriction enzymes and their corresponding buffers which target to various enzyme sites matched to the vectors. The reaction was as follows: Plasmid (50 ng/uL) 5 μl, NEB Buffer (10X) 2 μl, BSA (10X) 2 μl, Enzyme I 1 μl, Enzyme II 1 μl and they were made up to 20 μl by adding miliQ water. The mixture was incubated at 37 ℃ for three hours.

2.6.5 Ligation reaction

Ligation to pGEM®-T Easy Vector was performed by pGEM®-T Easy Vector System I (Promega) with the following system: 2X Rapid Ligation Buffer 5 μl, pGEM-T® Easy Vector (50 ng/μl) 0.3 μl, Insert DNA (50 ng/μl) 2 μl, T4 Ligase 0.5 μl and they were made up to 10 μl by adding miliQ water. The mixture was incubated at room temperature for four hours.

Normal ligation was performed by using T4 DNA Ligase (Thermo Fisher Scientific) with the following system: Insert Plasmid (20 ng/μl) 2 μl, Vector Plasmid eques to 3×insert plasmid concentration, T4 Ligase (5 U/μl) 0.5 μl, 10X T4 Buffer 1 μl and they were made up to 10 μl by adding miliQ water. The mixture was incubated at 16 ℃ overnight.

If the plasmid was digested by single enzyme, a dephosphorylation needed to be done before the ligation by Antarctic Phosphatase (NEB). A 1/10 volume of 10X Antarctic Phosphatase Reaction Buffer was added to 1-5 μg of DNA cut with any restriction endonuclease in any buffer. Antarctic Phosphatase (1 μl, 5U/ μl) was added to the mixture. The mixture was incubated for 15 min at 37 ℃ for 5 ´extensions, 60 min for 3 ´extensions and heat inactivated (or as required to inactivate the restriction enzyme) for five minutes at 65 ℃.

2.7 Sequencing and sequence analysis

2.7.1 Sequencing

Sequencing was performed by the BigDye® Terminator v3.1 Cycle Sequencing Kit (Thermo Fisher Scientific) with the following system: BigDye® Terminator 1 µl, BigDye Sequencing Buffer (5X) 2 µl, Primer (10 mM) 1 µl, Template 150 ng and they were made up to 10 µl by adding miliQ water. The sequencing PCR program was as follows: 96 ℃ for 4 min, 28 cycles of 96 ℃ for 30 s, 50 ℃ for 30 s and 60 ℃ for 4 min. BigDye was removed by DyeEx ™ 2.0 Spin Kit (QIAGEN). The sample was dried down in a vacuum centrifuge and processed by the Sanger Sequencing Service, ANU.

2.7.2 Sequence alignment and vector maps construction

Sequencing results were assembled and aligned by the Contig Assembly and Multi-Sequence Alignment programmes of the Vector NTI® Advance 11.3 Software. Gene sequence was further confirmed by the Basic Local Alignment Search Tool (BLAST®) programme from NCBI (http://blast.ncbi.nlm.nih.gov/Blast.cgi). Vector maps were constructed by the Vector NTI® Advance 11.3 Software based on the basic vector sequences.

2.8 Rice transformation

2.8.1 Callus inducement

The rice transformation method used in this study was modified from Toki et al. (2006). Wild type (WT, *cv. Nipponbare*) rice seeds were soaked in 70% ethanol for one minute and washed in sterile distilled water (SDW) for three times. The seeds were soaked in 50% bleach with 200 µl 0.01% Tween 20 for 15 min and washed in SDW five times. The seeds were soaked again in 50% bleach without Tween 20 for 15 min and washed in SDW five times. Sterile seeds were place on N6D media (**Table 2.2**) with 0.4% phytagel (25 seeds per plate) and cultured under 28 ℃ growth room with continuous lights (~600 µmol m^{-2} s^{-1}) for five to seven days.

2.8.2 Growth of Agrobacterium

Glycerol stocks (200 µl agrobacterium with target vector+200 µl 30% glycerol) was grown in 10 ml of LB medium at 28 ℃ with shaking for overnight. OD_{600} of the overnight broth was determined (it should be around OD_{600}=1.0) and diluted to OD_{600}=0.1 in AAM liquid medium (**Table 2.2**) with 1 µl of 1M Acetosyringone per 10 ml AAM. The broth was grown at 28 ℃ with shaking for two hours.

2.8.3 Inoculation of the callus

After five to seven days of callus growth, pre-cultured seeds were immersed in the Agrobacterium suspension by gently inverting the tube for 1.5 min. The seeds were blot dried with sterile filter paper to remove excess bacteria. A sterilized filter paper was moistened with 0.5 ml AAM medium and placed on 2N6-AS (**Table 2.2**) plate. The seeds were transferred onto the filter paper sitting on top of the 2N6-AS (20-22 seeds per plate). The plates were incubated at 24 ℃ in the dark for three days. After three days of co-culture in dark, the seeds were wash in SDW for five times and blot dried with sterile filter paper. The seeds were then transferred on N6D selection medium and placed under continuous light (~600 µmol m^{-2} s^{-1}) at 28 ℃ for 15-20 days.

2.8.4 Regeneration of plantlets

The calli were transfer to RE-Ⅲ medium (**Table 2.2**) plates and incubated under continuous light at 28 ℃ for two to three weeks. The plantlets were transferred to HF medium under continuous light at 28 ℃ for 10-14 days to grow bigger. The bigger plantlets were transferred to nutrient solution (as described in section **2.1.2**) and incubated under glasshouse condition (as described in section **2.1.2**) for 10-14 days. The plantlets then were transferred into soil and grown in phytotron (28 ℃ at daytime and 22 ℃ at night time with natural day/night cycle and light intensity) with water flooded condition. After few days, Fe-EDTA (2.4 g EDTA-Fe in 500 ml water with a drop of wetting agent or glycerol) was sprayed on the plants.

2.9 Statistical analyses

Statistical analysis was mostly performed with the SPSS™ statistical software package. Common tests were the t test and one-way analysis of variance (ANOVA) with the Tukey test. Where variances were non-homogeneous the data were transformed with either the square root function or the log function.

Results for gene expression (Chapter 6) are grouped into figures with a single control for convenience even though the figures sometimes represented several separate experiments. However the statistical analysis was performed on the raw data for each of these experiments using either a t-test or a one way ANOVA to test for differences from the control data in that experiment. Data with different letters are significantly different from its own control values. The 6 and 24 h data were tested separately and significant differences at $P<0.05$ are indicated as a and b or a' and b' respectively etc.

Some of the statistical analyses in this study followed the method described by Zhou et al. (2013) to test differences between relative changes. Many experiments in this study measured relative changes such as shoot biomass or root biomass in a specific treatment (e.g. salt or low light) compared with biomass in a control treatment (e.g. normal nutrient solution or normal light condition). This was done to account for the inherent differences among the genotypes or transgenic lines in control conditions. Since each measurement of the biomass has a mean and standard error (SE) associated with it the ratio of the means to estimate the relative change has a new accumulated standard error. For instance, relative biomass (RB) is calculated as the ratio of biomass in treatment condition to the control condition.

Therefore RB = x/y where x and y represent the mean biomass in the treatment and control conditions, respectively. The standard error (SE_{RB}) for this ratio estimated by Equ. 1:

$$SE_{RB} = RB\,[(SE_x/x)^2+(SE_y/y)^2]^{1/2}$$

where SE_x is SE of the treatment and SE_y is SE of the control.

Determining whether two RB values are different from one another is problematic if there is no *a priori* reason to pair the original plants in the treatment and control conditions. To

compare relative data we adapted an approach based on overlapping confidence limits (CL) described by Payton *et al*. (2003). In brief, Payton *et al*. (2003) showed that the 84% CL of means sampled from a normally distributed population will overlap 95% of the time (if the SE are similar sizes). As the two SE become less homogenous (ratio ≥ 2) the size of the CL increases to maintain the same probability of overlap. The present study used this principle to compare biomass difference between the treatment and control conditions. Initially, the values of SE_{RB} were calculated for the quotients (Equ. 1) and the 84% CL were calculated from the Z distribution by multiplying the SE by 1.33. If the CL did not overlap the means were considered significantly different from one another at $P_{0.05}$.

2.10 References

Livak KJ, Schmittgen TD (2001) Analysis of relative gene expression data using real-time quantitative PCR and the $2^{(-\Delta\Delta C(T))}$ Method. Methods 25: 402-408

Payton ME, Greenstone MH, Schenker N (2003) Overlapping confidence intervals or standard error intervals: What do they mean in terms of statistical significance? J Insect Sci 3: 34

Toki S, Hara N, Ono K, Onodera H, Tagiri A, Oka S, Tanaka H (2006) Early infection of scutellum tissue with *Agrobacterium* allows high-speed transformation of rice. Plant J 47: 969-976

Zhou G, Delhaize E, Zhou M, Ryan PR (2013) The barley MATE gene, *HvAACT1*, increases citrate efflux and $Al^{(3+)}$ tolerance when expressed in wheat and barley. Ann Bot 112: 603-612

Table 2.2 All the culture media used in the rice transformation

Composition	N6D(mg/l)	2N6-AS(mg/l)	AAM(mg/l)	RE-III(mg/l)	HF(mg/l)
Macronutrient components					
KNO_3	2,830	2,830		1,900	1,900
NH_4NO_3				1,650	1,650
$(NH_4)_2SO_4$	463	463			
$MgSO_4 \cdot 7H_2O$	185	185	250	370	370
$CaCl_2 \cdot 2H_2O$	166	166	150	440	440
$NaH_2PO \cdot 2H_2O$			150		
KH_2PO_4	400	400		170	170
KCl			3,000		
Micronutrient components					
Na_2EDTA	37.3	37.3		37.3	37.3
$FeSO_4 \cdot 7H_2O$	27.8	27.8		27.8	27.8
Fe-EDTA			40		
$MnSO_4 \cdot 4H_2O$	4.4	4.4	10	22.3	22.3
$ZnSO_4 \cdot 7H_2O$	1.5	1.5	2.0	8.6	8.6
$CuSO_4 \cdot 5H_2O$			0.025	0.025	0.025
$CoCl_2 \cdot 6H_2O$			0.025	0.025	0.025
KI	0.8	0.8	0.75	0.83	0.83
H_3BO_3	1.6	1.6	30.	6.2	6.2
$Na_2MoO \cdot 2H_2O$			0.25	0.25	0.25
Organic components					
Casamino acid	300	300	500	2,000	
Glycine	2.0	2.0	7.5	2.0	2.0
L-Arginine			176.7		
L-Proline	2,878				
L-Glutamine			900		
L-Aspartic acid			300		

Composition	N6D(mg/l)	2N6-AS(mg/l)	AAM(mg/l)	RE-III(mg/l)	HF(mg/l)
myo-Inositol	100	100	100	100	100
Nicotinic acid	0.5	0.5	1.0	0.5	0.5
Pyridoxine HCl	0.5	0.5	1.0	0.5	0.5
Thiamine HCl	1.0	1.0	10	1.0	1.0
Phytohormones					
2, 4-D	2.0	2.0			
NAA			0.02		
BAP			2.0		
Acetosyringone		20	20		
Carbon source					
Sucrose	30,000	30,000	68,500	30,000	30,000
Sorbitol				30,000	
Glucose		10,000	36,000		
Antibody					
Hygromycine	50			50	50
Coagulant					
Phytogel	3,500	3,500		3,500	3,500
pH	5.8	5.2	5.2	5.8	5.8

CHAPTER 3

Cloning of the *OsALMT1* coding and promoter regions and initial characterisation with on-line resources

3.1 Introduction

Rice (*Oryza sativa*) is one of the most important crops in the world which serves half of the world's population as a principal food (Lampe, 1995). The rice genome contains 12 chromosomes and it has the smallest genome among the major cereal crops at an estimated 400 to 430 Mb (Eckardt, 2000). The International Rice Genome Sequencing Project (IRGSP) completed a high quality draft sequence of the rice genome on December, 2002, and the sequence data for the entire rice genome is now available in the public domain deposited in public databases such as GenBank, EMBL and DDBJ for free access to all scientists worldwide (Wang *et al.*, 2011). The genomic resources and fully sequenced genome make rice a very convenient and important species in investigating gene function. More recently the 3,000 Rice Genomes Project has released the sequence of 3,000 accessions that cover the genetic and functional diversity of rice globally (Li *et al*., 2014). Furthermore, rice can be genetically transformed so this species has become a model species for cereal research (Chow *et al.*, 2000).

Members of the *ALMT* family were divided into five main clades (Barbier-Brygoo *et al.*, 2011). Those characterised form a number of sub-families in a phylogenetic tree which are loosely related to their putative functions in Al^{3+} resistance, stomatal function and other less well-defined functions (De Angeli *et al.*, 2013a; Meyer *et al.*, 2011; Pineros *et al.*, 2008; Sasaki *et al.*, 2004). There are nine *ALMT* members in rice located on five different chromosomes (**Table 3.1**). *OsALMT5* belongs to clade 1 along with *TaALMT1* and *ScALMT1*, which encode proteins conferring Al resistance, and other genes that encode proteins located on the plasma membrane of guard cells such as *HvALMT1* (Gruber *et al.*, 2011; Gruber *et al.*, 2010; Xu *et al.*, 2015). *OsALMT4* and *OsALMT7* are in clade 2 with other *ALMTs* localised to the tonoplast (*AtALMT6*) and plasma membrane (*AtALMT9*) of guard cells (De Angeli *et al.*, 2013b; Meyer *et al.*, 2011; Zhang *et al.*, 2013; Zhang *et al.*, 2014). OsALMT9 is in clade 3 along with *AtALMT12* which appears

to function as the rapid or R channel type anion channel in guard cells of *Arabidopsis* (Meyer *et al.*, 2010; Sasaki *et al.*, 2010). Clearly these clades are not entirely aligned with protein function since *CsALMT1*, also in clade 3, appears to be involved in Al tolerance and phosphorus nutrition in citrus roots (Yang *et al.*, 2012). *OsALMT1*, *OsALMT2* and *OsALMT3, OsALMT6, OsALMT8* belong to two clades with other members that have not been characterised (**Figure 3.1**). Since the *OsALMT1* and *OsALMT2* genes sit together on a separate branch in the phylogenetic tree they were chosen to have their molecular biology and function examined in more detail.

The four main aims of this chapter were: (1) to measure the expression of the *ALMT* genes in rice and choose members to investigate further; (2) investigate the available information about the selected genes *OsALMT1* and *OsALMT2* from on-line databases, (3) to clone the coding regions of selected genes *OsALMT1* and *OsALMT2*, and (4) to clone the promoter regions of these genes for further studies.

3.2 Materials and Methods

3.2.1 Expression analysis of rice *ALMT*s and cloning the *OsALMT1* coding region

Wild type rice (cv. *Nipponbare*) was grown by hydroponics as described in **Chapter 2.1.2**. cDNA was prepared from the leaves and roots of four-week old plants. The methods for RNA isolation, first-strand cDNA synthesis, purification of PCR product and sequencing are described in **Chapter 2**. The primers PRR 101 to 116 (**Table 2.1**) were used to amplify small diagnostic regions of each of the nine *ALMT1* genes. PCR products of the correct size were sequenced and compared to the database to confirm that fragments of the correct genes had been amplified.

Full-length *OsALMT1* cDNA was amplified from leaves with primers PRR-117 and PRR-119 (*Eco*RI and *Bam*HI enzyme sites included for subsequent ligation into the pWUbi palsmid). The PCR product was purified and ligated to pGEM®-T Easy vector (Promega, **Figure 3.2**). The resulting construct was transformed into *E. coli* DH5α and

Table 3.1 Sequence information of the ALMT members of rice (http://rice.plantbiology.msu.edu/cgi-bin/putative_function_search.pl)

	OsALMT1	OsALMT2	OsALMT3	OsALMT4	OsALMT5	OsALMT6	OsALMT7	OsALMT8	OsALMT9
Genomic sequence length	3434	2500	3342	2488	3334	2487	4689	2265	2757
CDS length	1575	933	1467	1755	1368	1542	1167	2007	1590
Protein length	525	311	489	585	456	514	389	669	530
Predicted molecular weight	59343.5	32702.3	52783.8	63759.2	48682.4	54001.7	41579.4	71022.9	58875.8
Predicted pI	7.6053	7.3127	6.3762	8.9287	8.313	6.3209	9.395	7.2224	8.6696
Predicted Transmembrane regions	6	6	6	5	5	5	5	7	6
Exons	6	4	3	6	6	3	6	--	6
Introns	5	3	2	5	5	2	5	--	5
Location	Chr1	Chr1	Chr2	Chr2	Chr4	Chr4	Chr6	Chr6	Chr10
Locus ID	Os01g12210	Os01g53570	Os02g45160	Os02g49790	Os04g34010	Os04g47930	Os06g15779	Os06g22600	Os10g42180
Expression in shoot	Yes	No	No	Yes	Yes	No	No	No	Yes
Expression in Root	Yes	No	Yes	No	Yes	No	No	Yes	Yes

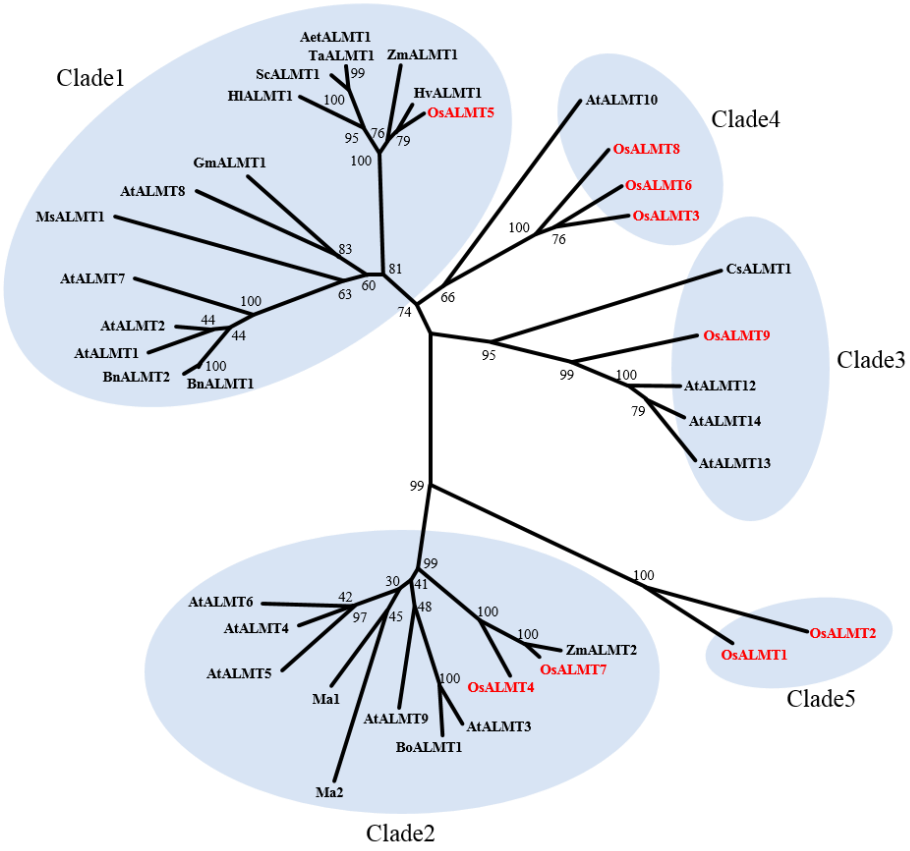

Figure 3.1 Phylogenetic tree of ALMT proteins from Arabidopsis and rice and some characterised members.

The red-coloured proteins are ALMT members from rice. The alignment of the full-length proteins of some known ALMTs was performed using ClustalW as part of the MEGA5.1 software package (Tamura *et al.*, 2011). The phylogenetic tree was constructed using the neighbour-joining method, and the bootstrap test of phylogeny performed using 10,000 replicates. Species prefixes and Genbank accession numbers: Aet, *Aegilops taushii* (AetALMT1: AAZ22853), At, *Arabidopsis thaliana* (AtALMT1: AAF22890, AtALMT2: NP_172320, AtALMT3: AAF25997, AtALMT4: NP_173919, AtALMT5: NP_564935, AtALMT6: NP_179338, AtALMT7: NP_180292, AtALMT8: NP_187774, AtALMT9: NP_188473, AtALMT10: CAB80900, AtALMT12: NP_193531, AtALMT13: AAX55201, AtALMT14: NP_199473); Bn, *Brassica napus* (BnALMT1: BAE97280, BnALMT2: BAE97281); Bo, *Brassica oleracea* (BoALMT1: AAW81734); Cs, *Citrus sinensis* (CsALMT1: AET22398.1); Gm, *Glycine max* (GmALMT1: NP_001237989.1); Hl, *Holcus lanatus* (HlALMT1: BAN78902.1); Hv, *Hordeum vulgare* (HvALMT1: EF424084); Ma, *Malus domestica* (Ma1: XP_008361730.1, Ma2: XP_008339686.1); Ms, *Medicago sativa* (MsALMT1: GU550122.1); Os, *Oryza sativa* (OsALMT1: NP_001042433, OsALMT2: BAD87020, OsALMT3: BAD29455, OsALMT4: BAD16367, OsALMT5: CAE01530, OsALMT6: CAE02072, OsALMT7: BAD54395, OsALMT8: BAD32958, OsALMT9: AAL86482); Sc, *Secale cereale* (ScALMT1: ABA62397); Ta, *Triticum aestivum* (TaALMT1: BAD10882); Zm, *Zea mays* (ZmALMT1: ABC86748). For ScALMT1 the ScALMT1-1 allele is shown (differs from the ScALMT1-2 allele at 6 amino acids). The protein encoded by AtALMT11 (At4g17585) of Arabidopsis was originally included as a member of the ALMT family but is excluded here because it is predicted to be soluble.

positive colonies were detected by PCR using primers PRR120 and PRR121 which straddle the site where the fragment was ligated in the pGEM®-T Easy vector. Selected colonies were further analysed by digestion with *Eco*RI and *Bam*HI. The full construct was sequenced to verify that PCR had not introduced mutations. The sequencing primers are PRR120, 121 and 104 as a middle primer for overlapping sequences.

3.2.2 *OsALMT1* promoter cloning

Sequence of the 4000 bp region upstream of *OsALMT1* was downloaded from the NCBI database (GenBank accession number NC_008394). The 2496 bp immediately upstream of the *OsALMT1* start codon was amplified from genomic DNA by the primers PRR128 and PRR129 which introduced *Pac*I and *Asc*I sites at each end. This region was considered the promoter of *OsALMT1*. The PCR product was subsequently cloned into pGEM® T-easy (Promega) to produce the plasmid pOsALMT1-promoter GEM-T Easy (**Figure 3.3**) and sequenced to confirm that errors had not been inadvertently introduced. PRR124 and PRR125 were used as middle primers for sequencing.

3.2.3 Investigating gene function using on-line resources

The predication software that placed *OsALMT1* into a gene family is Pfam 27.0 (http://pfam.xfam.org/) (Punta *et al.*, 2012). The secondary structure of the OsALMT1 protein was analysed by TMHMM (http://www.cbs.dtu.dk/services/TMHMM/), SOSUI (http://harrier.nagahama-i-bio.ac.jp/sosui//sosui_submit.html), Kyte-Doolittle (http://gcat.davidson.edu/rakarnik/kyte-doolittle.htm) and Protter (http://wlab.ethz.ch/protter/start/) (Doolittle, 1982; Hirokawa T., 1998; Omasits *et al.*, 2014).

The information about *OsALMT1* expression pattern was collected from the Rice Expression Profile Database (RiceXPro, http://ricexpro.dna.affrc.go.jp/) (Dash *et al.*, 2012; Junshi Yazaki, 2002) and Plant Expression Database (PLEXdb, http://www.plexdb.org/).

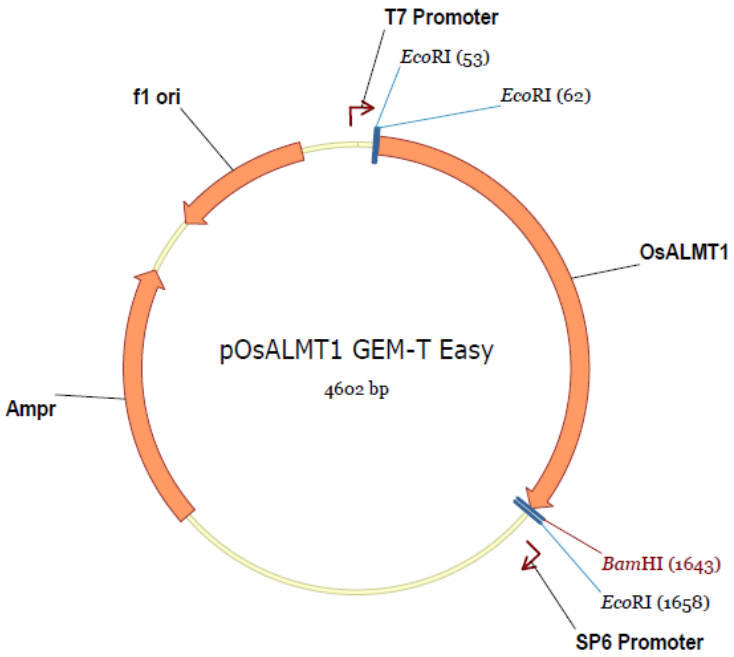

Figure 3.2 Vector map of pOsALMT1 GEM-T Easy

The orange arrows represent coding DNA sequence (CDS) except for *f1 ori* which is the origin of replication. The plasmid contains T7 and SP6 RNA polymerase promoters flanking a multiple cloning region within the α-peptide coding region of β-galactosidase. The *Ampr* confers ampicillin resistance to the cell by encoding a subunit of the enzyme beta lactamase which breaks down ampicillin and allows the positive clones to survive. The *f1 ori* (origin of replication) enables the production of a single stranded vector under appropriate conditions.

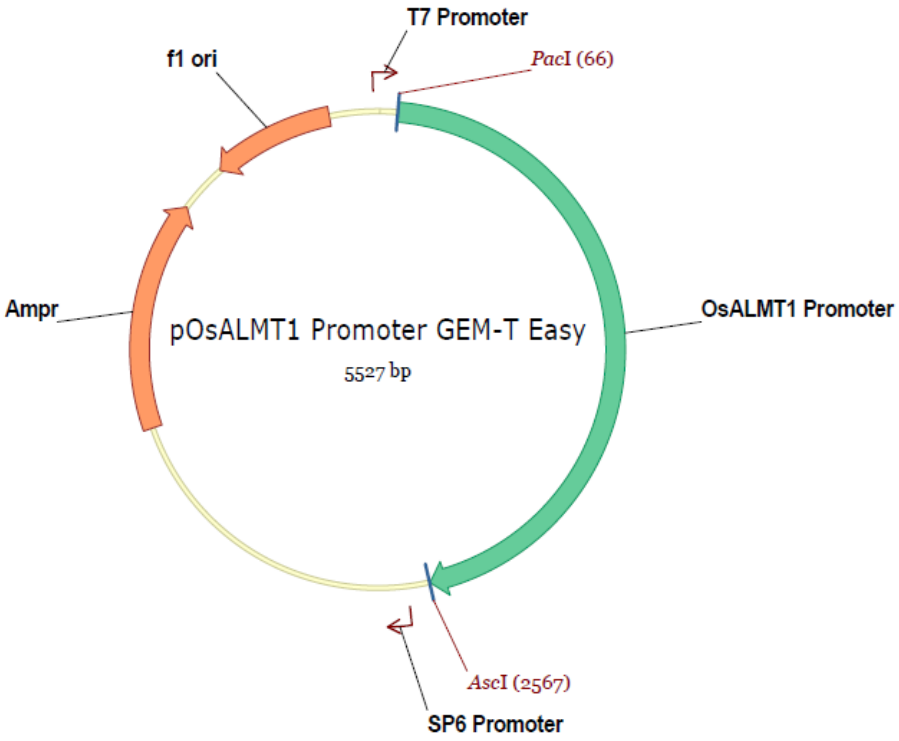

Figure 3.3 Vector map of pOsALMT1 promoter GEM-T Easy

The orange arrow represents coding DNA sequence (CDS) except for *f1 ori* which is the origin of replication. The green arrow represents promoter and the direction of the arrow is from 5'-3'. The plasmid contains T7 and SP6 RNA polymerase promoters flanking a multiple cloning region within the α-peptide coding region of β-galactosidase. The *Ampr* confers ampicillin resistance to the cell by encoding a subunit of the enzyme beta lactamase which breaks down ampicillin and allows the positive clones to survive. The *f1 ori* (origins of replication) enables the production of a single stranded vector under appropriate conditions.

The network of *OsALMT1* gene expression was predicted by the Rice Functional Related gene Expression Network Database (RiceFREND, http://ricefrend.dna.affrc.go.jp/), and the Search Tool for the Retrieval of Interacting Genes/Proteins (STRING, http://string-db.org/newstring_cgi/show_input_page.pl?UserId=bGNNaavo_9LH&sessionId=HrKcOL3y4cbv) (Szklarczyk *et al*., 2015).

3.2.4 On-line resources investigating the gene promoters

Transcription start site and regulatory motifs of *OsALMT1* promoter were predicted by Promoter 2.0 Prediction Server (http://www.cbs.dtu.dk/services/Promoter/) (Knudsen, 1999), Promoter Scan (PROSCAN, http://www-bimas.cit.nih.gov/molbio/proscan/) and Plant Cis-Acting Regulatory Elements database (PlantCARE, http://bioinformatics.psb.ugent.be/webtools/plantcare/html/) (Lescot *et al.*, 2002).

3.3 Results

3.3.1 Expression of *ALMT* genes in roots and shoots and structure of the *OsALMT1* coding region and promoter

The complementary DNA (cDNA) was prepared from the leaves and roots of rice cultivar *Nipponbare*. By using the gene specific primers, we found that the *OsALMT1* expression could be detected from both the root and leaf tissues. *OsALMT4* showed little expression in the leaf tissue while *OsALMT3* and *OsALMT8* were expressed in roots (**Table 3.1**). Expression of *OsALMT2*, *OsALMT6* and *OsALMT7* was not detected in either roots or shoots. *OsALMT5* expression was detected in both roots and shoots and *OsALMT9* was expressed mainly in the shoots (**Table 3.1**). Examination of the on-line sequence of *OsALMT2* indicated that it likely contained a premature stop codon (at the 966-968 bp region of *OsALMT1*) which would encode a truncated protein. Note that the primers used to measure expression of *OsALMT2* were upstream of this predicted stop codon.

This project chose the *OsALMT1* and *OsALMT2* genes to investigate further because they were closely related, their expression was easily measured and because they sit together are on a separate branch of the phylogenetic tree (**Figure 3.1**). However since expression of *OsALMT2* could not be detected in the roots or shoots this project focused on *OsALMT1*. Sequence analysis from NCBI predicted that the *OsALMT1* gene has five introns and six exons with a coding region of 1575 bp. The predicted protein contains 524 amino acid residues with 34% identity to TaALMT1 and 31% identity to AtALMT1 (http://blast.ncbi.nlm.nih.gov). The 2496 bp immediately upstream from the *OsALMT1* start codon was used as the *OsALMT1* promoter in this study (**Figure 3.4**).

3.3.2 On-line resources investigating *OsALMT1* biology

The *OsALMT1* coding region is predicted to encode a protein of 524 amino acids with a molecular weight of 59343 and isoelectric point of 7.45. This protein has features in common with other ALMT family members including a PF11744 domain (aluminum activated malate transporter) from 43 to 513 AA (**Figure 3.5**). OsALMT1 is predicted to have six transmembrane regions with different algorithms yielding different predictions for their orientations (**Figure 3.6**). The programs TMHMM and SOSUI predicted that both ends would be extracellular while Protter predicted that they would be directed towards the inside of the cell. The CELLO programme predicted that the OsALMT1 has high potential of localising on the plasma membrane (**Figure3.7**).

OsALMT1 is shown to be widely expressed in the rice plant during various growth stages (**Figure 3.8a and 3.9a**). Abiotic stresses such as drought, salt, cold, heat and phosphorus (P) and iron (Fe) deficiency as well as some hormones (ABA, GA, IAA and BAP) alter *OsALMT1* expression according to some online resources (**Figure 3.8b and 3.9b-e**) but this information is difficult to interpret since relative expression data is provided and tissue types are sometimes unclear. Nevertheless this information might indicate that *OsALMT1* has multiple roles.

The program RiceFREND predicted that *OsALMT1* expression may be regulated by the transcription factor Os01g0625300 (similar to heat shock transcription factor 31) (**Figure 3.10a**). The program also predicted that OsALMT1 interacts with Os06g0141200 (similar to RNA-binding protein EWS), Os07g0160400 (Glyoxalase/bleomycin resistance protein/dioxygenase domain containing protein),

Os07g0162100 (3-oxo-5-alpha-steroid 4-dehydrogenase, C-terminal domain containing protein), Os08g0101700 (similar to cytochrome b561), Os08g0412500 (4346901, protein of unknown function UPF0041 family protein), Os08g0557200 (metallophosphoesterase domain containing protein) and Os09g0373000 (4345559, similar to brain protein 44-like protein) (**Figure 3.10a**). Another program, STRING, also predicted interactions between OsALMT1 (4324653) and Os08g0412500 (4346901) and Os09g0373000 (4345559). The functions of most of these proteins are uncertain and the predicted roles are unconfirmed. Nevertheless the expression in different tissues and possible interactions with other proteins could indicate that OsALMT1 has multiple roles throughout the plant.

3.3.3 Analysis of the *OsALMT1* promoter

The genomic region (3947 bp) between the coding region of *OsALMT1* (Os01g0221600) and the next gene upstream (Os01g0221500) was analysed with various on-line programmes. The most likely promoter region was predicted to be within the initial 1800 bp upstream of *OsALMT1* (**Figure 3.11**). Therefore the 2496 bp region upstream of the *OsALMT1* start site encompassed this region and was considered the promoter for this study.

As part of the process to understand the function of *OsALMT1* and how the promoter is regulated, the occurrence of cis-elements along the 2496bp region was also predicted. The predictions show that the *OsALMT1* promoter not only contains fundamental elements for promoter function such as a CAAT-box and TATA-box, but also includes predicted regulators for various abiotic stresses and hormone response such as Box-4, G-box, GT1-motif, MNF1, MER and spl for light responsiveness, Box-W1 for fungal elicitor responsive, CAT-box related to meristem expression, GCN4_motif and Skn-1_motif involved in endosperm expression, HSE for heat stress responsiveness, O2-site involved in zein metabolism regulation, TC-rich repeats involved in defense and stress responsiveness, circadian involved in circadian control ABRE for abscisic acid responsiveness, CGTCA-motif and TGACG-motif for MeJA-responsiveness and GARE-motif for gibberellin-responsive (**Table 3.2**). These predictions indicate that the expression of *OsALMT1* might be responsive to certain hormones and abiotic stresses.

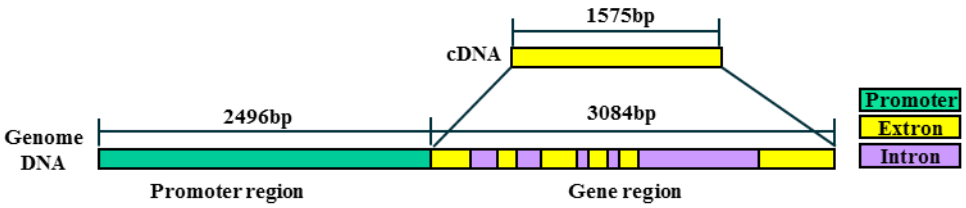

Figure 3.4 Predicted structure of the *OsALMT1* gene

Exons are shown as six yellow boxes that comprise of 1575 bp for the *OsALMT1* coding region. The exons are separated by five introns which are shown as purple boxes with a total combined length of 1509 bp. The region used as a promoter in this study (green box) was 2496 bp upstream from the *OsALMT1* initiation codon.

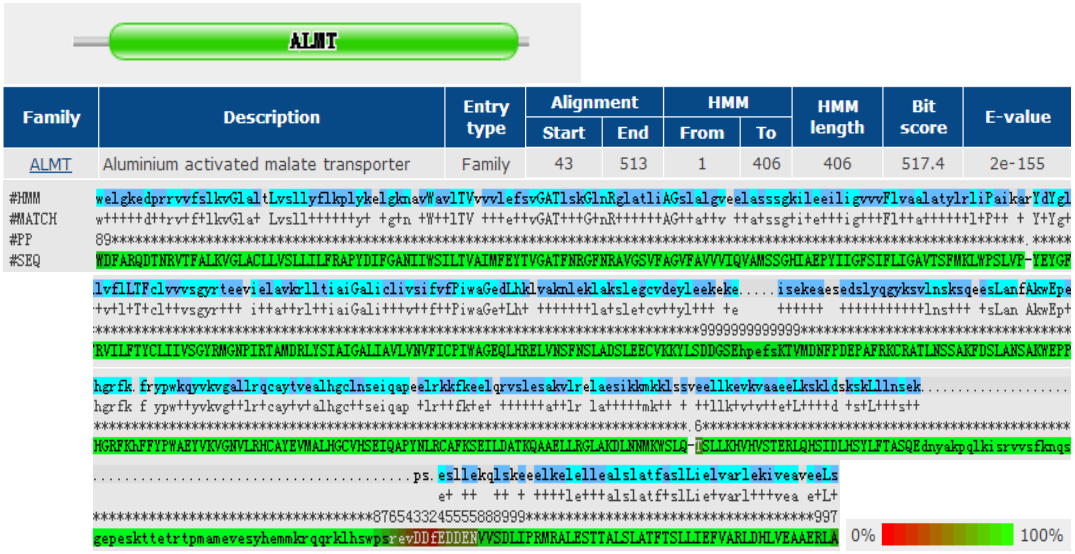

Figure 3.5 Significant Pfam-A matches of OsALMT1 to the family of ALMTs

OsALMT1 matched one Pfam-A (shown as "ALMT") domain from 43-513 AA, but no Pfam-B matches were found. The alignment row for each hit shows the alignment between OsALMT1 and the matching ALMT. The alignment fragment includes the following rows:

#HMM: consensus of the HMM (Hidden Markov Models). Capital letters indicate the most conserved positions;

#MATCH: the match between OsALMT1 and the ALMT HMM. A '+' indicates a positive score which can be interpreted as a conservative substitution;

#PP: posterior probability. The degree of confidence in each individual aligned residue: 0 means 0-5%, 1 means 5-15% and so on; 9 means 85-95% and a '*' means 95-100% posterior probability;

#SEQ: query sequence. A '-' indicate deletions in the query sequence with respect to the ALMT HMM. Columns are colored according to the posterior probability showed on the right bottom corner.

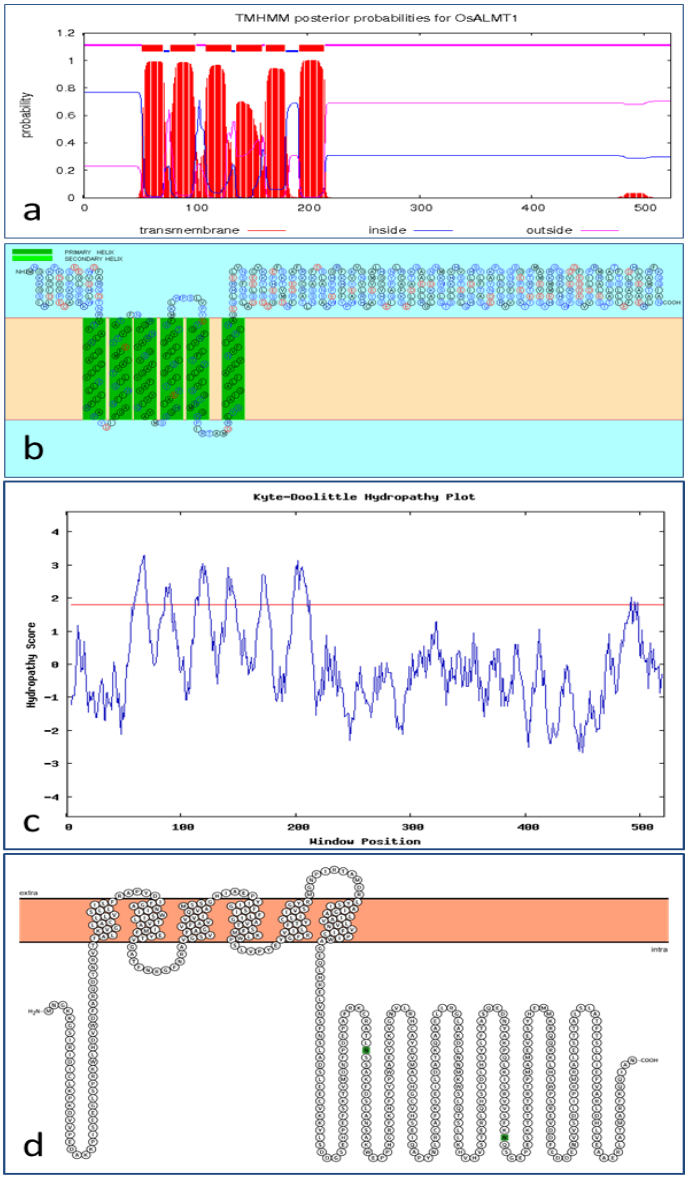

Figure 3.6 Predictions for the secondary structure of OsALMT1

The secondary structure of OsALMT1 was predicted by TMHMM (a), SOSUI (b), Kyte-Doolittle (c), and Protter (d) methods. For TMHMM the predicted number of transmembrane helices is six (from amino acids 53-71, 78-100, 110-132, 137-159, 163-180 and 193-215) but one is not predicted to cross the membrane completely so the N-terminus orientated to the cytoplasmic side (proability 0.77) and the C terminus is orientated towards the outside. SOSUI predicts six transmembrane helices with an average hydrophobicity of -0.03 (from amino acids 53-75, 79-101, 104-126, 129-151, 162-184, and 193-215). The Kyte-Doolittle method predicated six transmembrane helices when using a window size of nine amino acids. Strong negative peaks indicate possible surface regions of globular proteins. The Window Position values shown on the x-axis of the graph reflect the average hydropathy of the entire window, with the corresponding amino acid as the middle element of that window. Protter also predicted six transmembrane regions with both ends located on the intra-cellular side. The N in green box indicates N-glyco motifs (possible sites for sugar chain additions at the amide nitrogen on the side-chain of the asparagine).

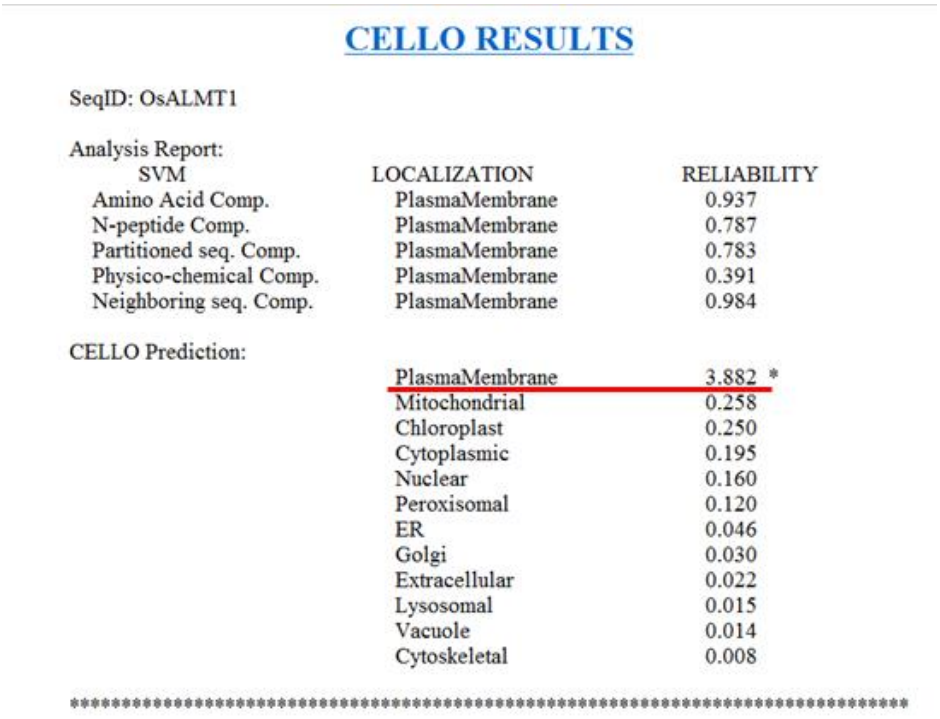

CELLO RESULTS

SeqID: OsALMT1

Analysis Report:

SVM	LOCALIZATION	RELIABILITY
Amino Acid Comp.	PlasmaMembrane	0.937
N-peptide Comp.	PlasmaMembrane	0.787
Partitioned seq. Comp.	PlasmaMembrane	0.783
Physico-chemical Comp.	PlasmaMembrane	0.391
Neighboring seq. Comp.	PlasmaMembrane	0.984

CELLO Prediction:

PlasmaMembrane	3.882 *
Mitochondrial	0.258
Chloroplast	0.250
Cytoplasmic	0.195
Nuclear	0.160
Peroxisomal	0.120
ER	0.046
Golgi	0.030
Extracellular	0.022
Lysosomal	0.015
Vacuole	0.014
Cytoskeletal	0.008

****

Figure 3.7 Prediction for the sub-cellular localisation of OsALMT1

Sub-cellular localisation of OsALMT1 using the CELLO program predicted that a plasma membrane localization was most likely.

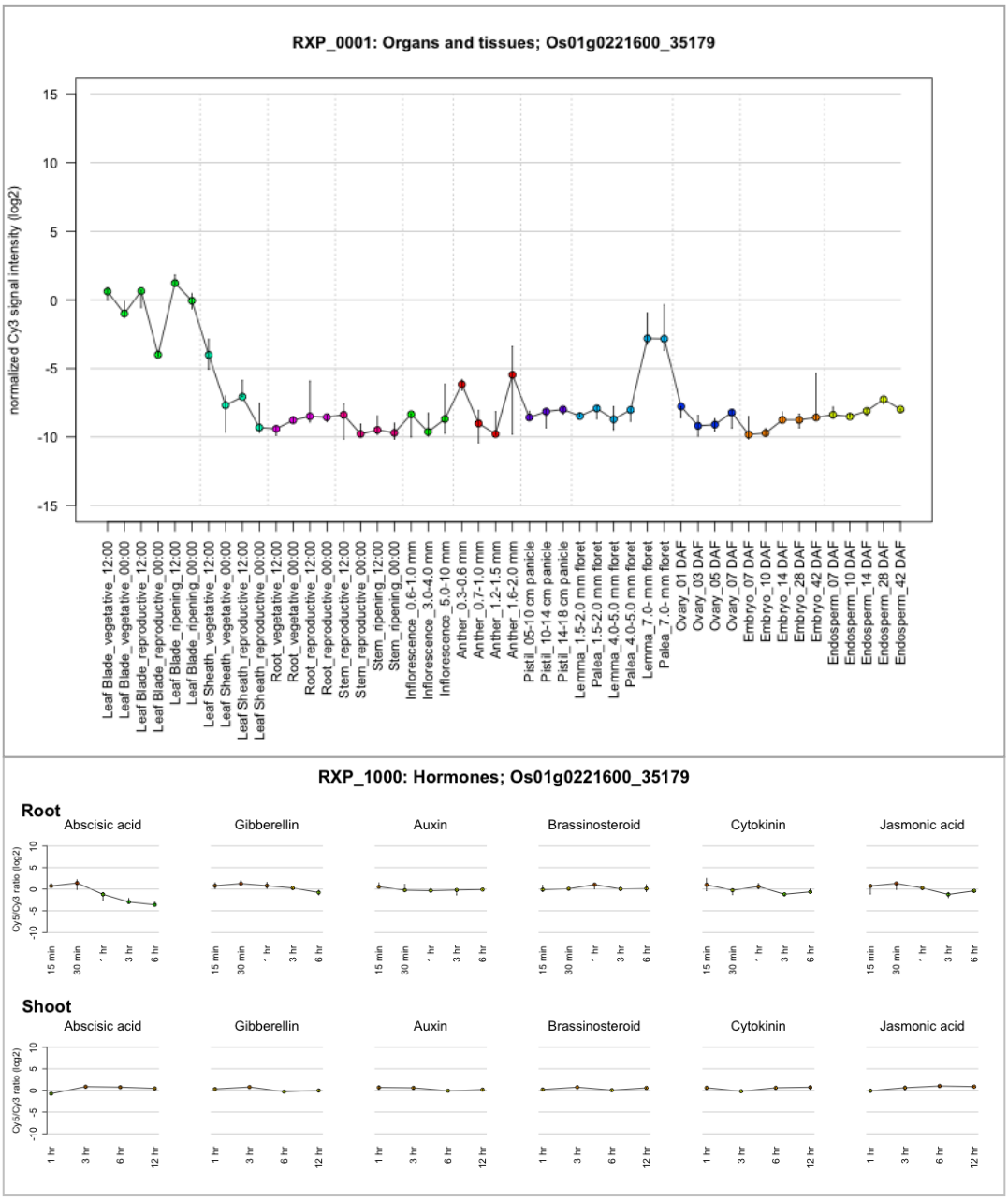

Figure 3.8 Pattern of *OsALMT1* expression as predicted by the on-line resource RiceXPro

The expression data represent raw signal intensity normalized to a log2 scale transformation. Expression data were normalized by adjusting to a 75 percentile baseline (when all expression data are arranged in increasing order, the expression level corresponding to 75% of the distribution). Three replicates are used for each point. The dots represent the median and the bars represent highest and lowest values among triplicates.

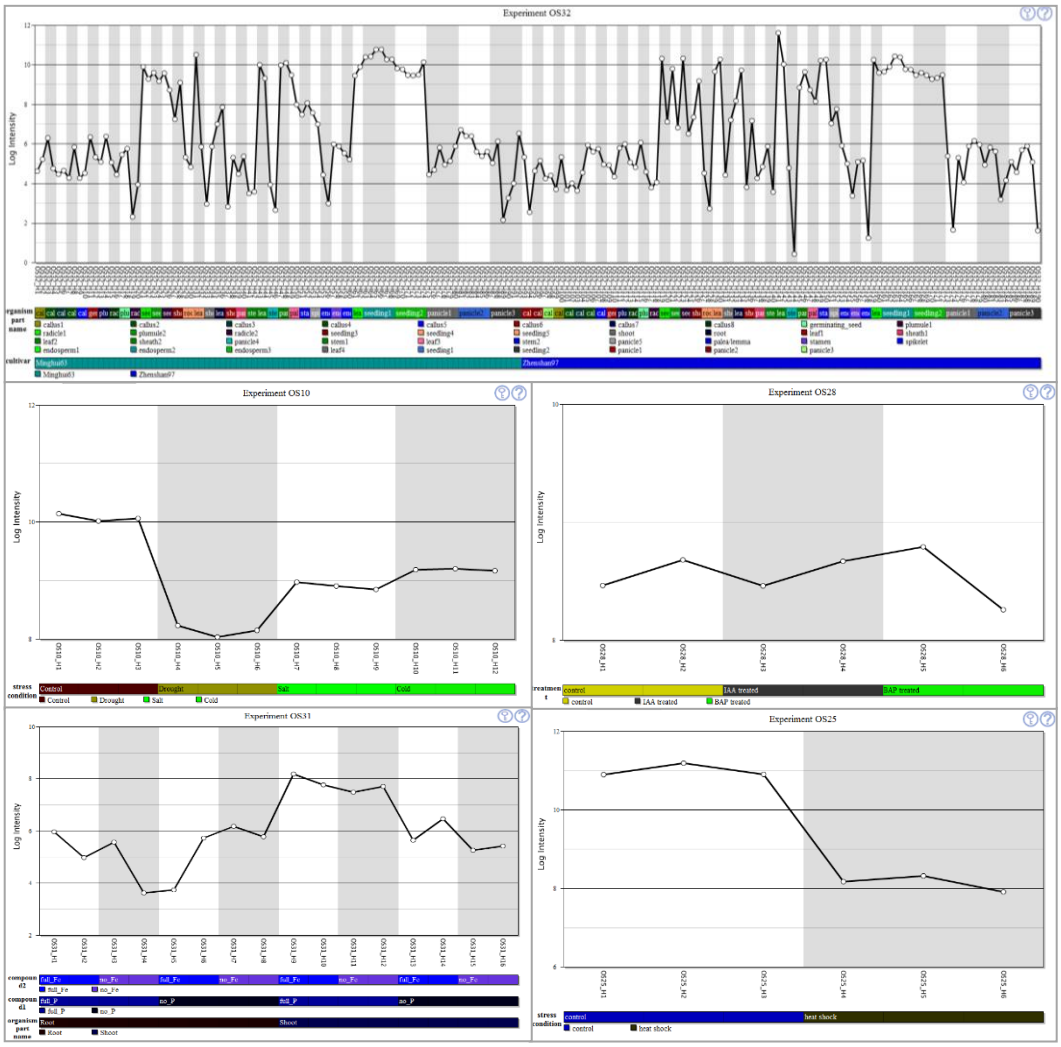

Figure 3.9 Pattern of *OsALMT1* expression as predicted by the online resource PLEXdb

The expression data are based on the Rice 57k microarray by using the probe target OsALMT1 (ID Os.26807.1.S1_at)**.** The expression graphs were calculated by MAS 5.0. Normalization and log intensity is shown on the graph. All hybridizations are shown in the graph as cycles and each cycle represents a replicate. Plant cultivar, treatment and tissue information are show under the expression graph by various color blocks. The different experiment means: OS10-Expression data for stress treatment in rice seedlings, OS25-Expression data for heat shock in rice seedlings, OS28-Rice seedling hormone treatment, OS31-Transcriptome analysis of iron and phosphorus interaction in rice seedlings and OS32: Dissecting the developmental transcriptomes of rice. IAA is indole-3-acetic acid and BAP is 6-benzylaminopurine.

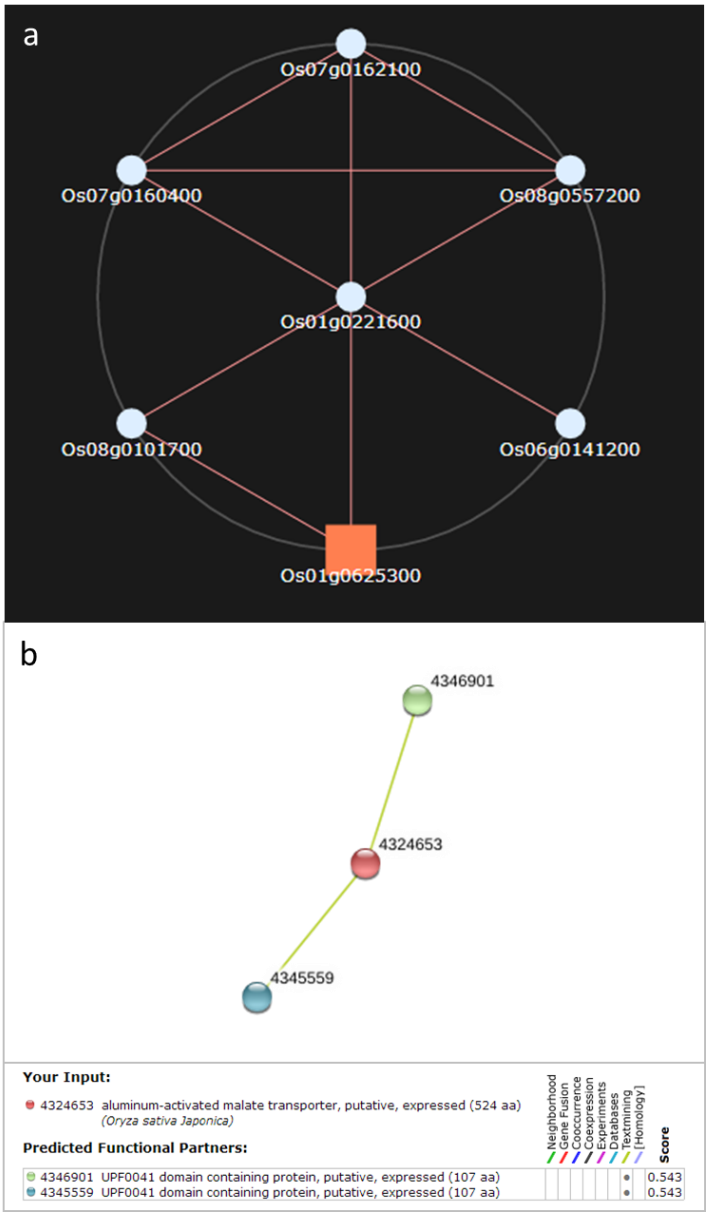

Figure 3.10 Predicted gene and protein networks with on-line resources

The *OsALMT1* gene was predicted to be related to various genes by RiceFREND (a) and STRING (b). (a) The *OsALMT1* gene (central dot) was predicted to be related with 5 other genes (white dots) and a transcription factor (red square). The parameter settings for this prediction is Hierarchy=1, Mutual Rank=20, Node=7, Edge=10. (b) Evidence for networks of the OsALMT1 protein. Different line colors represent the types of evidence for the association. For the network display: Nodes are either colored (if they are directly linked to the input - as in the table) or white (nodes of a higher iteration/depth). Edges, i.e. predicted functional links, consist of up to eight lines: one color for each type of evidence.

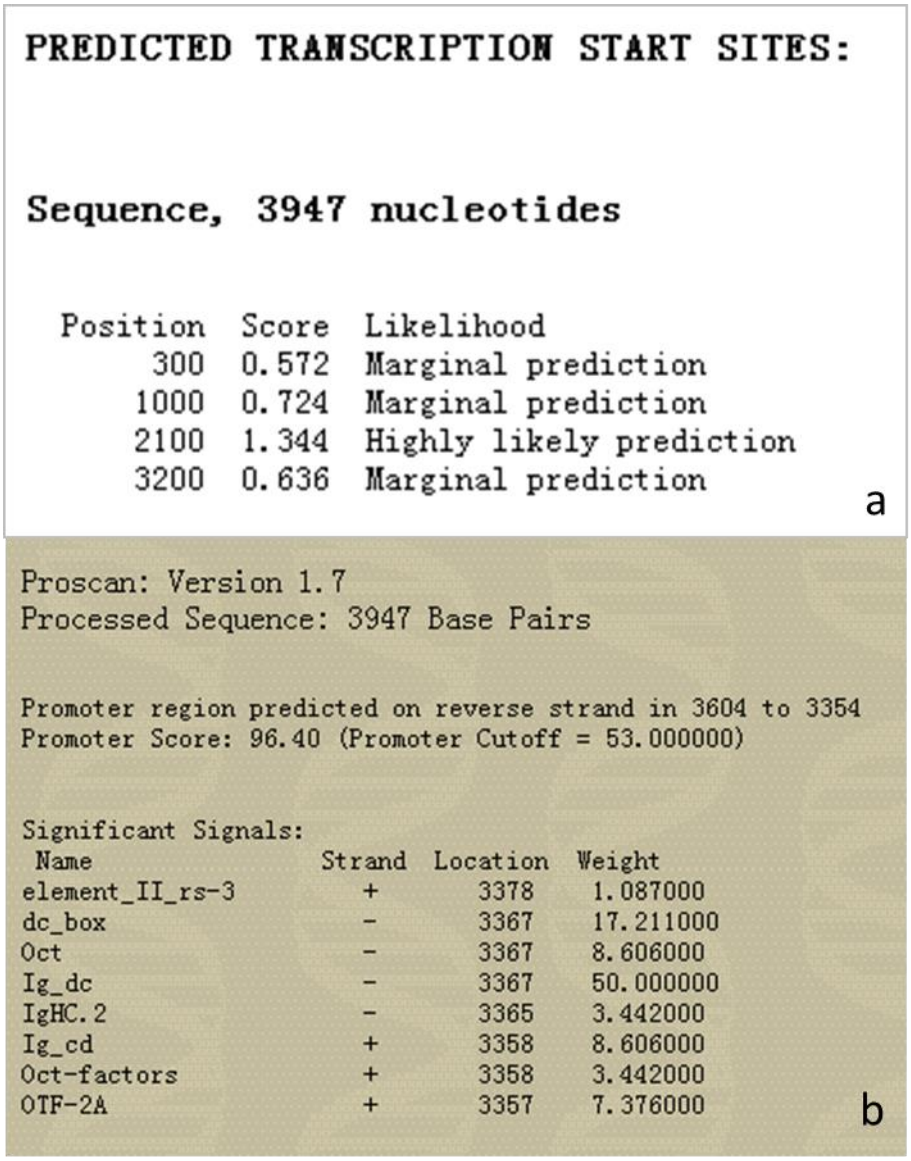

PREDICTED TRANSCRIPTION START SITES:

Sequence, 3947 nucleotides

Position	Score	Likelihood
300	0.572	Marginal prediction
1000	0.724	Marginal prediction
2100	1.344	Highly likely prediction
3200	0.636	Marginal prediction

a

Proscan: Version 1.7
Processed Sequence: 3947 Base Pairs

Promoter region predicted on reverse strand in 3604 to 3354
Promoter Score: 96.40 (Promoter Cutoff = 53.000000)

Significant Signals:

Name	Strand	Location	Weight
element_II_rs-3	+	3378	1.087000
dc_box	-	3367	17.211000
Oct	-	3367	8.606000
Ig_dc	-	3367	50.000000
IgHC.2	-	3365	3.442000
Ig_cd	+	3358	8.606000
Oct-factors	+	3358	3.442000
OTF-2A	+	3357	7.376000

b

Figure 3.11 Predicted transcription start sites for *OsALMT1*

The transcription start site for *OsALMT1* was predicted by Promoter 2.0 Prediction Server (a) and ProScan (b). Promoter 2.0 predicts transcription start sites of vertebrate PolII promoters in DNA sequences. It has been developed as an evolution of simulated transcription factors that interact with sequences in promoter regions**.** It builds on principles that are common to neural networks and genetic algorithms. ProScan predicts promoter regions based on scoring homologies with putative eukaryotic PolII promoter sequences. The analysis is done using the PROSCAN Version 1.7 suite of programs developed by Dr. Dan Prestridge, Advanced Biosciences Computing Center, University of Minnesota.

Table 3.2 Cis-element prediction by PlantCARE

Site Name	Organism	Position	Strand	Matrix score.	sequence	function
Box 4						
Box 4	*Petroselinum crispum*	962	+	6	ATTAAT	part of a conserved DNA module involved in light responsiveness
Box 4	*Petroselinum crispum*	1256	+	6	ATTAAT	part of a conserved DNA module involved in light responsiveness
G-Box						
G-Box	*Antirrhinum majus*	1285	-	6	CACGTA	cis-acting regulatory element involved in light responsiveness
G-box	*Daucus carota*	1285	+	6	TACGTG	cis-acting regulatory element involved in light responsiveness
GT1-motif						
GT1-motif	*Solanum tuberosum*	455	+	10	ATGGTGGTTGG	light responsive element
GT1-motif	*Arabidopsis thaliana*	1346	-	6	GGTTAA	light responsive element
MNF1						
MNF1	*Zea mays*	421	+	7	GTGCCC(A/T)(A/T)	light responsive element
MRE						
MRE	*Petroselinum crispum*	763	+	7	AACCTAA	MYB binding site involved in light responsiveness
Sp1						
Sp1	*Zea mays*	1308	+	5.5	CC(G/A)CCC	light responsive element
Sp1	*Zea mays*	1373	+	5	CC(G/A)CCC	light responsive element
Box-W1						
Box-W1	*Petroselinum crispum*	858	-	6	TTGACC	fungal elicitor responsive element
CAT-box						
CAT-box	*Arabidopsis thaliana*	935	+	6	GCCACT	cis-acting regulatory element related to meristem expression
GCN4_motif						
GCN4_motif	*Oryza sativa*	172	-	7	TGTGTCA	cis-regulatory element involved in endosperm expression

Site Name	Organism	Position	Strand	Matrix score.	sequence	function
Skn-1_motif						
Skn-1_motif	*Oryza sativa*	295	-	5	GTCAT	cis-acting regulatory element required for endosperm expression
Skn-1_motif	*Oryza sativa*	959	+	5	GTCAT	cis-acting regulatory element required for endosperm expression
Skn-1_motif	*Oryza sativa*	505	+	5	GTCAT	cis-acting regulatory element required for endosperm expression
HSE						
HSE	*Brassica oleracea*	793	+	9	AAAAAATTTC	cis-acting element involved in heat stress responsiveness
O2-site						
O2-site	*Zea mays*	501	-	9	GATGACATGG	cis-acting regulatory element involved in zein metabolism regulation
TC-rich repeats						
TC-rich repeats	*Nicotiana tabacum*	1205	+	9	ATTCTCTAAC	cis-acting element involved in defense and stress responsiveness
circadian						
circadian	*Lycopersicon esculentum*	501	+	6	CAANNNNATC	cis-acting regulatory element involved in circadian control
circadian	*Lycopersicon esculentum*	1232	+	6	CAANNNNATC	cis-acting regulatory element involved in circadian control
ABRE						
ABRE	*Arabidopsis thaliana*	1285	+	6	TACGTG	cis-acting element involved in the abscisic acid responsiveness
CGTCA-motif						
CGTCA-motif	*Hordeum vulgare*	1289	-	5	CGTCA	cis-acting regulatory element involved in the MeJA-responsiveness
GARE-motif						
GARE-motif	*Brassica oleracea*	972	+	7	TCTGTTG	gibberellin-responsive element
GARE-motif	*Brassica oleracea*	1355	-	7	TCTGTTG	gibberellin-responsive element
TGACG-motif						
TGACG-motif	*Hordeum vulgare*	1289	+	5	TGACG	cis-acting regulatory element involved in the MeJA-responsiveness

3.4 Discussion

No previous study has investigated the function of a rice member of the *ALMT* family in detail. Expression of all the *OsALMT*s was tested in the roots and leaves of rice plants and the *OsALMT1* was chosen for further analysis because its expression was easily measured and because it sat on a separate branch of the phylogenetic tree (**Figure 3.1**). The expression of *OsALMT2* could not detected in isolated RNA from leaves or roots and the sequence of *OsALMT2* appeared to contain a truncation in the coding region which may render it non-functional. In contrast, *OsALMT1* expression could easily be detected and thus a comprehensive description of *OsALMT1* biology was possible. OsALMT1 was predicted to have all the attributes associated with the ALMT family including a PF11744 domain. Several algorithms predicted six transmembrane regions in the N-terminal half of the protein, but with various orientations of the N and C terminal ends towards either the inside or outside the cell. In general, ALMT members are predicted to have five to seven transmembrane regions in the N-terminal region and a long "tail" in the C-terminal half (see Chapter 1). Detailed topological analyses have been performed to further characterise the structure-function relationship of some ALMTs. The first experimental study of the secondary structure of TaALMT1 used an immunocytochemical method to analyse secondary structure. That study concluded that the C-terminal half (240 amino acids) is extracellular and the N-terminal region is also extracellular. There may also be an additional transmembrane domain in the N-terminus but this is unconfirmed (Motoda *et al.*, 2007). More recent studies have questioned this topology and instead suggested that the C-terminal half of the TaALMT1 and other proteins is intracellular (Dreyer *et al.*, 2012; Meyer *et al.*, 2010; Mumm *et al.*, 2013; Ryan *et al.*, 2011). Similarly, experiments need to be undertaken to establish the secondary structure of OsALMT1 and to compare to the predicted secondary structures.

The on-line databases indicate that *OsALMT1* is expressed in leaf, seedling and flower parts. Some other members of the ALMT family that are highly expressed in leaves are expressed in the guard cells and contribute to stomatal function. For example *AtALMT6*, *AtALMT9*, *AtALMT12* and *HvALMT1* are highly expressed in the guard cells and the proteins encoded by these genes are important for guard cell function in Arabidopsis and barley (De Angeli *et al.*, 2013b; Gruber *et al.*, 2011; Gruber *et al.*, 2010; Kovermann *et al.*, 2007; Meyer *et al.*, 2010; Meyer *et al.*, 2011; Sasaki *et al.*, 2010; Xu

et al., 2015; Zhang *et al.*, 2013; Zhang *et al.*, 2014). All these genes are also expressed in other tissues. For instance, *AtALMT6* is expressed in stem and flowers, *AtALMT9* is expressed in the stem and along the root, *AtALMT12* is expressed in seedlings and roots, while *HvALMT1* is expressed in the root and in grain (Gruber *et al.*, 2011; Kovermann *et al.*, 2007; Meyer *et al.*, 2010; Meyer *et al.*, 2011; Xu *et al.*, 2015). The functions of all these proteins in tissues other than leaves are unclear except for HvALMT1 which facilitates malate efflux from the aleurone of grain during germination (Xu *et al* 2015).

The online databases explored here suggest that *OsALMT1* expression in root tissue is affected by drought, heat and abscisic acid. Cis-elements involved in ABA and GA-responsive also can be found at the promoter region. Repeated copies of abscisic acid response element (ABRE) can confer ABA responsiveness to a minimal promoter, which proved to be involved in the regulation of various abiotic processes, including stomatal closure, seed and bud dormancy, and physiological responses to cold, drought, osmotic and salinity stresses (Kim *et al.*, 2011; Narusaka *et al.*, 2003). *OsALMT1* expression was also predicted to change under different abiotic stresses such as drought, salt, cold, heat and P and Fe deficiency. The network predictions indicate the *OsALMT1* expression is regulated by a transcription factor Os01g0625300 which is similar to heat shock transcription factor 31. Although the mechanism of stress activation of heat shock transcription factor 31 is not yet understood, the other heat shock transcription factor such as HSF1, 2, 3, 4 and 29 are proved to be linked to cellular signalling pathways under heat and oxidative stress conditions as well as functions not associated with stress such as cell cycle regulation, embryonic development, cellular differentiation, and spermatogenesis (Pirkkla *et al.*, 2001; Zhong *et al.*, 1998). These results indicated that the *OsALMT1* might participant in plant responses to abiotic stresses involving hormones, light, heat, stress and defence responsiveness. Experiments should consider these treatments when exploring the possible function of the OsALMT1 protein in rice.

3.5 References

Barbier-Brygoo H, De Angeli A, Filleur S, Frachisse JM, Gambale F, Thomine S, Wege S (2011) Anion channels/transporters in plants: from molecular bases to regulatory networks. Annu Rev Plant Biol 62: 25-51

Chow TY, Chao YT, Liu SM, Wu HP, Chu MK, Chen CS, Hsing YIC (2000) Characterization of a 10 cM region of rice chromosome 5. Bot Bull Acad Sinica 42: 159-166

Dash S, Van Hemert J, Hong L, Wise RP, Dickerson JA (2012) PLEXdb: gene expression resources for plants and plant pathogens. Nucl Acids Res 40: 1194-1201

De Angeli A, Baetz U, Francisco R, Zhang J, Chaves MM, Regalado A (2013a) The vacuolar channel VvALMT9 mediates malate and tartrate accumulation in berries of Vitis vinifera. Planta 238: 283-291

De Angeli A, Zhang JB, Meyer S, Martinoia E (2013b) AtALMT9 is a malate-activated vacuolar chloride channel required for stomatal opening in *Arabidopsis*. Nat Commun 4: 1804

Delhaize E, Gruber BD, Ryan PR (2007) The roles of organic anion permeases in aluminium resistance and mineral nutrition. FEBS Lett 581: 2255-2262

Doolittle RF, Kyte J (1982) A simple method for displaying the hydropathic character of a protein. J Mol Biol 157: 105-132

Dreyer I, Gomez-Porras JL, Riano-Pachon DM, Hedrich R, Geiger D (2012) Molecular evolution of slow and quick anion channels (SLACs and QUACs/ALMTs). Front Plant Sci 3: 263

Eckardt NA (2000) Sequencing the Rice Genome. Plant Cell 12: 2011-2018.

Gruber BD, Delhaize E, Richardson AE, Roessner U, James RA, Howitt SM, Ryan PR (2011) Characterisation of *HvALMT1* function in transgenic barley plants. Funct Plant Biol 38: 163-175

Gruber BD, Ryan PR, Richardson AE, Tyerman SD, Ramesh S, Hebb DM, Howitt SM, Delhaize E (2010) HvALMT1 from barley is involved in the transport of organic anions. J ExpBot 61: 1455-1467

Hirokawa T. B-CS, and Mitaku S. (1998) SOSUI: classification and secondary structure prediction system for membrane proteins. Bioinformatics 14: 378-379

Junshi Yazaki NK, Masahiro Ishikawa and Shoshi Kikuchi (2002) Rice Expression Database:the gateway to rice functional genomics. Trends Plant Sci 12: 563-564

Kim JS, Mizoi J, Yoshida T, Fujita Y, Nakajima J, Ohori T, Todaka D, Nakashima K, Hirayama T, Shinozaki K, Yamaguchi-Shinozaki K (2011) An ABRE promoter sequence is involved in osmotic stress-responsive expression of the DREB2A gene, which encodes a transcription factor regulating drought-inducible genes in Arabidopsis. Plant Cell Physiol 52: 2136-2146

Knudsen S (1999) Promoter 2.0: for the recognition of PolII promoter sequences. Bioinformatics 15: 356-361

Kovermann P, Meyer S, Hortensteiner S, Picco C, Scholz-Starke J, Ravera S, Lee Y, Martinoia E (2007) The Arabidopsis vacuolar malate channel is a member of the ALMT family. Plant J 52: 1169-1180

Lampe K (1995) Rice research: Food for 4 billion people. GeoJournal 35: 253-261

Lescot M, Dehais P, Thijs G, Marchal K, Moreau Y, Peer YVd, Rouze P, Rombauts S (2002) PlantCARE, a database of plant cis-acting regulatory elements and a portal to tools for in silico analysis of promoter sequences. NuclAcids Res 30: 325-327

Li JY, Wang J, Zeigler RS (2014) The 3,000 rice genomes project: new opportunities and challenges for future rice research. GigaScience 3:8

Meyer S, Mumm P, Imes D, Endler A, Weder B, Al-Rasheid KAS, Geiger D, Marten I, Martinoia E, Hedrich R (2010) AtALMT12 represents an R-type anion channel required for stomatal movement in Arabidopsis guard cells. Plant J 63: 1054-1062

Meyer S, Scholz-Starke J, De Angeli A, Kovermann P, Burla B, Gambale F, Martinoia E (2011) Malate transport by the vacuolar AtALMT6 channel in guard cells is subject to multiple regulation. Plant J 67: 247-257

Motoda H, Sasaki T, Kano Y, Ryan PR, Delhaize E, Matsumoto H, Yamamoto Y (2007) The membrane topology of ALMT1, an aluminum-activated malate transport protein in wheat (*Triticum aestivum*). Plant signal behav 2: 467-472

Mumm P, Imes D, Martinoia E, Al-Rasheid KA, Geiger D, Marten I, Hedrich R (2013) C-terminus-mediated voltage gating of Arabidopsis guard cell anion channel QUAC1. Mol Plant 6: 1550-1563

Narusaka Y, Nakashima K, Shinwari ZK, Sakuma Y, Furihata T, Abe H, Narusaka M, Shinozaki K, Yamaguchi-Shinozaki K (2003) Interaction between two cis-acting elements, ABRE and DRE, in ABA-dependent expression of Arabidopsis rd29A gene in response to dehydration and high-salinity stresses. Plant J 34: 137-148

Omasits U, Ahrens CH, Muller S, Wollscheid B (2014) Protter: interactive protein feature visualization and integration with experimental proteomic data. Bioinformatics 30: 884-886

Pineros MA, Cancado GMA, Maron LG, Lyi SM, Menossi M, Kochian LV (2008) Not all ALMT1-type transporters mediate aluminum-activated organic acid responses: the case of *ZmALMT1* - an anion-selective transporter. Plant J 53: 352-367

Pirkkla L, Nykänen P, Sistonen L (2001) Roles of the heat shock transcription factors in regulation of the heat shock response and beyond. FASEB J 15: 1118-1131

Punta M, Coggill PC, Eberhardt RY, Mistry J, Tate J, Boursnell C, Pang N, Forslund K, Ceric G, Clements J, Heger A, Holm L, Sonnhammer EL, Eddy SR, Bateman A, Finn RD (2012) The Pfam protein families database. Nucl Acids Res 40: 290-301

Ryan PR, Tyerman SD, Sasaki T, Furuichi T, Yamamoto Y, Zhang WH, Delhaize E (2011) The identification of aluminium-resistance genes provides opportunities for enhancing crop production on acid soils. J Exp Bot 62: 9-20

Sasaki T, Mori IC, Furuichi T, Munemasa S, Toyooka K, Matsuoka K, Murata Y, Yamamoto Y (2010) Closing plant stomata requires a homolog of an aluminum-activated malate transporter. Plant Cell Physiol 51: 354-365

Sasaki T, Yamamoto Y, Ezaki B, Katsuhara M, Ahn SJ, Ryan PR, Delhaize E, Matsumoto H (2004) A wheat gene encoding an aluminum-activated malate transporter. Plant J 37: 645-653

Szklarczyk D, Franceschini A, Wyder S, Forslund K, Heller D, Huerta-Cepas J, Simonovic M, Roth A, Santos A, Tsafou KP, Kuhn M, Bork P, Jensen LJ, von Mering C (2015) STRING v10: protein-protein interaction networks, integrated over the tree of life. Nucl Acids Res 43: 447-452

Tamura K, Peterson D, Peterson N, Stecher G, Nei M, Kumar S (2011) MEGA5: molecular evolutionary genetics analysis using maximum likelihood, evolutionary distance, and maximum parsimony methods. Mol Biol Evol 28: 2731-2739

Wang J, Kong L, Zhao S, Zhang H, Tang L, Li Z, Gu X, Luo J, Gao G (2011) Rice-Map: a new-generation rice genome browser. BMC Genomics 12: 165

Xu M, Gruber BD, Delhaize E, White RG, James RA, You J, Yang Z, Ryan PR (2015) The barley anion channel, HvALMT1, has multiple roles in guard cell physiology and grain metabolism. Physiol Plant 153: 183-193

Yang LT, Jiang HX, Qi YP, Chen LS (2012) Differential expression of genes involved in alternative glycolytic pathways, phosphorus scavenging and recycling in response to aluminum and phosphorus interactions in Citrus roots. Mol Biol Rep 39: 6353-6366

Zhang J, Baetz U, Krugel U, Martinoia E, De Angeli A (2013) Identification of a probable pore-forming domain in the multimeric vacuolar anion channel AtALMT9. Plant Physiol 163: 830-843

Zhang J, Martinoia E, De Angeli A (2014) Cytosolic nucleotides block and regulate the Arabidopsis vacuolar anion channel AtALMT9. J Biol Chem 289: 25581-25589

Zhong M, Orosz A, Wu C (1998) Direct sensing of heat and oxidation by drosophila heat shock transcription factor. Mol Cell 2: 101-108

CHAPTER 4

Sub-cellular localisation of OsALMT1

4.1 Introduction

The subcellular localization of a protein provides key insights into its function. A variety of methods can be used to identify the location of proteins or protein complexes in subcellular compartments (Sadowski *et al*., 2008). Some of these include in situ localization with antibodies to the target proteins or to epitopes tags on the protein, separation of cellular functions and antibody detection after gel separation, in-frame fusions with fluorescence probes such as green fluorescence protein (GFP) and mass spectrometry. The localization of membrane proteins with antibodies can be challenging at times because the preparation of membrane fractions need to be free of contaminants.

The cloning of the jellyfish *Green Fluorescent Protein* (*GFP*) gene and its successful modification for expression in plant cells provided a new suite of methods for localizing membrane proteins in cells (Köhler, 2001). In-frame ligations of the coding regions of fluorescence probes can be added to the 5' or 3' ends of the open reading frame (ORF) of the gene of interest (GOI) so that the fluorescencing protein tags on the N or C-terminal ends of the protein can be detected under fluorescent microscopes. These tags can alter the subcellular localisation of some protein. By using reverse transfection microarrays, Palmer and Freeman (2004) showed that N-terminal tagging with GFP can sometimes affect protein localization more than C-terminal tags which generally maintain localization patterns of the native protein (Palmer and Freeman, 2004).

In addition to GFP, other fluorescent probes with different excitation and emission wavelength are available and widely used as reporters. These are often described by the colour associated with the emission spectra (e.g. red, orange and yellow fluorescent proteins). The different excitation and emission wavelengths of these reporter proteins enables different proteins to be tagged and detected separately within the same cell (Shaner *et al.*, 2004). Other resources available to cell biologists are collections of control genes with known localization to membranes and sub-cellular organelles that are tagged with a variety of different fluorescent probes. These enable co-localisation studies

to be undertaken with different control genes and the gene of interest (GOI). Such an approach can help determine whether the GOI targets a particular membrane or organelle (Nelson *et al.*, 2007).

The subcellular localization of several members of the ALMT-protein family have been established using immunodetection or fluorescent reporters with stably transformed plants or with transient expression in protoplasts or other tissues such as tobacco (*Nicotiana benthamiana*) leaves or onion (*Allium cepa* L.), leek (*Allium ampeloprasum* var. porrum) tissues. Those ALMT proteins examined so far localise to different membranes but most reside on the plasma membrane. By using immunodetection and transient expression in onion epidermal cells and tobacco suspension-cultured cells, the TaALMT1 was probed to target to the plasma membrane (Yamaguchi *et al.*, 2005). The BnALMT1, ZmALMT2 and GmALMT1 proteins are localized in the plasma membrane by transiently expressing the fusion constructs in Arabidopsis leaf protoplasts (Liang *et al.*, 2013; Ligaba *et al.*, 2006; Ligaba *et al.*, 2012). Subcellular localization of ZmALMT1, HlALMT1 and ZmALMT2 are also target to the plasma membrane of onion epidermal cells by transient expression of the fusion proteins (Chen *et al.*, 2013a; Ligaba *et al.*, 2012; Pineros *et al.*, 2008). The AtALMT12 from Arabidopsis was localised to the plasma membrane by Meyer *et al*. (2010) using isolated protoplasts and Arabidopsis guard cell stably expressing AtALMT12-GFP fusion protein. Sasaki *et al*. (2010) by contrast concluded that AtALMT12 localized to the plasma membrane as well as unidentified endomembranes by particle bombardment of onion epidermal cells and *Vicia faba* guard cells (Meyer *et al.*, 2010; Sasaki *et al.*, 2010). The barley protein HvALMT1 was also detected on multiple membranes including the plasma membrane and motile vesicles within the cytoplasm (Gruber *et al.*, 2010). The transient expression of the fusion constructs in Arabidopsis and onion epidermal cells by particle bombardment demonstrated that AtALMT9 resides on the tonoplast. This result was further confirmed in guard cells of *Vicia faba* as the complex vacuolar membrane system in guard cells makes localization to the tonoplast easier to visualise (Kovermann *et al.*, 2007). AtALMT6 was also detected on the tonoplast by various systems such as transient expression in onion epidermal cells, and Arabidopsis mesophyll protoplasts as well as in stably-transformed Arabidopsis guard cells (Meyer *et al.*, 2011). AtALMT5 is an Arabidopsis protein with unknown function but transient expression of AtALMT5-GFP fusion proteins in Arabidopsis and onion epidermal cells found it localised to the

endoplasmic reticulum (ER) (Kovermann *et al.*, 2007). Localisation in the ER can sometimes be an artifact of the protein not moving correctly through the targeting system.

The aim of this chapter is to determine the sub-cellular localization of the OsALMT1 protein as an initial step for investigating its function in rice plants.

4.2 Materials and Methods

4.2.1 Plant materials

Tobacco (*Nicotiana benthamiana*) seeds were germinated and sprinkled onto a small, well-watered pot and left to grow for about 10 days (24 ℃; 16/8 light/dark cycles). Tobacco seedlings then were thinned to larger (15 cm diameter) pots with a "cereal" soil (from CSIRO potting shed standard mix of soil and compost) and grown at the same conditions for a further two weeks. The leaves of these tobacco plants are receptive to infiltration and transgene expression for many weeks into maturity.

Fresh leek (*Allium ampeloprasum* var. porrum) plants were bought from the local store and roots kept in water. The pale tissue from the base of the plant was used for bombardment. Tissue segments were prepared on the day of bombardment by slicing sections approximately 0.5 x 1.0 cm in size and lining five to ten of these next to one another on damp Kleenex tissue in the central region of a petri dish. Three to five such dishes were prepared for each construct.

4.2.2 Vector construction

Both the N and C-terminal fusions of GFP to OsALMT1 were constructed. For the N-terminal fusion, GFP::OsALMT1, the *OsALMT1* and *GFP* fragments were amplified with primers PRR117/PRR130 and PRR131/PRR132 respectively. The PCR products were purified and fused by a fusion PCR reaction using primers PRR117 and PRR132 (see **Chapter 2**). For the C-terminals fusion OsALMT1::GFP, the OsALMT1 and GFP fragments were amplified with primers PRR133/PRR134 and PRR135/PRR119. The

PCR products were purified and fused to one another by a fusion PCR reaction using primers PRR133 and PRR119. These PCR products was purified and ligated to pGEM®-T Easy vector (Promega). The resulting construct was transformed into *E. coli* DH5α and positive colonies were detected by PCR using primers PRR120 and PRR121. These primers straddle the GOI in the pGEM®-T Easy vector to demonstrate whether an insert is present of the correct size. The full construct was sequenced to confirm the absence of mutations due to PCR. For OsALMT1::GFP sequencing, primers PRR-103 and PRR-104 were used as middle primers, and for GFP::OsALMT1 sequencing, primers PRR-101 and PRR-102 were used as middle primers. Plasmids confirmed to have the correct insert were digested by *Eco*RI and *Bam*HI and the fragments ligated into the pART vector digested with the same emzymes (**Figure 4.1**). pART has the CaMV35S promoter. pART vectors with ligation products were transformed into *E. coli* DH5α and positive colonies were tested with PCR and enzyme digestion to ensure they contained vectors with the correct inserts. Confirmed clones were used to bombard leek tissues and for the construction of vectors for the transformation of *Nicotiana benthamiana* leaf tissue by infiltration.

To construct the vectors for tobacco transformation the pART7-OsALMT1::GFP and pART7- GFP::OsALMT1 plasmids were digested by *Not*I and ligated into the pWBVec8 vector (**Figure 4.2**). *E. coli* DH5α was then transformed with 2 µL of the ligation reaction and positive clones were detected by PCR and enzyme digestion. The positive clones were transformed into competent cells of AGI agrobacterium for later infiltration of tobacco leaves.

4.2.3 Leek bombardment

Biolistic® PDS-1000/He Particle Delivery System was used for leek bombardment.

Preparing gold particles: Gold particles (40 mg of Heraeus particles 0.4-1.2 µm in diameter or BIO-RAD Sub-micron particles 0.6µm in diameter) were weighed into a 1.5 ml Eppendorf tube with 1 ml 100% ethanol and sonicated for 2 min. Tubes were centrifuged for a 3 s pulse and supernatant removed. This step was repeated twice more before 1 mL sterile distilled water was added and sonicated for 2 min. The tubes were

centrifuged again for a 3 s pulse and the supernatant was removed. The pellet of gold was resuspended in 1 mL sterile distilled water and aliquoted into 50 µL volumes in sterile Eppendorfs while vortexing between each aliquot. All tubes were stored at -20 ℃.

Coating of gold particles: Aliquots of gold particles (50 µl) were thawed and sonicated for 1 to 2 min. Then 5 µL DNA (0.5 to 1 mg/µL) was added to the appropriate tubes and vortexed briefly to mix. Then 50 µL 2.5 M $CaCl_2$ and 20 µL 0.1 M spermidine was placed on the inner side of the open lid of the tubes and mixed together, and then vortexed onto the gold particles. This stabilized the DNA precipitation onto the gold particles. When ready to use 10 µL of the gold particles loaded with DNA were pipetted onto the macro carrier discs and allowed to spread and dry in the laminar flow cabinet.

Shooting the particles: The biolistic chamber was surface sterilized by wiping with 70% ethanol. The sterile rupture disk (~900 psi) was loaded at the top of bombardment chamber and tightened with a torque wrench. The macrocarrier with gold particles and stopping screen was loaded into the launch assembly. Prepared leek tissue was placed under the launch assembly and the chamber was closed and evacuated to a vacuum of approximately 8.5 kPa (26 inches Hg). The release button was fired. After the bombardment, the vacuum was released and tissues kept at room temperature in the dark. Images were captured after 6 to 28 hours using a Leica TCS SP2 confocal laser scanning.

4.2.4 Tobacco leaf infiltration

This method is a slight modification upon the protocol used in Wood *et al.* (2009) and Petrie *et al.* (2010).

Preparing the Agrobacterium: Agrobacterium colonies containing each of the various vectors prepared were suspended in 5 mL LB with antibiotics for selection (rifampicillin) until the optical density (OD_{600nm}) was 1.0 - 1.5. Acetosyringone (AS) was added to each culture to a final concentration of 100 µM from a 100 mM stock (DMSO stored at -20 ℃) and left for a further 2-3 hours to induce the virulence genes required for infection. Three hours prior to use the plants were taken from the growth cabinets to a well-light room (28 ℃) and watered to promote stomata opening.

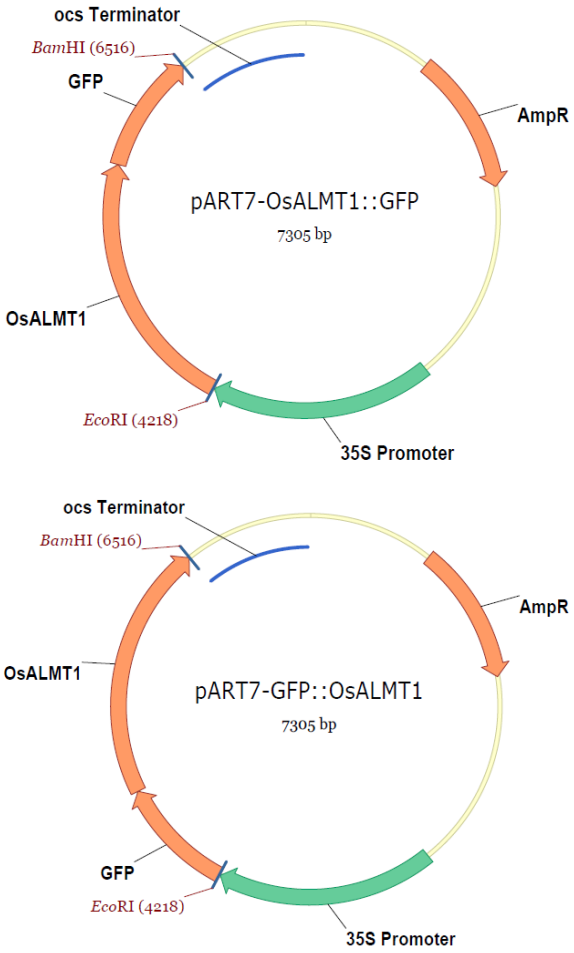

Figure 4.1 Vector maps of pART7-OsALMT1::GFP and pART7-GFP::OsALMT1

Vector maps of pART7-OsALMT1::GFP and pART7-GFP::OsALMT1 used for sub-cellular localization in leek cells. The orange arrow represents coding DNA sequence (CDS) and the direction of the arrow is the same as the gene transcription direction.

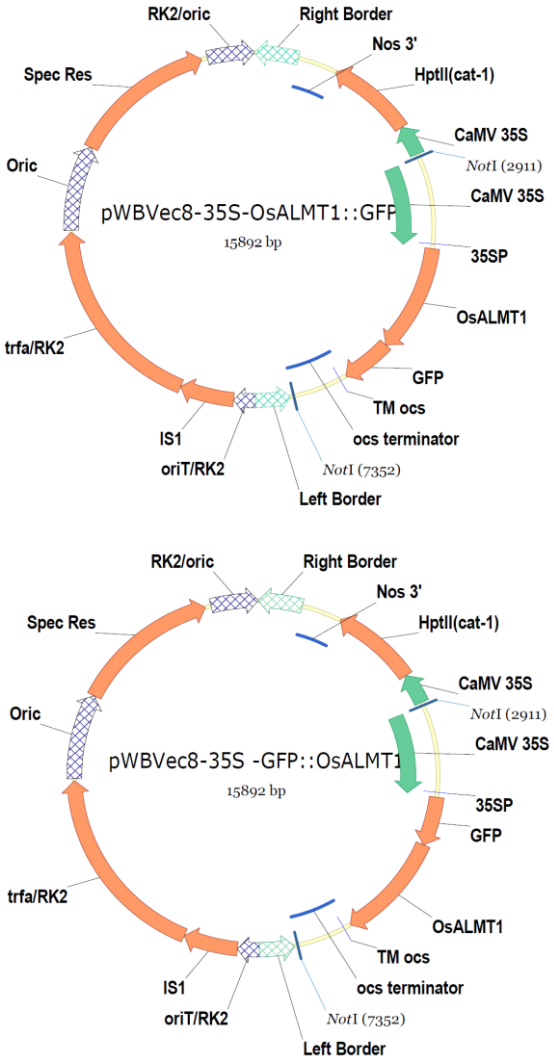

Figure 4.2 Vector maps used for sub-cellular localisation of OsALMT1

Vector used for localization in tobacco leaves. Coloured arrows represent different elements: Orange arrows represent coding DNA sequence (CDS) and the direction of the arrow is the same as the gene transcription direction, dark green arrow represents promoter, light hollow green arrow represents transfer border and bold blue line along the plasmid represents terminator. The fine blue line cross the plasmid represents primer binding site (e.g. 35SP) and the bold blue line cross the plasmid represent restriction enzyme site. This plasmid contains cauliflower mosaic virus (CaMV) 35S promoter (35S promoter) which is a very strong constitutive promoter causing high levels of gene expression in dicot plants, ocs and nos3' terminators which are transcriptional terminators for transgenes in plants, the *hptII* conferring hygromycin resistance for selection in planta, the "*Spec Res"* gene for spectinomycin selection in Agrobacteria. Transfer is initiated at the right border and terminated at the left border.

Infiltration: Agrobacterium cultures were transferred to 10 mL tubes and centrifuged at 4000 rpm in a Sigma benchtop centrifuge at room temperature for 5 minutes. The supernatant was removed and cells gently resuspended in ~2.5 mL Infiltration Media (5 mM $MgCl_2$ and 5 mM MES, adjusted to pH 5.7 with KOH or NaOH) and 100 µM AS. The OD_{600nm} of the cultures was adjusted to approximately 1.0 with Infiltration Media with 100 µM AS. The cultures were returned to the growth room for a further 20 minutes while final calculations were made regarding the solution and dilutions required. The cultures were then adjusted to OD_{600nm} 0.3. Finally a 1 mL syringe (no needle) was used to draw up the culture. It was placed flat on the underside of the leaf surface and the culture gently pushed into the tissue. The wetness can be seen spreading through the tissue. The area of the leaf was then marked with a pen so it can be distinguished at a later date.

After infiltration: Gene expression is strongest three to four days after infiltration but continues for more than 10 d. Plants were watered well. GFP fluorescence was visualised with a BlueStar flashlight packages (BLS2 - BlueStar Flashlight and Model VG2 barrier filter and glasses, Electron Microscopy Sciences). Images were captured after three to five days using a Leica TCS SP2 confocal laser scanning.

4.2.5 Co-localization system

Co-infiltration of tobacco leaves agrobacterium containing different constructs allowed two proteins tagged with different fluorophores. This enabled control proteins with known localization characteristics to be expressed in the same cells as the GOI. A plasma membrane localized control protein named pm-rk with the mCherry fluorophore was obtained (Stock 4011591933, http://www.bio.utk.edu/cellbiol/markers/) (Nelson *et al.*, 2007) (**Figure 4.3**). The pm-rk is an aquaporin gene from the *PIP* family. The mCherry fluorophore has suitably different excitation and emission wavelengths so that overlap of the signals from GFP and mCherry is minimized. For GFP, the excitation laser wavelength was set at 488 nm and the emission collection bin was range between 480-600 nm. For mCherry, the excitation laser wavelength was set at 587 nm and the emission collection bin was range between 600-680 nm. The pm-rk plasmid was isolated

and transformed into AGI agrobacterium competent cells. These cultures were prepared as above and then mixed with the GFP constructs prior to infiltration.

The same control contruct that expresses pm-rk (plasma membrane-localizing protein fused with the mCherry fluorophore) was also co-bombarded in leek. A plasmid preparation was made (1 mg/µl) and mixed with both the pART7-OsALMT1::GFP or pART7-GFP::OsALMT1 plasmids and treated as described above. Software in confocal microscope software enables images from these two fluorescent probes to be recorded and then overlaid to determine whether they co-localise or not.

4.3 Results

4.3.1 Sub-cellular localization in leek

OsALMT1 was transiently expressed in leek with GFP fused to either the C or N-terminal ends. A control construct included in these experiments expressed soluble GFP using the CaMV35S promoter. Fluorescence detected from control cells (expressing GFP only) showed the typical distribution of a soluble protein with strong signals in the nucleus (**Figure 4,4 a-b**). For the N-terminal (GFP::OsALMT1) and C-terminal (OsALMT1::GFP) constructs fluorescence could be observed around the cell periphery but not in any other internal organelles which is consistent with OsALMT1 localising to the plasma membrane (**Figure 4.4 c-f**).

4.3.2 Sub-cellular localization in tobacco

OsALMT1 was transiently expressed in tobacco leaf cells with GFP fused to either the C or N- terminal ends. The GFP control generated strong signals in the nucleus and around the periphery which is consistent with soluble protein in the cytosol (**Figure 4.5 a-b**). Fluorescent signals from the N-terminal (GFP::OsALMT1) and C-terminal (OsALMT1::GFP) GFP fusions could be also be detected around the cell periphery but not any other internal organelles (**Figure 4.5 c-f**). These results are consistent with OsALMT1 localising to the plasma membrane.

In order to test the idea that OsALMT1 localises to the plasma membrane tobacco cells expressing the GFP::OsALMT1 fusion were plasmolysed by gently applying drops of 50% sucrose to the surface of the leaf. After several minutes water begins to move out of the cells and the plasma membrane retracts from the cell walls (**Figure 4.5 g-h**). As the plasma membrane retracts Hechtian strands appear (Lang-Pauluzzi and Gunning, 2000). These are residual connections between the cell wall and the plasma membrane. Since the Hechtian strands show strong GFP fluorescence it supports the hypothesis that OsALMT1 is located on the plasma membrane (**Figure 4.5 i)**.

A second test for the localisation of OsALMT1 involved co-expressing GFP::OsALMT1 fusion with a control protein known to localise to the plasma membrane. The control protein, denoted as pm-rk, is tagged with a different fluorophore, mCherry, so it can be detected in a cell that is also expressing GFP (Nelson *et al.*, 2007). GFP::OsALMT1 and the pm-rk control were transiently expressed in the same leek cells. GFP and mCherry fluorescence was detected in the periphery of the same cell but nowhere internally (**Figure 4.6 a-c**). When these signals were laid over one another there was a good co-incidence of the signals (**Figure 4.6 d**). Similar results were obtained in tobacco tissue co-infiltrated with the GFP::OsALMT1 and pm-rk constructs (**Figure 4.6 e-h**). The areas where the overlap were not perfect will be, in part, due to the slight offset of the lasers from one another but it could also reflect differences in fluorophore intensities. Taken together, these results indicate that the OsALMT1 protein localises to the plasma membrane.

4.4 Discussion

The function of a protein is closely linked with its subcellular localization, and so determining the subcellular localization of a protein is an essential step for inferring its function. OsALMT1 was predicted to have six transmembrane regions by different algorithms and to likely reside on the plasma membrane (see **Chapter 3**). In order to determine subcellular localisation of OsALMT1 experimentally, the reporter gene GFP was fused to the N- and C- terminal ends of the protein. Fusions at both ends were generated since protein localisation can sometimes be disrupted by these fusions. Some reports indicate that N-terminal tagging with GFP adversely affects the protein

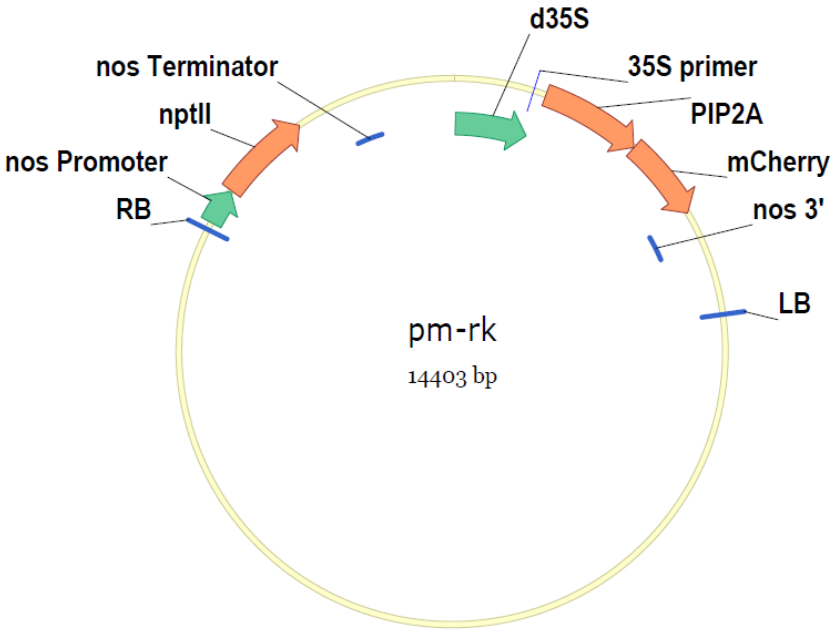

Figure 4.3 Vector map of the plasma-membrane localising control protein pm-rk fused with the mCherry fluorophore

The construct was made by the Arabidopsis Biological Resource Centre (stock # CD3-1007 with the TAIR accession of Stock 4011591933). This plasma membrane-mCherry marker was constructed by using CaMV35S promoter to drive expression of the *Arabidopsis thaliana* plasma membrane intrinsic protein 2a (PIP2A, GenBank: X75883.1) fused with mCherry. The fused fragment was ligated to PBIN20 vector background and selected for kanamycin resistance based on the *nptII* gene.

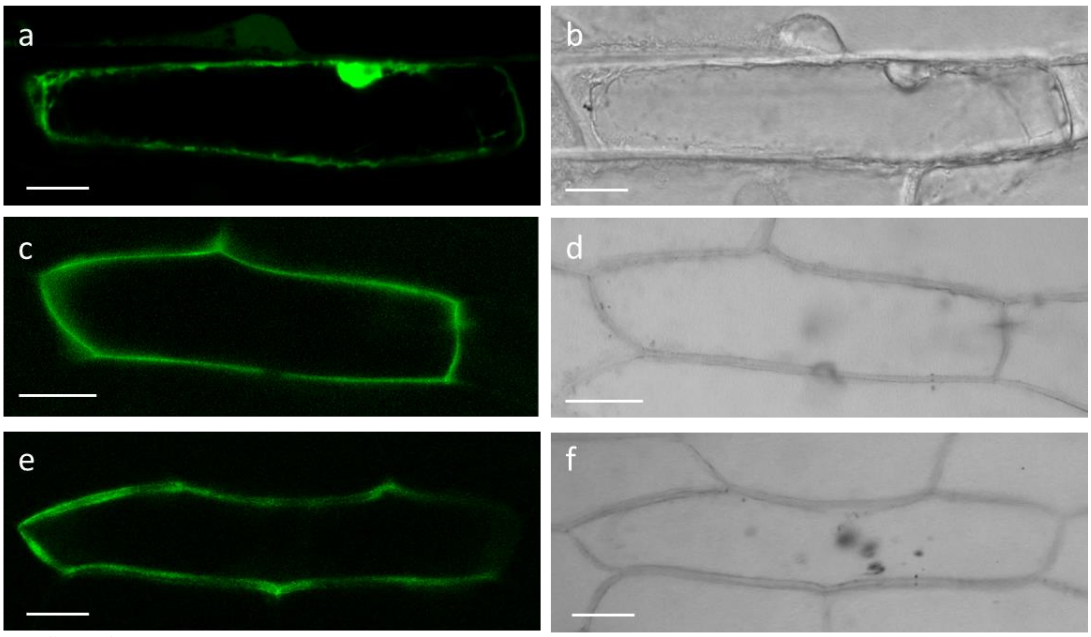

Figure 4.4 OsALMT1 protein localises to the periphery of leek cells

GFP was fused to the N- and C-terminal ends of OsALMT1 protein and transiently expressed in leek epidermal cells by bombardment. Soluble GFP was expressed as a control. a, Fluorescence image of leek tissue bombarded with a construct containing soluble GFP showing the fluorescence in the nucleus indicating presence in the cytosol; b, Bright-field image of the tissue in a; c, Fluorescence image of GFP::OsALMT1 showing GFP fluorescence around the periphery of a single cell but not in the nucleus; d, Bright-field image of the tissue in c; e, Fluorescence image of the OsALMT1::GFP construct showing GFP fluorescence around the periphery of a single cell but not in the nucleus; f, Bright-field image of the same tissue in e. Scale bar=50 µm

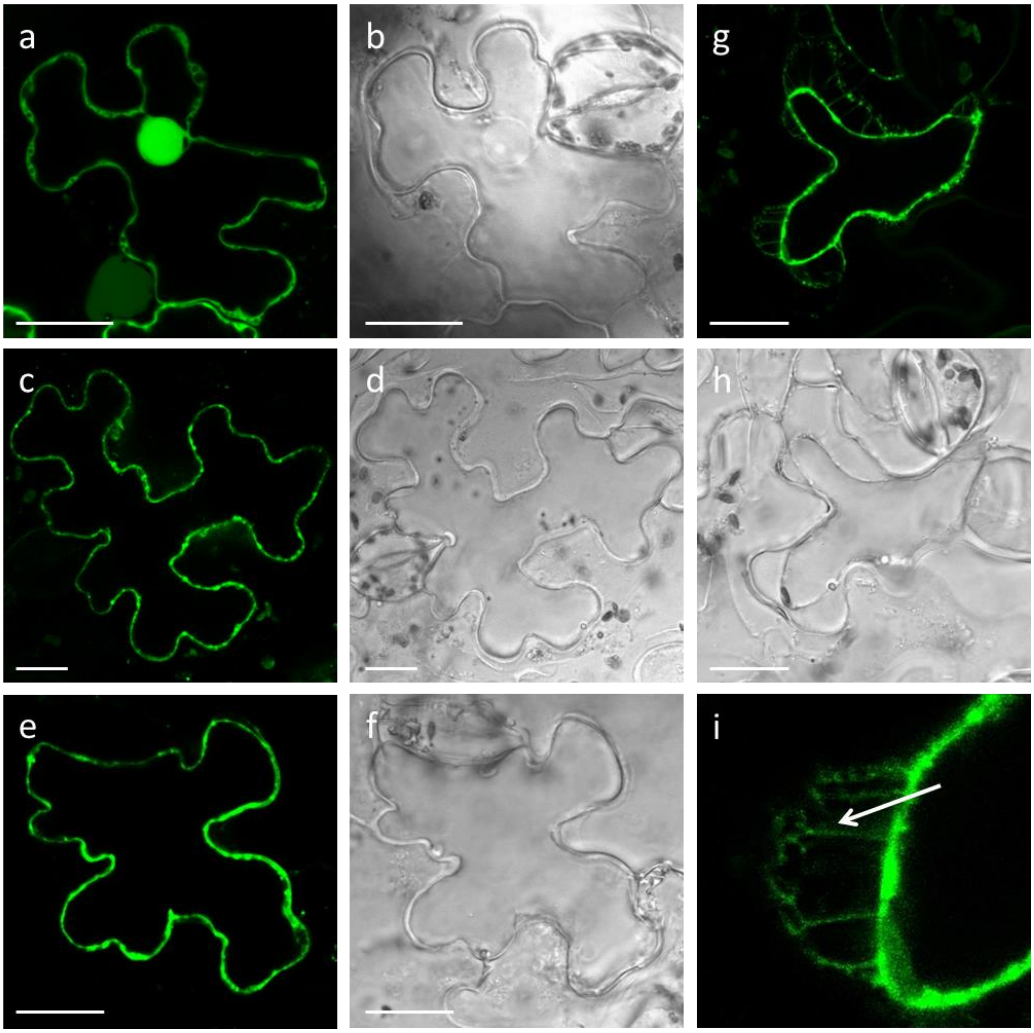

Figure 4.5 OsALMT1 localises to the plasma membrane of tobacco cells

GFP was fused to the N- and C-terminal ends of OsALMT1 protein and transiently expressed in tobacco cells by Agrobacteria infiltration. The GFP-only construct was infiltrated separately as a control. a, Fluorescence image of tobacco tissue transformed with the control construct showing fluorescence in the nucleus and cytosol; b, Bright-field image of the same tissue with a; c, Fluorescence image of the N-terminal fusion of GFP to OsALMT1 showing GFP fluorescence around the periphery of a single cell; d, Bright-field image of the same tissue with c; e, Fluorescence image of the C-terminal fusion of GFP to OsALMT1 showing GFP fluorescence around the periphery of a single cell; f, Bright-field image of the same tissue with e; g, A tobacco cell expressing the N-terminal fusion of GFP to OsALMT1 after plasmolysis with 0.5 M sucrose; h, Bright-field image of the same tissue with g; i, The Hechtian strands that connect the cell wall with the retreating protoplast (arrow). Scale bar=20 μm.

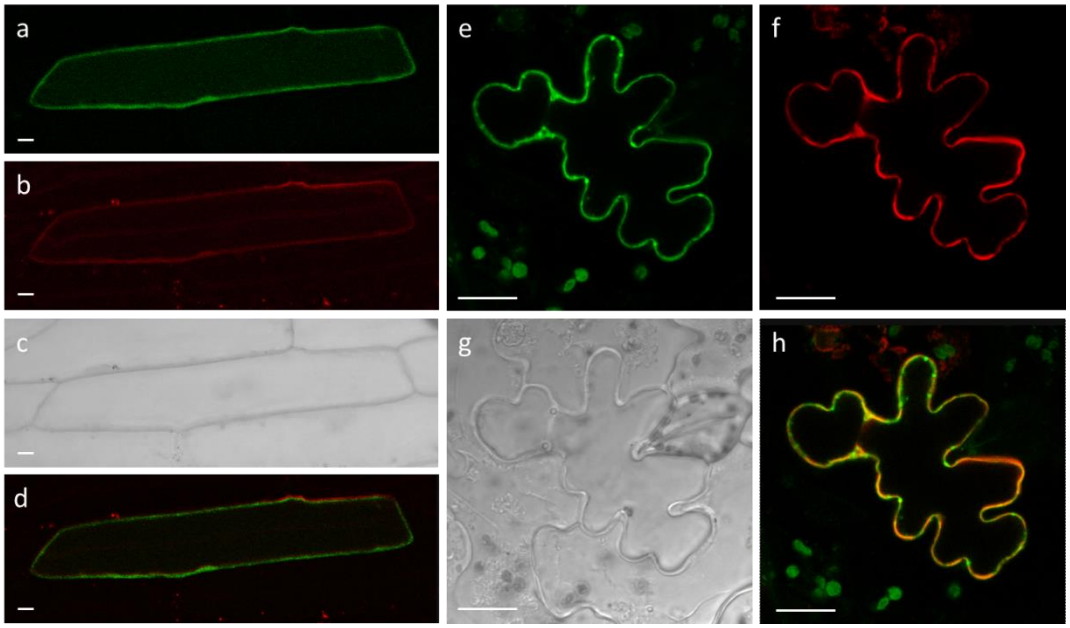

Figure 4.6 Co-localisation of OsALMT1 with the plasma membrane marker

Transient expression of the GFP::OsALMT1 fusion protein and plasma membrane control protein tagged with the mCherry fluorophore in the leek and tobacco cells. a, GFP fluorescence image of leek tissue transformed with a construct containing OsALMT1 N-terminal GFP fusion showing the fluorescence around the periphery of a single cell; b, DsRed fluorescence image of leek tissue transformed with a construct containing plasma membrane mCherry marker showing the fluorescence around the periphery of a single cell; c, Bright-field image of the same tissue with a and b; d, Merged image of a and b; e, GFP fluorescence image of tobacco leaf cell transformed with a construct containing OsALMT1 N-terminal GFP fusion showing the fluorescence around the periphery of a single cell; f, DsRed fluorescence image of tobacco leaf cell transformed with a construct containing plasma membrane mCherry marker showing the fluorescence around the periphery of the same cell; g, Bright-field image of the same tissue with e and f; h, Merged image of e and f. Scale bar=20 μm

localization in reverse transfection assays, while tagging with GFP at the C-terminal end was generally better in preserving the localization of the native protein (Palmer and Freeman, 2004). In our study, the localisation results for the GFP::OsALMT1 and OsALMT1::GFP constructs showed strong fluorescence largely around the periphery of single tobacco and leek cells but not other cellular compartments which provided the first indication that OsALMT1 likely localized to the plasma membrane (Collings, 2013).The results from leek cells and tobacco leaf tissues are consistent with each other and these results are also identified with the CELLO prediction. To confirm the subcellular localisation of OsALMT1 two independent approaches were used with the transient systems. These involved looking for Hechtian strands in plasmolysed cells (Lang-Pauluzzi and Gunning, 2000) and co-localisation of the OsALMT1 protein with a control protein known to localise to the plasma membrane. The latter approach used a plasma membrane-localized water channel protein fused with the mCherry reporter gene marker. The results for both were consistent with OsALMT1 localising to the plasma membrane but futher confirmation with immunolocalisation with antibodies on fixed tissues would be helpful. This chapter established that the OsALMT1 protein is localised to the plasma membrane.

4.5 References

Chen Q, Wu KH, Wang P, Yi J, Li KZ, Yu YX, Chen LM (2013a) Overexpression of *MsALMT1*, from the aluminum-sensitive *Medicago sativa*, enhances malate exudation and aluminum resistance in tobacco. Pl Mol Biol Rep 31: 769-774

Chen ZC, Yokosho K, Kashino M, Zhao FJ, Yamaji N, Ma JF (2013b) Adaptation to acidic soil is achieved by increased numbers of cis-acting elements regulating *ALMT1* expression in *Holcus lanatus*. Plant J 76: 10-23

Collings D (2013) Subcellular localization of transiently expressed fluorescent fusion proteins. Meth Mol B 1069: 227-258

De Angeli A, Baetz U, Francisco R, Zhang J, Chaves MM, Regalado A (2013a) The vacuolar channel VvALMT9 mediates malate and tartrate accumulation in berries of *Vitis vinifera*. Planta 238: 283-291

De Angeli A, Zhang JB, Meyer S, Martinoia E (2013b) AtALMT9 is a malate-activated vacuolar chloride channel required for stomatal opening in *Arabidopsis*. Nat Commun 4: 1804

Gruber BD, Ryan PR, Richardson AE, Tyerman SD, Ramesh S, Hebb DM, Howitt SM, Delhaize E (2010) HvALMT1 from barley is involved in the transport of organic anions. J Exp Bot 61: 1455-1467

Köhler MRHaRH (2001) GFP imaging: methodology and application to investigate cellular compartmentation in plants. J Exp Bot 52: 529-539

Kovermann P, Meyer S, Hortensteiner S, Picco C, Scholz-Starke J, Ravera S, Lee Y, Martinoia E (2007) The *Arabidopsis* vacuolar malate channel is a member of the ALMT family. Plant J 52: 1169-1180

Lang-Pauluzzi I, Gunning BES (2000) A plasmolytic cycle: the fate of cytoskeletal elements. Protoplasma 212: 174-185

Liang CY, Pineros MA, Tian J, Yao ZF, Sun LL, Liu JP, Shaff J, Coluccio A, Kochian LV, Liao H (2013) Low pH, aluminum, and phosphorus coordinately regulate malate exudation through *GmALMT1* to improve soybean adaptation to acid soils. Plant Physiol 161: 1347-1361

Ligaba A, Katsuhara M, Ryan PR, Shibasaka M, Matsumoto H (2006) The *BnALMT1* and *BnALMT2* genes from rape encode aluminum-activated malate transporters that enhance the aluminum resistance of plant cells. Plant Physiol 142: 1294-1303

Ligaba A, Maron L, Shaff J, Kochian L, Pineros M (2012) Maize ZmALMT2 is a root anion transporter that mediates constitutive root malate efflux. Plant Cell Environ 35: 1185-1200

Meyer S, Mumm P, Imes D, Endler A, Weder B, Al-Rasheid KAS, Geiger D, Marten I, Martinoia E, Hedrich R (2010) AtALMT12 represents an R-type anion channel required for stomatal movement in *Arabidopsis* guard cells. Plant J 63: 1054-1062

Meyer S, Scholz-Starke J, De Angeli A, Kovermann P, Burla B, Gambale F, Martinoia E (2011) Malate transport by the vacuolar AtALMT6 channel in guard cells is subject to multiple regulation. Plant J 67: 247-257

Nelson BK, Cai X, Nebenfuhr A (2007) A multicolored set of in vivo organelle markers for co-localization studies in *Arabidopsis* and other plants. Plant J 51: 1126-1136

Palmer E, Freeman T (2004) Investigation into the use of C- and N-terminal GFP fusion proteins for subcellular localization studies using reverse transfection microarrays. Compar Funct Genom 5: 342-353

Petrie JR, Shrestha P, Liu Q, Mansour MP, Wood CC, Zhou XR, Nichols PD, Green AG, Singh SP (2010) Rapid expression of transgenes driven by seed-specific constructs in leaf tissue: DHA production. Plant Methods 6: 8

Pineros MA, Cancado GMA, Maron LG, Lyi SM, Menossi M, Kochian LV (2008) Not all ALMT1-type transporters mediate aluminum-activated organic acid responses: the case of ZmALMT1 - an anion-selective transporter. Plant J 53: 352-367

Sadowski PG, Groen AJ, Dupree P, Lilley KS (2008) Sub-cellular localization of membrane proteins. Proteomics 8: 3991-4011

Sasaki T, Mori IC, Furuichi T, Munemasa S, Toyooka K, Matsuoka K, Murata Y, Yamamoto Y (2010) Closing plant stomata requires a homolog of an aluminum-activated malate transporter. Plant Cell Physiol 51: 354-365

Shaner NC, Campbell RE, Steinbach PA, Giepmans BN, Palmer AE, Tsien RY (2004) Improved monomeric red, orange and yellow fluorescent proteins derived from *Discosoma* sp. red fluorescent protein. Nat Biotechnol 22: 1567-1572

Wood CC, Petrie JR, Shrestha P, Mansour MP, Nichols PD, Green AG, Singh SP (2009) A leaf-based assay using interchangeable design principles to rapidly assemble multistep recombinant pathways. Plant Biotechnol J 7: 914-924

Yamaguchi M, Sasaki T, Sivaguru M, Yamamoto Y, Osawa H, Ahn SJ, Matsumoto H (2005) Evidence for the plasma membrane localization of Al-activated malate transporter (ALMT1). Plant Cell Physiol 46: 812-816

CHAPTER 5

Tissue-specific expression of *OsALMT1*

5.1 Introduction

Where a gene is expressed in the plant and when it is expressed is linked with its physiological functions. Therefore determining the location and timing of expression in a plant is another important step for understanding its function. Transcriptional regulation is largely controlled by the promoter region of the gene which initiates transcription. Promoters have been defined as modulatory DNA structures containing an array of *cis*-acting regulatory elements required for accurate and efficient initiation of transcription and for controlling expression of a gene (Ven, 1996). Therefore promoters are regions of DNA upstream of the transcription start site and coding region of a gene which affect its expression: when, where and how much. The length of promoters are difficult to ascertain but in plants that usually range between 100 bp to 2,000 bp. While this is the most important region controlling gene expression sometimes other regions of the non-coding regions of a gene (e.g. introns or regions downstream of the coding region) can also affect expression (Parra *et al.*, 2011)

Expression in more than one tissue or plant developmental stage may require distinct combinations of tissue specific transcription factors, especially if the gene responds to extracellular signals as well as having tissue-specific or cell-specific expression (Ven, 1996). The *cis*-elements, to which tissue-specific, development-specific, or stress-related transcription factors bind on a promoter, individually or in combination, determine the spatio-temporal expression pattern of transcriptional level (Tjian, 2000).

Relative gene expression can be measured in tissues with quantitative reverse transcription polymerase chain reaction (qRT-PCR). The limitation of this technique is that RNA is extracted from a target tissue and cell specificity is lost. For instance, it is impossible to determine whether expression of a gene occurred evenly throughout the tissue extracted or whether it only occurred in a subset of cells in that tissue. The development of reporter genes over the last 20 years does allow this information to be obtained because these techniques link gene expression in specific tissues or cell types

with colour reactions or spectrophotometric signals. In general terms, this approach relies on a promoter of interest being cloned and ligated into a plasmid to drive the expression of a reporter gene in a transgenic cell or organism. When a colour change is detected in that tissue then it indicates that the promoter was active at that time and place and this helps elucidate what functions the gene is linked with in wild type plants. Common reporter genes include the *E. coli LacZ* gene which encodes β-galactosidase, and was originally used as a reporter gene in single-celled systems like *C. elegans* (Fire A *et al.*, 1990). However plants have endogenous β-galactosidase activity so *lacZ* cannot be employed as a reporter gene in plants. Instead the transient or stable expression of the *E. coli* 3-glucuronidase (GUS) (Jefferson *et al.*, 1987) or green fluorescent protein (*GFP*) genes (Martin Chalfie *et al.*, 1994) in transgenic plants are now widely used to map gene expression and analyse promoter function. The primary advantage of GFP over GUS is the ability to visualize reporter gene expression in live cells rather than in fixed preparations. The same plant tissue can also be visualized through time with the GFP technique.

Information on the tissue-specific expression of *ALMT*s is only available for a small number of members. The *ALMT*s that are involved with Al resistance in wheat, rye and Arabidopsis are known to be expressed mainly in the root apices but a detailed investigation of these genes throughout those plants is not available (Collins *et al.*, 2008; Hoekenga *et al.*, 2006; Sasaki *et al.*, 2004). The rye (*Secale cereale L.*) *Alt4* Al-tolerance locus contains a cluster of genes homologous to the single-copy *TaALMT1* gene of wheat. Tolerant (M39A-1-6) and intolerant (M77A-1) rye haplotypes contain five and two genes, respectively, of which (*ScALMT1-M39.1* and *ScALMT1-M39.2*) and (*ScALMT1-M77.1*) are highly expressed in the root tip which is an important site for Al tolerance in plants (Collins *et al.*, 2008). The *TaALMT1* homologs from rape (*Brassica napus*), *BnALMT1* and *BnALMT2*, were also appear to confer Al resistance because the expression of these genes were induced in roots by treatment with Al and some other trivalent cations (e.g. lanthanum, ytterbium and erbium) (Ligaba *et al.*, 2006). *ALMT*s likely to be involved in Al tolerance in alfalfa (*Medicago sativa*), soybean (*Glycine max*) and Yorkshire fog (*Holcus lanatus*) (ie. *MsALMT1, GmALMT1* and *HlALMT1* respectively) were also found to be expressed in the root tissue (Chen *et al.*, 2013a; Chen *et al.*, 2013b; Liang *et al.*, 2013). Ryan *et al.* (2010) used the GFP reporter gene in transgenic rice plants to demonstrate that the tandem repeats present in the promoter of *TaALMT1* in Al-tolerant

genotypes of wheat increase expression in the root apices but a detailed analysis of other tissues was not undertaken (Ryan *et al.*, 2010).

Some *ALMT*s showing strong expression in guard cells are involved with regulating stomatal aperture. For example, transgenic Arabidopsis plants expressing the *GUS* reporter gene with the *AtALMT12* promoter showed strong GUS activity in guard cells as well as various other tissues including pollen and the root stele (Meyer *et al.*, 2010; Sasaki *et al.*, 2010). Similarly, Arabidopsis plants expressing *GUS* under the control of a 1.881 bp promoter region from *AtALMT6* also showed high expression in guard cells although some expression was also detected in stems and floral organs (Meyer *et al.*, 2011). Similar constructs with the *AtALMT9* promoter demonstrated that this gene is expressed widely in the plant but, in leaves, GUS activity was almost exclusively in guard cells and mesophyll cells (De Angeli *et al.*, 2013; Kovermann *et al.*, 2007). The barley (*Hordeum vulgare*) gene *HvALMT1* shows a high identity to *TaALMT1* from wheat but instead of contributing to Al tolerance, it is expressed in guard cells (Gruber *et al.*, 2010; Xu *et al.*, 2015). Once again this was determined in transgenic barley plants in which GFP expression was driven by the 2.906 bp upstream of *HvALMT1*. Fluorescence was also observed in the roots of those plants particularly in a region behind the root tip, at the site of emerging lateral roots, and in newly emerged lateral roots. Further investigation also found *HvALMT1* is expressed in the nucellar projection, the aleurone layer and the scutellum of developing barley grain (Gruber *et al.*, 2010; Xu *et al.*, 2015). All these results provided valuable information about the pattern of expression of these genes and give clues to their function.

The aim of this chapter is to investigate the tissue-specific expression of *OsALMT1* in rice.

5.2 Materials and methods

5.2.1 Vector construction

The plasmid vector used to map *OsALMT1* expression in transgenic rice was modified from the construct used to investigate the *HvALMT1* promoter in barley (Gruber *et al.*, 2010). The 2496 bp region upstream of the *OsALMT1* transcription start site was cloned

(see **Chapter 3**) and ligated into the plasmid called "PS1aGFP-OsALMT1 promoter" using restriction sites *Pac*I and *Asc*I (**Figure 5.1**). The promoter was used to drive GFP expression. A maize *Adh1* intron was inserted between the promoter and the *GFP* coding region to enhance expression levels. The plasmid was transformed into *E. coli* DH5α and positive clones were detected by PCR and enzyme digestion. Positive clones were then transformed into competent cells of AGL agrobacterium and prepared for rice transformation. Transgenic rice lines were generated as described in **Chapter 2**.

5.2.2 Tissue collection time and method

The transgenic plants were grown in glasshouse conditions in hydroponics and in soil (see **Chapter 2**). At various stages of growth leaf, root and flower tissues and developing grain were collected and examinied for GFP signals. T1 seed collected from the T0 plants was germinated and seedlings examined at different stages of development. Non-transformed wild type (WT) plants were also included to account for any background auto-fluorescence that might be present.

The root and leaf tissues were collected two weeks after transferring plants to nutrient solution from the tissue culture. The flower tissues were collected at ~10:00 am on the day of flowering. Developing grains were collected and checked 14 d (for milk stage) and 28 d (for dough stage) after flowering and the germination of mature grain was monitored daily from 10 d after germination. GFP fluorescence was examined and photographed with a Leica MZFLIII fluorescence dissecting microscope (Excitation filter: 425-60 nm, Barrier filter: 480 nm) and Leica SP2 confocal laser scanning microscope (Excitation laser wavelength: 488 nm, emission collection bin: 480-600 nm). Plant tissues were examined as quickly as possible after dissection to eliminate the auto-fluorescence which is sometimes associated with cell death.

5.3 Results

5.3.1 Distribution of *OsALMT1* expression in rice roots

Transgenic T0 rice plants in which GFP expression was driven by the *OsALMT1* promoter (*OsALMT1* promoter::GFP) were removed from their tissue culture pots to hydroponics and grown for two weeks. Wild type plants were also grown in hydroponics to provide non-transgenic controls. The plants were removed from hydroponics and transferred to the microscopy laboratory in a beaker with growth solution. Examination of newly grown roots under the dissecting microscope detected GFP signals at the root apices near the meristematic region (**Figure 5.2 a-b**). No similar fluorescence was detected in wild-type plants. Transverse sections were prepared from newly emerged roots when they were two to three centimeters long and fluorescence was detected in most cell layers. Fluorescence in the central vascular tissue and exodermis was particularly strong. Transverse sections of more mature root tissues also showed high fluorescence in the central vascular tissue and also the root hairs (**Figure 5.2 c-h**). Transverse sections through different root growth zones shows fluorescence in all cell layers especially in the exodermis layer near the root apex (**Figure 5.3 a**) while cross-sections of the mature root show high fluorescence in what appears to be the sclerenchymatous layer, exodermis, root hairs and epidermal layers of newly emerging lateral roots (**Figure 5.3 b, d and f**).

5.3.2 Distribution of *OsALMT1* expression in rice leaves

In two week old plants fluorescence was observed in both abaxial surface of leaf blade and outer surface of leaf sheath (**Figure 5.4 a-d**) but no expression was detected in the guard cells. These plants were treated with darkness prior to measurements to reduce background fluorescence. High GFP expression was also observed in the ligule and auricle which occur at the junction of the leaf blade and sheath (**Figure 5.4 e-h**). Transverse sections of newly emerged tillers also showed fluorescence especially in the vascular bundles and xylem parenchyma tissues (**Figure 5.4 i-l**).

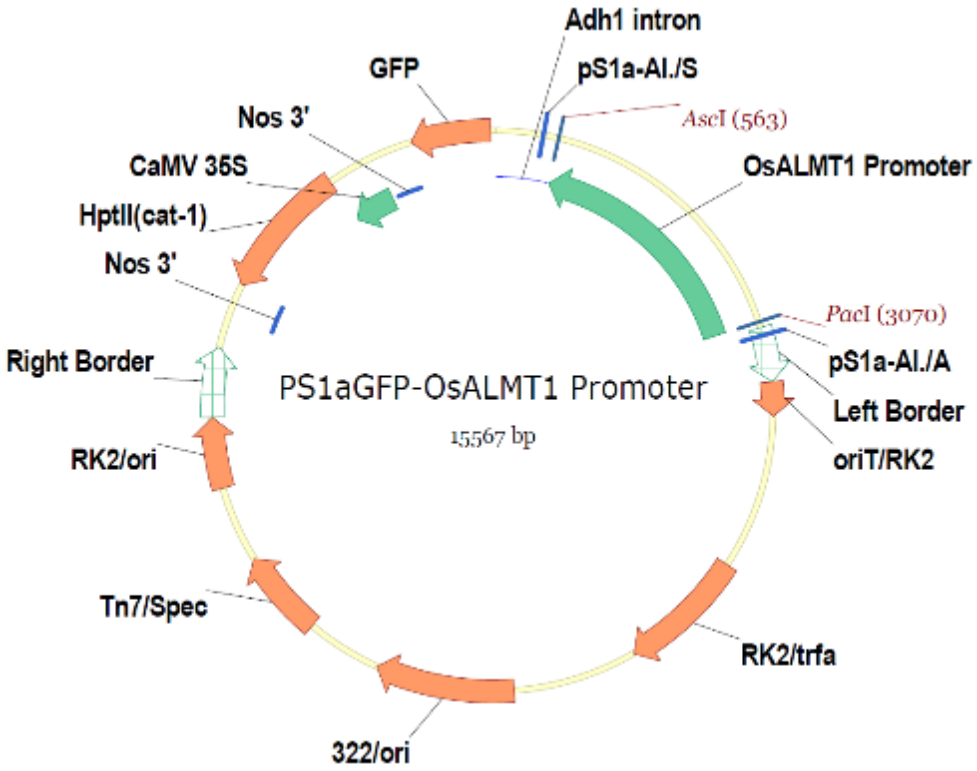

Figure 5.1 Vector maps of pS1a-OsALMT1 Promoter::GFP

The arrows represent different elements with the following colours: orange arrow represents coding DNA sequence (CDS), dark green arrow represents promoter, light hollow green arrow represents transfer border, bold blue line along the plasmid represents the Nos 3' terminator, and fine blue line along the plasmid represents the Adh1 intron. The bold blue line cross the plasmid represents primer binding site and the fine blue line cross the plasmid represent restriction enzyme site. The plasmid contains the cauliflower mosaic virus 35S promoter (CaMV35S) which is a strong constitutive promoter causing high levels of gene expression in dicotyledons and monocotyledons, the Nos 3' terminator which is widely used as a transcriptional terminator in plant expression vectors, the *Spec* resistance gene for spectinomycin selection in Agrobacteria, and the *hptII* gene which confers hygromycin resistance for selection in plants. Transfer is initiated at the right border and terminated at the left border.

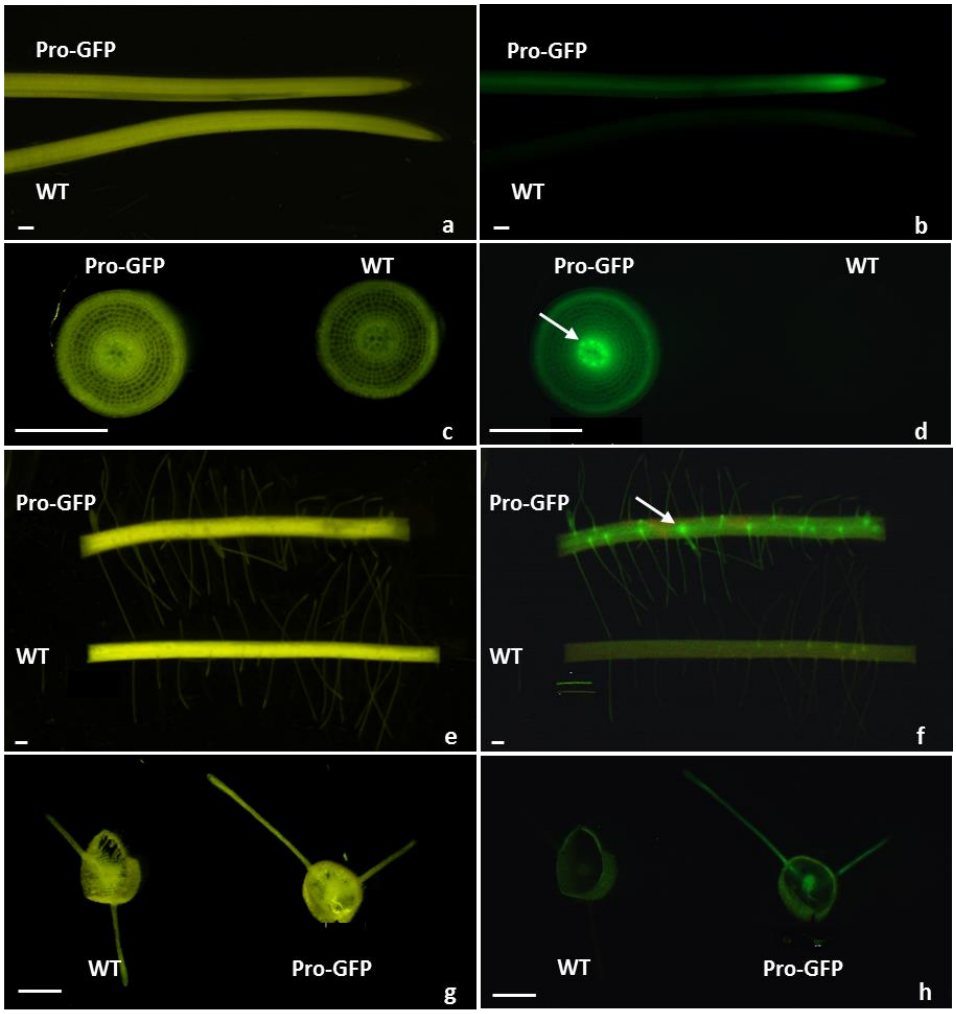

Figure 5.2 Rice roots expressing *GFP* with the *OsALMT1* promoter

Roots of rice plants transformed with the *OsALMT1* promoter::GFP (Pro-GFP) construct were examined under Leica MZFLIII fluorescence dissecting microscope in different stages. Wild type (WT) plants were also included as controls for auto-fluorescence. a, Bright-field image of young root; b, Fluorescence image of the same tissue in a; c, Bright-field image of young root transverse section (3 mm from root tips); d, Fluorescence image of the same tissue in c showing high signals in the vascular tissues (arrow); e, Bright-field image of mature root (3-4 cm from root tips); f, Fluorescence image of same tissue in e showing high signals in the root hair cells (arrow); g, Bright-field image of mature root transverse section (3-4 cm from root tips); h, Fluorescence image of the same tissue with g. Scale bar=500 μm.

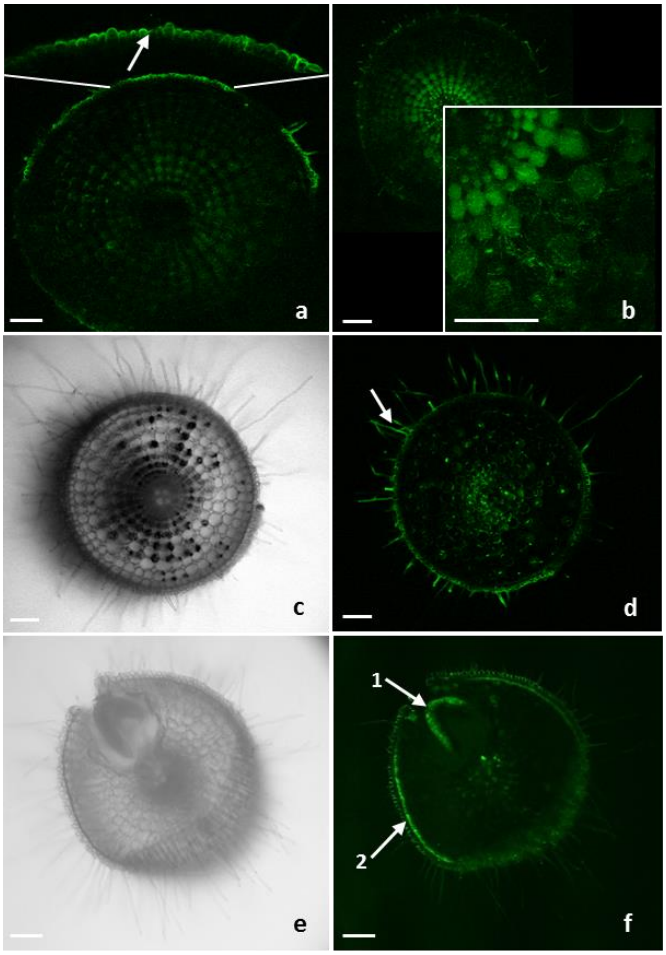

Figure 5.3 Detailed images of GFP fluorescence in root tissue

Different regions of the roots of rice plants transformed with the *OsALMT1* promoter::GFP construct were examined under Leica MZFLIII fluorescence dissecting microscope. a, Fluorescence image of a transverse section at the root apex near the meristematic zone. The insert shows a magnified region of the epidermis layer cells indicated by the white lines and arrow. (Note the projections out from the epidermis are not root hairs but damaged epidermal cells from the dissection); b, Fluorescence image of a transverse section near the elongation zone with an insert showing a magnified area of the middle cell layers (lower right); c, Bright-field image of mature root transverse section; d, Fluorescence image of the same tissue in c showing high signals in the root hairs (arrow); e, Bright-field image of transverse section of emerging lateral root and sclerenchymatous; f, Fluorescence image of the same tissue in e showing the emerging lateral root (arrow 1) and sclerenchymatous (arrow 2). Scale bar=100 μm.

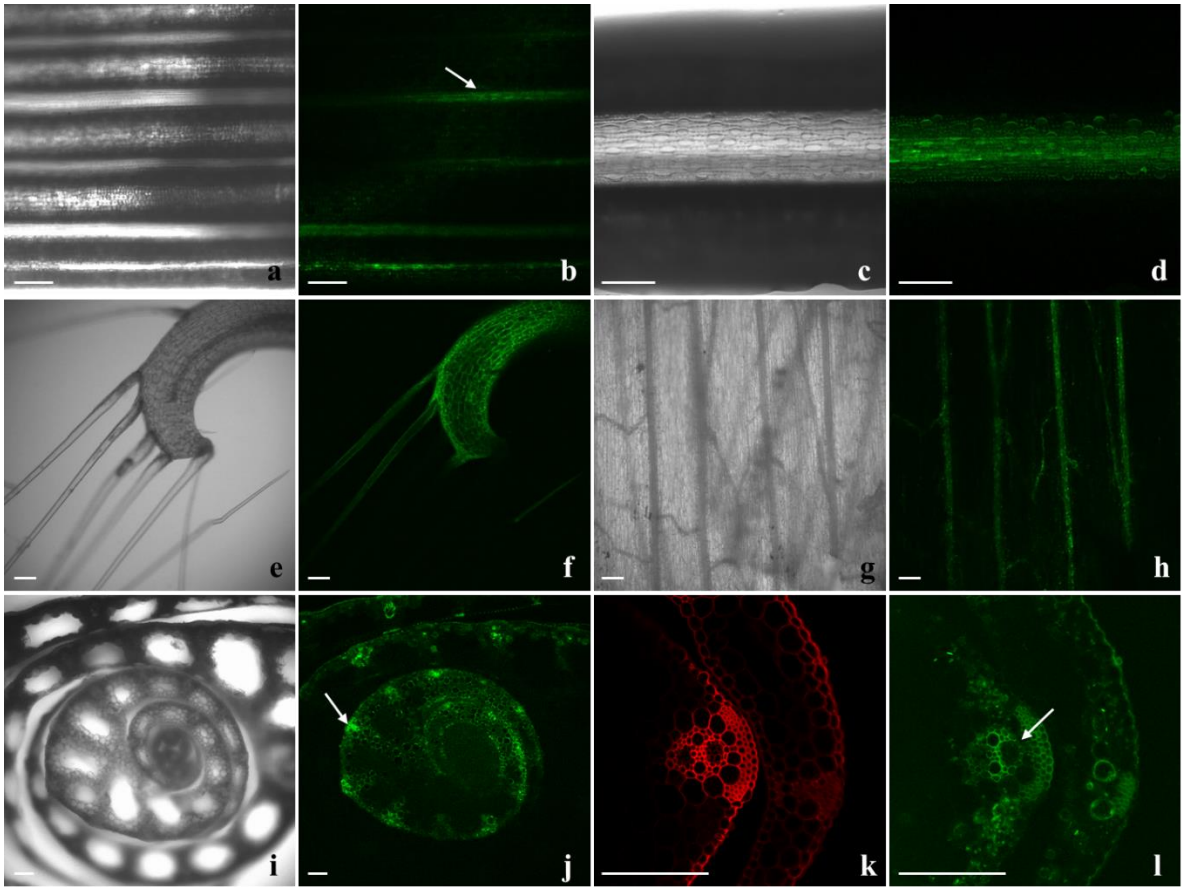

Figure 5.4 Fluorescence in leaves of rice expressing *GFP* with the *OsALMT1* promoter

Two week old transgenic *OsALMT1* promoter::GFP plants were examined under the confocal laser scanning microscope. a, Bright-field image of abaxial surface of leaf blade; b, Fluorescent image of the tissue shown in a showing high signals in the leaf ribs (arrow); c, Bright-field image of the midrib on the outer surface of leaf sheath; d, Fluorescent image of the tissue in c; e, Bright-field image of the auricle; f, Fluorescent image of auricle shown in e; g, Bright-field image of the ligule; h, Fluorescent image of the ligule shown in g; i, Bright-field image of a transverse section through a newly emerged tiller; j, Fluorescent image of the same tissue in i showing high signals in the vascular tissue (arrow); k, Ultra violet image of a transverse section through a newly emerged tiller showing cell wall; l, GFP fluorescence from the same tissue in k showing high expression around the xylem and xylem parenchyma (arrow). Scale bar=100 μm.

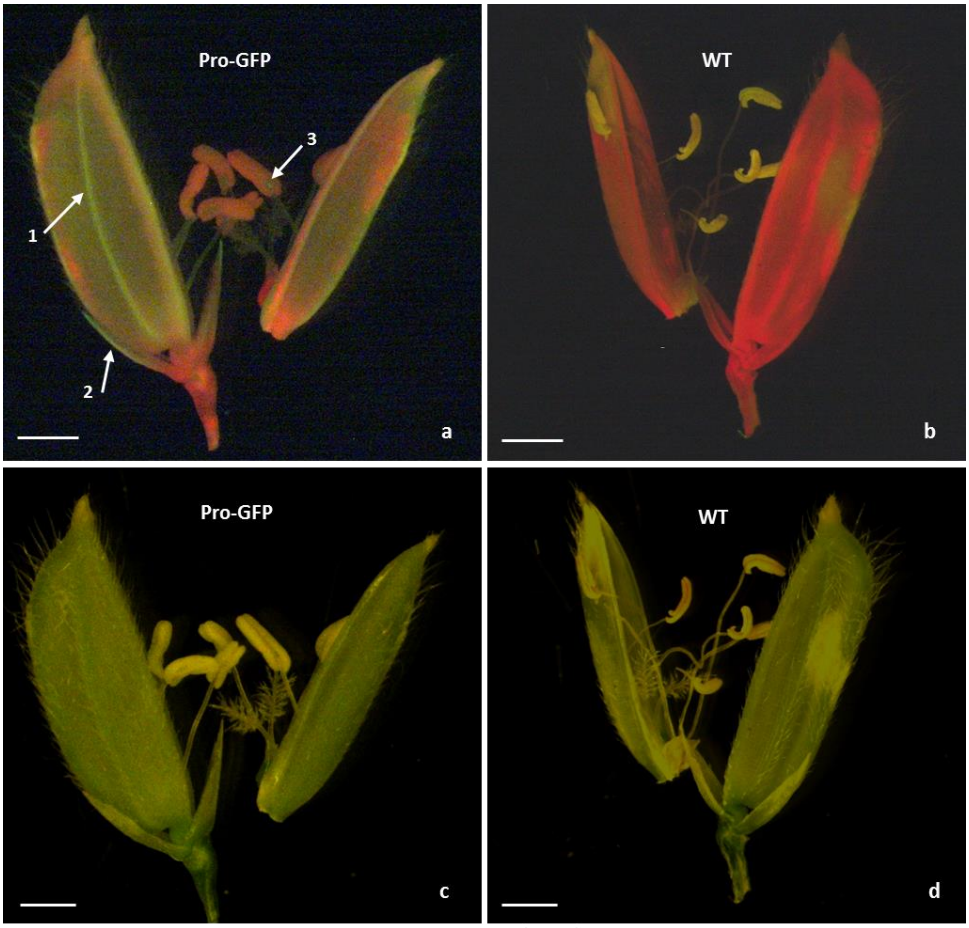

Figure 5.5 Fluorescence in the whole flower of rice plants expressing *GFP* with the *OsALMT1* promoter

Flowers from transgenic and wild-type rice plants were examined under a Leica MZFLIII fluorescence dissecting microscope. a, Fluorescent image from a transgenic plant showing signals in the lemma (arrow 1), sterile lemma (arrow 2) and anther (arrow 3); b, Fluorescent image from a wild type plant; c, Bright-field image of the same image in a; d, Bright-field image of the same image in b. Scale bar=1 mm

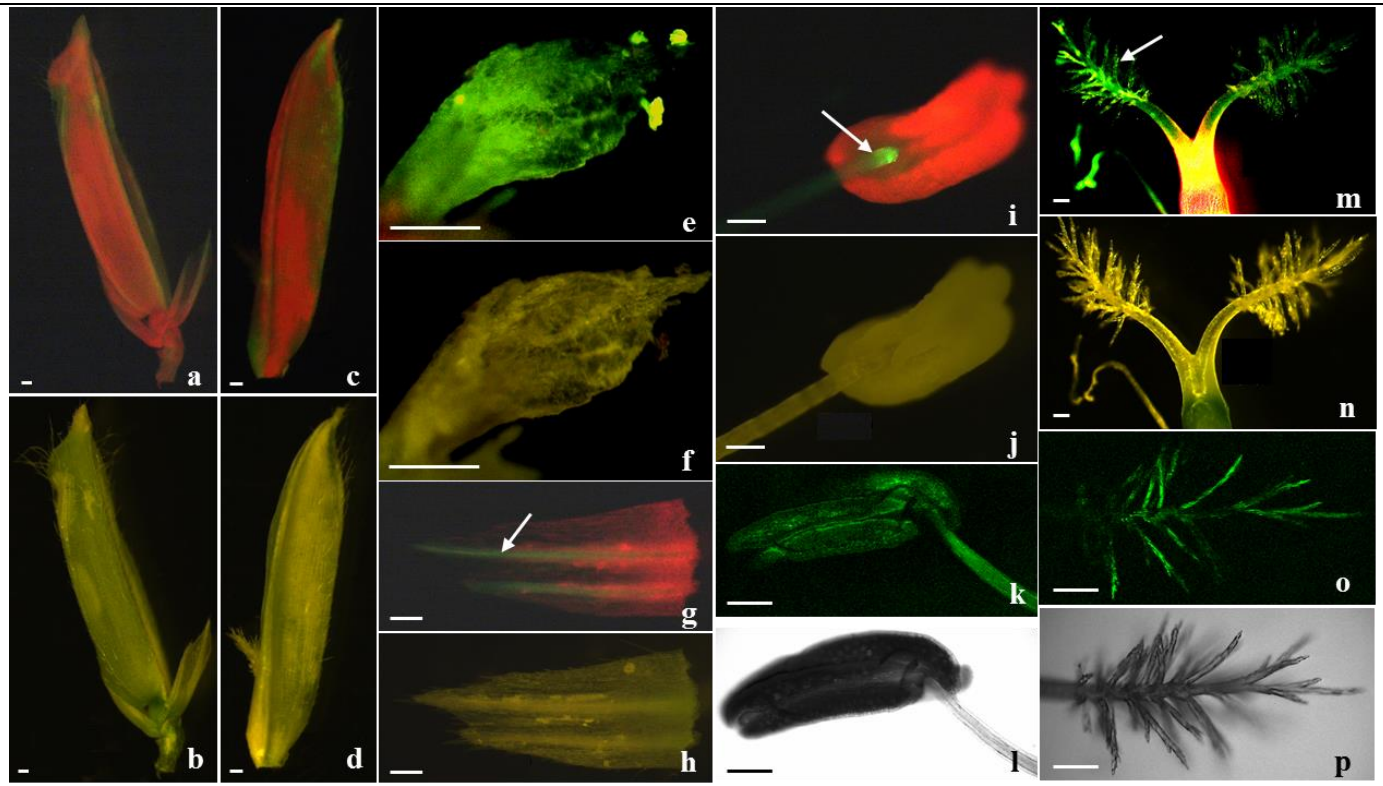

Figure 5.6 Fluorescence in different parts of the flower of rice plants expressing *GFP* with the *OsALMT1* promoter

a, Fluorescent image of a lemma; b, Bright-field image of the image in a; c, Fluorescent image of a palea; d, Bright-field image of the image in c; e, Fluorescent image of a lodicule; f, Bright-field image of the lodicule in e; g, Fluorescent image of a sterile lemma showing high expression in vascular ribs (arrow); h, Bright-field image of with the image in g; i, Fluorescent image of a stamen showing high expression in the filament at the junction with the anther; j, Bright-field image of the image in i; k, Fluorescent image of an anther and filament under confocal microscope; l, Bright-field image of the image in k; m, Fluorescent image of a carpel showing high expression in the stigmas (arrows); n, Bright-field image of the carpel in m; n, Fluorescent image of a stigma under confocal microscope ; l, Bright-field image of the same tissue in k. Scale bar=200 μm

5.3.3 Distribution of *OsALMT1* expression in flower parts

Fluorescence was detected in specific parts of the flower in the transgenic rice expressing *OsALMT1*promoter::GFP which were not observed in the wild type controls (**Figure 5.5**). Fluorescence was detected in the stigma and style of the carpel, stamens, lodicules, the lemma and sterile lemma, and palea (**Figure 5.6 a-j, m, n**). Auto-fluorescence was found in the anther with the Leica MZFLIII fluorescence dissecting microscope, but high GFP expression can be found in the filament at the junction with the anther. GFP fluorescence was able to be detected in the anthers with the Leica SP2 confocal laser scanning microscope (**Figure 5.6 i-l**). Flower parts from wild-type plants were examined at the same time and they did not show comparable fluorescence. Some of the images do not fully show the very distinct differences in GFP fluorescence between the transgenic and wild type plants but the differences were clear under the microscopes.

5.3.4 Fluorescent images in developing rice grain

GFP fluorescence was detected in developing grains. At the milk stage of grain development (14 d after flowering) fluorescence was detected on the outer side of the seed coat and transverse sections show high expression in the nucellar projection (**Figure 5.7 a-d**). Little or no fluorescence was observed in the dough stage of grain development (28 d after flowering). No differences could be found between the transgenic and the WT grain when viewed from the outside. However, when part of the seed coat was peeled back fluorescence could be detected indicating expression in the aleurone layer (**Figure 5.7 e-h**). The presence of GFP signals in the seed coat and aleurone layer were confirmed with the confocal microscope which could remove the auto-florescence by narrowing the Emission range between 510-570nm (**Figure 5.7 i-l**). GFP fluorescence was also found in the empty glumes and the emerged region of the rachilla (**Figure 5.7 m, n**).

5.3.5 Fluorescent images in developing rice grain

The primary generation of transgenic rice (T0) were planted and T1 grain were harvested.

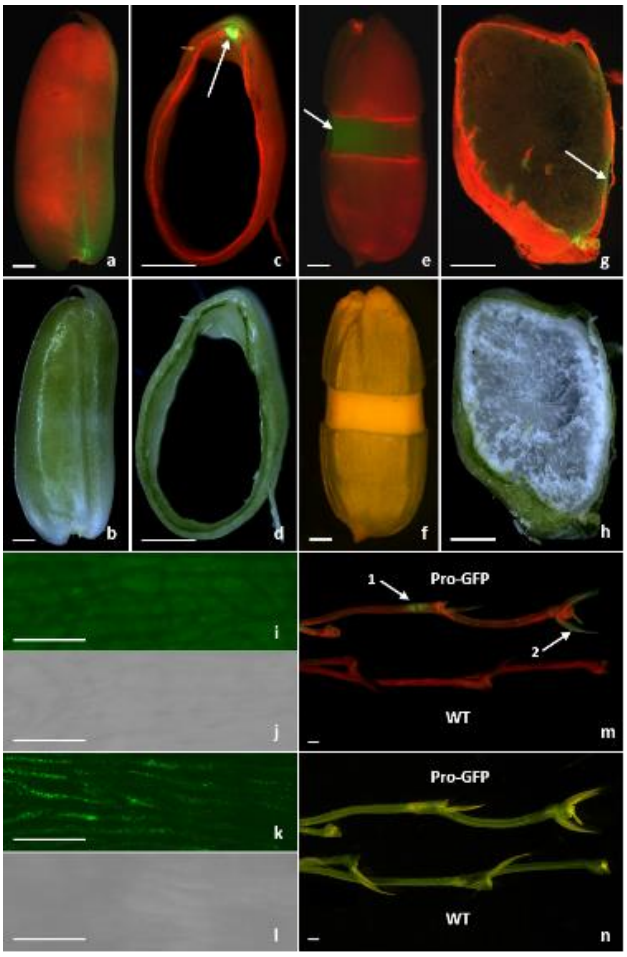

Figure 5.7 GFP fluorescence in developing grain

Developing grain from transgenic rice expressing *OsALMT1* promoter::GFP and wild type plants were examined under a fluorescence dissecting microscope and a confocal laser scanning microscope. a, Fluorescent image of grain at the milk stage; b, Bright-field image of the image in a; c, Fluorescent image of a transverse section through grain at the milk stage showing high expression in the nucellar projection (arrow); d, Bright-field image of the image in c; e, Fluorescent image of the dough stage of grain development showing GFP signals in the aleurone layer when part of the seed coat was peeled back (arrow); f, Bright-field image of the tissue in e; g, Fluorescent image of a transverse section through grain at the dough stage showing GFP signals in the aleurone layer (arrow); h, Bright-field image of the tissue in g; i, Fluorescent image of the aleurone layer with a confocal microscope; j, Bright-field image of the tissue in i; k, Fluorescent image of a seed coat with a confocal microscope; l, Bright-field image of the same tissue in k; m, Fluorescence image of a rachilla showing GFP signals in the empty glumes (arrow 1) and the emerged region of the rachilla (arrow 2); n, Bright-field image of the same tissue in m. Scale bar=500 μm (Scale bar in i, j, k and l=50 μm).

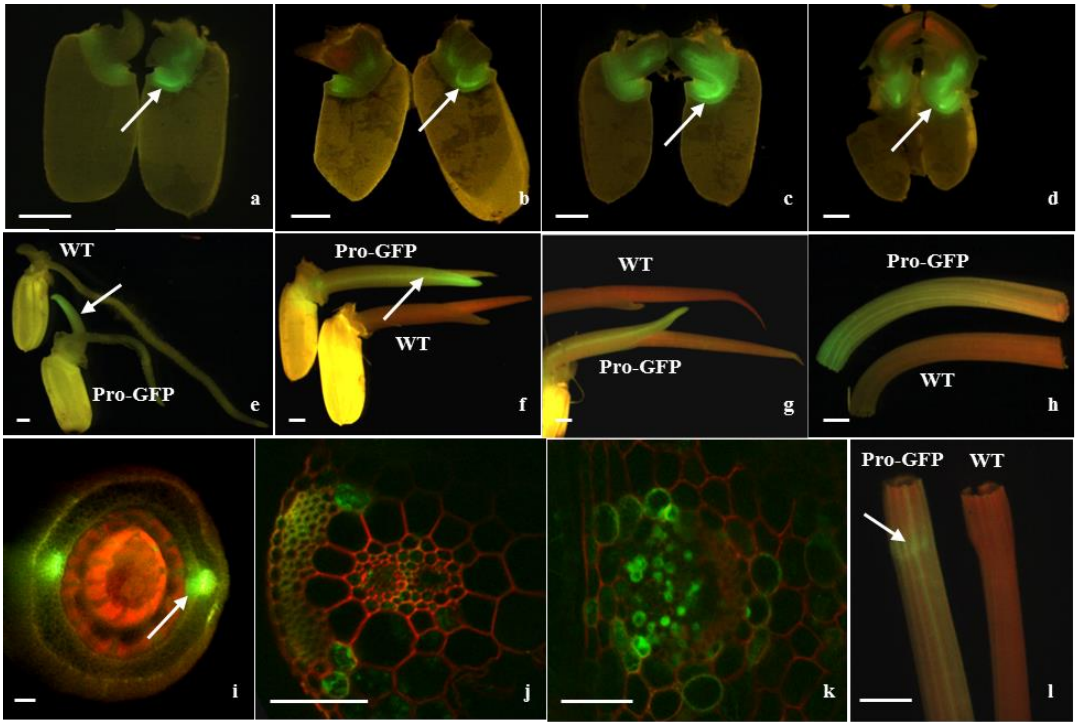

Figure 5.8 GFP fluorescence in germinating grain, coleoptiles and shoots

Transgenic rice expressing OsALMT1promoter::GFP and wild type germinating seeds were examined under fluorescence dissecting microscope and a confocal laser scanning microscope. a-d, Fluorescent image of a longitudinal section through a grain two days, five days, seven days, and nine days after imbibing showing high expression in the embryo (arrows); e, Fluorescent image of newly emerged shoot two days after imbibing showing high GFP signals in the newly emerged shoot (arrow); f, Fluorescent image of newly emerged shoot five days after imbibing showing high expression at the tips and in the vascular bundles of the coleoptiles (arrow); g, Fluorescent image of newly emerged shoot seven days after imbibing showing decrease GFP signal in coleoptiles but strong signals remained in the vascular tissues (arrow); H, Fluorescent image of an excised section of a newly emerged shoot nine days after imbibing; i, Fluorescent image of a transverse section of newly emerged shoot nine days after germination showing high expression in the vascular bundle of the coleoptiles (arrow); j, Fluorescent and UV merged images of a transverse section of vascular tissue of the newly emerged leaf shown in i; k, Fluorescent and UV merged images of a transverse section of vascular bundle of the coleoptiles from the same tissue using in i; l, Fluorescent image showing high expression in the collar region between the leaf sheath and leaf blade (arrow). Scale bar=1mm (Scale bar in i, j and k=50 µm).

These grain were imbibed on moist tissue paper and examined for fluorescent signals through time. Fluorescence was detected in the embryo two days after germination and this increased in intensity in subsequent days. No GFP signals were detected in the endosperm (**Figure 5.8 a-d**). After five days from imbibing the emerging root and shoot were too long to photograph intact so these were removed and examined separately. GFP fluorescencewas initially high in the coleoptiles but this became weaker and strong signals remained in the vascular tissues only (**Figure 5.8, e-h**). Transverse sections of tissue nine days after imbibing showed expression in most cells of young leaves especially in the vascular tissue of coleoptiles and newly emerged leaves (**Figure 5.8 i-k**). After 10 days the first leaf formed and GFP signals were found at the collar which is the junction between the blade and the sheath (Figure 5.8 l). These results indicate strong fluorescence in the embryo and vascular bundles of coleoptiles and leaves.

5.4 Discussion

These experiments mapped the fluorescence in transgenic plants in which *GFP* expression was driven by the OsALMT1 promoter. GFP fluorescence was detected in the roots and shoots and in floral tissues and grain. It is assumed that this distribution reflects the expression of the *OsALMT1* gene *in vivo*. The wide expression of *OsALMT1* indicates that it contributes to multiple functions throughout the rice plant, perhaps based on a single type of transport activity. Expression was consistently high in the vasculature tissues of roots and leaves. Vasculature tissues include the xylem and phloem and associated companion cells and vascular parenchyma (Wilson, 1966). Xylem tissues transport water and minerals to the shoot in the transpiration stream while the phloem distribute photosynthetic products from their source to sinks as well as redistribute mobile nutrients and other compounds from senescencing tissues. The GFP signals were highest around the larger vessels in the vascular tissues and so more consistent with xylem localisation than phloem. In rice the ligule is thought to contain vascular tissues and performs function of water control between leaf blade and leaf sheath (J. Chaffey, 1985; Moon *et al.*, 2013). The high expression of *OsALMT1* around vascular tissue could indicate that OsALMT1 releases anions into the xylem stream as a means of balancing charge or osmolarity during nutrient loading or for accompanying mineral nutrients to shoots. ALMTs from other

species have been assigned roles in ion homeostasis and charge balance. For instance, the ZmALMT1 and ZmALMT2 proteins from maize were predicted to be involved in the selective transport of mineral anions for mineral nutrient acquisition and transport (Ligaba *et al.*, 2012; Pineros *et al.*, 2008).

In addition to the vascular tissues GFP signals were also detected in the floral parts, and in grain during development and germination. Flowers of eudicots can be divided into four concentric whorls of organs (sepals, petals, stamens, and carpels) which arrange sequentially from the floral meristem. In the male reproductive organ or stamen, the filament transmits water and nutrients to the anther and positions it to aid pollen dispersal (Scott *et al.*, 2004). OsALMT1 could be involved in this process.

The distribution of *OsALMT1* expression shows some similarity with other *ALMT* genes. For instance, *HvALMT1* is also widely expressed throughout barley plants including developing grain and during germination but is also expressed in guard cells (Gruber *et al.*, 2011; Gruber *et al.*, 2010; Xu *et al.*, 2015). Both the *OsALMT1* and *HvALMT1* are highly expressed in nucellar projection, aleurone layers and early embryo. The nucellar projection is a part of the nucellar tissue which faces the vascular tissue and coordinates the movement of nutrients to the endosperm transfer cells in developing grain (Sreenivasulu *et al.*, 2010). When fertilization is completed, the nucellar cells and nucellar projection undergo a degenerative processes which are recognized as programmed cell death (PCD) (Dom ńguez *et al.*, 2001; Krishnan and Dayanandan, 2003). After fertilization, the nucellus degrades which promotes nutrient supply for the young embryo and endosperm (Krishnan and Dayanandan, 2003; Sreenivasulu *et al.*, 2010). Previous studies demonstrated that manipulation of expression of the MADS29 transcription factor suppresses the degradation of the nucellus and nucellar projection during rice seed development which leads to altered grain morphology and reduced biomass (Yin and Xue, 2012). Nutrients delivered to the developing grain via the nucellar projection are then transported to the starchy endosperm either by the multiple aleuronic layers adjacent to the nucellar projection or by the nucellar epidermis and aleurone cells (Krishnan and Dayanandan, 2003). Since *HvALMT1* and *OsALMT1* are expressed in aleurone layers these proteins could facilitate the release of anions from the aleurone cells to the endosperm which might help the delivery of nutrients from the aleurone layer to the starchy endosperm. This is supported by previous experiments on transgenic barley plants in which *HvALMT1* expression was reduced with

RNAi. Those lines showed a lower release of malate from isolated aleurone layers during germination than a null transgenic control line (Xu *et al.*, 2015). Further experiments need to be performed to check whether a similar changes occur in aleurone function in the RNAi rice plants with reduced *OsALMT1* expression. Additional experiments could also monitor the effects of reduced *OsALMT1* expression on grain germination or early shoot elongation. These results indicate that the function of OsALMT1 in the nucellar projection and aleurone layers might be related to nutrient redistribution during seed filling.

OsALMT1 expression is also high in the areas of high metabolic activity and growth such as the root apex, lateral root emergence, collar of the leaf, flower parts, emerging regions of the rachillas, developing grain and early embryonic tissues. The *OsALMT1* promoter region contains potential *cis*-acting elements including a CAT-box (GCCAAT) at 935 bp from the transcription start site. This widely spread element is sometimes related to expression in the meristem expression and seems to be required to ensure sufficient transcript is produced (**Chapter 3**). The CAT box *cis*-element was first identified in a maize H3 promoter as a nuclear factor-binding site (Brignon and Chaubet, 1993) and a reversed CAT motif was found in the Arabidopsis *H4A748* gene promoter and behaved as a strong positive *cis*-element (Chaubet *et al.*, 1996). The CAT-box is conserved among various plant species including monocotyledons and dicotyledons (Meshi *et al.*, 2000). The Arabidopsis H4A748 promoters which contains the CAT-box have the ability to express in meristematic tissues in rice and in Arabidopsis. The alfalfa a histone H3 (*ALH3-1.1*) gene, with a CAT-box in its promoter region, also directs expression in meristematic tissues of transgenic tobacco (Kapros *et al.*, 1993; Meshi *et al.*, 2000). These result indicate that the high expression of *OsALMT1* in various meristems might be regulated by the CAT-box in the promoter region. The large demand for nutrients and transport activities in meristems need to be controlled and balanced with the counter movement of other ions.

In this chapter, the 2496 bp *OsALMT1* promoter was used to drive expression of the *GFP* reporter gene in transgenic rice. *OsALMT1* was found to be widely expressed throughout the rice plant and especially in the vascular tissue, meristems and developing grain.

5.5 References

Brignon P, Chaubet N (1993) Constitutive and cell-division-inducible protein-DNA interactions in two maize histone gene promoters. Plant J 4: 445-457

Chaubet N, Flénet M, Clément B, Brignon P, Gigot C (1996) Identification of *cis*-elements regulating the expression of an *Arabidopsis* histone H4 gene. Plant J 10: 425-435

Chen Q, Wu KH, Wang P, Yi J, Li KZ, Yu YX, Chen LM (2013a) Overexpression of *MsALMT1*, from the aluminum-sensitive *Medicago sativa*, enhances malate exudation and aluminum resistance in Tobacco. Pl Mol Biol Rep 31: 769-774

Chen ZC, Yokosho K, Kashino M, Zhao FJ, Yamaji N, Ma JF (2013) Adaptation to acidic soil is achieved by increased numbers of cis-acting elements regulating *ALMT1* expression in *Holcus lanatus*. Plant J 76: 10-23

Collins NC, Shirley NJ, Saeed M, Pallotta M, Gustafson JP (2008) An *ALMT1* gene cluster controlling aluminum tolerance at the *Alt4* locus of rye (*Secale cereale* L.). Genetics 179: 669-682

De Angeli A, Zhang JB, Meyer S, Martinoia E (2013b) AtALMT9 is a malate-activated vacuolar chloride channel required for stomatal opening in *Arabidopsis*. Nat Commun 4: 1804

Domínguez F, Moreno J, Cejudo F (2001) The nucellus degenerates by a process of programmed cell death during the early stages of wheat grain development. Planta 213: 352-360

Fire A, Harrison SW, Dixon D (1990) A modular set of *lacZ* fusion vectors for studying gene expression in Caenorhabditis elegans. Gene 93: 189-198

Gruber BD, Delhaize E, Richardson AE, Roessner U, James RA, Howitt SM, Ryan PR (2011) Characterisation of *HvALMT1* function in transgenic barley plants. Funct Plant Biol 38: 163-175

Gruber BD, Ryan PR, Richardson AE, Tyerman SD, Ramesh S, Hebb DM, Howitt SM, Delhaize E (2010) HvALMT1 from barley is involved in the transport of organic anions. J Exp Bot 61: 1455-1467

Hoekenga OA, Maron LG, Pineros MA, Cancado GMA, Shaff J, Kobayashi Y, Ryan PR, Dong B, Delhaize E, Sasaki T, Matsumoto H, Yamamoto Y, Koyama H, Kochian LV (2006) *AtALMT1*, which encodes a malate transporter, is identified as one of several genes critical for aluminum tolerance in *Arabidopsis*. PNAS 103: 9738-9743

J.Chaffey N (1985) Structure and function in the grass ligule: presence of veined and membranous ligules on the same culm of british grasses. New Phytol 101: 613-621

Jefferson RA, Kavanagh TA, Bevan MW (1987) GUS fusions: Beta-glucuronidase as a sensitive and versatile gene fusion marker in higher plants. EMBO J 6: 3901-3907

Kapros T, Stefanov I, Magyar Z, Ocsovszky I, Dudits D (1993) A short histone H3 promoter from alfalfa specifies expression in s-phase cells and meristems. In Vitro Cell Dev Biol - Plant 29: 27-32

Kovermann P, Meyer S, Hortensteiner S, Picco C, Scholz-Starke J, Ravera S, Lee Y, Martinoia E (2007) The *Arabidopsis* vacuolar malate channel is a member of the ALMT family. Plant J 52: 1169-1180

Krishnan S, Dayanandan P (2003) Structural and histochemical studies on grain-filling in the caryopsis of rice (*Oryza sativa* L.). J Biosciences 28: 455-469

Liang CY, Pineros MA, Tian J, Yao ZF, Sun LL, Liu JP, Shaff J, Coluccio A, Kochian LV, Liao H (2013) Low pH, aluminum, and phosphorus coordinately regulate malate exudation through *GmALMT1* to improve soybean adaptation to acid soils. Plant Physiol 161: 1347-1361

Ligaba A, Katsuhara M, Ryan PR, Shibasaka M, Matsumoto H (2006) The *BnALMT1* and *BnALMT2* genes from rape encode aluminum-activated malate transporters that enhance the aluminum resistance of plant cells. Plant Physiol 142: 1294-1303

Ligaba A, Maron L, Shaff J, Kochian L, Pineros M (2012) Maize ZmALMT2 is a root anion transporter that mediates constitutive root malate efflux. Plant Cell Environ 35: 1185-1200

Martin Chalfie, Yuan Tu, Ghia Euskirchen, William W. Ward, Prasherf DC (1994) Green fluorescent protein as a marker for gene expression. Science 263: 802-805

Meshi T, Taoka K-i, Iwabuchi M (2000) Regulation of histone gene expression during the cell cycle. Plant Mol Biol 43: 643–657

Meyer S, Mumm P, Imes D, Endler A, Weder B, Al-Rasheid KAS, Geiger D, Marten I, Martinoia E, Hedrich R (2010) AtALMT12 represents an R-type anion channel required for stomatal movement in Arabidopsis guard cells. Plant J 63: 1054-1062

Meyer S, Scholz-Starke J, De Angeli A, Kovermann P, Burla B, Gambale F, Martinoia E (2011) Malate transport by the vacuolar AtALMT6 channel in guard cells is subject to multiple regulation. Plant J 67: 247-257

Moon J, Candela H, Hake S (2013) The liguleless narrow mutation affects proximal-distal signaling and leaf growth. Development 140: 405-412

Parra G, Bradnam K, Rose AB, Korf I (2011) Comparative and functional analysis of intron-mediated enhancement signals reveals conserved features among plants. Nucl Acids Res 39: 5328-5337

Pineros MA, Cancado GMA, Maron LG, Lyi SM, Menossi M, Kochian LV (2008) Not all ALMT1-type transporters mediate aluminum-activated organic acid responses: the case of *ZmALMT1* - an anion-selective transporter. Plant J 53: 352-367

Ryan PR, Raman H, Gupta S, Sasaki T, Yamamoto Y, Delhaize E (2010) The multiple origins of aluminium resistance in hexaploid wheat include *Aegilops tauschii* and more recent *cis* mutations to *TaALMT1*. Plant J 64: 446-455

Sasaki T, Mori IC, Furuichi T, Munemasa S, Toyooka K, Matsuoka K, Murata Y, Yamamoto Y (2010) Closing plant stomata requires a homolog of an aluminum-activated malate transporter. Plant Cell Physiol 51: 354-365

Sasaki T, Yamamoto Y, Ezaki B, Katsuhara M, Ahn SJ, Ryan PR, Delhaize E, Matsumoto H (2004) A wheat gene encoding an aluminum-activated malate transporter. Plant J 37: 645-653

Scott RJ, Spielman M, Dickinson HG (2004) Stamen structure and function. Plant Cell 16: Suppl, S46-60

Sreenivasulu N, Borisjuk L, Junker BH, Mock H-P, Rolletschek H, Seiffert U, Weschke W, Wobus U (2010) Chapter 2 - Barley Grain Development: Toward an Integrative View, Int Rev Cell Mol Biol 281: 49-89

Tjian BLaR (2000) Orchestrated response: a symphony of transcription factors for gene control. Gene Dev 14: 2551-2569

Ayoubi TA , Van De Ven WJ (1996) Regulation of gene expression by alternative promoters. FASEB J 10: 453-460

Xu M, Gruber BD, Delhaize E, White RG, James RA, You J, Yang Z, Ryan PR (2015) The barley anion channel, HvALMT1, has multiple roles in guard cell physiology and grain metabolism. Physiol Plant 153: 183-193

Yin LL, Xue HW (2012) The MADS29 transcription factor regulates the degradation of the nucellus and the nucellar projection during rice seed development. Plant Cell 24: 1049-1065

CHAPTER 6

Changes in *OsALMT1* expression in response to different stress and hormone treatments

6.1 Introduction

Plants are consistently exposed to many biotic and abiotic stresses which affect their growth and development and have evolved various mechanisms to sense, respond, and adapt to a wide range of stress conditions. For instance, salinity and drought affect growth by disrupting the ionic and osmotic equilibrium of cells which reduces transpiration and photosynthesis. Plants have evolved a wide range of responses to osmotic stress at the molecular, cellular and plant levels such as morphological and developmental changes (e.g. change of life cycle, inhibition of shoot growth and enhancement of root growth), adjustment in ion transport (such as uptake, extrusion or sequestration of ions) and metabolic changes (e.g. carbon metabolism and the synthesis of compatible solutes) (Xiong and Zhu, 2002). Continuous exposure to high oxygen can result in cellular damage because molecular oxygen is reduced within cells to various forms of reactive oxygen species (ROS), especially the free radical superoxide anion (O_2^-) and hydrogen peroxide (H_2O_2) (Scandalios, 2005). Although plants use light to produce their own energy and metabolites via photosynthesis, excess light can still adversely affect plants due to photo-oxidative damage (Osakabe and Osakabe, 2001). By contrast, continuous low light or darkness inhibits photosynthesis and alters growth habit (Frances and Thompson, 1997). Plants can differentiate and develop in response to different light intensities (known as photomorphogenesis) which allows them to optimize their use of light and space (Han *et al.*, 2007). Aluminium (Al) toxicity is a common stress in acid soils because Al^{3+} cations inhibit root growth (Delhaize and Ryan, 1995) and plants have evolved resistance mechanisms to survive from the Al toxicity. Exclusion mechanisms decrease Al uptake and Al concentrations in the cell wall, or reduce Al interactions with root cells by the exudation of organic ligands which bind Al^{3+} and limit its uptake into the cytosol. Tolerance mechanisms minimise oxidative stress and sequester Al that does enter the cytosol to subcellular compartments such as the vacuole (Ryan *et al.*, 2011).

Under normal growth conditions as well as in stressful environments hormones form a signalling network that regulate cellular metabolism and affect growth. Hormones are structurally diverse compounds that are active at nanomolar or micromolar concentrations. In plants they were generally divided into five main groups: auxins (IAA), abscisic acid (ABA), gibberellins (GA), cytokinins (CK) and ethylene. Additional compounds like the jasmonates (JA), salicylates (SA), strigolactones (SL), brassinosteroids (BR), polyamines and some peptides are now also considered as plant hormones (Peleg and Blumwald, 2011). IAA is present in all parts of a plant at various concentrations and subject to tight regulation through both metabolic and transport processes. IAA has an aromatic ring and a carboxylic acid group and participates in phototropism, geotropism, hydrotropism and other developmental changes by affecting both cell division and cellular expansion (Benková *et al.*, 2003; Friml, 2003). ABA is another widely studied plant hormone associated with water and osmotic stress and regulation of stomatal aperature (Wilkinson and Davies, 2010). It also is involved in responses to cold by integrating signalling pathways involving sugar and reactive oxygen species (Xue-Xuan *et al.*, 2010) and also plays a role in plant resistance to pathogens (Ton *et al.*, 2009). GA is involved with cellular growth and has been linked with responses to stress and to stress tolerance. Reduced GA concentrations lead to growth restriction during cold, salt and osmotic stress (Colebrook *et al.*, 2014). Altered GA concentrations are also linked with responses to light and dark treatments and during de-etiolation (O'Neill *et al.*, 2000). SA is involved with multiple aspects of plant growth and development such as seed germination, vegetative growth, photosynthesis, respiration, thermogenesis, flower formation, seed production and senescence. It is involved in plant responses against pathogens and biotic stresses (Vlot *et al.*, 2009) as well as abiotic stresses including drought, chilling, heavy metal toxicity, heat and osmotic stress (Rivas-San Vicente and Plasencia, 2011). JA is a lipid-derived compound involved with responses to wounding and biotic stress (Wasternack, 2007). JA and its methyl ester, MeJA, can influence the growth and physiology of root growth (Wasternack and Hause, 2013).

Plants respond to stresses by activating tolerance mechanisms at multiple levels of organization (molecular, tissue, anatomical, and morphological), by adjusting the membrane system and the cell wall architecture, by altering the cell cycle and rate of cell division, and by metabolic tuning (Atkinson and Urwin, 2012). At the molecular level,

responses to stress involves the induction or repression of many genes via intricate and precise regulation of signalling networks and transcription factors (Delano-Frier *et al.*, 2011). The responses of genes and proteins to a stress or environmental condition can be measured at three levels: changes in transcript, post-transcriptional modifications and post-translational changes. At each level, gene responses depend on specific molecular elements as well as molecular networks and cascades (Duque *et al.*, 2013). The amount of mRNA in polysomes can increase or decrease depending on the treatment (Mazzucotelli *et al.*, 2008). The development of real-time PCR allows the precise quantification of mRNA levels of genes of interest under various conditions.

Expression levels of some members of the *ALMT* family are altered in response to abiotic stresses and to certain hormones. For example, *MsALMT1* from *Medicago sativa*, *CsALMT1* from *Citrus sinensis* and *HlALMT1* from Yorkshire fog (*Holcus lantanus*) are some genes whose expression are up-regulated by Al stress (Chen *et al.*, 2011; Chen *et al.*, 2013; Yang *et al.*, 2012). Expression of *GmALMT1* from soybean was suppressed by low pH but enhanced in roots by the addition of Al and P while *AtALMT1* from Arabidopsis was induced by low pH and Al treatments (Kobayashi *et al.*, 2007; Liang *et al.*, 2013). Expression of *BnALMT1* from rape (*Brassica napus*) increased in root tissue by treatment with Al, lanthanum (La), erbium (Er), and ytterbium (Yb) (Ligaba *et al.*, 2006). Foliar infection of Arabidopsis leaves with the pathogen *Pseudomonas syringae pv tomato* (Pst DC3000), flagellin22 (*flg22*) and coronatine induced *AtALMT1* expression in roots and increased malate efflux even in the absence of Al (Lakshmanan *et al.*, 2012; Rudrappa *et al.*, 2008). Other studies showed that *AtALMT1* expression was also induced by IAA, ABA and hydrogen peroxide (Kobayashi *et al.*, 2013a). However the induction of *AtALMT1* expression by Al and *flg22* was independent of the hormone pathway.

The aim of this chapter is to examine how *OsALMT1* expression changes in response to a range of abiotic stresses and phytohormones in order to reveal possible functions of this gene.

6.2 Materials and methods

6.2.1 Treatments and gene expression

Wild type rice seeds (cv. Nipponbare) were surface sterilised, germinated on half MS media for seven days and grown hydroponically as described in **Chapter 2**. Plants were then transferred to tubs containing ~10 L of fresh nutrient solution for seven days. The solutions were changed after seven days and different treatments initiated as shown in **Table 6.1**. After 6 and 24 h in the various treatments or specific growth conditions the first totally expanded leaf and roots were collected for expression analysis. The only exception was for the "drying roots" treatment. This treatment consisted simply of lifting the seedlings out of the growth solution and resting them above an empty tank so that the roots were no longer in contact with solution. For this treatment tissue was collected after one and two hours because longer treatments caused the roots to dry too much and become shrivelled. Total RNA and first-strand cDNA were prepared as described in **Chapter 2**. Quantitative RT-PCR was performed with *OsALMT1*-specific primer pairs (PRR142 and PRR143, see **Chapter 2**) using SYBR Green (BIO-RAD) and the CFX96 Real-Time System (BIO-RAD) following the manufacturer's instructions. Reactions were performed with three biological replicates (ie. separate RNA isolations from independently treated material) and three technical replicates for each sample. Transcript levels of *OsALMT1* were normalized with two reference genes: *glyceraldehyde-3-phosphate dehydrogenase* (*GAPDH*, GenBank: GQ848049.1) and *elongation factor-1 alpha* (*eEF-1a,* GenBank: GQ848073.1). Relative gene expression is described in **Chapter 2**.

6.3 Results

6.3.1 Effect of osmotic stress, light and low Cl^- treatments on *OsALMT1* expression

To gain insight into the function of OsALMT1, we monitored changes in transcript levels in *Nipponbare* in response to 6 and 24 h exposure with various treatments. The osmotic treatments and ionic challenges included salt and mannitol. A 200 mM NaCl solution

caused little change in expression in the roots but reduced expression in the shoot by ~20-fold (**Figure 6.1**). A solution of 350 mM mannitol that has the same osmolarity as 200 mM NaCl (see Materials and Methods) also reduced *OsALMT1* expression in the shoots by 30% and 70% after 6 and 24 h respectively but the changes were only significant after 24 h. In contrast to NaCl, mannitol induced *OsALMT1* expression in roots by about six-fold. Treatment with 20% PEG6000 also caused *OsALMT1* expression in shoots to decrease to ~5% of controls while roots showed a three-fold higher expression after 6 h but no difference from controls at 24 h. This same general pattern in expression (decrease in shoots and increase in roots) was also induced by lifting roots out from the growth solution. Expression in shoots decreased by 60 and 85% after plants were lifted out of the solution for one and two hours respectively. In the roots expression increased seven-fold after one hour but then was similar to controls after two hours. However the changes were only significant in the shoots for the longer treatment and in root tissues after the shorter treatment. Note that these treatments were one and two hours instead of 6 and 24 h. Treatment in a Cl^--free solution tended to increase *OsALMT1* expression in the shoots by ~50% after 24 h but this was not significant. There were not changes of expression in the roots in the Cl^--free solution (**Figure 6.1**).

6.3.2 Changes in *OsALMT1* expression with hormone treatments

OsALMT1 expression was measured in response to hormones and signalling compounds (**Figure 6.2**). Abscisic acid (ABA) treatment had no effect on expression in shoots after 6 h but tended to decrease expression after 24 h but this was not significant. Expression in the roots decreased significantly with ABA to 10% of controls after 6 h and 5% of controls after 24 h. Indole-3-acetic acid (IAA) also induced a large and rapid decrease in *OsALMT1* expression in roots which was maintained for 24 h. IAA increased *OsALMT1* expression significantly in shoots four-fold after 6 h but levels were similar to controls after 24 h.

Salicylic acid (SA) increased expression five to seven-fold in roots and shoots after 6 h. After 24 h expression in roots and shoots returned to control levels. No changes in *OsALMT1* expression were associated with gibberellin (GA_3) or methyl jasmonic acid (MeJA) treatments. Gamma amino butyric acid (GABA) caused no changes in

expression in shoots and expression in the roots dropped to 30% of controls after 6 h but was significantly greater than controls after 24 h (**Figure 6.2**).

6.3.3 *OsALMT1* expression pattern under other stress conditions

Low pH (pH 4.5) solution caused little or no changes in expression in roots or shoots and the combination of low pH and 100 μM $AlCl_3$ (pH 4.5) had no effect either (**Figure 6.3**). Continual darkness for 6 h had no effect on *OsALMT1* expression in roots or shoots but after 24 h of continual darkness expression in roots increased five-fold compared to control plants (**Figure 6.3**). Continual light for 6 h had little effect on expression in roots or shoots but after 24 h expression in the shoots increased 10-fold. Hydrogen peroxide treatment significantly increased expression in the roots by almost three-fold but only after 24 h.

6.4 Discussion

The reason for performing these experiments was to identify treatments that alter *OsALMT1* expression in order to gain insight into OsALMT1 function. Treating rice seedlings with salt, mannitol and PEG and also lifting seedlings out of the growth solution caused qualitatively similar responses in *OsALMT1* expression: reduced expression in leaves and increased expression in roots. Further investigation of the signals involved in these changes will reveal aspects of OsALMT1 function. All the osmotic treatments would reduce the water potential gradient between the root and growth solution which would decrease the pull for water movement into the roots. But why these treatments should induce opposing changes in *OsALMT1* expression in roots and leaves is difficult to interpret. If it is assumed, for discussions sake, that OsALMT1 is important for malate movement into the xylem then reducing *OsALMT1* expression in leaves would reduce malate efflux from those cells and maintain a lower water potential in the leaves. This could help extract water from the xylem and keep the shoots hydrated and turgid. By contrast, increasing *OsALMT1* expression in roots could increase malate concentrations in the vasculature system which re-establishes the gradient in water potential between the root xylem and soil which could help drive water uptake by roots. These ideas need further investigation.

The effect of a Cl^- free treatment *OsALMT1* expression was tested because it was predicted that the absence of this prevalent inorganic anion might increase the importance of alternative anions (ie. organic anions) for charge balance and osmotic adjustment. The Cl^- free treatment had no effect after 24 h but this may have been too short a period to induce changes in the Cl- status of the plants - especially since they had been grown in a complete nutrient solution for several weeks prior to the treatment. Similar experiments should be repeated with longer periods of Cl^- deprivation to determine if *OsALMT1* expression is affected.

Metabolic responses to hormones can be very complex and transient and the changes in *OsALMT1* expression during treatment with exogenously applied hormones are difficult to interpret. ABA treatments were investigated because the concentration of this hormone increases during drier conditions and water stress (Passioura, 1982). Our results indicate that ABA tended to decrease *OsALMT1* expression in roots whereas the osmotic stress (salt and mannitol etc) tended to increases *OsALMT1* expression in roots. This suggests that the changes induced by osmotic stress were unlikely mediated by ABA. Of course ABA is not usually applied externally so this might have some different effects from endogenous changes in ABA concentrations. Changes to *OsALMT1* expression in the shoots with ABA and osmotic stress treatments were more similar except that they were significantly smaller for ABA than for the osmotic treatments. Both ABA and IAA inhibit root growth at higher concentrations (Luo *et al.*, 2014) so it is possible that reduced *OsALMT1* expression in these treatments reflects a slower root growth rate.

SA increased *OsALMT1* expression by four to six fold in roots and shoots after 6 h. Expression levels were similar or lower than control levels by 24 h. Other studies indicate that low concentrations (normally less than 0.5 mM) of external SA reduce plant sensitivity to abiotic stresses, while high concentrations decreased tolerance to abiotic stresses because they induce oxidative stress. However different species vary in their sensitivity to SA (Hara *et al.*, 2012). SA can affect membrane properties by altering membrane transport activity and membrane potential, possibly by activating potassium, calcium and chloride channels (Claire Lurin, 1996; Vadim Demidchik, 2002). Perhaps the finding here that SA induced relatively rapid increases in *OsALMT1* expression in roots and shoots could be a response to changes in other transports to help balance ion movements across membranes. Further experiments are needed to check if external SA

Table 6.1 Treatments for measuring changes in *OsALMT1* expression in WT rice

Treatment type	Description	Conditions*
Control	Standard nutrient solution (As described in **Chapter 2**)	pH 5.6, GH with prevailing light and dark cycles
Light	Continual darkness	Cover over boxes
	Continuous high light	~600 μmoles m^{-2} s^{-1}
Hormones	Indole-3-acetic acid (IAA)	100 μM
	Abscisic acid (ABA)	100 μM
	Gibberellic acid (GA_3)	100 μM
	Methyl jasmonic acid (MeJA)	100 μM
	Salicylic acid (SA)	100 μM
Osmotic stress**	Mannitol	350 mM
	Sodium chloride	200 mM
	Polyethylene glycol	20% PEG6000
Water stress	Drying roots	Seedlings lifted out of solution for 1 and 2 h.
Miscellaneous	Oxidative stress	300 μM H_2O_2
	Low pH	pH 4.5
	Aluminium chloride	100 μM (pH 4.5)
	Low chloride	[Cl^-] reduced from 502.6 μM to 2.6 μM by replacing Cl^- with NO_3^- and SO_4^{2-} (**See Table S3**)
	Gamma amino butyric acid	2 and 10 mM

* All solutions contained the standard nutrients at pH 5.6 unless stated otherwise.
** The 200 mM NaCl and 350 mM mannitol solutions were calculated to have the similar osmotic pressure of ~0.92 MPa (**See Table S1 and S2).**
GH = glasshouse

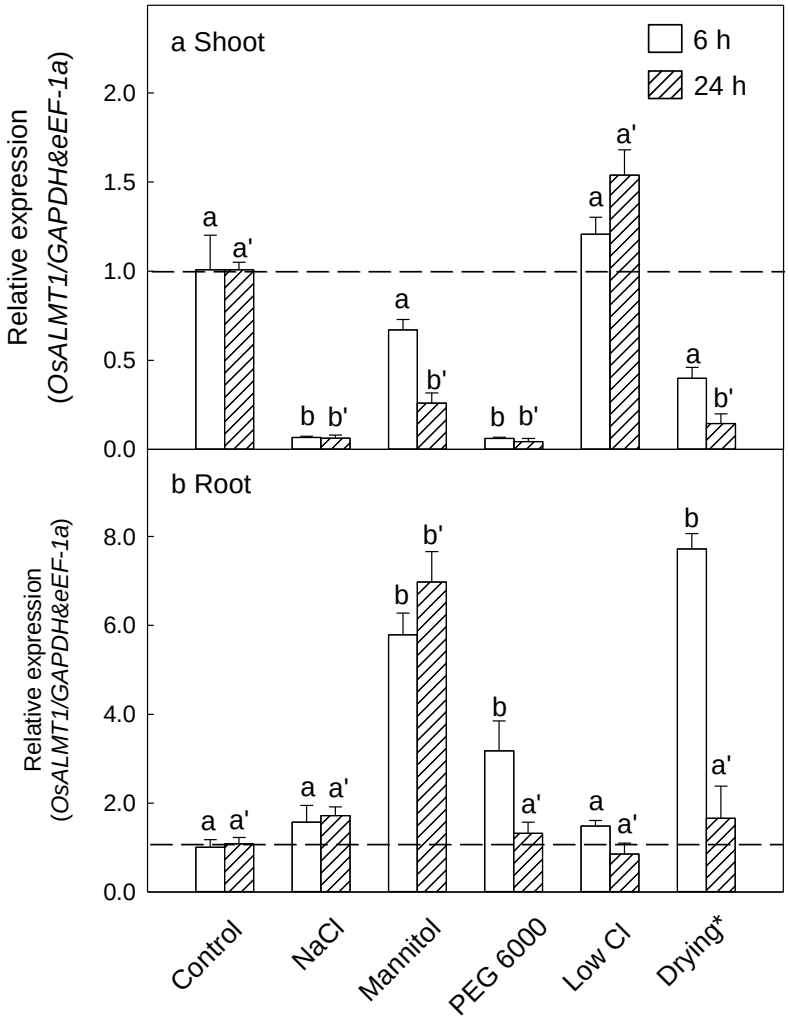

Figure 6.1 Changes in *OsALMT1* expression with osmotic treatments

OsALMT1 expression in root and shoot tissue was measured using qRT-PCR in 15 day-old rice seedlings. Seedlings were measured after 6 h and 24 h exposure to different osmotic treatments. (*) The only exception was the "drying" treatment where plants were lifted out of the growth solution and sampled after one and two hours. Treatments included 200 mM NaCl, 350 mM mannitol (same osmolarity as the NaCl treatment, **Appendix 1**) and 20% PEG6000 which were added to the nutrient solution. The chloride-free treatment required modifying the growth solution (**Table 6.1**). Plants in control treatment were harvested at each time point for comparison. Results from the two reference genes (*GAPDH* and *eEF-1α*) were combined to provide a single result according to the software in Bio-Rad CFX Manager**.** Data show mean and SE from three biological replicates and three technical replicates. For convenience the results are presented with a single control even though the figure represents several separate experiments. The statistical analyses were performed on the raw data for each experiment with its own control. Data with different letters are significantly different from its own control values. The 6 and 24 h data were tested separately and differences indicated as a and b or a' and b' respectively.

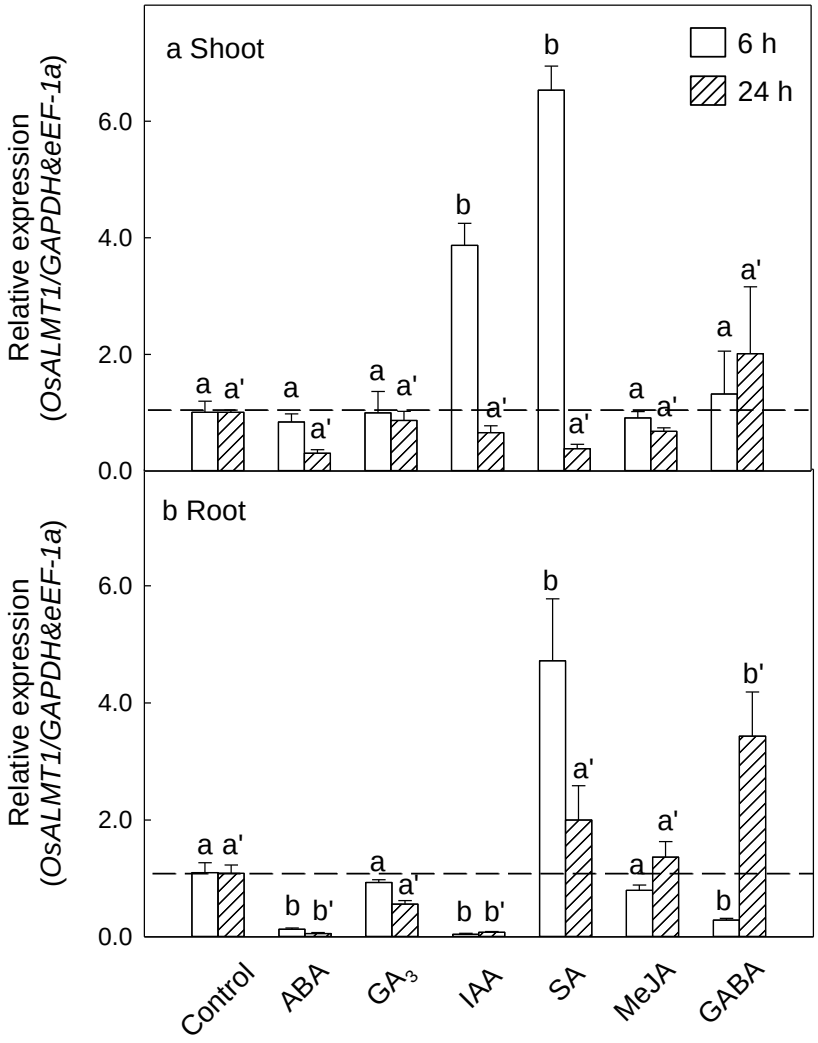

Figure 6.2 Changes in *OsALMT1* expression with hormone treatments

OsALMT1 expression in root and shoot tissue was measured using qRT-PCR in seedlings after 6 h and 24 h exposure to different hormones. Treatments included (100 µM) abscisic acid, gibberellin (GA_3), indole acetic acid (IAA), salicylic acid (SA), methyl jasmonic acid (MeJA) and 1 mM γ-amino butyric acid (GABA) added to the nutrient solution. Plants in control treatment were harvested at each time point for comparison. Results from the two reference genes (*GAPDH* and *eEF-1α*) were combined to provide a single result according to the software in Bio-Rad CFX Manager. Data show mean and SE from three biological replicates and three technical replicates. For convenience the results are presented with a single control even though the figure represents several separate experiments. The statistical analyses were performed on the raw data for each experiment with its own control. Data with different letters are significantly different from its own control values. The 6 and 24 h data were tested separately and differences indicated as a and b or a' and b' respectively.

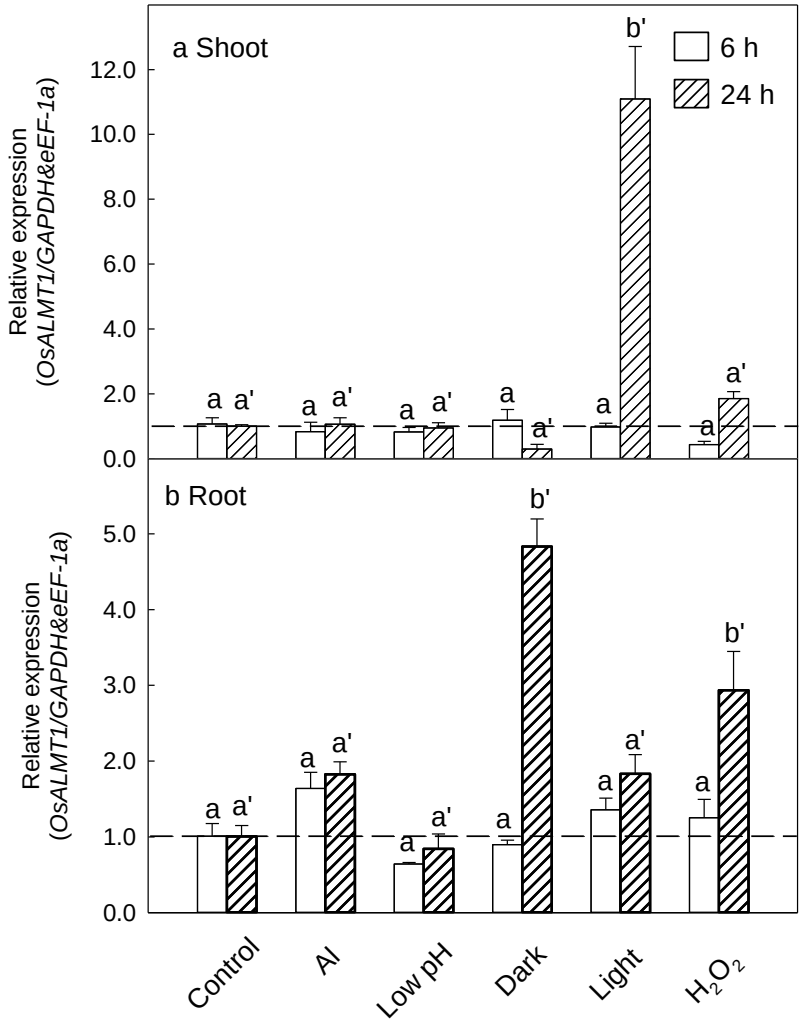

Figure 6.3 Changes in *OsALMT1* expression with different abiotic stresses

OsALMT1 expression in root and shoot tissue was measured using qRT-PCR in seedlings after 6 h and 24 h exposure to different stress conditions. Treatments included low pH (pH 4.5) alone, 100 μM $AlCl_3$ at pH 4.5, continual darkness, continual light and 300 μM hydrogen peroxide. Plants in control treatment were harvested at each time point for comparison. Results from the two reference genes (*GAPDH* and *eEF-1α*) were combined to provide a single result according to the software in Bio-Rad CFX Manager. Data show mean and SE from three biological replicates and three technical replicates. For convenience the results are presented with a single control even though the figure represents several separate experiments. The statistical analyses were performed on the raw data for each experiment with its own control. Data with different letters are significantly different from its own control values. The 6 and 24 h data were tested separately and differences indicated as a and b or a' and b' respectively.

directly affects OsALMT1 function.

OsALMT1 expression was not affected by methyl jasmonate or GA_3 and this was similar to reports previous for *AtALMT1* expression (Kobayashi *et al.*, 2013b). Online databases indicate that *OsALMT1* expression in roots is decreased under ABA treatment which is consistent with our result, and they also indicate little or no expression change in leaf tissues with GA_3, IAA and jasmonic acid treatments (**Chapter 3**).

The responses of *OsALMT1* expression to ABA, IAA and SA deserve further investigation because they contrast with the responses reported for *AtALMT1* in Arabidopsis (Kobayashi *et al.*, 2013b). In that study *AtALMT1* expression was strongly induced by IAA and ABA but not by SA. There are *cis*-acting regulatory elements in the *OsALMT1* promoter region which are potentially involved in ABA, GA_3, IAA and MeJA responsiveness. Detailed experiments are needed to determine whether these have biological activity.

Constant darkness or light for 6 h did not affect *OsALMT1* expression. This may not be surprising since 6 h still reflects a normal diurnal cycle. After 24 hours of continuous light expression increased significantly in the shoots. This could reflect increased metabolic activity and the requirement to transport and redistribute fixed carbon as sugars and other compounds throughout the plant in the vasculature. All these electrogenic transport processes need to be balanced by equal and opposite movements of other ions and the transport of malate could contribute to this.

Ten cis-acting regulatory elements involved in light responsiveness were found within the 1500 bp *OsALMT1* promoter region might be indicative that *OsALMT1* responds to the light/dark conditions (see **Chapter 3**). After 24 h in the darkness, *OsALMT1* transcript levels decreased slightly in the leaf but increased significantly in root tissue. It is hard to interpret these results. Under continuous darkness plants cannot photosynthesise so perhaps there is a greater requirement for recycling carbon and redistributing it from reserves in the roots to the shoots. Increasing *OsALMT1* expression in the roots might be involved with this recycling or with releasing more malate into the xylem for movement to the shoots when the light and transpiration returns. Some mycoheterotrophic plants which have no chlorophyll to obtain energy from sunlight

instead get nutrients and energy from organic matter in the soil (Klooster and Culley, 2009) so other plants might recycle their carbon in a similar way.

OsALMT1 expression did not change in a low pH solution or with Al treatment which is consistent with it not being involved with Al resistance. The *AtALMT1* gene in Arabidopsis is involved with Al tolerance and its expression is induced by both low pH and by Al treatment (Kobayashi *et al.*, 2007).

We conclude that *OsALMT1* expression in roots and shoots changes in response to a range of different stresses and especially osmotic stress and certain hormone treatments. Changes in the roots and shoots can occur in different directions. A general pattern observed for osmotic stress in hydroponics was a decrease in *OsALMT1* expression in the shoots and an increase in the roots.

6.5 References

Atkinson NJ, Urwin PE (2012) The interaction of plant biotic and abiotic stresses: from genes to the field. J Exp Bot 63: 3523-3543

Benková E, Michniewicz M, Sauer M, Teichmann T, Seifertová D, Jürgens G, Friml J (2003) Local, efflux-dependent auxin gradients as a common module for plant organ formation. Cell 115: 591-602

Chen Q, Zhang XD, Wang SS, Wang QF, Wang GQ, Nian HJ, Li KZ, Yu YX, Chen LM (2011) Transcriptional and physiological changes of alfalfa in response to aluminium stress. J Agr Sci 149: 737-751

Chen ZC, Yokosho K, Kashino M, Zhao FJ, Yamaji N, Ma JF (2013) Adaptation to acidic soil is achieved by increased numbers of cis-acting elements regulating *ALMT1* expression in *Holcus lanatus*. Plant J 76: 10-23

Lurin C, Geelen D, Barbier-Brygoo H, Guern J, Maurel C (1996) Cloning and functional expression of a plant voltage-dependent chloride channel. Plant Cell 8: 701-711

Colebrook EH, Thomas SG, Phillips AL, Hedden P (2014) The role of gibberellin signalling in plant responses to abiotic stress. J Exp Bot 217: 67-75

Delano-Frier JP, Aviles-Arnaut H, Casarrubias-Castillo K, Casique-Arroyo G, Castrillon-Arbelaez PA, Herrera-Estrella L, Massange-Sanchez J, Martinez-Gallardo NA, Parra-Cota FI, Vargas-Ortiz E, Estrada-Hernandez MG (2011) Transcriptomic analysis of grain amaranth (*Amaranthus hypochondriacus*) using 454 pyrosequencing: comparison with *A. tuberculatus*, expression profiling in stems and in response to biotic and abiotic stress. BMC Genomics 12: 363

Delhaize E, Ryan PR (1995) Aluminum toxicity and tolerance in plants. Plant Physiol 107: 315-321

Duque AS, Almeida AMd, Silva ABd, Silva JMd, Farinha AP, Santos D, Fevereiro P, Araújo SdS(2013). Abiotic Stress Responses in Plants: Unraveling the Complexity of Genes and Networks to Survive, Abiotic Stress - Plant Responses and Applications in Agriculture, Dr. Kourosh Vahdati (Ed.), ISBN: 978-953-51-1024-8, InTech

Frances S, Thompson WF (1997) The dark-adaptation response of the de-etiolated pea mutant lip7 is modulated by externa1 signals and endogenous programs. Plant Physiol 115: 23-28

Friml J (2003) Auxin transport — shaping the plant. Curr Opin Plant Biol 6: 7-12

Han YJ, Song PS, Kim JI (2007) Phytochrome-mediated photomorphogenesis in plants. J Plant Biol 50: 230-240

Hara M, Furukawa J, Sato A, Mizoguchi T, Miura K (2012) Abiotic stress and role of salicylic acid in plants. Abiotic Stress Responses in Plants 13: 235-251

Klooster MR, Culley TM (2009) Comparative analysis of the reproductive ecology of monotropa and monotropsis: two mycoheterotrophic genera in the monotropoideae (*Ericaceae*). Amer J Bot 96: 1337-1347

Kobayashi Y, Hoekenga OA, Itoh H, Nakashima M, Saito S, Shaff JE, Maron LG, Pineros MA, Kochian LV, Koyama H (2007) Characterization of *AtALMT1* expression in aluminum-inducible malate release and its role for rhizotoxic stress tolerance in arabidopsis. Plant Physiol 145: 843-852

Kobayashi Y, Kobayashi Y, Sugimoto M, Lakshmanan V, Iuchi S, Kobayashi M, Bais HP, Koyama H (2013a) Characterization of the Complex Regulation of *AtALMT1* Expression in Response to Phytohormones and Other Inducers. Plant Physiol 162: 732-740

Kobayashi Y, Lakshmanan V, Kobayashi Y, Asai M, Iuchi S, Kobayashi M, Bais HP, Koyama H (2013b) Overexpression of AtALMT1 in the Arabidopsis thaliana ecotype Columbia results in enhanced Al-activated malate excretion and beneficial bacterium recruitment. Plant Signal Behav 8: 25561-25564

Lakshmanan V, Kitto SL, Caplan JL, Hsueh YH, Kearns DB, Wu YS, Bais HP (2012) Microbe-associated molecular patterns-triggered root responses mediate beneficial rhizobacterial recruitment in Arabidopsis. Plant Physiol 160: 1642-1661

Liang CY, Pineros MA, Tian J, Yao ZF, Sun LL, Liu JP, Shaff J, Coluccio A, Kochian LV, Liao H (2013) Low pH, aluminum, and phosphorus coordinately regulate malate exudation through *GmALMT1* to improve soybean adaptation to acid soils. Plant Physiol 161: 1347-1361

Ligaba A, Katsuhara M, Ryan PR, Shibasaka M, Matsumoto H (2006) The *BnALMT1* and *BnALMT2* genes from rape encode aluminum-activated malate transporters that enhance the aluminum resistance of plant cells. Plant Physiol 142: 1294-1303

Luo X, Chen Z, Gao J, Gong Z (2014) Abscisic acid inhibits root growth in Arabidopsis through ethylene biosynthesis. Plant Jo 79: 44-55

Mazzucotelli E, Mastrangelo AM, Crosatti C, Guerra D, Stanca AM, Cattivelli L (2008) Abiotic stress response in plants: When post-transcriptional and post-translational regulations control transcription. Plant Sci 174: 420-431

O'Neill DP, Ross JJ, Reid JB (2000) Changes in Gibberellin A1 levels and response during de-etiolation of pea seedlings. Plant Physiol 124: 805-812

Osakabe K, Osakabe Y (2001) Plant Light Stress. eLS: John Wiley & Sons Ltd, Chichester.

Lange OL (2012). Physiological Plant Ecology II: Water relations and carbon assimilation. 12: Springer Science & Business Media

Peleg Z, Blumwald E (2011). Hormone balance and abiotic stress tolerance in crop plants. Curr Opin Plant Biol 14: 290-295

Rivas-San Vicente M, Plasencia J (2011) Salicylic acid beyond defence: its role in plant growth and development. J Exp Bot 62: 3321-3338

Rudrappa T, Czymmek KJ, Pare PW, Bais HP (2008) Root-secreted malic acid recruits beneficial soil bacteria. Plant Physiol148: 1547-1556

Ryan PR, Tyerman SD, Sasaki T, Furuichi T, Yamamoto Y, Zhang WH, Delhaize E (2011) The identification of aluminium-resistance genes provides opportunities for enhancing crop production on acid soils. J Exp Bot 62: 9-20

Scandalios JG (2005) Oxidative stress: molecular perception and transduction of signals triggering antioxidant gene defenses. Brazilian Journal of Medical and Biological Research 38: 995-1014

Ton J, Flors V, Mauch-Mani B (2009) The multifaceted role of ABA in disease resistance. Trends Plant Sci 14: 310-317

Vadim Demidchik SNS, Katherine B. Coutts, Mark A. Tester and Julia M. Davies (2002) Free oxygen radicals regulate plasma membrane Ca^{2+}-and K^{+}-permeable channels in plant root cells. J Cell Sci 116: 81-88

Vlot AC, Dempsey DA, Klessig DF (2009) Salicylic Acid, a multifaceted hormone to combat disease. Annu Rev Phytopathol 47: 177-206

Wasternack C (2007) Jasmonates: an update on biosynthesis, signal transduction and action in plant stress response, growth and development. Ann Bot 100: 681-697

Wasternack C, Hause B (2013) Jasmonates: biosynthesis, perception, signal transduction and action in plant stress response, growth and development. An update to the 2007 review in Annals of Botany. Ann Bot 111: 1021-1058

Wilkinson S, Davies WJ (2010) Drought, ozone, ABA and ethylene: new insights from cell to plant to community. Plant Cell Environ 33: 510-525

Xiong L, Zhu JK (2002) Molecular and genetic aspects of plant responses to osmotic stress. Plant Cell Environ 25: 131-139

XueXuan X, HongBo S, YuanYuan M, Gang X, JunNa S, DongGang G, Cheng-iang R (2010) Biotechnological implications from abscisic acid (ABA) roles in cold stress and leaf senescence as an important signal for improving plant sustainable survival under abiotic-stressed conditions. Crit Rev Biotechnol 30: 222-230

Yang LT, Jiang HX, Qi YP, Chen LS (2012) Differential expression of genes involved in alternative glycolytic pathways, phosphorus scavenging and recycling in response to aluminum and phosphorus interactions in Citrus roots. Mol Biol Rep 39: 6353-6366

CHAPTER 7

Generation of transgenic rice plants with altered levels of *OsALMT1* expression

7.1 Introduction

Genetic engineering is the direct manipulation of an organism's genome using biotechnology to create a genetically modified organism (GMO). There are many different types of genetic manipulation which are useful for different purposes. Some types require DNA to be inserted into the genome of another organism where it is transcribed and translated into protein to introduce a new trait into that GMO or enhance an existing trait. Others types of genetic manipulation do not require transcription of inserted DNA but rely on the random or targeted insertion of DNA into a host genome in order to disrupt or alter endogenous gene expression or function. Another type of genetic manipulation reduces gene expression without knocking out gene function totally. This method relies on RNA interference (RNAi) technology. RNAi is a biological process in which RNA molecules inhibit gene expression by inducing the degradation of specific mRNA molecules (Younis *et al.*, 2014).

The process of genetic engineering can be described in general terms as follows. A length of DNA containing a coding region of a protein is isolated from one organism and copied using molecular cloning methods. It is then ligated into a plasmid vector and transformed into the genome of a host organism by one of several methods (Alberts, 2002). The expression of a gene can be altered in plants or other systems to help discover the function of the proteins they encode. One method involves attaching the gene to a strong promoter to examine what phenotypes develop when the transgene and the protein it encodes are expressed to much higher values than occur in wild type plants. Another method relies on knocking-out gene expression totally or reducing it with RNAi methods to see whether new or altered phenotypes occur.

The promoter of a gene is region upstream of the coding region which controls when a gene is expressed, how strongly and in which tissues. The promoters used in biotechnology vary according to the intended purpose of the resulting transgenic lines. They can be

generally divided into constitutive promoters, specific promoters, inducible promoters and synthetic promoters (Potenza *et al.*, 2004). Constitutive promoters induce gene expression in all cells and tissues irrespective of environmental or developmental factors. The Cauliflower mosaic virus 35S promoter, which also named CaMV 35S promoter or 35S promoter, is one of the most widely used constitutive promoters (Odell *et al.*, 1985). The 35S promoter is a very strong constitutive promoter that drives high gene expression in eudicot plants. However, it can sometimes be less effective in monocotyledons, especially in cereals (Wilmink *et al.*, 1995). Therefore for research with monocotyledons other plant promoters are available to drive high constitutive transgene expression such as plant promoter from the *ubiquitin* gene (*Ubi*), *actin 1* promoter (Act-1) and *alcohol dehydrogenase 1* promoter (*Adh-1*). Ubiquitin is one of the most highly conserved proteins and the maize *ubiquitin 1* promoter (*pUbi*) promoter is a popular choice for cereals (Christensen *et al.*, 1992). In stably transformed rice plants, the maize *pUbi* promoter and its first intron generated higher levels of gene expression although this promoter can be slightly less active in the older tissues (Cornejo *et al.*, 1993). The next type of promoters are "specific" promoters which only operate in particular cells, tissues, at certain developmental stages of a plant. In this case the transgenes will only be expressed in particular tissues, cells or stages and leave the rest of the plant unmodified (Potenza *et al.*, 2004). In plants, various types of stresses, both biotic and abiotic, induce a large number of genes. Inducible promoters only function in response to certain environmental triggers (heat, cold, ion toxicities etc) or in the presence of specific chemical compounds. These compounds can include antibiotics, herbicides or hormones. Inducible promoters can also be tissue- or development-specific (Gatz, 1996; Holtorf *et al.*, 1995). Lastly, "synthetic" promoters are promoters manually assembled in the laboratory by bringing together the primary elements of a promoter (transcription start sites, *cis*-motifs etc) perhaps from diverse origins. The use of these promoters allows gene expression to be controlled in a very detailed way as long as the components are understood well (Venter, 2007).

When the genetic manipulation involves altering the expression of an endogenous gene (from the same species) it is described as a homologous expression system whereas when a gene from one species is expressed in a host organism from a different species it is a heterologous expression system (Costa *et al.*, 2010). The function of some ALMTs has already been investigated this way both in homologous and heterologous expression systems (**Table 7.1**).

The aim of this chapter was: (i) to generate transgenic rice lines with increased and reduced *OsALMT1* expression, (ii) to provide an initial characterisation these lines to help understand its function in rice.

7.2 Materials and Methods

7.2.1 Vector construction

To over-express *OsALMT1* in rice the vectors pWUbi and pGEM-OsALMT1-T Easy plasmids were digested by *Eco*RI and *Bam*HI and isolated from an agarose gel after electrophoresis separation. *OsALMT1* cDNA was ligated into pWUbi vector which contains the ubiquitin (Ubi) promoter and transformed into electro-competent DH5α *E. coli* cells. Positive colonies were detected by enzyme digestion and inserts sequenced using the primers UbiP and TM/pWUbi. A correct clone was digested with the *Not*I restriction enzyme and the excised fragment ligated into pWBVec8 (**Figure 7.1**). Positive clones were transformed into AGLI *Agrobacterium* competent cells for rice transformation. The rice transformation method is described in **Chapter 2**.

Knockout mutations in the *OsALMT1* gene of rice were not available from the rice genomic resource centre when this project started (http://signal.salk.edu/RiceGE/RiceGE_Data_Source.html) so instead RNAi technology was used to generate transgenic rice lines with reduced *OsALMT1* expression. An RNAi construct was prepared by amplifying the 1108-1335bp region of *OsALMT1* cDNA using primers PRR136 and PRR-137 (see **Chapter 2**). This fragment was unique to *OsALMT1* and so this construct would not be expected to reduce expression of any other member of the family. The fragment was ligated into pGEM-T Easy vector and positive colonies were selected by sequencing. The positive sequenced fragment was firstly inserted into digested pStarling (a) pretty vector by *Kpn*I and *Spe*I to form the pStarling-OsALMT1 RNAi Reverse plasmid. The pStarling-OsALMT1 RNAi Reverse plasmid was transformed into DH5α Electro competent *E. coli* cells. The pGEM- OsALMT1 RNAi-T Easy and pStarling-OsALMT1 RNAi Reverse plasmids then secondly were digested and ligated by *Bam*HI and *Xma*I and transformed into DH5α Electro competent cells. Positive colonies

Table 7.1 Homologous and heterologous expression of ALMT members

Gene function	Gene	Source species	Species transformed	Modification method	Promoter used	Transgenic phenotype	Reference
Al Resistance	*TaALMT1*	Wheat	*Xenopus* oocytes	Over-expression	T7 promoter	Al-activated malate efflux	(Sasaki *et al.*, 2004)
				Over-expression	T7 promoter	TaALMT1 is also permeable to Cl^-, NO_3^- and SO_4^{2-}	(Pineros *et al.*, 2008a)
			Rice	Over-expression	CaMV 35S	Al-activated malate efflux	(Sasaki *et al.*, 2004)
			Cultured tobacco cells	Over-expression	CaMV 35S	Increased tolerance to Al treatment	(Sasaki *et al.*, 2004)
				Over-expression	CaMV 35S	TaALMT1 functions as an Al^{3+} activated $malate^{2-}$ channel	(Zhang *et al.*, 2008)
			wheat	Over-expression	CaMV 35S	Enhanced Al^{3+} resistance	(Pereira *et al.*, 2010)
			Arabidopsis	Over-expression	CaMV 35S	Enhanced Al^{3+} resistance and malate release	(Ryan *et al.*, 2011)
			Barley	Over-expression	Ubiquitin promoter	High level of Al tolerance	(Delhaize *et al.*, 2004)
				Over-expression	Ubiquitin promoter	Enhanced phosphorus nutrition and grain production on acid soil	(Delhaize *et al.*, 2009)
	AtALMT1	*Arabidopsis*	*Xenopus* oocytes	Over-expression	T7 promoter	Associated with Al tolerance	(Hoekenga *et al.*, 2006)
			Arabidopsis	Knockout mutant	NA	The mutant was much more Al sensitive	(Hoekenga *et al.*, 2006)
				Knockout mutant	NA	The mutant exhibited inhibited root growth and malate release	(Kobayashi *et al.*, 2007)
				Over-expression	CaMV 35S	Enhanced malate excretion and beneficial bacterium recruitment	(Kobayashi *et al.*, 2013)

Gene function	Gene	Source species	Species transformed	Modification method	Promoter used	Transgenic phenotype	Reference
Al Resistance	*BnALMT1*	Rape	Cultured tobacco cells	Over-expression	CaMV 35S promoter	Enhanced malate efflux when exposed to Al	(Ligaba *et al.*, 2006)
			Xenopus oocytes	Over-expression	SP6 promoter	Enhanced malate efflux when exposed to Al	(Ligaba *et al.*, 2006)
	BnALMT2	Rape	Cultured tobacco cells	Over-expression	CaMV 35S promoter	Enhanced malate efflux when exposed to Al	(Ligaba *et al.*, 2006)
			Xenopus oocytes	Over-expression	SP6 promoter	Enhanced malate efflux when exposed to Al	(Ligaba *et al.*, 2006)
	MsALMT1	*Medicago sativa*	Tobacco	Over-expression	CaMV 35S promoter	Enhances malate exudation and aluminum resistance in tobacco	(Chen *et al.*, 2013a)
	GmALMT1	Soybean	*Xenopus* oocytes	Over-expression	T7 promoter	GmALMT1 mediates malate efflux in an extracellular pH-dependent and Al-independent manner.	(Liang *et al.*, 2013)
			Arabidopsis	Over-expression	CaMV 35S promoter	Transgenic *Arabidopsis* conferring a significant increase in Al tolerance	(Liang *et al.*, 2013)
			Soybean hairy roots	Over-expression	CaMV 35S promoter	Higher malate exudation and less Al accumulation in the root	(Liang *et al.*, 2013)
			Soybean hairy roots	RNAi	CaMV 35S	Lower malate exudation	(Liang *et al.*, 2013)
	HlALMT1	Yorkshire fog	*Xenopus* oocytes	Over-expression	T7 promoter	*HlALMT1* has Al activated malate efflux ability	(Chen *et al.*, 2013a)

			Rice	Over-expression	HlALMT1 promoter	HlALMT1 driven by the tolerance promoter showed more Al-induced malate secretion	(Chen *et al.*, 2013b)
Gene function	**Gene**	**Source species**	**Species transformed**	**Modification method**	**Promoter used**	**Transgenic phenotype**	**Reference**
Stomatal Functions	*HvALMT1*	Barley	*Xenopus* oocytes	Over-expression	T7 promoter	HvALMT1 conferred both inward and outward currents to a range of anions including malate	(Gruber *et al.*, 2010)
			Barley	Over-expression	Ubiquitin promoter	HvALMT1contribute to anion homeostasis in the cytosol and osmotic adjustment	(Gruber *et al.*, 2011)
				RNAi	Ubiquitin promoter	The RNAi line maintained higher stomatal conductance in low light intensity and lost water more rapidly from excised leaves	(Xu *et al.*, 2015)
	AtALMT12	*Arabidopsis*	*Arabidopsis*	Mutants	NA	Guard cell protoplasts isolated from *atalmt12* mutants revealed reduced R-type currents	(Meyer *et al.*, 2010)
				Mutant	NA	The nutation showed impaired stomatal closure induced by ABA, calcium and darkness	(Sasaki *et al.*, 2010)
				Mutant	NA	Site-directed mutations and deletions at the C terminus resulted in altered voltage-dependent channel activity	(Mumm *et al.*, 2013)
			Xenopus oocytes	Over-expression	Not mentioned	Voltage-dependent anion currents reminiscent to R-type channels could be activated	(Meyer *et al.*, 2010)

				Over-expression	T7 promoter	AtALMT12 facilitates chloride and nitrate currents but not those of organic solutes	(Sasaki *et al.*, 2010)
Gene function	**Gene**	**Source species**	**Species transformed**	**Modification method**	**Promoter used**	**Transgenic phenotype**	**Reference**
Stomatal Functions	*AtALMT6*	*Arabidopsis*	*Arabidopsis*	Mutant	NA	Guard cell vacuoles isolated from *Atalmt6* knock-out plants displayed reduced malate currents	(Meyer *et al.*, 2011)
	AtALMT9	*Arabidopsis*	*Tobacco* leaves	Over-expression	CaMV 35S promoter	Enhanced malate current densities across the mesophyll tonoplasts	(Kovermann *et al.*, 2007)
				Over-expression	Not mentioned	Cytosolic nucleotides and vacuolar anions directly modulate AtALMT9 intracellular transport	(Zhang *et al.*, 2014)
				Over-expression	CaMV 35S promoter	AtALMT9 is a chloride channel and activated by malate-dependent increase	(De Angeli *et al.*, 2013b)
				Over-expression	CaMV 35S promoter	Citrate is an “open channel blocker” of AtALMT9	(Zhang *et al.*, 2013)
				Over-expression	T7 promoter	Induced anion currents	(Kovermann *et al.*, 2007)
			Arabidopsis	Mutant	NA	Reduced vacuolar malate channel activity and malate content in mesophyll protoplasts	(Kovermann *et al.*, 2007)
			Xenopus oocytes	Mutant	NA	The mutants impaired stomatal opening and wilt more slowly than the wild type	(De Angeli *et al.*, 2013b)

				Mutant	NA	AtALMT9 is a tetramer and the TMa5 domains contribute to form the pore of this anion channel	(Zhang *et al.*, 2013)
Gene function	**Gene**	**Source species**	**Species transformed**	**Modification method**	**Promoter used**	**Transgenic phenotype**	**Reference**
Mineral Nutrition	*ZmALMT1*	Maize	*Xenopus* oocytes	Over-expression	T7 promoter	This transporter is implicated in the selective transport of anions involved in mineral nutrition and ion homeostasis processes	(Pineros *et al.*, 2008b)
	ZmALMT2	Maize	*Xenopus* oocytes	Over-expression	T7 promoter	Mediated an Al-independent electrogenic transport of organic and inorganic anion efflux	(Ligaba *et al.*, 2012)
			Arabidopsis	Over-expression	CaMV 35S promoter	Al-independent constitutive root malate efflux	(Ligaba *et al.*, 2012)
Vacuolar Malate Balance	*VvALMT9*	Maize Grape	*Tobacco* leaves	Over-expression	CaMV 35S promoter	VvALMT9 is able to mediate malate and tartrate accumulation in the vacuole of grape berries	(De Angeli *et al.*, 2013a)

NA – Not applicable

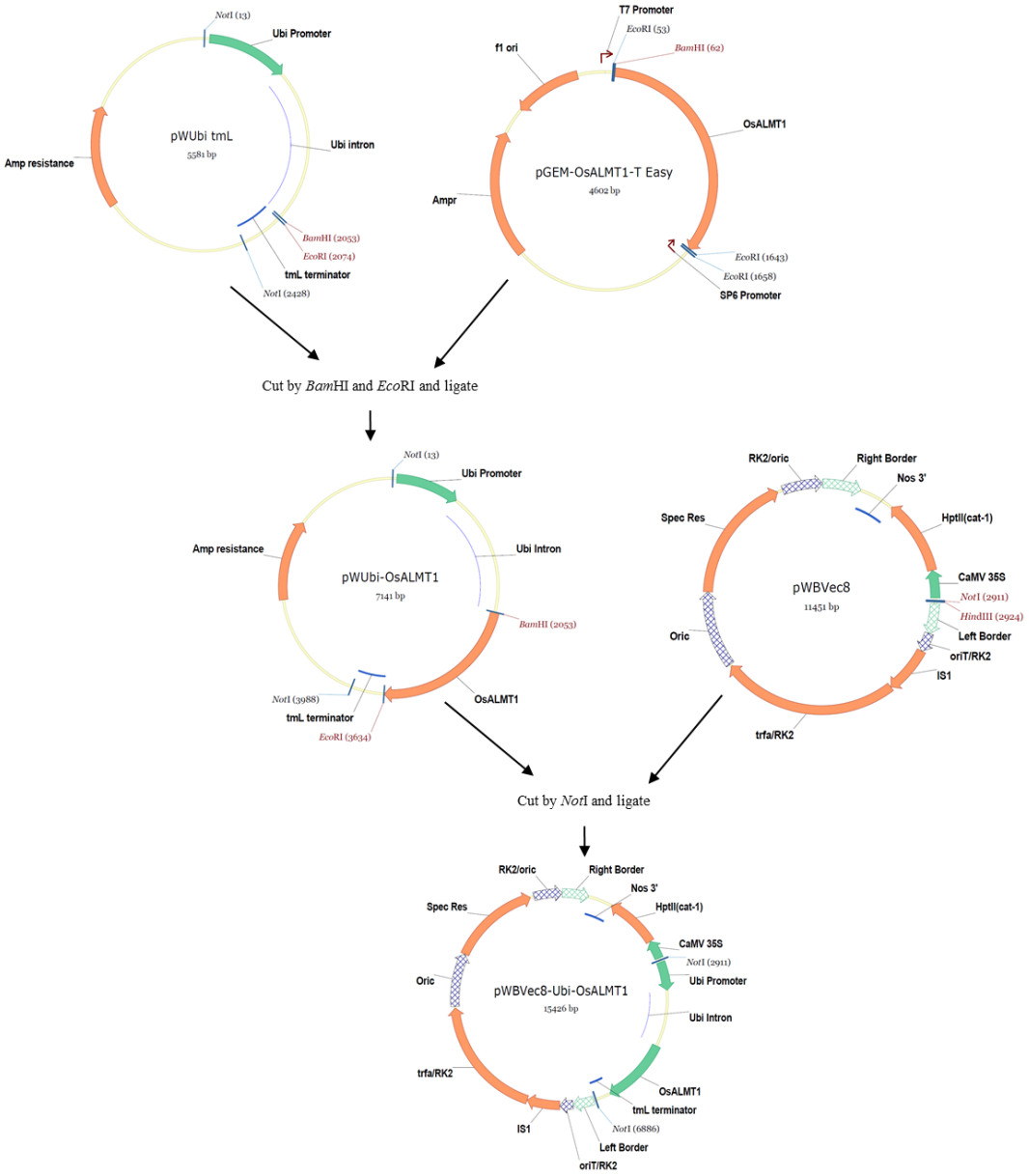

Figure 7.1 Construction of the pWBVec8-Ubi-OsALMT1 plasmid vector

Construction of the pWBVec8-Ubi-OsALMT1 vector used to overexpress *OsALMT1* in rice. The orange arrows represents coding DNA sequence (CDS) and the direction of the arrows is the same as the gene transcription direction, dark green arrows represent promoters, light hollow green arrows represent transfer borders, bold blue lines along the plasmid represent terminators, and fine blue lines along the plasmid represent introns. The fine blue lines cross the plasmid represent primer binding sites and the bold blue lines cross the plasmid represent restriction enzyme sites. CaMV35S is a strong constitutive promoter, the ubiquitin promoter (Ubi) is a strong constitutive promoter in monocotyledons, the tumor morphology larger terminator (tml terminator) is a transcriptional terminator in plants, the *hptII* gene confers hygromycin resistance for selection of transgenic plant lines, and the *Spec Res* gene is for spectinomycin resistance selection of transformed agrobacteria. Transfer is initiated at the right border and terminated at the left border.

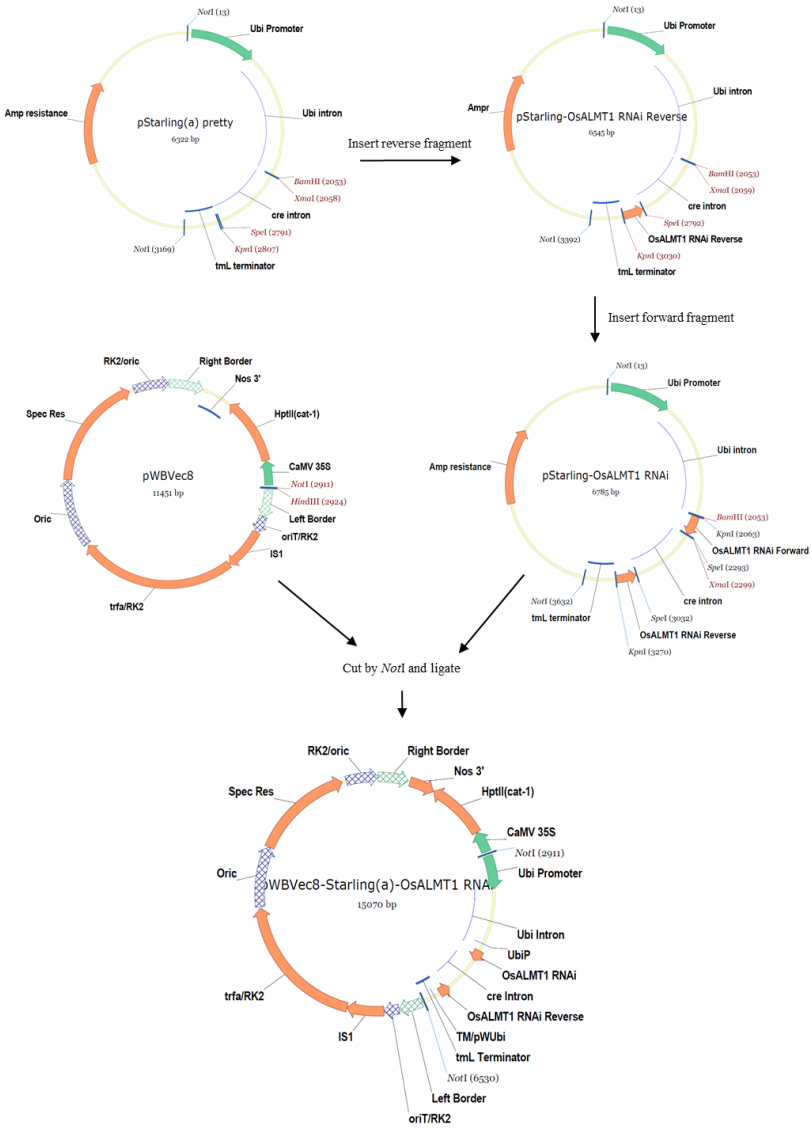

Figure 7.2 Construction of the pWBVec8-Starling(a)-OsALMT1 RNAi plasmid vector

Construction of the pWBVec8-Starling(a)-OsALMT1 RNAi plasmid for generate OsALMT1 RNAi plants. The orange arrows represents coding DNA sequence (CDS) and the direction of the arrows is the same as the gene transcription direction, dark green arrows represent promoters, light hollow green arrows represent transfer borders, bold blue lines along the plasmid represent terminators, and fine blue lines along the plasmid represent introns. The fine blue lines cross the plasmid represent primer binding sites and the bold blue lines cross the plasmid represent restriction enzyme sites. CaMV35S is a strong constitutive promoter, the ubiquitin promoter (Ubi) is a strong constitutive promoter in monocotyledons, the tumor morphology larger terminator (tml terminator) is a transcriptional terminator in plants, the *hptII* gene which confers hygromycin resistance for selection of transgenic plant lines, and the *Spec Res* gene for spectinomycin resistance selection of transformed agrobacteria. Transfer is initiated at the right border and terminated at the left border.

were detected by enzyme digestion and sequencing by using the primers UbiP and TM/pWUbi and the subsequent steps are the same as described above (**Figure 7.2**).

7.2.2 System for naming transgenic materials

The primary transgenic plants from tissue culture were called T0 plants. The seed harvested from T0 plants were called T1 seed. When several individual T1 seed were grown, each plant is named in a systematic way (gene_T1_line): the gene name followed by the generation name, and finally the line number. The T2 and T3 lines are derived from seed collected from individual plants. For the later generations some lines are nulls which means they are no longer transgenic because the transgenes were segregated away. In these cases the 'Null' was added to the names to make it easier to interpret the data **(Figure 7.3)**.

7.2.3 Identifying homozygous and null lines

Genomic DNA was extracted from more than 30 independent T0 plants and PCR used to confirm which were transgenic using the PRR80F/PRR80R primers which target to the *Ubi* promoter and *Ubi* intron (see above and **Chapter 2.5.1**). *OsALMT1* expression was then measured in positive T0 plants over-expressing *OsALMT1* and RNAi plants as described in **Chapter 2**. These measurements used the PRR142/PRR143 primers to target *OsALMT1* and the *OsGAPDHF*/*OsGAPDHR* and *OseEF-1αF/OseEF-1αR* primers for the two reference genes (see **Chapter 2**).

Several T0 plants were selected and grown in pots to collect T1 seed. For a single transgene insert, the T1 seed will segregate in a ratio of 1:2:1 for homozygous plants, hemizygous (one copy of the transgene) and null plants (without a transgene) (**Figure 7.3**). Therefore 25% of T1 seed will be null plants and 75% will be transgenic. For each independent transgenic event T1 seed were grown in soil and PCR tests on leaf material was used to find null segregant plants (no transgene). The T2 seed collected from these was used to find null segregant plants (no transgene). The T2 seed collected from these null plants were later used as controls. T1 plants that were transgenic were either

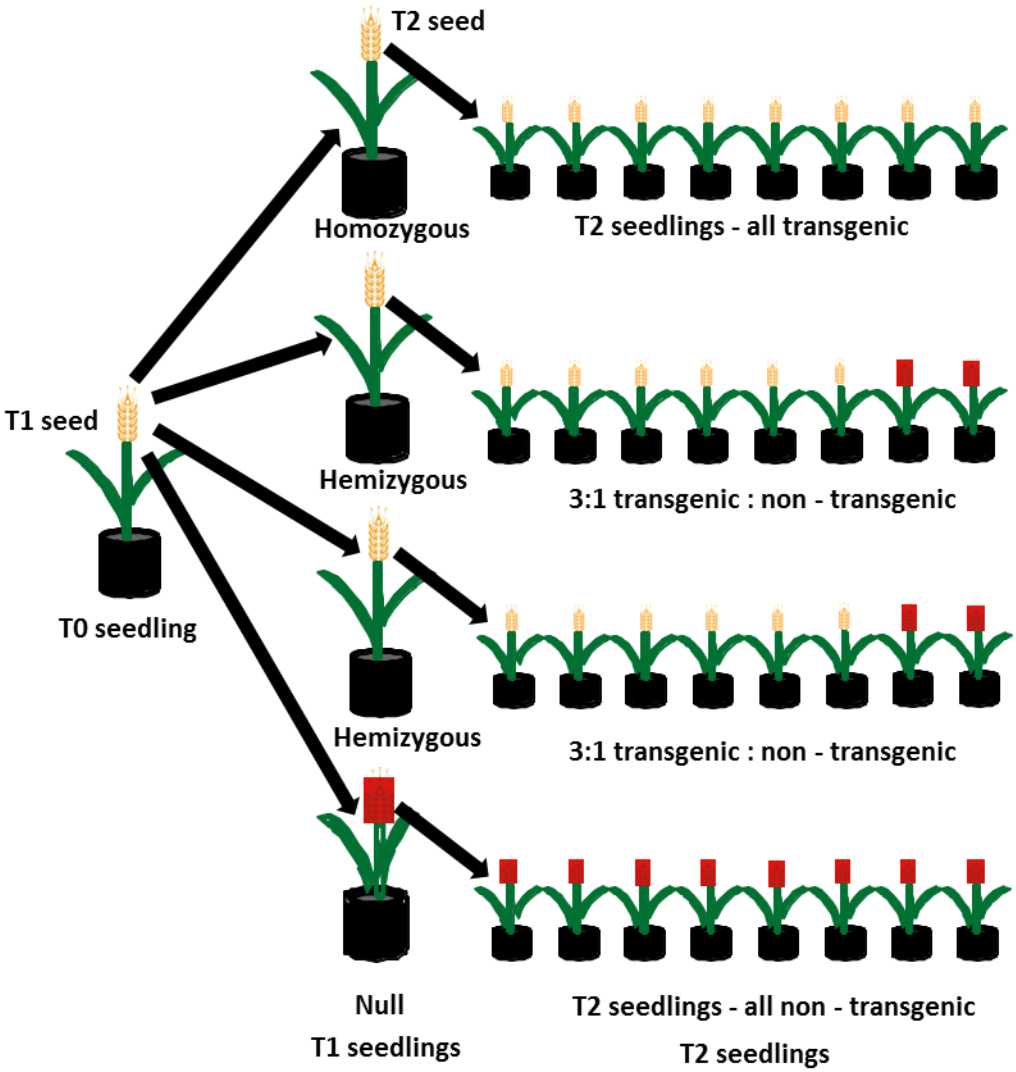

Figure 7.3 Nomenclature of transgenic plants and likely ratios for a single transgene insert.

For a single transgene insert, the segregation ratio of transgenic and non-transgenic plants in the T1 generation is 3:1 (where the transgenics include homozygous and hemizygous plants). All of the T2 seedlings from homozygous T1 are transgenic; T2 seedlings from hemizygous T1 have 3:1 segregation ratio (transgenic:non-transgenic); all of the T2 seedlings from null T1 are non-transgenic. Yellow spikelets represents transgenic plants and red spikelets represents non-transgenic plants.

hemizygous (66%) or homozygous (33%) if a single insert was present. T2 seed was collected from these transgenic plants and then 20 seed from each of six different plants (families) were grown in soil **(Figure 7.3)**. Genomic DNA was extracted from each of the 20 plants and tested with PCR for the presence of the transformation vector as described above. Those T2 lines in which all 20 plants contained the vector were considered homozygous lines. T2 lines which contained a mixture of transgenic and non-transgenic were hemizygous. The ratio of null plants to transgenic plants within the T1 and T2 families provided information on the likely copy number of transgene inserts (**Figure 7.3**).

7.2.4 Examining appearance of the leaf phenotype on transgenic lines

Two lines over-expressing *OsALMT1* and their relative null lines were germinated as described in **Chapter 2**. After one week of growth in the medium, the plants were transferred into pots with flooded soil and placed in different growth glasshouse and cabinets with different growth conditions: A = Glasshouse (high light and high temperature, 29/22 ˚C, natural day/night cycle with light intensity of ~350-1500 µmol m^{-2} s^{-1}), B = Growth Cabinet (high light and high temperature, 29/24 ˚C, 16/8 hours day/night cycle with light intensity of ~600 µmol m^{-2} s^{-1}), C = Growth Cabinet (high light and low temperature, 22/20 ˚C, 16/8 hours day/night cycle with light intensity of ~600 µmol m^{-2} s^{-1}) and D = Growth Cabinet (low light and high temperature, 29/24 ˚C, 16/8 hours day/night cycle with light intensity of ~300 µmol m^{-2} s^{-1}). The severity of leaf spot symptoms were checked frequently after planting and scored for severity. The severity of leaf spot symptoms were scored as : 0 = No visible symptoms; 1 = Mild (few small brown spots); 2 = Medium (larger and denser brown spots); 3 = Strong (leaf has a higher density of larger brown spots). Photographs of these are shown in the Results

7.2.5 Oxidative determination of the transgenic rice leaf

The method to visualize relative O_2^- and H_2O_2 concentrations was modified from Giraud *et al.*, (2008) (Giraud *et al.*, 2008). Rice leaves from two transgenic overexpressing *OsALMT1* and their relative null lines were grown in flooded soil under glasshouse

conditions until the brown spot phenotype appeared. Three plants with either no phenotype (no spots), moderate phenotype (moderate size and density of spots) or strong phenotype (larger and denser spots) were examined and three leaves from each plant were sampled and assayed as follows. Excised leaves were placed in 6 mM nitroblue tetrazolium for O_2^- detection or 5 mM 3,3'-diaminobenzidine for H_2O_2 detection. Leaf segments were infiltrated in the stain solution under vacuum for 30 minutes and incubated for three more hours. After three hours, the leaves were placed into 100% boiling ethanol and incubated for 30 minutes to remove the chlorophyll. The leaves were stored in 40% (v/v) glycerol until examined.

7.2.6 Growth experiments for biomass measurements

Two lines over-expressing *OsALMT1*, and their relative null lines, and two RNAi lines with reduced expression, and their relative null lines, were germinated as described in **Chapter 2**. After one week of growth in the medium, the plants were transferred into nutrient solution or flooded soil (as described in **Chapter 2**) in various growth conditions: Hydroponic in glasshouse (29/22 ˚C, natural day/night cycle with light intensity of ~350-1500 µmol m^{-2} s^{-1}), hydroponic in growth cabinet (29/22 ˚C, 16/8 hours day/night cycle with light intensity of ~600 µmol m^{-2} s^{-1}), flooded soil in glasshouse (29/22 ˚C, natural day/night cycle with light intensity of ~350-1500 µmol m^{-2} s^{-1}), flooded soil in growth cabinet (29/22 ˚C, 16/8 hours day/night cycle with light intensity of ~600 µmol m^{-2} s^{-1}). Plants were harvested after three to eight weeks of being transferred into these conditions. For the hydroponically grown plants, root and shoot tissues were harvested and dried separately for 72 h at 65 ˚C. For the flooded soil grown plants, the up-ground shoot tissue was harvested and dried for 72 h at 65 ˚C.

7.2.7 Mineral analysis in leaf tissue

Mineral analyses were performed in leaves collected from plants grown under normal soil conditions. The plants included transgenic lines overexpressing *OsALMT1*, transgenic RNAi lines with reduced expression as well as null control lines. The leaf tissue were dried at 70 ℃ for 24 hours. Between 50 to 250 mg dry tissue was digested by

8 mL concentrated nitric acid and 2 mL hydrochloric acid and digested at 170 ℃ in microwave oven for 1.5 h. The samples were diluted in 40 mL milliQ water and elements analysed by Analytical Chemistry Group, CSIRO, with inductively coupled plasma mass spectrometry (ICP) analysis.

7.2.8 Weight of the T3 generation seed

Three plants from two T2 lines overexpressing *OsALMT1* and two T2 lines with reduced expression (RNAi), and their respective nulls, were grown under normal glasshouse flooded soil condition. T3 generation seeds were harvested and dried for 72 hours at 42 ˚C. Weight of 100 T3 seed from each line was measured.

7.3 Results

7.3.1 *OsALMT1* expression in T_0 plants

OsALMT1 expression was measured in 31 positive T0 plants over-expressing *OsALMT1* and 35 T0 RNAi plants (**Figure 7.4**). Plants transformed with the over-expression construct showed a wide range of expression levels from 2 to 95 fold higher of wild type plants (WT). T0 plants transformed with the RNAi vector plants showed expression at 0.89 to 0.001 levels relative to wild type plants.

7.3.2 Identifying homozygous and null lines

Seven plants containing the overexpression construct and seven plants with the RNAi constructs with a range of expression levels were selected to generate T1 seed. Twenty T1 plants for each line were grown and tested whether they were transgenic or not using PCR to target the transformation plasmid (**Table 7.2**). Lines with single transgene inserts were preferred for further study since they are more likely to display stable phenotypes in the subsequent generations. Therefore the segregation data together with *OsALMT1* expression levels measured in the T0 plants was used to select three T1 lines over-

expressing *OsALMT1* and three RNAi lines with reduced *OsALMT1* expression for further experiments (**Table 7.2**). Among the over-expression lines OE2, OE5 and OE8 had high relatively expression and a segregation ratio consistent with a single transgene insert. Among the lines with reduced *OsALMT1* expression R24, R58 and R78 had relatively low expression levels and a segregation ratio consistent with a single transgene insert. T2 seed was then collected from the selected lines. Twenty T_2 seed were planted for each of the selected families and PCR used to score for the transformation plasmid so that three homozygous lines with higher expression and three lines with reduced expression, along with their corresponding null sister lines, were selected for further experiments.

Relative expression of *OsALMT1* was then measured in the three independent homozygous lines over-expressing *OsALMT1* (OE5-5, OE2-18 and OE8-5) and their respective null sister lines (OE5-13_null, OE2-8_null and OE8-16_null). The homozygous OE lines showed 18 to 40-fold higher *OsALMT1* expression than their null sister lines which were similar to wild type plants (**Figure 7.5**). Relative expression of *OsALMT1* was also measured in the three independent homozygous lines with reduced *OsALMT1* expression (R24-15, R58-1 and R8-5) and their respective null sister lines (R24-20_null, R58-5_null and R78-6_null). Expression in the homozygous RNAi lines was 10 to 24% the levels of their null sister lines which were similar to wild type plants (**Figure 7.5**).

7.3.3 General phenotypes of the transgenic lines.

The transgenic lines over-expressing *OsALMT1* plants developed a phenotype of brown spots on the leaves after approximately 40 d of growth in flooded soil, non-flooded soil and hydroponics (**Figure 7.6**). These spots appeared on the older leaves but timing was variable and depended on the growth conditions (see later). These spots appeared first on the OE5-5 homozygous line, then OE2-18 and lastly the OE8-5 homozygous lines and so the severity of this phenotype was generally correlated with the level of *OsALMT1* expression. This indicated that higher *OsALMT1* expression may lead to some imbalance or sensitivity to stress which leads the spotted phenotype. This phenotype did not appear

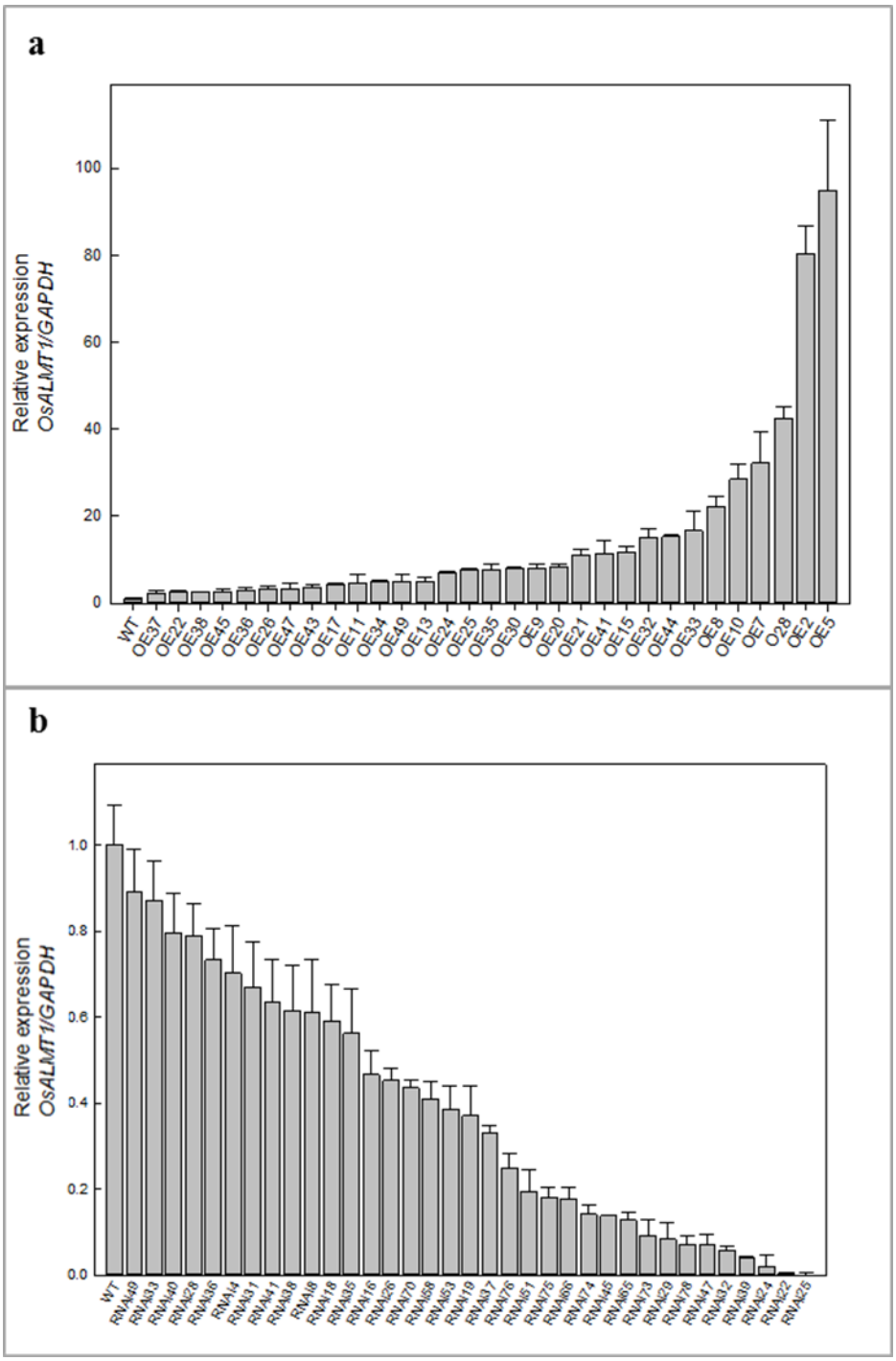

Figure 7.4 Relative expression of *OsALMT1* in T0 plants

Relative expression of *OsALMT1* was measured in T0 plants using qRT-PCR and *GAPDH* as a reference gene. (a) The range of T0 plants over-expressing *OsALMT1*. (b) The range of RNAi T0 plants with reduced *OsALMT1* expression. Data represent three technical replicates from a single plant.

Table 7.2 Initial characterisation of the transgenic rice plants

Shown are 20 T1 plants from seven individual T0 lines examined for OsALMT1 expression levels and segregation ratio. The segregation ratio was calculated by Transgenic/Non-Transgenic T1 plants. Three lines were selected based on a 3:1 ratio which is likely to contain a single copy of the transgene (red ones).

Transgenic Line	Relative *OsALMT1* expression in T0 plants	#Transgenic T1 plants	#Non-transgenic T1 plants	Segregation ratio
Over-expression lines				
OE2	80.3704	15	5	**3:1**
OE5	94.8661	14	6	**2.3:1**
OE8	22.1757	15	5	**3:1**
OE9	8.0694	17	3	5.7:1
OE10	28.4341	16	4	4:1
OE17	4.3774	20	0	20:0
OE30	7.9206	20	0	20:0
RNAi lines				
RNAi19	0.3703	20	0	20:0
RNAi24	0.0206	15	5	**3:1**
RNAi29	0.0836	16	4	4:1
RNAi45	0.1376	18	2	9:1
RNAi58	0.4106	15	5	**3:1**
RNAi76	0.2490	19	1	19:1
RNAi78	0.0714	15	5	**3:1**

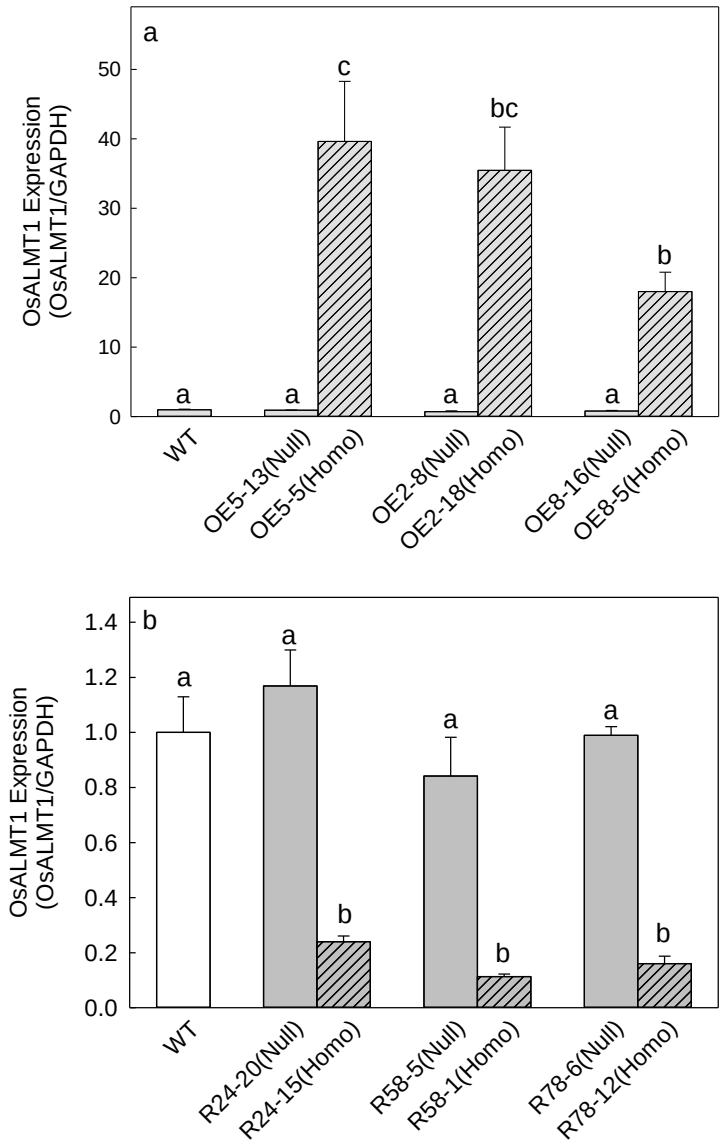

Figure 7.5 Relative expression of *OsALMT1* in transgenic T_2 lines

Expression of *OsALMT1* was measured in (a) three homozygous lines with increased and (b) three homozygous lines with decreased expression as well as their corresponding null lines. Data represent three biological replicates from three technical replicates. Reference gene was *GAPDH*. Data were analysed with a one way ANOVA after transformation to the square root to satisfy the requirement for homogeneous variances. Data with different letters are significantly different at $P<0.05$.

in any of the null lines, the RNAi lines or WT plants (**Figure 7.6**). The spots might be caused by mineral stress due to metal accumulation or oxidative stress. Transgenic overexpressing and RNAi lines and nulls were grown in soil and elemental analysis performed on the leaves (**Figure 7.7**). The OE5-5 line, which showed the strongest leaf symptoms showed significantly greater concentrations of Cu, Cr and Fe than the null sister line while the RNAi line showed reduced B, Ca and Mn concentrations. However these findings should be viewed cautiously since they were not always observed in subsequent experiments where tissues of different ages were measured. As a general trend higher concentrations of Mn were observed in lines over-expressing OsALMT1 but this was not a consistent result. Similarly the changes in mineral concentration of the RNAi line were also variable. This variability is investigated later in this Chapter.

The appearance of this brown spot phenotype was monitored in plants under different growth conditions which included high and low light intensity and high and low temperatures. The treatments were as follows: A = Glasshouse (high light and high temperature, 29/22 ˚C, natural day/night cycle with light intensity of ~350-1500 µmol m^{-2} s^{-1}), B = Growth Cabinet (high light and high temperature, 29/24 ˚C, 16/8 hours day/night cycle with light intensity of ~600 µmol m^{-2} s^{-1}), C = Growth Cabinet (high light and low temperature, 22/20 ˚C, 16/8 hours day/night cycle with light intensity of ~600 µmol m^{-2} s^{-1}) and D = Growth Cabinet (low light and high temperature, 29/24 ˚C, 16/8 hours day/night cycle with light intensity of ~300 µmol m^{-2} s^{-1}). The severity of leaf spot symptoms were checked frequently after planting and scored for severity from 0 (no spots) to 3 (larger and denser spots). Results indicated that the brown spots on lines overexpressing *OsALMT1* lines tended to appear earlier under higher light intensity and higher temperature conditions (**Table 7.3**). This is consistent with Mn toxicity. Therefore Mn concentration in leaves from the overexpressing lines was measured in different experiments using leaves of different ages. The results in **Table 7.4** show that in some experiments the Mn concentrations in the overexpressing lines were significantly greater than the null lines but this was not observed in every case. Furthermore the appearance of the brown spots was not directly correlated with total Mn concentration in the leaves.

The earliest development of the spotted phenotype on the over-expressing lines occurred when high light was combined with high temperature. These brown spots and their increased occurrence with high light and temperature are consistent with the symptoms

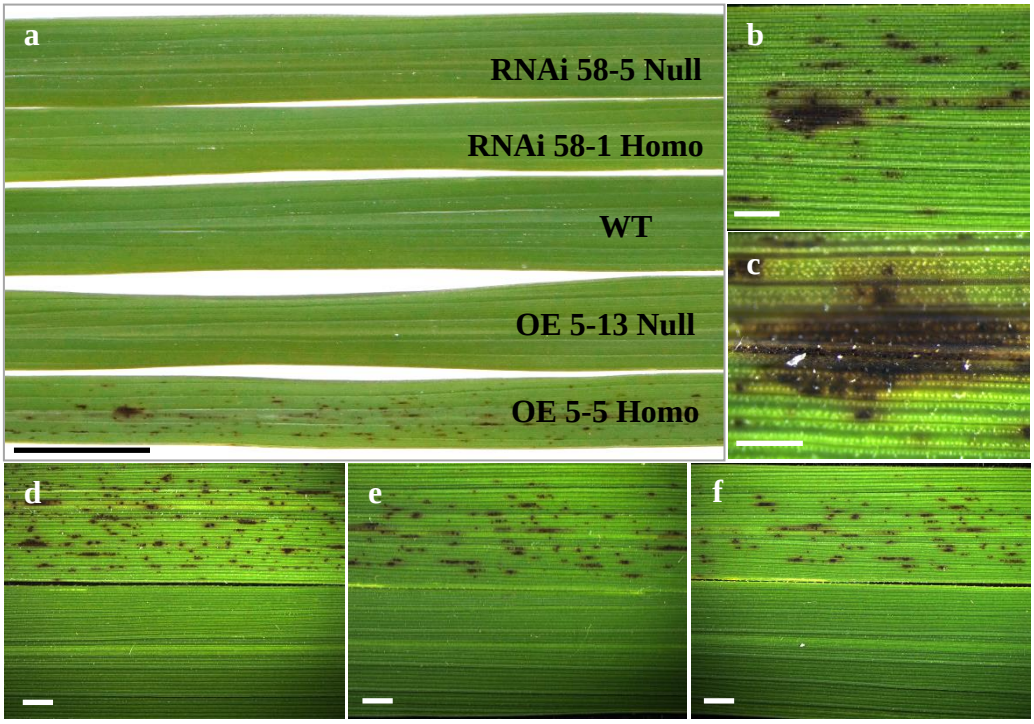

Figure 7.6 Leaf phenotype on rice plants showing increased *OsALMT1* expression

A consistent phenotype observed on rice plants over-expressing *OsALMT1* was brown spots which appear after about four weeks growth, depending on growth conditions. These were not observed in the null lines or in any of the RNAi lines or wild type plants. (a) Photographs of different rice lines with altered *OsALMT1* expression. Notice the brown spots on the OE5-5 line with highest expression; (b) Brown spots from OE5-5 line under Leica MZFLIII fluorescence dissecting microscope; (c) Detailed image of the brown spot under Leica MZFLIII fluorescence dissecting microscope; (d) Comparison of OE5-5 homozygous line (upper) with the null sister line OE5-13 (lower); (e) Comparison of OE2-18 homozygous (upper) with the null sister line OE2-8 (lower); (f) Comparison of OE8-5 homozygous (upper) with the null sister line OE8-16 (lower). Scale bars in figure a, b, c and d-f represent 1 cm, 1 mm, 500 µm and 2 mm, respectively.

of oxidative stress. Preliminary tests then compared the O_2^- and H_2O_2 concentrations in transgenic and null plants using the nitroblue tetrazolium and 3,3'-diaminobenzidine reagents. However no consistent differences were detected between leaves with the spots and without (data not shown). Rice OE 5-5 and OE 2-18 lines over-expressing *OsALMT1* tended to be smaller and accumulate less root and shoot biomass compared with their nulls in hydroponics. These lines also accumulated less shoot biomass under flooded soil conditions compared with their nulls. These observations are shown in **Table 7.5** which summarises data collected from many experiments throughout this whole project. By the contrast, the RNAi lines with reduced expression accumulated similar biomass to their null sister lines in most cases. This result indicates that the higher *OsALMT1* expression, which is associated with the brown spot phenotype on leaves, affects plant growth in both flooded soils and hydroponic conditions.

The effect of *OsALMT1* expression level on seed size was also measured by weighing 100 seeds collected from three plants in a set of T3 lines (**Figure 7.8**). The OE5-5 and OE2-18 lines showed a trend to lower seed weight compared to their nulls but this was significant for the OE2-18 line only. The RNAi lines R24-15 and R58-1 showed no significant differences in grain weight compared to their null sister lines. These results indicate that the level of *OsALMT1* expression can affect the seed development to some extent.

7.4 Discussion

Examination of the transgenic lines over-expressing *OsALMT1* can help to understand the function of the OsALMT1 protein but since a constitutive promoter was used not all the phenotypes induced will necessarily reflect function in WT plants. Although *OsALMT1* appears to be widely expressed in the rice, expression in cells or tissues that do not usually express this gene in WT plants (such as guard cells) could result in complex phenotypes. Therefore, the changes occurring in transgenic lines constitutively overexpressing a gene should be considered cautiously to avoid making wrong conclusions about function. More informative are the phenotypes observed in the RNAi lines. While the phenotypes in these plants still need to be examined carefully, the loss or reduction of function is more easily interpreted.

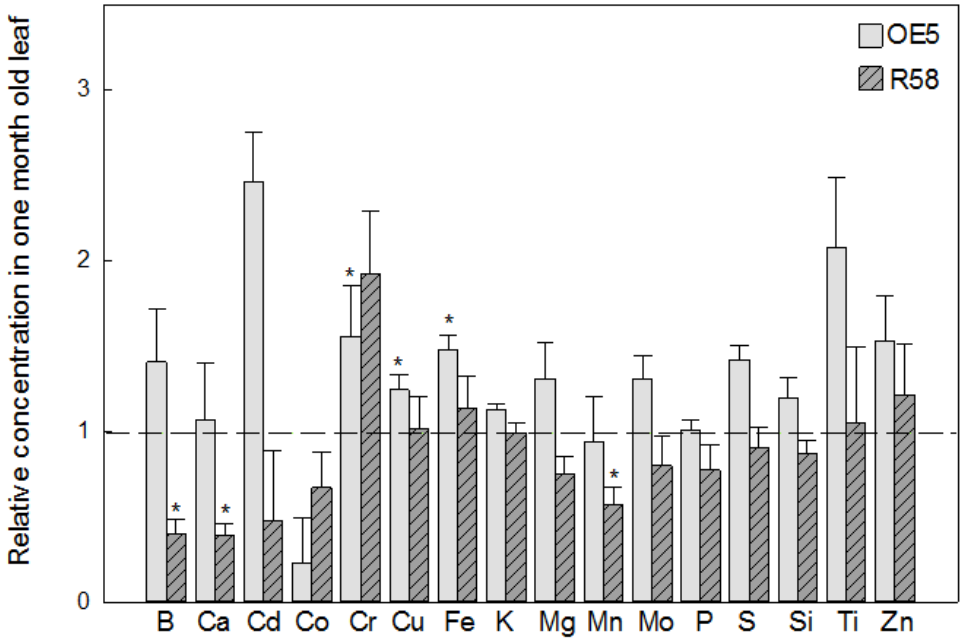

Figure 7.7 Mineral composition of leaves

Relative mineral concentrations in leaves from an over-expressing *OsALMT1* transgenic line (OE5-5) and an RNAi line with reduced *OsALMT1* expression (R58-1) were measured with inductively coupled plasma mass spectrometry (ICP) analysis. Results show the concentrations of each element in each line relative to their own null sister lines: OE5-13_null and R58-5_null. The plants were about four weeks old. Data show mean, SE (n=3). Raw data is presented in **Table S4**. Statistical analyses were performed on the raw data for each element whereby each transgenic line was compared to its null sister line and significant differences ($P<0.05$) indicated by an asterisk.

Table 7.3 Leaf phenotype appearance time line

The table shows symptoms appear time after plant into soil (Days).
Growth Conditions: A = Glasshouse (High light+High Temperature)
B = Growth Cabinet (High light+High Temperature)
C = Growth Cabinet (High light+Low Temperature)
D = Growth Cabinet (Low light+High Temperature)

		7D	14D	21D	28D	35D	42D	49D	56D
OE 5-5 (Homo)	A	0	0	**1**	**1**	**2**	**2**	**3**	**3**
	B	0	0	0	0	**1**	**1**	**2**	**2**
	C	0	0	0	0	0	0	**1**	**1**
	D	0	0	0	0	0	0	0	**1**
OE5-13 (Null)	A	0	0	0	0	0	0	0	0
	B	0	0	0	0	0	0	0	0
	C	0	0	0	0	0	0	0	0
	D	0	0	0	0	0	0	0	0
OE2-18 (Homo)	A	0	0	0	**1**	**1**	**2**	**2**	**3**
	B	0	0	0	0	0	**1**	**1**	**1**
	C	0	0	0	0	0	0	0	**1**
	D	0	0	0	0	0	0	0	0
OE2-8 (Null)	A	0	0	0	0	0	0	0	0
	B	0	0	0	0	0	0	0	0
	C	0	0	0	0	0	0	0	0
	D	0	0	0	0	0	0	0	0

Key: Severity of leaf spot symptoms (scale bar is 5 mm):

0 = None;

1 = Mild;

2 = Medium;

3 = Strong.

Table 7.4 Concentration of Mn in the leaves of lines overexpressing *OsALMT1* and their nulls from different experiments and different ages

	Mn concentration (mg/kg DW)					
Lines	1 month old leaf	3 month old leaf	Old leaf (+sym)	New leaf (+sym)	New leaf (-sym)	Leaf (+sym)
OE5-5	252 ± 68	59 ± 11	136 ±	44 ± 5	38 ± 2	913 ±
OE5-13-null	268 ± 25	54 ± 5	51 ± 25	34 ± 2	52 ± 18	394 ± 41
OE2-18	-	-	-	-	-	889 ± 258
OE2-8_null	-	-	-	-	-	342 ± 199

Asterisks indicate significant difference ($P_{0.05}$) using a t test between the OE line and its null sister line for that experiment.

$^{\Psi}$(-sym) and (+sym) indicate the absence and presence of the brown spot symptoms in the homozygous lines, respectively. No symptoms appeared in the nulls.

Table 7.5 Dry weight of transgenic lines grown in hydroponic and water-flooded soil conditions

Dry weight (g) was measured after 3-8 weeks (W) grown under different conditions and samples were drying for 72 hours at 65 ˚C. Value represent average ± SE (n=4-6). Asterisks indicate significant differences (P=0.05) using a t test to compare the raw shoot or root biomass of a specific transgenic line and its corresponding null line. GH: Glasshouse, GC: Growth cabinet

		Hydroponic in GH (4W)	Hydroponic in GH (4W)	Hydroponic in GH (6W)	Hydroponic in GC (4W)	Hydroponic in GC (3W)	Flooded soil in GC (8W)	Flooded soil in GC (4W)	Flooded soil in GH (8W)	Flooded soil in GH (6W)
OE5-5	Shoot	0.37 ±0.05*	0.31 ±0.07*		0.84 ±0.05*	0.80 ±0.15	13.69 ±0.42*		9.23 ±0.73	
(Homoz)	Root	0.11 ±0.01*	0.10 ±0.03*		0.32 ±0.02*	0.25 ±0.05	-		-	
OE5-13	Shoot	0.91 ±0.08	0.79 ±0.14		1.11 ±0.06	0.66 ±0.07	16.94 ±0.80		13.98 ±2.19	
(Null)	Root	0.26 ±0.02	0.32 ±0.05		0.57 ±0.05	0.28 ±0.03	-		-	
OE2-18	Shoot	0.59 ±0.05*	0.60 ±0.03		0.81 ±0.07*		14.41 ±1.16		9.42 ±0.69*	
(Homoz)	Root	0.14 ±0.01*	0.18 ±0.01*		0.30 ±0.02*		-		-	
OE2-8	Shoot	0.91 ±0.06	0.84 ±0.09		1.15 ±0.03		17.55 ±0.72		13.60 ±0.92	
(Null)	Root	0.26 ±0.01	0.35 ±0.03		0.53 ±0.03		-		-	
R24-15	Shoot	0.37 ±0.06		1.11 ±0.09	1.11 ±0.03	0.49 ±0.10		2.53 ±0.38		3.41 ±0.61
(Homoz)	Root	0.10 ±0.01		0.59 ±0.03	0.56 ±0.01	0.21 ±0.04		-		-
R24-20	Shoot	0.42 ±0.04		0.96 ±0.10	1.13 ±0.08	0.71 ±0.09		3.03 ±0.34		5.27 ±0.30
(Null)	Root	0.12 ±0.01		0.47 ±0.05	0.54 ±0.04	0.31 ±0.04		-		-
R58-1	Shoot	0.41 ±0.01*		1.06 ±0.09	1.15 ±0.04			2.15 ±0.15		4.50 ±0.81
(Homoz)	Root	0.11 ±0.00		0.55 ±0.06	0.55 ±0.02			-		-
R58-5	Shoot	0.30 ±0.04		1.20 ±0.18	1.09 ±0.06			2.43 ±0.28		6.49 ±0.52
(Null)	Root	0.08 ±0.01		0.63 ±0.09	0.54 ±0.02		-	-		-

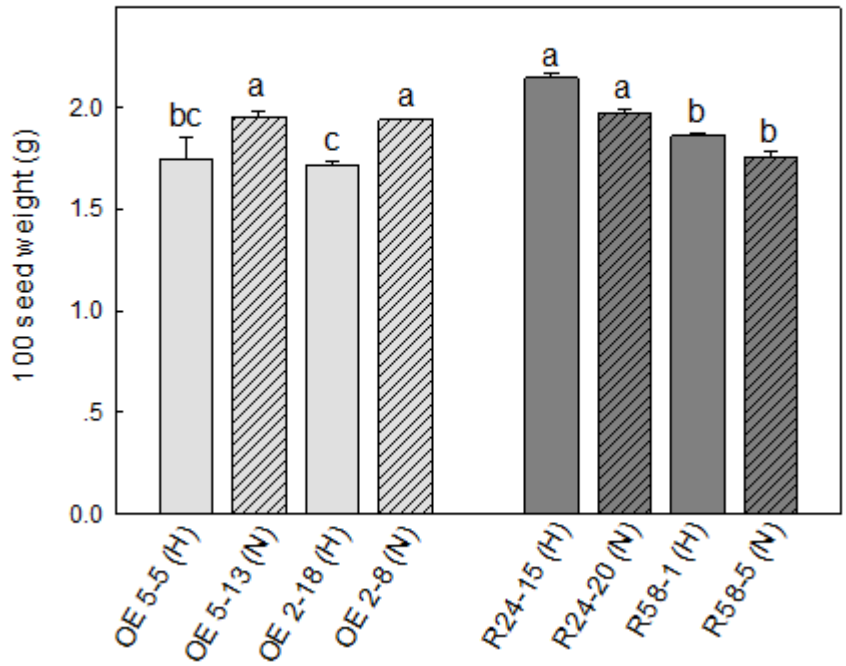

Figure 7.8 Weight of 100 grains from different transgenic lines

100 seed weight was measured by using T3 seed. For each line, three individual T3 lines were measured and three replicates were measured for each individual line. Data show the mean of total 100 seed weight (g) and standard error (n=9). H: homozygous, N: Null. Data were analysed with a one-way ANOVA and significant differences indicated by different letters using the Tukey test.

Homozygous transgenic rice lines with higher and lower expression of *OsALMT1* were generated. The transgenic plants over-expressing *OsALMT1* showed a phenotype of brown spots on the leaves. This phenotype can be caused by a number of processes but they are often associated with hypersensitive responses (HR). Many pathogens and diseases induce the HR and cause brown spots in rice. For example the fungus *Cochliobolus miyabeanus* is one of the most prevalent rice diseases in around the world but this is unlikely to be causing the phenotypes here because no fungal spores could be found on the leaf and the nulls did not show the symptoms. Furthermore this disease is typically associated with water-stressed plants (low water) and in nutrient poor soils neither of which are relevant to the growth conditions used here (Barnwal *et al.*, 2013). Necrotic brown spots are also indicators of the manganese phytotoxicity and those spots were identified as oxidized Mn and phenolic compounds present in the cell walls (Wissemeier and Horst, 1991). Excess accumulation of other metal elements can sometimes generate oxidative stress the development of brown spots (Bahadur *et al.*, 2015; Kampfenkel *et al.*, 1995). An elemental analysis of leaves in these experiments showed that the concentration of several elements were higher in transgenic lines overexpressing *OsALMT1* compared with their null lines. In this experiment certain micronutrients such as Fe and Cu were higher in the OE line but this was not a consistent finding and the metal accumulation could be very dependent on leaf age and environmental conditions including the levels of soluble metals in the soil. These results indicated that the brow spots potentially could be related to metal accumulation and this phenotype requires further investigation.

The brown spots appeared earlier when the growth conditions had higher light intensity and a higher temperature indicating that the brown spot might be caused by oxidative stress. Heat and high light intensity are also closely related to oxidative stress and Mn accumulation can exacerbate these processes. Light with a high proportion of energy in the blue wavelength spectrum (350 to 560 nm) has significantly more ability to induce physical leaf spot on barley than light with a pronounced red (photosynthetically active radiation) spectrum (580 to 650 nm) (Wu and Tiedemann, 2004). Interestingly, the rice with a knock-out mutation in the heat stress transcription factor *Spl7* showed brown spots on its leaves under various light and heat conditions (Yamanouchi *et al.*, 2002). However the finding here that the same phenotype was observed in independent

transgenic lines indicates that it is very unlikely to be caused by an insertional mutation in a particular gene.

Lesion mimic, is the spontaneous formation of lesions which resemble the HR lesions in the absence of a pathogen. This is occasionally found to accompany the expression of different, mostly unrelated, transgenes in plants. Unlike other types of brown spot formation, lesion mimic necrosis is not due to the formation of a simple compound which kills the cells, but related to the activation of programmed cell death (PCD) pathway (Mittlerl and Rizhsky, 2000).

No difference in O_2^- and H_2O_2 concentrations were detected here in preliminary tests between lines with or without the brown spots. However more detailed or quantitative experiments would be recommended. Further experiments to investigate the cause of the spotting phenotype on the leaves are described in later Chapters. Those experiments investigate further the possible role of Mn accumulation in inducing the phenotype.

Plants over-expressing *OsALMT1* accumulated less biomass in most experiments when grown under both hydroponic and non-flooded soil conditions. The brown spot phenotype also occurred in both conditions. Whether the brown spots cause this reduction in biomass through the reduction of photosynthetic surface or other stress-related changes, or whether the slower growth and spots occur by independent pathways (but linked through high *OsALMT1* expression) is unclear.

Previous results showed that *OsALMT1* is highly expressed in vascular tissue and may function to balance charge during nutrient loading or to accompany mineral nutrients to the shoots in the xylem stream. RNAi plants may be slightly compromised in these processes or less competent at adjusting cellular osmolarity which could retard plant growth and vigour. Nevertheless growth of the homozygous RNAi plants was similar to their nulls in most experiments. A decrease in shoot biomass was detected in only two out of nine experiments and in one experiment an RNAi line had a significantly higher shoot biomass than its null line.

In conclusion homozygous lines were generated with 20 to 40-fold higher *OsALMT1* expression and significantly reduced expression. Lines with higher expression showed a spotted phenotype on the leaves which tended to appear more rapidly when grown under higher light intensities and in higher temperatures. These lines also tended to be

smaller than their null lines. Reducing *OsALMT1* expression to 10 to 20% of WT levels had less effect on plant biomass and resulted in no observable phenotypes on the leaves.

7.5 References

Alberts B JA, Lewis J (2002) Studying gene expression and function. Molecular Biology of the Cell. 4th edition. New York: Garland Science

Bahadur B, Rajam MV, Sahijram L, Krishnamurthy KV (2015) Plant biology and biotechnology. Volume II: Plant Genomics and Biotechnology. Springer India

Barnwal MK, Kotasthane A, Magculia N, Mukherjee PK, Savary S, Sharma AK, Singh HB, Singh US, Sparks AH, Variar M, Zaidi N (2013) A review on crop losses, epidemiology and disease management of rice brown spot to identify research priorities and knowledge gaps. Eur J Plant Pathology 136: 443-457

Chen Q, Wu KH, Wang P, Yi J, Li KZ, Yu YX, Chen LM (2013) Overexpression of *MsALMT1*, from the aluminum-sensitive *Medicago sativa*, enhances malate exudation and aluminum resistance in Tobacco. Pl Mol Biol Rep 31: 769-774

Chen ZC, Yokosho K, Kashino M, Zhao FJ, Yamaji N, Ma JF (2013) Adaptation to acidic soil is achieved by increased numbers of cis-acting elements regulating *ALMT1* expression in *Holcus lanatus*. Plant J 76: 10-23

Christensen A, Sharrock R, Quail P (1992) Maize polyubiquitin genes: structure, thermal perturbation of expression and transcript splicing, and promoter activity following transfer to protoplasts by electroporation. Plant Mol Biol 18: 675-689

Cornejo MJ, Luth D, Blankenship K, Anderson O, Blechl A (1993) Activity of a maize ubiquitin promoter in transgenic rice. Plant Mol Biol 23: 567-581

Costa F, Alba R, Schouten H, Soglio V, Gianfranceschi L, Serra S, Musacchi S, Sansavini S, Costa G, Fei Z, Giovannoni J (2010) Use of homologous and heterologous gene expression profiling tools to characterize transcription dynamics during apple fruit maturation and ripening. BMC Plant Biol10: 229

De Angeli A, Baetz U, Francisco R, Zhang J, Chaves MM, Regalado A (2013a) The vacuolar channel VvALMT9 mediates malate and tartrate accumulation in berries of *Vitis vinifera*. Planta 238: 283-291

De Angeli A, Zhang JB, Meyer S, Martinoia E (2013b) AtALMT9 is a malate-activated vacuolar chloride channel required for stomatal opening in *Arabidopsis*. Nat Commun 4: 1804

Delhaize E, Ryan PR, Hebb DM, Yamamoto Y, Sasaki T, Matsumoto H (2004) Engineering high-level aluminum tolerance in barley with the *ALMT1* gene. PNAS 101: 15249-15254

Delhaize E, Taylor P, Hocking PJ, Simpson RJ, Ryan PR, Richardson AE (2009) Transgenic barley (*Hordeum vulgare* L.) expressing the wheat aluminium resistance

gene (*TaALMT1*) shows enhanced phosphorus nutrition and grain production when grown on an acid soil. Plant Biotechnol J 7: 391-400

Gatz C (1996) Chemically inducible promoters in transgenic plants. Curr Opin Biotechnol 7: 168-172

Giraud E, Ho LH, Clifton R, Carroll A, Estavillo G, Tan YF, Howell KA, Ivanova A, Pogson BJ, Millar AH, Whelan J (2008) The absence of *alternative oxidase1a* in Arabidopsis results in acute sensitivity to combined light and drought stress. Plant Physiol 147: 595-610

Gruber BD, Delhaize E, Richardson AE, Roessner U, James RA, Howitt SM, Ryan PR (2011) Characterisation of *HvALMT1* function in transgenic barley plants. Funct Plant Biol 38: 163-175

Gruber BD, Ryan PR, Richardson AE, Tyerman SD, Ramesh S, Hebb DM, Howitt SM, Delhaize E (2010) HvALMT1 from barley is involved in the transport of organic anions. J Exp Bot 61: 1455-1467

Hoekenga OA, Maron LG, Pineros MA, Cancado GMA, Shaff J, Kobayashi Y, Ryan PR, Dong B, Delhaize E, Sasaki T, Matsumoto H, Yamamoto Y, Koyama H, Kochian LV (2006) *AtALMT1*, which encodes a malate transporter, is identified as one of several genes critical for aluminum tolerance in *Arabidopsis*. PNAS 103: 9738-9743

Holtorf S, Apel K, Bohlmann H (1995) Comparison of different constitutive and inducible promoters for the overexpression of transgenes in *Arabidopsis thaliana*. Plant Mol Biol 29: 637-646

Kampfenkel K, Montagu MV, Inzé D (1995) Effects of iron excess on *Nicotiana plumbagnifolia* plants. Plant Physiol 107: 725-735

Kobayashi Y, Hoekenga OA, Itoh H, Nakashima M, Saito S, Shaff JE, Maron LG, Pineros MA, Kochian LV, Koyama H (2007) Characterization of *AtALMT1* expression in aluminum-inducible malate release and its role for rhizotoxic stress tolerance in arabidopsis. Plant Physiol 145: 843-852

Kobayashi Y, Lakshmanan V, Kobayashi Y, Asai M, Iuchi S, Kobayashi M, Bais HP, Koyama H (2013) Overexpression of AtALMT1 in the Arabidopsis thaliana ecotype Columbia results in enhanced Al-activated malate excretion and beneficial bacterium recruitment. Plant Signal Behav 8: 25561-25564

Kovermann P, Meyer S, Hortensteiner S, Picco C, Scholz-Starke J, Ravera S, Lee Y, Martinoia E (2007) The Arabidopsis vacuolar malate channel is a member of the ALMT family. Plant J 52: 1169-1180

Liang CY, Pineros MA, Tian J, Yao ZF, Sun LL, Liu JP, Shaff J, Coluccio A, Kochian LV, Liao H (2013) Low pH, aluminum, and phosphorus coordinately regulate malate exudation through *GmALMT1* to improve soybean adaptation to acid soils. Plant Physiol 161: 1347-1361

Ligaba A, Katsuhara M, Ryan PR, Shibasaka M, Matsumoto H (2006) The *BnALMT1* and *BnALMT2* genes from rape encode aluminum-activated malate transporters that enhance the aluminum resistance of plant cells. Plant Physiol 142: 1294-1303

Ligaba A, Maron L, Shaff J, Kochian L, Pineros M (2012) Maize ZmALMT2 is a root anion transporter that mediates constitutive root malate efflux. Plant Cell Environ 35: 1185-1200

Meyer S, Mumm P, Imes D, Endler A, Weder B, Al-Rasheid KAS, Geiger D, Marten I, Martinoia E, Hedrich R (2010) AtALMT12 represents an R-type anion channel required for stomatal movement in Arabidopsis guard cells. Plant J 63: 1054-1062

Meyer S, Scholz-Starke J, De Angeli A, Kovermann P, Burla B, Gambale F, Martinoia E (2011) Malate transport by the vacuolar AtALMT6 channel in guard cells is subject to multiple regulation. Plant J 67: 247-257

Mittlerl R, Rizhsky L (2000) Transgene-induced lesion mimic. Plant Mol Biol 44: 335-344

Mumm P, Imes D, Martinoia E, Al-Rasheid KA, Geiger D, Marten I, Hedrich R (2013) C-terminus-mediated voltage gating of Arabidopsis guard cell anion channel QUAC1. Mol Plant 6: 1550-1563

Odell JT, Nagy F, Chua NH (1985) Identification of DNA sequences required for activity of the cauliflower mosaic virus 35S promoter. Nature 313: 810-812

Pereira JF, Zhou GF, Delhaize E, Richardson T, Zhou MX, Ryan PR (2010) Engineering greater aluminium resistance in wheat by over-expressing *TaALMT1*. Ann Bot 106: 205-214

Pineros MA, Cancado GMA, Kochian LV (2008a) Novel properties of the wheat aluminum tolerance organic acid transporter (TaALMT1) revealed by electrophysiological characterization in *Xenopus* oocytes: functional and structural implications. Plant Physiol 147: 2131-2146

Pineros MA, Cancado GMA, Maron LG, Lyi SM, Menossi M, Kochian LV (2008b) Not all ALMT1-type transporters mediate aluminum-activated organic acid responses: the case of *ZmALMT1* - an anion-selective transporter. Plant J 53: 352-367

Potenza C, Aleman L, Sengupta-Gopalan C (2004) Targeting transgene expression in research, agricultural, and environmental applications: Promoters used in plant transformation. In Vitro Cell Dev Biol - Plant 40: 1-22

Ryan PR, Tyerman SD, Sasaki T, Furuichi T, Yamamoto Y, Zhang WH, Delhaize E (2011) The identification of aluminium-resistance genes provides opportunities for enhancing crop production on acid soils. J Exp Bot 62: 9-20

Sasaki T, Mori IC, Furuichi T, Munemasa S, Toyooka K, Matsuoka K, Murata Y, Yamamoto Y (2010) Closing plant stomata requires a homolog of an aluminum-activated malate transporter. Plant Cell Physiol 51: 354-365

Sasaki T, Yamamoto Y, Ezaki B, Katsuhara M, Ahn SJ, Ryan PR, Delhaize E, Matsumoto H (2004) A wheat gene encoding an aluminum-activated malate transporter. Plant J 37: 645-653

Venter M (2007) Synthetic promoters: genetic control through cis engineering. Trends Plant Sci 12: 118-124

Wilmink A, van de Ven BCE, Dons JJM (1995) Activity of constitutive promoters in various species from the Liliaceae. Plant Mol Biol 28: 949-955

Wissemeier AH, Horst WJ (1991) Simplified methods for screening cowpea cultivars for manganese leaf-tissue tolerance. Crop Sci 31: 435-439

Wu YX, Tiedemann Av (2004) Light-Dependent oxidative stress determines physiological leaf spot formation in barley. Phytopathology 94: 584-592

Xu M, Gruber BD, Delhaize E, White RG, James RA, You J, Yang Z, Ryan PR (2015) The barley anion channel, HvALMT1, has multiple roles in guard cell physiology and grain metabolism. Physiol Plant153: 183-193

Yamanouchi U, Yano M, Lin H, Ashikari M, Yamada K (2002) A rice spotted leaf gene, *Spl7*, encodes a heat stress transcription factor protein. PNAS 99: 7530-7535

Younis A, Siddique MI, Kim CK, Lim KB (2014) RNA interference (RNAi) induced gene silencing: A promising approach of hi-tech plant breeding. Int J Biol Sci 10: 1150-1158

Zhang J, Baetz U, Krugel U, Martinoia E, De Angeli A (2013) Identification of a probable pore-forming domain in the multimeric vacuolar anion channel AtALMT9. Plant Physiol 163: 830-843

Zhang J, Martinoia E, De Angeli A (2014) Cytosolic nucleotides block and regulate the Arabidopsis vacuolar anion channel AtALMT9. J Biol Chem 289: 25581-25589

Zhang WH, Ryan PR, Sasaki T, Yamamoto Y, Sullivan W, Tyerman SD (2008) Characterization of the TaALMT1 protein as an Al^{3+}-activated anion channel in transformed tobacco (*Nicotiana tabacum* L.) cells. Plant Cell Physiol 49: 1316-1330

CHAPTER 8
Characterisation of transgenic plants with altered *OsALMT1* expression

8.1 Introduction

The generation of transgenic plants can help reveal the functions of gene products. This analysis can be approached in different ways but, in general, they rely on changing the expression levels of transgenes to manipulate biological processes. The goal is to generate gain-of-function or loss-of-function changes which result in phenotypes that can be observed and measured (Curtis and Grossniklaus 2003). Gain-of-function changes can be achieved by placing a gene under the transcriptional control of a promoter to generate a phenotype that helps to elucidate protein function. It is possible that no phenotype will be detected if, for example, the protein encoded by the gene is not a rate-limiting part of the biochemical/metabolic process or if cellular metabolism maintains some equilibrium despite the changes in expression. It is also possible that the protein is under post-translational regulation or feedback regulation which prevents a phenotype from being generated. Reducing gene expression with knock-out mutations or with antisense or RNAi constructs generally produce loss-of-function phenotypes but this is not always the case. Similarly it is not uncommon for knock-out mutations or RNAi lines to have no phenotype either due to redundancy (where other genes contribute to the same phenotype) (Griffiths et al. 2000). Nevertheless the phenotypes that arise in transgenic lines can give clues to transgene function.

Transgenic approaches investigating other *ALMT*s in various expression systems indicate that they encode transport proteins, and specifically anion channels, that release organic and/or inorganic anions from cells. Increasing expression of the wheat gene *TaALMT1* in rice, barley, Arabidopsis and wheat all showed higher malate efflux from roots and greater Al resistance in most cases (Delhaize et al. 2004; Sasaki et al. 2004; Pereira et al. 2010). Increasing expression of *AtALMT1* in the *Arabidopsis* ecotype Columbia also enhanced Al-activated malate excretion (Kobayashi et al. 2013). Similarly, Arabidopsis plants and soybean hairy roots expressing *GmALMT1* and barley plants expressing *HvALMT1* all

showed increased malate exudation from roots and improved Al tolerance (Liang et al. 2013; Gruber et al. 2011). Overexpression of the maize *ZmALMT2* gene in an Al-hypersensitive *Arabidopsis* mutant line lacking Al tolerance genes (*AtALMT1* and *AtMATE*) resulted in constitutive efflux of malate from roots (Ligaba et al. 2012).

The function of plant proteins can also be examined in animal cells such as the oocytes of the African clawed frog, *Xenopus laevis*. This system is very useful for the electrophysiological characterisation of transporter proteins and provides means for assessing the permeability of transporters to different substrates. Several *ALMT*s genes have been examined in *Xenopus* oocytes. Some are more permeable to the organic anions such as malate and succinate while others are more permeable to inorganic anions such as Cl^- and NO_3^- (Sasaki et al. 2004; Zhang et al. 2008; Ligaba et al. 2006; Liang et al. 2013; Chen et al. 2013a; Gruber et al. 2010; Kovermann et al. 2007; De Angeli et al. 2013); (Pineros et al. 2008b; Ligaba et al. 2012). The *Xenopus* expression system demonstrated that *TaALMT1* was permeable to malate and to a lesser extent to succinate, and that HvALMT1 was permeable to malate and fumarate (Pineros et al. 2008a; Gruber et al. 2010). It also showed that VvALMT9 from grape mediated malate and tartrate currents, that AtALMT9 and AtALMT12 from Arabidopsis were permeable to inorganic anions like Cl^- but not organic anions (Sasaki et al. 2010; De Angeli et al. 2013)

The transport activity of some ALMTs are known to be sensitive to specific treatments and these responses can provide clues to their regulation and *in situ* function. For instance, all ALMTs currently known to be involved in Al resistance are activated by external Al to release malate (Kobayashi et al. 2013; Sasaki et al. 2004; Ligaba et al. 2006; Chen et al. 2013a; Liang et al. 2013; Chen et al. 2013b). Furthermore some are sensitive to protein kinase inhibitors such as K-252a which effectively blocks the Al-induced malate efflux from wheat roots (Osawa and Matsumoto 2001). K-252a reduced malate efflux by 60% from transgenic Arabidopsis plants over-expressing *AtALMT1*, while staurosporine (kinase inhibitor) and calyculin A (phosphatase inhibitor) both blocked changes in *AtALMT1* gene expression and thus inhibited malate release (Kobayashi et al. 2007). Therefore the effects of the phosphorylation on AtALMT1 function are complex and appear to involve direct changes to the protein and indirect regulation of gene expression. The anion channel blockers niflumic acid, anthracene carboxylic acid and 5-nitro-2-(3-phenylpropylamino)-benzoic acid (NPPB) effectively reduced the malate efflux from wheat roots (Ryan et al.

1995) and ZmALMT2 function was also blocked by niflumic acid (Ligaba et al. 2012). Citrate competitively inhibited malate uptake across the tonoplast and acted as an "open channel blocker" of AtALMT9 (Zhang et al. 2013). The hormone salicylic acid increased Al resistance in soybean and *Cassia tora* by modulating of citrate efflux from roots (Liu et al. 2011; Yang et al. 2003). More recently, millimolar concentrations of γ amino butyric acid (GABA) and micromolar concentrations of muscimol, an analogue of GABA, were shown to inhibit ALMT-dependent inward currents in *Xenopus* oocytes (Ramesh et al. 2015). GABA expression often increases during stress but its function was never very clear but it has been linked with stress responses (heat, salinity and herbivory) and pH regulation (Kinnersley and Turano 2000; Bouché and Fromm 2004). The identification of ALMT proteins as likely GABA receptors highlights intriguing parallels between GABA function in plant and animal cells and suggests that ALMTs might form fundamental links in stress-related signalling processes.

Malate concentrations and transport processes are important in grain germination. Malate synthase transcripts increase over several days following the onset of germination and malate concentrations also increase, especially during the initial 24 h (Pracharoenwattana et al. 2010; Smith and Leaver 1986; Ren and Bewley 1999). The aleurone layer releases compounds like citric, malic and phosphoric acids which begin to acidify the starchy endosperm (Koehler and Ho 1990; Martínez-Camacho et al. 2004).

Members of the *ALMT* gene family characterised previously were shown to encode anion channels. The aim of this chapter is to further examine the function OsALMT1 by examining its transport activity in transgenic plants and how its activity varies with different treatments and pharmacological agents. This Chapter begins to examine some direct consequences of these transport processes on plant biology.

8.2 Materials and methods

8.2.1 Measuring organic anion efflux from rice plants.

Organic anion efflux from intact rice roots was measured using two methods. The analysis of all organic anions was made using HPLC at the University of Western

Australia using methods described previously (Cawthray 2003; Uloth et al. 2015). Malate and citrate were also assayed individually using enzymatic reactions by modifying the methods described by Ryan *et al*. (2009).

For the enzymatic approach, 15 seeds from each line were surface sterilized and pre-germinated in sterile conditions as described in **Chapter 2**. Three germinated seeds were transferred to 125 mL flasks containing 20 mL of ½ strength nutrient solution (see **Chapter 2**). Foil was used to cover the lids of the flasks before they were placed on a shaker (60 rpm) in a growth room at 28 ℃ at low light (~40 μmol $m^{-2}s^{-1}$). After four days the solutions were gently poured out from the flasks and seedlings were rinsed twice with 40 mL of the same sterile control solution or a treatment solution. After rinsing, 15 mL of control or treatment solution was added to each flask and returned to the shaker in the same conditions for 6 to 20 h depending on the experiment. At the end of the incubation period 0.6 mL solution was collected from each flask for malate assays and 1.0 or 2.0 mL was collected for citrate assays. The measurements of malate efflux from excised root apices was similar except individual root apices (apical 5 mm of roots) were first excised and washed as described in detail by Ryan *et al*. (1995).

For the enzymatic malate measurements a stock reaction buffer was prepared by dissolving 34.2 g glycine with 75 ml hydrazine hydrate in 0.9 L water) as well as a fresh solution of NAD (N-0632, Sigma) by dissolving 30 mg NAD in 1 ml H_2O. Malate measurements were made by adding 0.4 mL buffer and 20 μL NAD to 600 μL sample. These were mixed in a spectrophotometer cuvette with a pipette and the absorbance at 340 nm on a Cary 50 Bio Spectrophotometer was set to zero. Once absorbance was stable, 1 μl malate dehydrogenase (M-7383, Sigma) was added and mixed gently to avoid creating bubbles. Absorbance (ΔABS_{340nm}) increased as NADH was formed in a stoichiometric ratio with the malate present. Once ΔABS_{340nm} stabilised the change in absorbance was measured and the initial malate content calculated from a standard curved using L-malate (Note: the enzymatic reaction does not recognise D-malate). For citrate measurements, stock solutions included 1 M Tris•Cl (pH 7.8), an equal mixture of lactate dehydrogenase and lactate dehydrogenase (Sigma M-7383, and Roche 107042) and NADH solution prepared by dissolving 16 mg NADH and 15 mg $NaHCO_3$ in 2 ml H_2O. A reaction solution was then prepared by mixing 120 μl 1 M Tris•Cl, 1 ml water, 4 μl LDH/MDH and 15 μl NADH solution. The 1.0 or 2.0 mL samples collected for citrate assay were dried on a rotary

vacuum drier and re-dissolved in 100 µl of the reaction solution and mixed in a spectrophotometer cuvette with pipette and the absorbance at 340 nm set to zero. The enzymatic reaction was initiated by adding 1 µl citrate lyase (C0897, Sigma, prepared by dissolving 10 mg citrate lyase in 100 µL H_2O). The absorbance decreases as NADH disappears in a stoichiometric ratio with the citrate present. The final change ΔABS_{340nm} was recorded and initial citrate content calculated from a standard curve.

For the HPLC method, 15 mL of 0.5 mM $CaCl_2$ was added to each flask after rinsing and returned to the shaker in the same conditions 24 h. At the end of the incubation period 15 mL of the solution was collected and frozen and used for organic acid analysis (Cawthray *et al*., 2003).

8.2.2 Measurements of Al^{3+} resistance in hydroponic culture

Seed were sterilized and pre-germinated and nutrient solution prepared as described in **Chapter 2**. To measure Al^{3+} resistance, six day old seedlings were transferred to hydroponic condition (pH 5.6; **Chapter 2**) and grown for two days. The solution was replaced with similar treatment solution but with lower concentration (1 µM) KH_2PO_4 and adjusted pH to 4.5 or the same solution with a range of $AlCl_3$ concentrations (0, 200 and 400 µM $AlCl_3$). The solutions were aerated and replaced every three days. After seven days of growth, the longest root length was measured and the relative root growth (RRG) was calculated. RRG was estimated as: (root length in Al^{3+} treatment/root length in control solution)×100%. Standard errors of the relative root growth (SERRG) were calculated as follows:

$SERRG = RRG \times [(SEx/x)^2 + (SEy/y)^2]^{1/2}$, where x and y represent the mean of root length under control and Al^{3+} treatments, and SEx and SEy represent the standard errors of those means. Testing significant differences between proportions is described in **Chapter 2**.

8.2.3 Effect of different treatments on malate efflux from roots

Malate efflux from the whole root system was measured in response to different chemical

compounds and different environmental conditions. Plants were grown as described above. Stock solutions for niflumic acid, salicylic acid and muscimol were 20 mM in ethanol. The highest final ethanol concentration used was 0.5% which does not affect malate efflux (Ryan et al. 1995). The low pH nutrient solution treatment was pH 4.3, and the Al treatment had 100 μM $AlCl_3$ at pH 4.3. The "high light" treatment was continuous light of 600 μmoles $m^{-2}s^{-1}$ intensity in a growth cabinet at 28 ℃. For the dark treatment flasks were covered by aluminium foil in the same conditions.

8.2.4 Measuring malate concentrations in xylem sap

Six week old plants were used for xylem sap collection using the method described previously (Yokosho et al. 2009). Plants were grown hydroponically as described in **Chapter 2**. The nutrient solution was renewed every five days and also on the day before xylem sap was collection. To collect sap the plants were cut about 3 cm above the roots with a scalpel. Sap slowly extruded from the cut surface and this was collected with a glass micropipette over 60 min. Collected samples were immediately placed on ice to prevent evaporation. Final volume of samples varied from 20 to 100 uL. To measure malate concentration 1 μL of the sap sample was added to 99 μL of the reaction mixture (0.75 mL hydrazine buffer, 0.68 mL H_2O, and 50 μL NAD solution) and the malate assay started as described above.

8.2.5 Mineral analysis in grain

Mineral analyses were performed on grain collected from plants grown under normal soil conditions. The plants included WT plants, homozygous transgenic lines over-expressing *OsALMT1*, transgenic RNAi lines with reduced expression as well as null control lines. The grain were dried at 70 ℃ for 24 hours. Between 50 to 250 mg dry tissue was digested by 8 mL concentrated nitric acid and 2 mL hydrochloric acid and digested at 170 ℃ for 1.5 h in Microwave Digestion System (Milestone^{TM}). The samples were diluted in 40 mL milliQ water and elements analysed by Analytical Chemistry Group, CSIRO, with inductively coupled plasma mass spectrometry (ICP) analysis.

8.2.6 Qualitative estimates of endosperm pH

Endosperm pH of germinating grain was visualised by staining with a pH indicator using a modified method described previously (Dominguez and Cejudo 1999). Rice grains from two independent over-expression and RNAi lines and their relative null lines were sterilised and germinated on sterile filter paper imbibed in water as described in **Chapter 2**. At different times from the start of germination, the shoots and roots were cut and the grains were dissected longitudinally with a razor blade. Dissected grains were then incubated for 15 min at room temperature in a solution containing 0.1 g of the pH indicator Bromcresol purple (Sigma, B-5880) in 250 mL of water and 37 mL of 5 N NaOH. Dissected grains were then washed in water for 2 min, observed under a Leica MZFLIII microscope, and photographed in dark field. Colour changes from yellow to purple indicates pH changes from acid to alkaline with a pK_a of ~ 6.1.

8.3 Results

8.3.1 Organic anion release from the root of transgenic rice plants over-expressing *OsALMT1*

The aim of this experiment was to determine the substrate transported by OsALMT1. Organic anion efflux was first measured from the roots of the three independent homozygous lines and their null sister lines as well as WT plants. Exudates were collected over 16 h in sterile conditions. WT and null plants from all lines showed little or no malate efflux from the root system but all three overexpression homozygous lines showed significant malate efflux of 1 to 3 nmol seedling^{-1} h^{-1} (**Figure 8.1**). Citrate efflux was also measured from these same plants. In WT and null plants citrate efflux was ~0.8 nmol seedling^{-1}hour^{-1}. In the three homozygous lines over-expressing *OsALMT1* citrate efflux from OE8-5 was similar to its null whereas efflux from OE5-5 the OE2-18 lines was significantly less than their null lines (**Figure 8.2**). In some experiments there appeared to be an inverse relationship between the magnitude of malate efflux and citrate efflux among the homozygous lines which is plotted in **Figure 8.3**. Estimates of malate efflux did vary between experiments. Variation in background fluxes occurred and small changes in

absorbance could lead to significant changes to the calibration curve. Therefore null lines were included as controls in most experiments to compare with the transgenic lines.

These enzyme assays are specific for the target anions only. Therefore organic anion efflux was also measured by HPLC which has the capacity to detect a wide range of organic anions at once. Using HPLC method to measure organic anions significant malate and fumarate efflux was detected from the OE5-5 transgenic line but not from the null line OE5-13 (**Table 8.1**). This indicates that OsALMT1 can mediate malate and fumarate efflux (**Figure 8.4**). Interestingly, no citrate efflux was detected in any of the HPLC samples. The reason for this is unclear and does not appear to due to detection limits since fumarate efflux is less than the predicted citrate efflux using enzymatic analysis. Perhaps it is a feature of the sample preparation. This requires further examination.

Malate efflux was also measured from isolated root apices of the OE5-5 line so the fluxes could be directly compared to Al-resistant wheat. The fluxes were approximately 0.5 nmol $apex^{-1}$ h^{-1} greater than the null line which is similar to the rates commonly reported for the Al-activated malate release from excised root apices of wheat of ~1.0 nmol $apex^{-1}$ h^{-1}.

8.3.2 Greater malate release from transgenic rice over-expressing *OsALMT1* increases their tolerance to Al toxicity

Organic anion efflux from roots is a major mechanism for Al tolerance in many plant species (see **Chapter 1**). The aim of this experiment was to determine whether the greater malate efflux from the root apices of the transgenic rice lines enhanced their Al tolerance. Al tolerance was estimated from relative root growth (RRG) by measuring root growth after seven days in 0, 200 and 400 μM Al concentrations in two T3 homozygous lines (OE2-18, OE5-5) and their nulls (OE2-8_null, OE5-13_null). In the control treatment (no Al) root growth in the two homozygous lines was 20 to 40% smaller than their null lines. Both Al treatments significantly inhibited root growth in the homozygous and null lines. Nevertheless absolute root growth at 200 μM was greater in the homozygous lines compared to their respective null lines. Furthermore, RRG of the OE2-18 and OE5-5 homozygous lines was two-fold greater and significantly different ($P_{0.05}$) from the null lines at both Al concentrations. (**Figure 8.4**).

8.3.3 Effect of different treatments on malate efflux from transgenic rice

Previous research has demonstrated that the anion channels encoded by *ALMT* genes are inhibited by some treatments. The aim of the following experiments was to determine how specific pharmacological agents (niflumic acid, γ amino butyric acid, muscimol), hormones (ABA, IAA, SA), ions (Al) and environmental conditions (pH, light intensity) affect malate and citrate efflux from the OE5-5 homozygous line over-expressing *OsALMT1* and its null sister line OE5-13_null. The outcomes will help compare the function of OsALMT1 with other members of the family characterised previously. Control experiments used glass beakers with nutrient solution (pH 5.6), a low light intensity of ~40 µmol $m^{-2}s^{-1}$ and 28 ^{o}C. Treatment with 10 mM γ amino butyric acid (GABA) inhibited malate efflux from the homozygous line by 40% but there was no effect at 2 mM (**Figure 8.5 a**). Treatment with 100 µM muscimol, an agonist of GABA, increased malate efflux by 50% (**Figure 8.5 b**). Previous reports for some ALMTs including TaALMT1 from wheat found 10 µM muscimol inhibited malate efflux. Treatment with 100 µM niflumic acid completely inhibited malate efflux to equal the null lines (**Figure 8.5 b**) which is consistent with responses in some other ALMTs. Treatment with 20 to 100 µM salicylic acid (SA) reduced the malate efflux by 20 to 80% respectively (**Figure 8.5 c**). The highest SA concentrations reduced the pH of the treatment solutions slightly to pH 5.1 Therefore additional experiments were performed with solutions buffered to pH 5.6 and 100 µM SA still significantly reduced malate efflux at this pH also (**Figure 8.5 d**). Treatments with 100 µM ABA or 100 µM IAA for 6 h inhibited malate efflux by approximately 50% (data not shown) but these results need verifying since the control values in this experiment were lower than normal. The inhibition after 24 h was smaller for both these hormones. Continual darkness had no effect on efflux compared to control conditions which already had a relatively low light intensity (~40 µmol $m^{-2}s^{-1}$) (**Figure 8.5 d**). Continual high light intensity of 600 µmol $m^{-2}s^{-1}$ increased malate efflux two-fold compared to the control treatment. Reducing pH from 6.5 to 4.3 decreased malate efflux slightly but the difference was not significant ($P_{0.05}$). The addition of 100 µM Al at pH 4.3 decreased efflux by 80%. This contrasts with other ALMT members involved in Al tolerance which are activated by external Al (**Figure 8.5 d**).

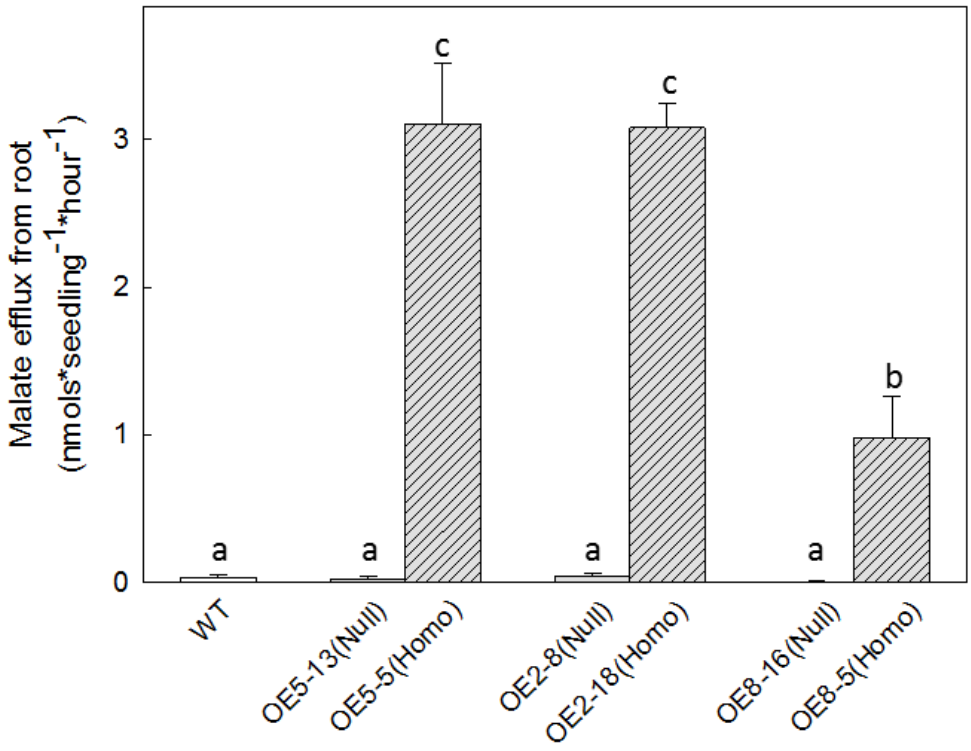

Figure 8.1 Malate efflux from transgenic lines over-expressing *OsALMT1* and nulls

Malate efflux was measured from the whole root system of three pairs of T2 homozygous and null lines as well as WT rice plants. Data show the mean and standard error (n=3). Data were transformed with the square root function to overcome the non-homogeneity of variances and then tested with a one way ANOVA. Differences at $P<0.05$ are indicated with different letters.

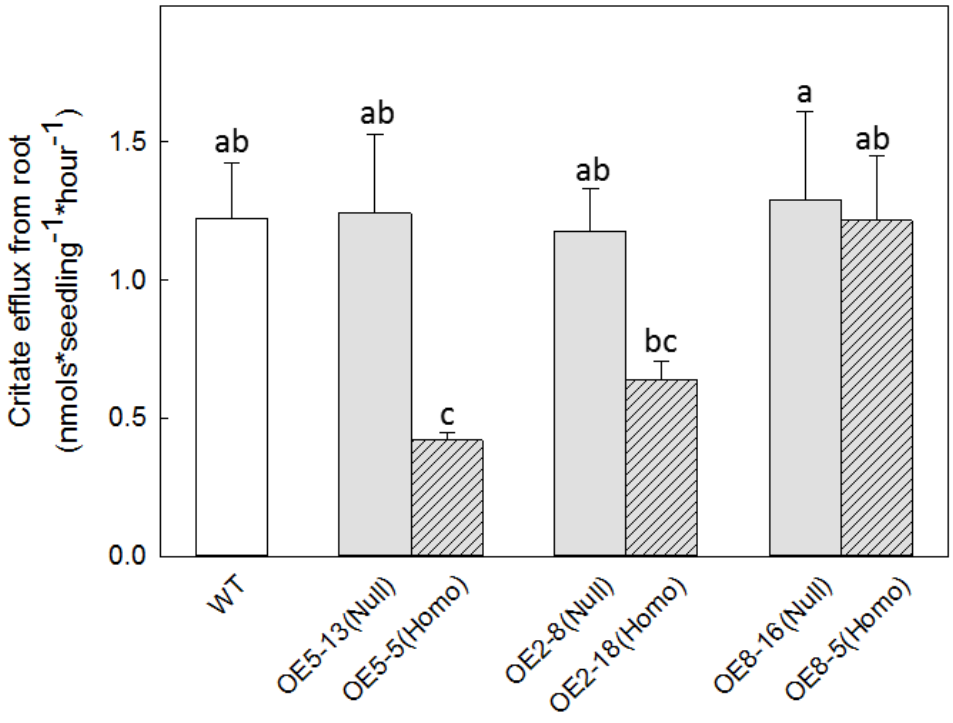

Figure 8.2 Citrate efflux from transgenic lines over-expressing *OsALMT1* and nulls

Citrate efflux was measured from the whole root system of three pairs of T2 homozygous and null lines as well as WT rice plants. Data show the mean and standard error (n=3). Data were transformed with the square root function to overcome the non-homogeneity of variances and then tested with a one way ANOVA. Differences at $P<0.05$ are indicated with different letters.

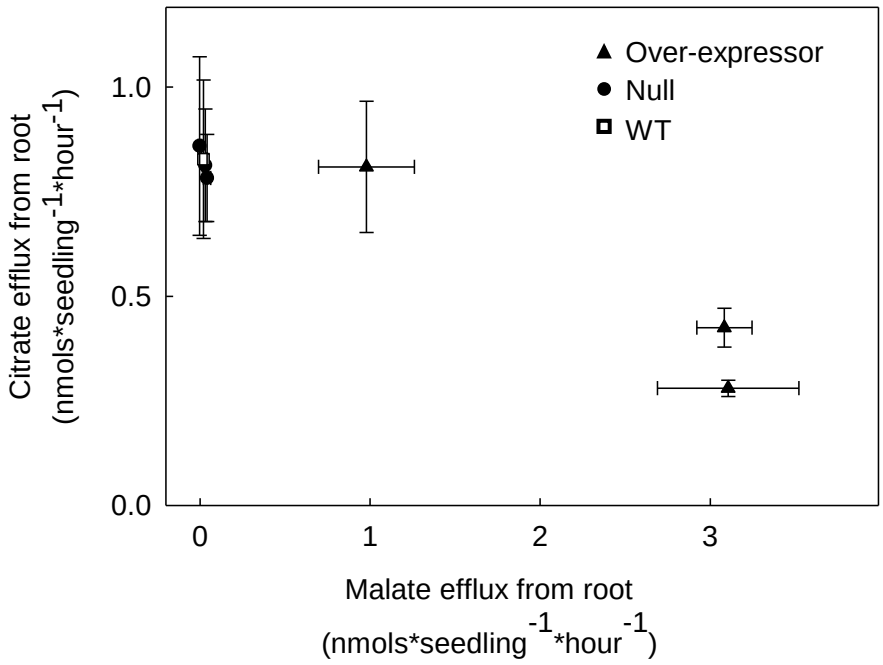

Figure 8.3 Relationship between malate and citrate efflux from homozygous T2 lines over-expressing *OsALMT1* and nulls

Data replotted from **Figures 8.1 and 8.2**. Data show the mean and standard error (n=3)

Table 8.1 Organic anion efflux measured from transgenic rice by HPLC

Organic anion efflux measured from one homozygous transgenic line over-expressing *OsALMT1* (OE5-5) and its null sister line (OE5-13). Data show the final concentration of organic anions in the treatment solution and the calculated efflux. The data were analysed with a t test and differences ($P<0.05$) between the homozygous line and null line are indicated with an asterisk.

	Malate		Fumarate	
	Concentration (μM)	Efflux (nmol seedling^{-1} h^{-1})	Concentration (μM)	Efflux (nmol seedling^{-1} h^{-1})
Control (no plants)	nd		nd	
OE5-5 (Homo)	21.9 ± 4.5 *	4.6 ±0.9 *	0.34 ± 0.08 *	0.07 ± 0.02 *
OE5-13 (Null)	7.2 ± 0.4	1.5 ± 0.1	0.04 ± 0.01	0.01 ± 0.00

nd: not detectable

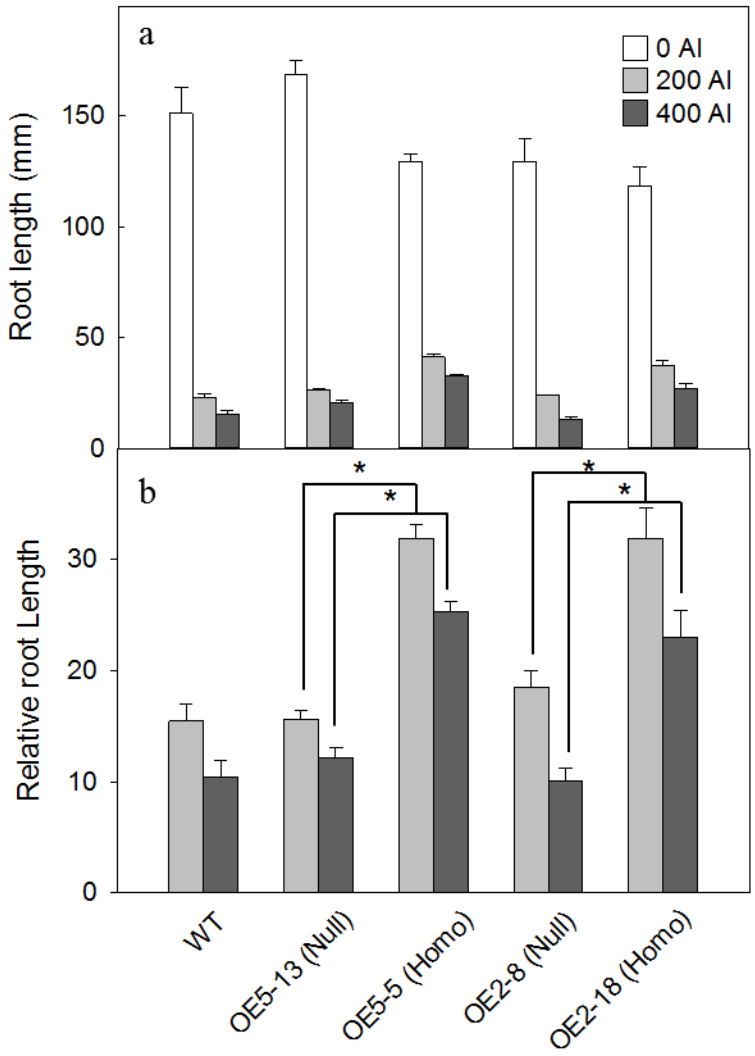

Figure 8.4 Relative Al tolerance of the transgenic rice over-expressing *OsALMT1*

Al tolerance of two transgenic T_3 homozygous lines and their null sister lines were measured in hydroponic solution. (a) The longest root length was measured after 7 d growth in 0 µM, 200 µM and 400 µM $AlCl_3$. (b) Relative root growth (RRG) is also shown. Data show the mean of relative root growth and standard error (n=4). Standard errors of the ratios in RRG are given by $SERRG = RRG \times [(SEx/x)^2 + (SEy/y)^2]^{1/2}$, where x and y represent the mean of root length under control and Al treatments, and SEx and SEy represent the standard errors of those means. Asterisks (*) indicate a significant difference ($P_{0.05}$) between the homozygous line and its relative null line as described in **Chapter 2**.

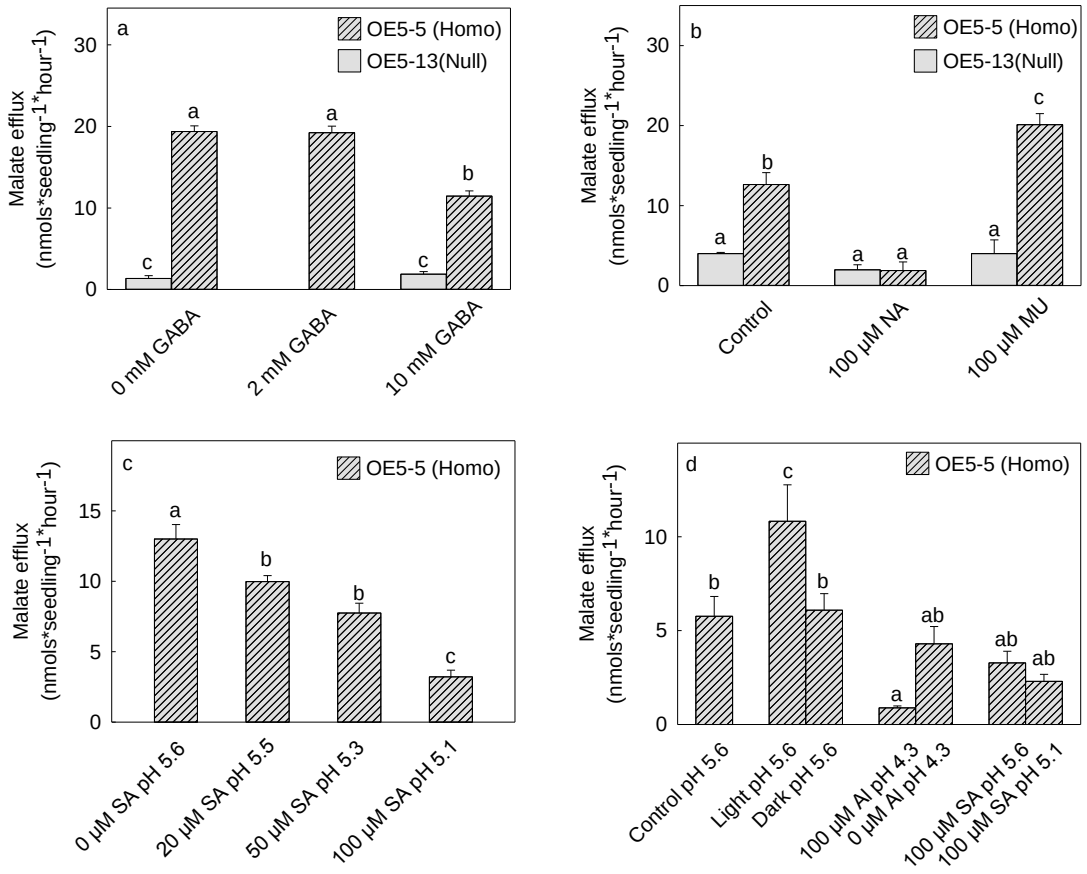

Figure 8.5 Effect of different treatments on the efflux of malate from homozygous rice over-expressing *OsALMT1*

Malate efflux measured from the whole root system of the T_3 homozygous line OE5-5 over 20 h in response to various treatments. Experiments in a and b also include results for the null line OE5-13_null. The treatments were as follows: (a) 2, 5 and 10 mM GABA; (b) 100 µM NA and 100 µM muscimol (MU); (c) salicylic acid (SA); (d) constant high light (600 µmol $m^{-2}s^{-1}$), constant darkness, lower solution pH (pH 4.3) and 100 µM Al (pH 4.3). Control conditions are pH 5.6 at low light intensity (50 µmol $m^{-2}s^{-1}$) and 28 ^{o}C. Data show the mean and standard error (n=3-4). Where necessary data were transformed with the square root function to overcome the non-homogeneity of variances and then tested with a one way ANOVA. Differences at $P<0.05$ are indicated with different letters.

8.3.4 Overexpression of *OsALMT1* increases malate concentration in the xylem sap

Chapter 5 indicated that OsALMT1 expression was high in the vasculature tissue of roots and leaves. Therefore it is possible that OsALMT1 functions in those cells to release malate into the xylem. These experiments were aimed at measuring the malate concentrations in the xylem sap and comparing them in the transgenic lines with higher and lower expression. Malate concentration in the sap of WT plants was approximately 1.2 mM and this was similar to the values measured in the homozygous RNAi lines R24-15 and R58-1 as well as their null sister lines R24-20_null and R58-5_null (**Figure 8.6**).Malate concentrations in the sap of the homozygous lines over-expressing *OsALMT1*, OE5-5 and OE2-18, were 2.0 and 2.3 mM, respectively. These are 60 and 100% greater, respectively, than concentrations in the null lines.

8.3.5 Effect of altered *OsALMT1* expression on grain mineral content

An important function of organic anions in the xylem is to facilitate the long-distance transport of mineral nutrients from the roots to shoots and finally to the developing grain. We analysed the mineral content of grain (**Figure 8.7**) harvested from two transgenic lines with higher OsALMT1 expression and two RNAi lines with reduced OsALMT1 expression grown in standard potting mix.

Both transgenic lines OE5-5 and OE2-18 with increased OsALMT1 expression had two-fold greater concentrations of B and OE5-5 also had small but significant increases in Cu, Mn, P and Zn in their grain than their corresponding null lines.. Average concentrations of these minerals in null lines were 7.1 mg kg^{-1}, 16.3 mg kg^{-1}, 0.36%, and 27.4 mg kg^{-1} respectively (**Table S5**). The OE2-18 line had a greater silicon (Si) concentration than its null sister line which was 149.7 mg Si kg^{-1} (**Figure 8.7 a**). No differences in the mineral content were detected between the two RNAi lines analysed and their corresponding nulls which is consistent with the malate concentration in the xylem sap not changing (**Figure 8.7 b**). The one exception is one RNAi line which showed greater B concentration.

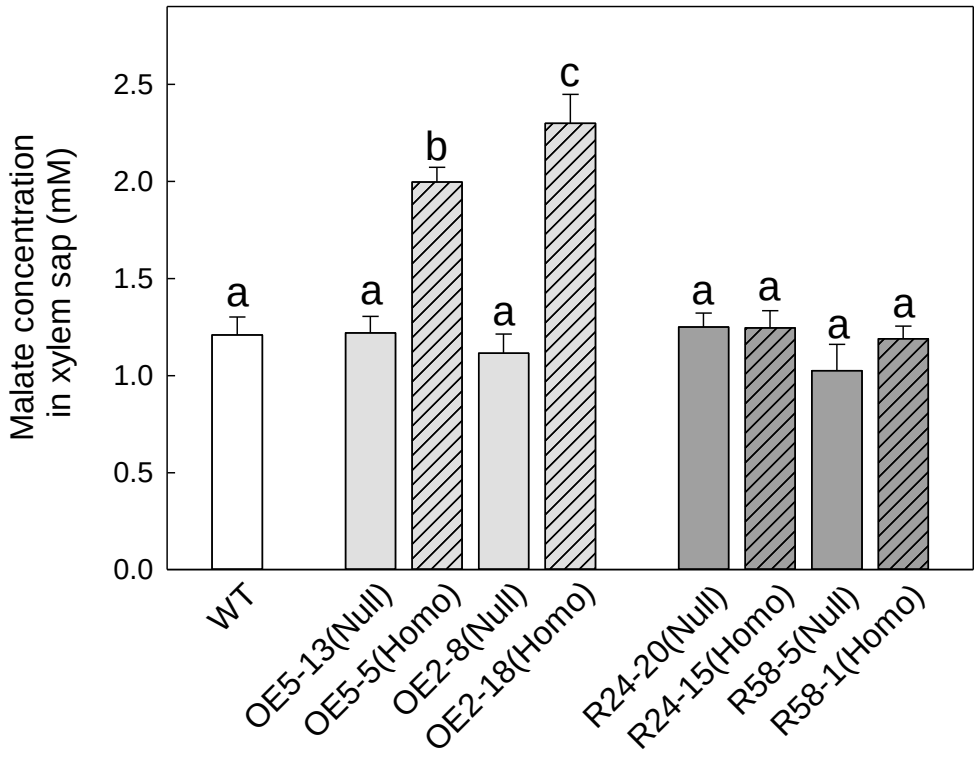

Figure 8.6 Malate concentrations in the xylem sap of transgenic rice lines with altered *OsALMT1* expression

Sap was collected from six week old wild-type plants (WT), T_3 lines over-expressing *OsALMT1* and their nulls (OE) and T_2 transgenic RNAi lines with reduced *OsALMT1* expression and their nulls (R). Data show the mean and standard error (n=4 separate plants for each line). Data were analysed with a one-way ANOVA and differences ($P<0.05$) indicated with different letters.

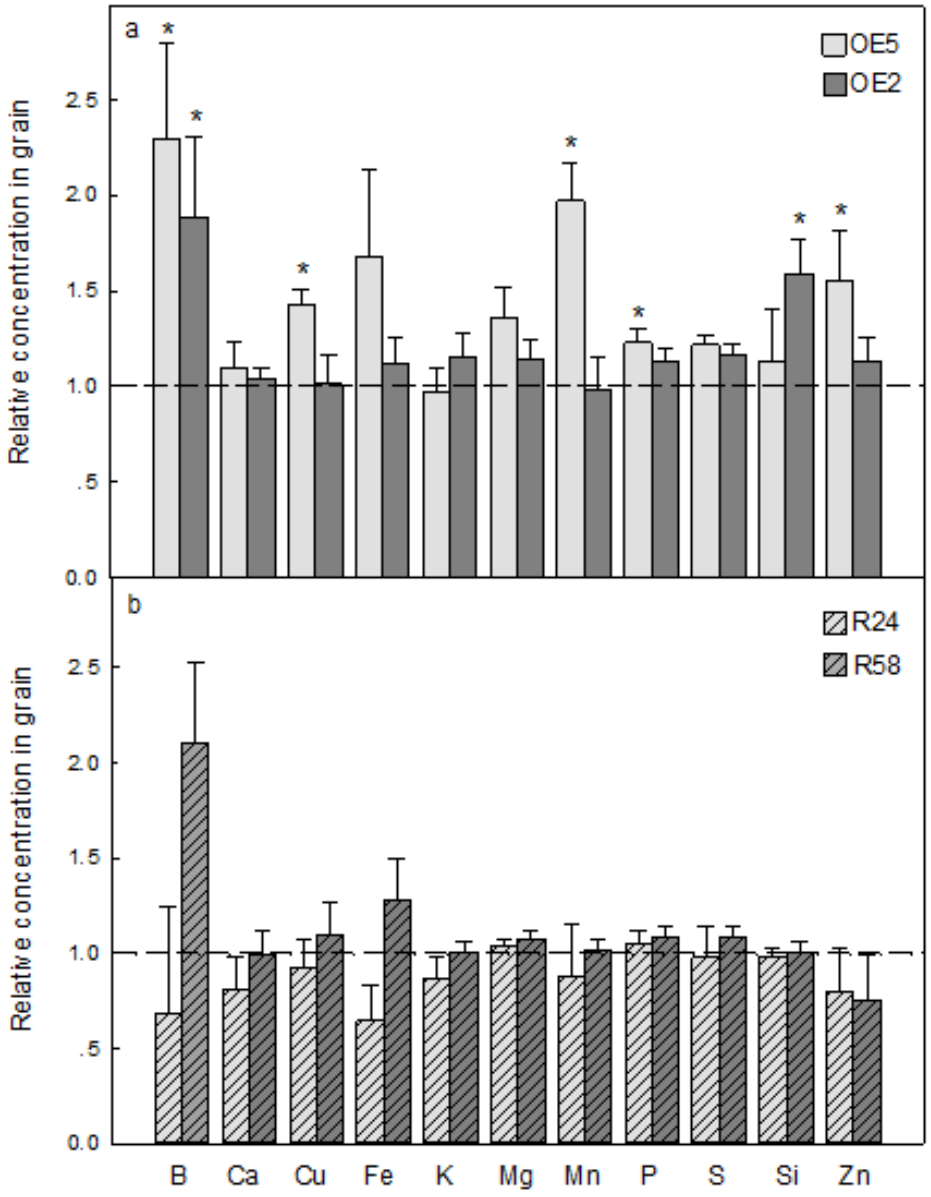

Figure 8.7 Mineral composition of rice grain

Relative mineral concentrations in grain from (a) two transgenic lines over-expressing *OsALMT1* (OE5-5 and OE2-18) and (b) two RNAi lines with reduced *OsALMT1* expression (R24-15 and R58-1) were measured with inductively coupled plasma mass spectrometry (ICP) analysis. Results show the concentrations of each mineral in the transgenic lines relative to their null sister line. Data show mean, SE (n=3). Raw data was presented in **Table S5**. The raw data for each element from the transgenic lines were compared to its null sister line and differences ($P<0.05$) indicated by an asterisk.

8.3.6 Pattern of starchy endosperm acidification in transgenic grains following germination

Bromcresol purple to study the variation of pH in the starchy endosperm among different lines with altered *OsALMT1* expression. A preliminary experiment stained first germinated grain for three days and then dissected and stained the grain. Colour of the two homozygous lines over-expressing *OsALMT1* were lighter and more yellowy than the nulls indicating they had a lower pH (**Figure 8.8**). A larger experiment then monitored pH through time in the overexpressing lines and RNAi lines along with their nulls. After 1 day of imbibing no difference in colour was detected among the overexpressing and RNAi lines compared to their relative null lines. After 3 days of germination, the overexpression seeds started to appear more acidic especially in the endosperm surrounding the embryo (**Figure 8.9**). After 5 days of germination, the acidic yellowy area in the overexpressing grain appeared to be larger and one of the OE5-5 gain was clearly more acidic over the whole endosperm area (**Figure 8.9**). There was still no pH difference found on RNAi lines compared with their corresponding null lines. These results indicate that altering *OsALMT1* expression can affect pH of the starchy endosperm during germination.

8.4 Discussion

This chapter examined the transgenic lines with altered *OsALMT1* expression to help understand *OsALMT1* function. Lines with high constitutive *OsALMT1* expression showed a constitutive release of malate and fumarate from their roots which was not detected in null segregate lines. The efflux was similar to the measured malate efflux from the roots of Al-tolerant wheat plants (Delhaize et al. 1993; Ryan et al. 1995). These results indicate that OsALMT1 mediates malate and fumarate efflux from cells. Whether OsALMT1 is also permeable to other anions, including inorganic anions, can be resolved with electrophysiological measurements in *Xenopus* oocytes in the future. A smaller but significant efflux of citrate was also detected from all plants and in some experiments there was an inverse relationship between malate and citrate efflux. Citrate and malate can be competitive inhibitors in some systems where the two anions are transported by the same pathway (Picault et al. 2002; Rentsch and Martinoia 1991). By using a combination of

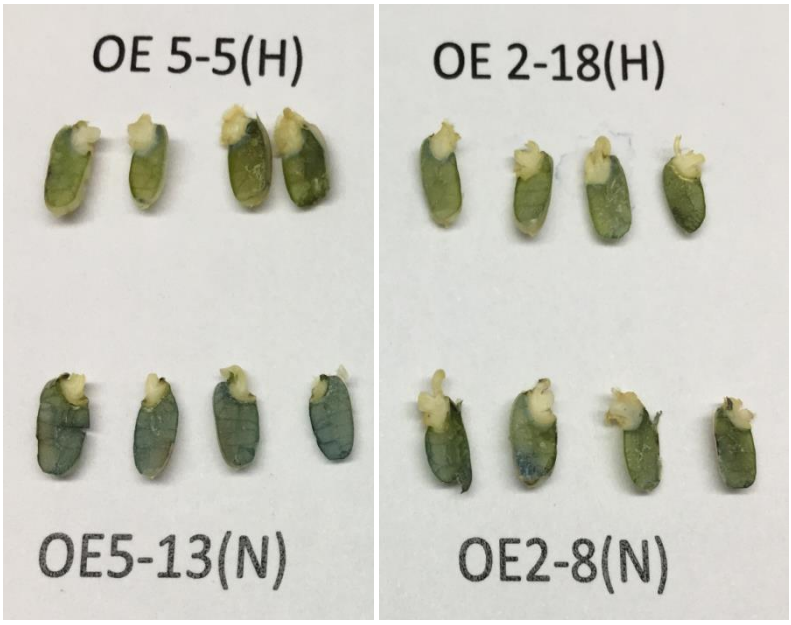

Figure 8.8 pH staining of grain endosperm 3 d after germination

Transgenic grains from two separate homozygous (H) lines over-expressing (OE) *OsALMT1* and their sister null lines three days after germination. The grains were longitudinally sectioned and stained with the pH indicator Bromcresol purple for 15 min. Colour changes from yellow to purple indicates pH changes from acid to alkaline.

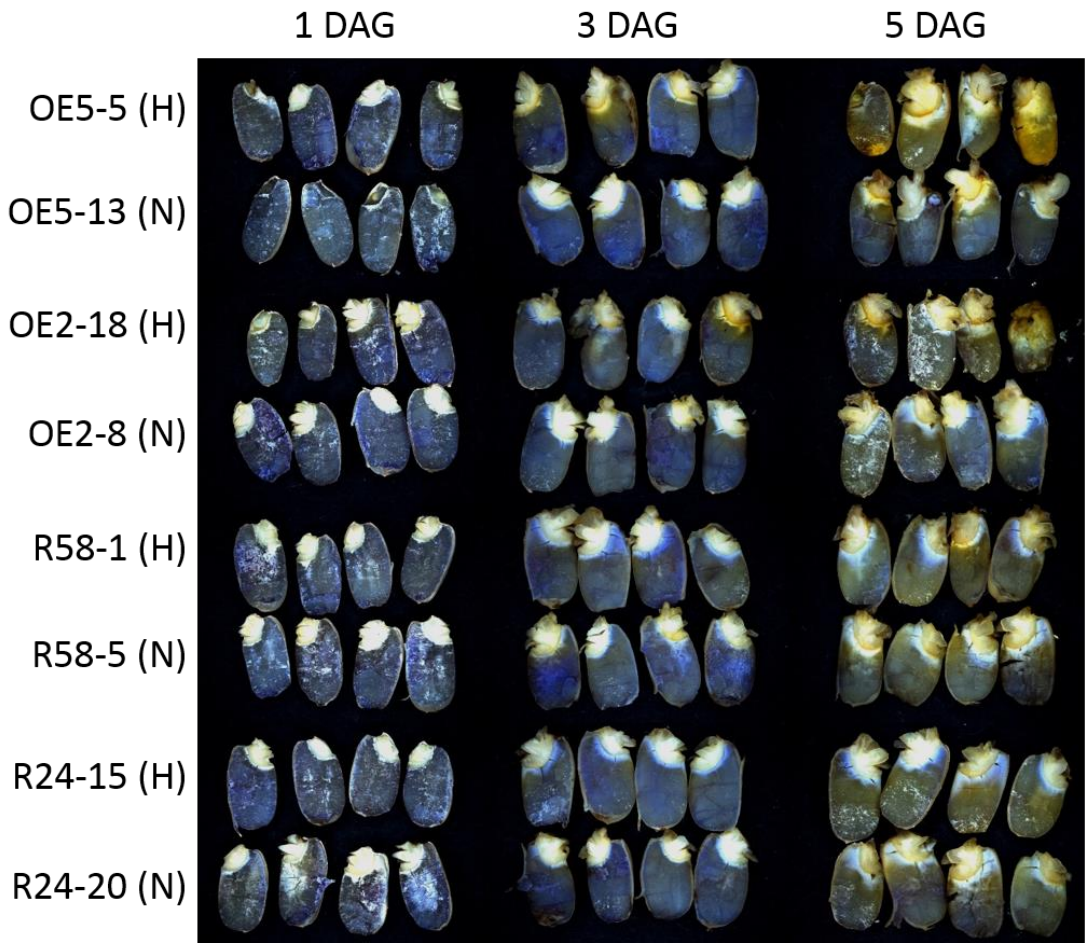

Figure 8.9 pH staining of the transgenic grain following germination

Transgenic grains from two separate homozygous (H) overexpression (OE) and RNAi (R) lines and their relative null (N) lines were germinated for 1day (1DAG), 3 days (3DAG) and 5 days (5 DAG). The grains were longitudinally sectioned and stained with the pH indicator Bromcresol purple for 15 min. A yellow colour indicates a low pH while a purple colour indicates a high pH.

pharmacological and mutagenesis approaches, Zhang *et al.* identified citrate as an "open channel blocker" of *AtALMT9* (Zhang et al. 2013). In the present experiments OsALMT1 expression was increased in the transgenic lines and therefore the inhibition of citrate efflux sometimes observed might reflect competition between transporters for the same pool of interchanging organic anions rather than citrate and malate competing for the same transporter. Malate and citrate are the most common organic acids released from roots for Al tolerance in a wide range of plant species (Magalhaes 2006). Therefore, we tested whether the high malate efflux from transgenic lines increased their tolerance to Al^{3+} toxicity. The homozygous lines showed greater relative root elongation in 200 and 400 μM Al which demonstrates over-expression of *OsALMT1* in rice did increase their Al tolerance. However this result from lines showing constitutive expression of *OsALMT1* does not indicate that *OsALMT1* necessarily confers Al tolerance in WT plants. In fact this conclusion is unlikely for two reasons: no malate efflux was detected in the WT plants with or without Al treatment, *OsALMT1* expression in roots was not affected by Al treatment as it is for all other ALMTs involved in Al tolerance except for TaALMT1 from wheat. Furthermore Al did not stimulate malate efflux in these over-expressing lines. Rice is the most Al^{3+}-tolerant of among all small-grain cereals and the mechanisms involved have been widely investigated with physiological and genetic approaches. These indicate that Al tolerance in rice is due to multiple mechanisms that operate in the root cell wall and the cytosol of root cells (Ma et al. 2002; Nguyen et al. 2001). Genes induced by the transcription factor ART1 (e.g. *Nrat1*, *STAR1/2*, *OsALS1*) have now been linked with Al tolerance in rice. These genes also include a MATE gene (*OsFRDL4*) which facilitates citrate efflux although this appears to play a minor role only. None of the known tolerance genes in rice are members of the ALMT family (Li et al. 2014; Huang et al. 2009; Huang et al. 2012; Tsutsui et al. 2011; Yokosho et al. 2011). Although rice is highly tolerant to Al by mechanisms that are less dependent on organic acid release, the enhanced efflux of malate from the roots in transgenic lines still increased tolerance in hydroponic experiments.

OsALMT1 function in the transgenic plants was sensitive to low concentrations of niflumic acid and to salicylic acid treatments. Niflumic acid is an anion channel blocker which effectively inhibits malate efflux via TaALMT1 in Al^{3+}-tolerant wheat (Ryan et al. 1995). The strong inhibition of malate efflux by the plant hormone salicylic acid was more surprising. Salicylic acid effectively decreased malate efflux with a half maximum

inhibition (Ki) of ~50 μM after 6 h. Salicylic acid is involved with growth, photosynthesis, respiration, gas exchange, nutrition, immunity and stress responses (Rivas-San Vicente and Plasencia 2011). Several studies have linked salicylic acid with increased Al^{3+} tolerance. Some attribute this response to the improved management of oxidative stress (Surapu et al. 2014; Pandey et al. 2013; Guo et al. 2014) while others correlate it with increased citrate efflux from roots via MATE transporters (Liu et al. 2011; Yang et al. 2003). This is the first study showing antagonistic interactions between salicylic acid and ALMT function and future studies will need to examine the regulation of this response in *OsALMT1* as well as in other ALMTs.

More recently, ALMTs were shown to function as receptors for GABA by transducing the fluctuations of GABA concentrations into ion movements and electrical signals (Ramesh et al. 2015). That study expressed a range of ALMTs from different species in *Xenopus* oocytes and showed that millimolar GABA and micromolar concentrations of muscimol, an analogue of GABA, inhibited ALMT-dependent inward currents. The authors identified a region in these ALMTs with similarity to the GABA binding site on $GABA_A$ receptors in humans (FFRQSWKDERLK) and demonstrated that targeted mutations in this region (e.g. F213C in TaALMT1) removed the inhibitory effects of GABA and muscimol on ALMT function (Ramesh *et al* 2015). In the present study 10 mM GABA inhibited malate efflux from transgenic rice by 50% but 100 μM muscimol actually increased efflux by ~50%. The reasons for this are unclear because OsALMT1 does possess the same 12 residue domain from (F209 to H220; FICPIWAGEQLH) which shows similarity to the GABA binding site. Future studies will express OsALMT1 in oocytes to determine whether it shows an altered sensitivity to these compounds.

Since *OsALMT1* expression is high in the vasculature tissue of roots and shoots (see **Chapter 5**) OsALMT1 function in WT plants could include facilitating malate efflux from the xylem parenchyma into the xylem. Consistent with this idea, transgenic plants over-expressing OsALMT1 showed an almost two-fold higher malate concentration in the xylem sap. Malate in the phloem is in the millimolar range also and plants can deliver and retrieve malate from that part of the vasculature system (van Dongen et al. 2003; Hijaz and Killiny 2014). Apoplastic pathways of loading and unloading photosynthetic assimilates and minerals often require the counter movement of ions for charge balance or osmotic adjustment. OsALMT1 could perform these roles in the phloem as well as in other tissues

where expression is also high such as the growing root apices, lateral root initiation and in the scutellum during grain germination. The expectation was that phenotypes in the RNAi lines would help to resolve these ideas but even when OsALMT1 expression was reduced to ~15% WT levels no strong phenotypes were detected in plant structure or function. This indicates either that low levels of OsALMT1 expression is adequate or that functional redundancy exists with other ALMTs or other transporters.

The transgenic lines over-expressing *OsALMT1* showed higher concentrations of B in their grain and also some other metal ions such as Mn and Cu and Zn. However all these changes were not observed in both transgenic lines so caution is required before concluding that these changes are directly related to greater OsALMT1 expression. Plants that do not normally hyperaccumulate metals take them up from the soil and store them in root cells, perhaps detoxified by the formation of complexes in the cytoplasm or storing them in vacuoles. Species that do hyperaccumulate metals normally accumulate them in the above ground tissues through long distance transport in the xylem from root to shoot (Grennan 2009). Organic acids can facilitate the long distance transport of metals in the vascular tissues and storage in the leaf cells (Sagner et al. 1998). Organic acids are able to bind metals, form complexes and produce a range of ligands for metal elements such as cadmium (Cd), copper (Cu), nickel (Ni), and zinc (Zn) (Parker et al. 2001). The high expression of OsALMT1 around vascular tissue could indicate that OsALMT1 releases malate into the xylem stream as a means of balancing charge during nutrient loading or for accompanying mineral nutrients to shoots. Consistent with this idea, transgenic plants over-expressing OsALMT1 showed an almost two-fold higher malate concentration in the xylem sap. While not proving a function of OsALMT1 this result demonstrates that high expression of this anion channel in the vascular bundle can influence malate concentration in the xylem sap. The translocation of certain micronutrients and heavy metals (including Fe, Zn and Cr) from roots to shoots rely on organic anions in the xylem as well as their transport proteins in the xylem parenchyma (Yokosho et al. 2009; Durrett et al. 2007). Several studies indicate that fast and efficient root-to-shoot translocation of heavy metals is accompanied by increased organic acids in vascular tissues. In the xylem sap moving from roots to leaves, citrate and histidine are the principal ligands for Cu, Ni, and Zn (Rauser 1999). Some members of the YSL (Yellow Strip1-Like) family mediate the loading into and unloading of nicotinamine–metal chelates to the xylem (especially nicotinamine–Ni and nicotinamine–Mn complexes) (Gendre et al. 2007; Colangelo and Guerinot 2006;

Sasaki et al. 2011). It was reported that the citrate transporters AtFRD3 loads citrate, an iron chelator, into the xylem necessary for the correct distribution of iron throughout the plant (Durrett et al. 2007). The OsFRDL1, a rice MATE family member, was also reported to function as a citrate transporter necessary for efficient translocation of Fe to the shoot by helping form Fe-citrate complexes in the xylem (Yokosho et al. 2009). Cr is reported to be transported through the maize plant xylem sap as an anionic organic complex (Juneja and Prakash 2006). Lu *et al*. (2013) also reported that while Zn is mainly transported in the xylem sap in *Sedum alfredii* as aqueous Zn a proportion is also associated with citric acid (Lu et al. 2013). Citrate is important in this respect but other anions including malate could also be involved. The experiments here showed that the over-expression of *OsALMT1* altered the mineral composition of grain. Those changes could result, in part, from the higher malate concentrations in the xylem and in part by the malate efflux from roots which enhances mineral availability in the soil. This could be tested by comparing the mineral composition of grain harvested from soil-grown plants and hydroponically-grown plants where nutrient availability is not restricted.

We also examined the pH of grain during germination as malate concentrations increase quickly (Ren and Bewley 1999). During the germination process, gibberellin is released from the early embryo and scutellum and the cells in the aleurone layer respond to the increased hormone by synthesizing and releasing hydrolytic enzymes into the endosperm such as α-amylase, cysteine proteases and ribonucleases that hydrolyze starch and storage proteins (Ritchie et al. 2000). In the meantime, the starchy endosperm becomes more acidic because acids such as citric, malic and phosphoric acids are released from the aleurone layer (Macnicol and Jacobsen 1992; Drozdowicz and Jones 1995). The barley HvALMT1 was highly expressed at the aleurone layer of germinating seed and the malate released from aleurone layer of the transgenic RNAi lines was inhibited (Xu et al. 2015). Interestingly, pH of the starchy endosperm of RNAi lines of barley with reduced *HvALMT1* expression was higher than null lines which is consistent with the changes observed here in rice grain overexpressing *OsALMT1*. The overexpressing lines showed more acidification in the endosperm surrounding the embryo which indicates that altering OsALMT1 activity can affect grain pH during germination. Further experiments are needed to quantify malate efflux from the aleurone layers. These experiments indicate that OsALMT1 likely functions as an organic anion channel which mainly facilitates organic anion (and mainly malate) efflux from cells.

8.5 References

Bouché N, Fromm H (2004) GABA in plants: just a metabolite? Trends Plant Sci 9: 110-115

Cawthray GR (2003) An improved reversed-phase liquid chromatographic method for the analysis of low-molecular mass organic acids in plant root exudates. J Chromatogr 1011: 233-240

Chen Q, Wu KH, Wang P, Yi J, Li KZ, Yu YX, Chen LM (2013a) Overexpression of *MsALMT1*, from the aluminum-sensitive *Medicago sativa*, enhances malate exudation and aluminum resistance in Tobacco. Pl Mol Biol Rep 31: 769-77

Chen ZC, Yokosho K, Kashino M, Zhao FJ, Yamaji N, Ma JF (2013b) Adaptation to acidic soil is achieved by increased numbers of cis-acting elements regulating *ALMT1* expression in *Holcus lanatus*. Plant J 76: 10-23

Colangelo EP, Guerinot ML (2006) Put the metal to the petal: metal uptake and transport throughout plants. Curr Opin Plant Biol 9: 322-330

Curtis MD, Grossniklaus U (2003) A gateway cloning vector set for high-throughput functional analysis of genes in planta. Plant Physiol 133: 462-469

De Angeli A, Baetz U, Francisco R, Zhang J, Chaves MM, Regalado A (2013a) The vacuolar channel VvALMT9 mediates malate and tartrate accumulation in berries of *Vitis vinifera*. Planta 238: 283-291

Delhaize E, Ryan PR, Hebb DM, Yamamoto Y, Sasaki T, Matsumoto H (2004) Engineering high-level aluminum tolerance in barley with the *ALMT1* gene. PNAS 101: 15249-15254

Delhaize E, Ryan PR, Randall PJ (1993) Aluminum Tolerance in Wheat (*Triticum aestivum* L.). Plant Physiol 103: 695-720

Dominguez F, Cejudo FJ (1999) Patterns of starchy endosperm acidification and protease gene expression in wheat grains following germination. Plant Physiol 119: 81-87

Drozdowicz YM, Jones RL (1995) Hormonal regulation of organic and phosphoric acid release by barley aleurone layers and scutella. Plant Physiol 108: 769-776

Durrett TP, Gassmann W, Rogers EE (2007) The FRD3-mediated efflux of citrate into the root vasculature is necessary for efficient iron translocation. Plant Physiol 144: 197-205

Gendre D, Czernic P, Conejero G, Pianelli K, Briat JF, Lebrun M, Mari S (2007) *TcYSL3*, a member of the *YSL* gene family from the hyper-accumulator *Thlaspi caerulescens*, encodes a nicotianamine-Ni/Fe transporter. Plant J 49: 1-15

Grennan AK (2009) Identification of genes involved in metal transport in plants. Plant Physiol 149: 1623-1624

Griffiths A, Miller J, Suzuki D (2000) An Introduction to Genetic Analysis. Mutant types, 7th edition. W. H. Freeman and company, New York.

Gruber BD, Delhaize E, Richardson AE, Roessner U, James RA, Howitt SM, Ryan PR (2011) Characterisation of *HvALMT1* function in transgenic barley plants. Funct Plant Biol 38: 163-175

Gruber BD, Ryan PR, Richardson AE, Tyerman SD, Ramesh S, Hebb DM, Howitt SM, Delhaize E (2010) HvALMT1 from barley is involved in the transport of organic anions. J Exp Bot 61: 1455-1467

Guo DY, Zhao SY, Huang LL, Ma CY, Hao L (2014) Aluminum tolerance in *Arabidopsis thaliana* as affected by endogenous salicylic acid. Biol Plant 58: 725-732

Hijaz F, Killiny N (2014) Collection and chemical composition of phloem sap from *Citrus sinensis* L. Osbeck (sweet orange). Plos One 9: e101830

Huang CF, Yamaji N, Chen Z, Ma JF (2012) A tonoplast-localized half-size ABC transporter is required for internal detoxification of aluminum in rice. Plant J 69: 857-867

Huang CF, Yamaji N, Mitani N, Yano M, Nagamura Y, Ma JF (2009) A bacterial-type ABC transporter is involved in aluminum tolerance in rice. Plant Cell 21: 655-667

Juneja S, Prakash S (2006) The chemical form of trivalent chromium in xylem sap of maize (*Zea mays* L.). Chem Spec Bioavailab 17: 161-169

Kinnersley AM, Turano FJ (2000) Gamma aminobutyric acid (GABA) and plant responses to stress. Crit Rev Plant Sci 19: 479-509

Kobayashi Y, Hoekenga OA, Itoh H, Nakashima M, Saito S, Shaff JE, Maron LG, Pineros MA, Kochian LV, Koyama H (2007) Characterization of *AtALMT1* expression in aluminum-inducible malate release and its role for rhizotoxic stress tolerance in arabidopsis. Plant Physiol 145: 843-852

Kobayashi Y, Lakshmanan V, Kobayashi Y, Asai M, Iuchi S, Kobayashi M, Bais HP, Koyama H (2013b) Overexpression of AtALMT1 in the Arabidopsis thaliana ecotype Columbia results in enhanced Al-activated malate excretion and beneficial bacterium recruitment. Plant Signal Behav8: 25561-25564

Koehler SM, Ho T-HD (1990) A major gibberellic acid-induced barley aleurone cysteine proteinase which digests hordein : purification and characterization. Plant Physiol 94: 251-258

Kovermann P, Meyer S, Hortensteiner S, Picco C, Scholz-Starke J, Ravera S, Lee Y, Martinoia E (2007) The Arabidopsis vacuolar malate channel is a member of the ALMT family. Plant J 52: 1169-1180

Li JY, Liu J, Dong D, Jia X, McCouch SR, Kochian LV (2014) Natural variation underlies alterations in Nramp aluminum transporter (NRAT1) expression and function that play a key role in rice aluminum tolerance. PNAS 111: 6503-6508

Liang CY, Pineros MA, Tian J, Yao ZF, Sun LL, Liu JP, Shaff J, Coluccio A, Kochian LV, Liao H (2013) Low pH, aluminum, and phosphorus coordinately regulate malate exudation through *GmALMT1* to improve soybean adaptation to acid soils. Plant Physiol 161: 1347-1361

Ligaba A, Katsuhara M, Ryan PR, Shibasaka M, Matsumoto H (2006) The *BnALMT1* and *BnALMT2* genes from rape encode aluminum-activated malate transporters that enhance the aluminum resistance of plant cells. Plant Physiol 142: 1294-1303

Ligaba A, Maron L, Shaff J, Kochian L, Pineros M (2012) Maize ZmALMT2 is a root anion transporter that mediates constitutive root malate efflux. Plant Cell Environ 35: 1185-1200

Liu N, You J, Shi W, Liu W, Yang Z (2011) Salicylic acid involved in the process of aluminum induced citrate exudation in *Glycine max* L. Plant Soil 352: 85-97

Lu L, Tian S, Zhang J, Yang X, Labavitch JM, Webb SM, Latimer M, Brown PH (2013) Efficient xylem transport and phloem remobilization of Zn in the hyperaccumulator plant species *Sedum alfredii*. New Phytol 198: 721-731

Ma J, Shen R, Zhao Z, Wissuwa M, Takeuch Y, Ebitani T, Yano M. (2002) Response of rice to Al stress and identification of quantitative trait loci for al tolerance. Plant Cell Physiol 43: 652-659

Macnicol PK, Jacobsen JV (1992) Endosperm acidification and related metabolic changes in the developing barley grain. Plant Physiol 98: 1098-1104

Magalhaes JV (2006) Aluminum tolerance genes are conserved between monocots and dicots. PNAS 103: 9749-9750

Mart ínez-Camacho JL, la Vara LG-d, Hamabata A, Mora-Escobedo R, Calder ón-Salinas V (2004) A pH-stating mechanism in isolated wheat (*Triticum aestivum*) aleurone layers involves malic acid transport. J Plant Physiol 161: 1289-1298

Nguyen VT, Burow MD, Nguye HT, Le BT, Le TD, Paterson AH (2001) Molecular mapping of genes conferring aluminum tolerance in rice (*Oryza sativa* L.). TAG 102: 1002-1010

Osawa H, Matsumoto H (2001) Possible involvement of protein phosphorylation in Aluminum-responsive malate efflux from wheat root apex. Plant Physiol 126: 411-420

Pandey P, Srivastava RK, Dubey RS (2013) Salicylic acid alleviates aluminum toxicity in rice seedlings better than magnesium and calcium by reducing aluminum uptake, suppressing oxidative damage and increasing antioxidative defense. Ecotoxicology 22: 656-670

Parker D, JF P, ZA A, M R (2001) Reevaluating the free-ion activity model of trace metal toxicity toward higher plants: experimental evidence with copper and zinc. Environ Toxicol Chem 20: 899-906

Pereira JF, Zhou GF, Delhaize E, Richardson T, Zhou MX, Ryan PR (2010) Engineering greater aluminium resistance in wheat by over-expressing *TaALMT1*. Ann Bot 106: 205-214

Picault N, Palmieri L, Pisano I, Hodges M, Palmieri F (2002) Identification of a novel transporter for dicarboxylates and tricarboxylates in plant mitochondria. Bacterial expression, reconstitution, functional characterization, and tissue distribution. J Biol Chem 277: 24204-24211

Pineros MA, Cancado GMA, Kochian LV (2008a) Novel properties of the wheat aluminum tolerance organic acid transporter (TaALMT1) revealed by

electrophysiological characterization in *Xenopus* oocytes: functional and structural implications. Plant Physiol 147: 2131-2146

Pineros MA, Cancado GMA, Maron LG, Lyi SM, Menossi M, Kochian LV (2008b) Not all ALMT1-type transporters mediate aluminum-activated organic acid responses: the case of *ZmALMT1* - an anion-selective transporter. Plant J 53: 352-367

Pracharoenwattana I, Zhou W, Smith SM (2010) Fatty acid beta-oxidation in germinating Arabidopsis seeds is supported by peroxisomal hydroxypyruvate reductase when malate dehydrogenase is absent. Plant Mol Biol 72: 101-109

Ramesh SA, Tyerman SD, Xu B, Bose J, Kaur S, Conn V, Domingos P, Ullah S, Wege S, Shabala S, Feijo JA, Ryan PR, Gillham M (2015) GABA signalling modulates plant growth by directly regulating the activity of plant-specific anion transporters. Nat Commun 6: 7879

Rauser WE (1999) Structure and function of metal chelators produced by plants. Cell Biochem Biophys 31: 1-19

Ren C, Bewley JD (1999) Developmental and germinative events can occur concurrently in precociously germinating Chinese cabbage (*Brassica rapa* ssp. *Pekinensis*) seeds. J Exp Bot 50: 1751–1761

Rentsch D, Martinoia E (1991) Citrate transport into barley mesophyll vacuoles comparison with malate-uptake activity. Planta 184: 532-537

Ritchie S, Swanson SJ, Gilroy S (2000) Physiology of the aleurone layer and starchy endosperm during grain development and early seedling growth: new insights from cell and molecular biology. Seed Sci Res 10: 193-212

Rivas-San Vicente M, Plasencia J (2011) Salicylic acid beyond defence: its role in plant growth and development. J Exp Bot 62: 3321-3338

Ryan PR, Delhaize E, Randall P (1995) Characterisation of Al-stimulated efflux of malate from the apices of Al-tolerant wheat roots. Planta 196: 103-110

Ryan PR, Raman H, Gupta S, Horst WJ, Delhaize E (2009) A second mechanism for Aluminum resistance in wheat relies on the constitutive efflux of citrate from roots. Plant Physiol 149: 340-351

Sagner S, Kneer R, Wanner G, Cosson J-P, Deus-Neumann B, Zenk MH (1998) Hyperaccumulation, complexation and distribution of nickel in Sebertia acuminata. Phytochemistry 47: 339-347

Sasaki A, Yamaji N, Xia J, Ma JF (2011) OsYSL6 is involved in the detoxification of excess manganese in rice. Plant Physiol 157: 1832-1840

Sasaki T, Mori IC, Furuichi T, Munemasa S, Toyooka K, Matsuoka K, Murata Y, Yamamoto Y (2010) Closing plant stomata requires a homolog of an aluminum-activated malate transporter. Plant Cell Physiol 51: 354-365

Sasaki T, Yamamoto Y, Ezaki B, Katsuhara M, Ahn SJ, Ryan PR, Delhaize E, Matsumoto H (2004) A wheat gene encoding an aluminum-activated malate transporter. Plant J 37: 645-653

Smith SM, Leaver CJ (1986) Glyoxysomal malate synthase of Cucumber: molecular cloning of a cDNA and regulation of enzyme synthesis during germination. Plant Physiol 81: 762-767

Surapu V, Ediga A, Meriga B (2014) Salicylic acid alleviates aluminum toxicity in tomato seedlings (*Lycopersicum esculentum* Mill.) through activation of antioxidant defense system and proline biosynthesis. Adv Bios Biot 5: 777-789

Tsutsui T, Yamaji N, Ma JF (2011) Identification of a cis-acting element of ART1, a C2H2-type zinc-finger transcription factor for aluminum tolerance in rice. Plant Physiol 156: 925-931

Uloth MB, You MP, Cawthray G, Barbetti MJ (2015) Temperature adaptation in isolates of *Sclerotinia sclerotiorum* affects their ability to infect *Brassica carinata*. Plant Pathol 64: 1140-1148

van Dongen JT, Schurr U, Pfister M, Geigenberger P (2003) Phloem metabolism and function have to cope with low internal oxygen. Plant Physiol 131: 1529-1543

Xu M, Gruber BD, Delhaize E, White RG, James RA, You J, Yang Z, Ryan PR (2015) The barley anion channel, HvALMT1, has multiple roles in guard cell physiology and grain metabolism. Physiol Plant153: 183-193

Yang ZM, Wang J, Wang SH, Xu LL (2003) Salicylic acid-induced aluminum tolerance by modulation of citrate efflux from roots of *Cassia tora* L. Planta 217: 168-174

Yokosho K, Yamaji N, Ma JF (2011) An Al-inducible MATE gene is involved in external detoxification of Al in rice. Plant J 68: 1061-1069

Yokosho K, Yamaji N, Ueno D, Mitani N, Ma JF (2009) OsFRDL1 is a citrate transporter required for efficient translocation of iron in rice. Plant Physiol 149: 297-305

Zhang J, Baetz U, Krugel U, Martinoia E, De Angeli A (2013) Identification of a probable pore-forming domain in the multimeric vacuolar anion channel AtALMT9. Plant Physiol 163: 830-843

Zhang WH, Ryan PR, Sasaki T, Yamamoto Y, Sullivan W, Tyerman SD (2008) Characterization of the TaALMT1 protein as an Al^{3+}-activated anion channel in transformed tobacco (*Nicotiana tabacum* L.) cells. Plant Cell Physiol 49: 1316-1330

CHAPTER 9

Growth experiments to investigate OsALMT1 function

9.1 Introduction

Transgenic technologies provide useful tools for investigating gene function because the phenotypes associated with changing expression of a gene can provide clues to the roles it performs (Pereira, 2000). The phenotypes can be associated with loss-of-function or gain-of-function alterations (Abdeeva *et al*., 2012). The conventional approach to analysing gene function in this way is to use induce loss-of-function or knock-out mutants. A population of grain containing random mutations throughout the genome is generated by exposing them to ionising radiation or treating them with mutagenic drugs such as ethyl methanosulfonate (M0 seed). The M2 generation is then screened for specific phenotypes. The gene causing a phenotype can then be identified by genetic mapping. In the present project the gene is known but its function is not known. Therefore targeted mutants can be obtained from resource centres but more recently CRISPR technology allows specific changes to be generated in a genome with standard engineering techniques (Belhaj *et al*., 2013). An alternative approach is to reduce gene expression with RNAi technology. RNAi usually decreases expression without stopping it entirely which has the advantage that it avoids generating lethal mutations if the target gene is essential for growth. However the disadvantage with RNAi is that it might not generate very pronounced phenotypes if its expression is simply reduced rather than knocked out. Nevertheless phenotypes associated with these changes may still help understand gene function (Ostergaard and Yanofsky, 2004). When genes are members of larger families, single gene disruptions may not show clear phenotypes due to redundancy (Abdeeva *et al*., 2012). Under these circumstances, gain-of-function approaches have been used as a complementary method to examine function in plants. Gain-of-function mutagenesis can be achieved by randomly inserting transcriptional enhancers into the genome and looking for changes in gene expression (Kondou *et al*., 2010) or by over-expressing the gene, if it is known, in a homologous or heterologous expression system.

In the previous Chapters, *OsALMT1* was confirmed to be one of the nine members *ALMT* gene family in rice which is widely expressed in roots and leaves of wild type plants. To characterise OsALMT1 function in more detail, transgenic rice lines were generated with either increased (~40 fold over-expression) or reduced (~0.2 of WT by RNAi) *OsALMT1* expression. Transgenic rice plants over-expressing OsALMT1 tended to have less root and shoot biomass and showed brown spots on the leaves but the RNAi plants didn't show any visible phenotype. The over-expressing plants also showed a constitutive release of malate and fumarate from their roots and the efflux of malate can be affected by pharmacological agents, hormones and certain ions (GABA, niflumic acid, muscimol, salicylic acid and Al) as well as some environmental conditions (pH and high light).

Previously in **Chapter 6** the responses of *OsALMT1* expression in wild type rice plants were monitored during various treatments. Expression levels were affected by various abiotic treatments including osmotic stress, salt stress, light treatments as well as some hormones. For instance, 200 mM NaCl and 350 mM mannitol generated similar changes in expression which comprised decreases in the shoot tissues and increases in the root tissues. Since *OsALMT1* expression is clearly sensitive to these osmotic treatments it was interesting to monitor growth of the transgenic plants over a longer period in similar treatments to test whether their changes in gene expression affect plant growth. Since *OsALMT1* encodes a malate channel it might contribute to the regulation of cellular osmolality and charge balance by moving malate anions out of cells. In the absence of Cl^-, a major inorganic anion in plants cells, the role of other anions such as malate in adjusting cytosolic conditions could become even more important. Interestingly there was no obvious and consistent affects of a low Cl^- treatment on *OsALMT1* expression after 24 h (see **Chapter 6**). However this period might have been too short to trigger differences in expression so longer term treatments of the transgenic lines with higher and lower expression when Cl^- availability is restricted could be informative. *OsALMT1* also showed large changes in expression during continuous light and darkness (see **Chapter 6**) and later in **Chapter 7** when the leaf phenotypes were being investigated the plants overexpressing *OsALMT1* appeared to grow more poorly in low light compared to their null sister lines (see **Chapter 7**). Considering these results, growth of the transgenic material under low light could be informative for investigating *OsALMT1* function. Growth experiments in higher concentrations of boric acid were also performed here because boron (B) concentrations in the grain of transgenic plants over-expressing

OsALMT1 were about two-fold greater than the nulls (see **Chapter 7**). Longer growth experiments in a higher and toxic B treatment could provide additional hints to OsALMT1 function as well. The previous results also showed relative higher Mn accumulation in both leaf and grain tissues of the transgenic overexpressing lines compared with their null lines (see **Chapter 7 and 8**). A long term growth experiment also done under various Mn concentration to test the sensitivity of these lines to higher Mn concentrations.

The aim of this chapter is further characterise the *OsALMT1* function by performing longer-term growth experiments under specific conditions.

9.2 Materials and methods

9.2.1 Stress conditions

Homozygous transgenic lines with higher and lower levels of *OsALMT1* expression and null lines were germinated as described in **Chapter 2**. Seven days old seedlings were transferred from MS media to nutrient solution (pH 5.6) and adapted for another seven days. The solutions were then changed to control again or control solution with the addition of 100 mM NaCl, 50 mM mannitol, 5 mM H_3BO_3, 250/500 µM $MnCl_2$ or a similar control solution without added chloride (pH 5.6). Preliminary tests indicated that the 200 mM NaCl and 350 mM mannitol treatments used in **Chapter 6** to measure changes in *OsALMT1* expression of WT plants are too high and damaging for longer term growth experiments (data not shown). For this reason only 100 mM NaCl and 50 mM mannitol treatments are used here. The 100 mM NaCl solution also included 12 mM $CaCl_2$ to minimise this treatment displacing Ca from the root membranes and causing Ca deficiency and other membrane damage. The low Cl^- solution was described in **Chapter 6**. All the solutions were renewed every three to four days and the plants were harvested after four weeks.

For the light intensity treatment, the over-expressing lines and null plants were germinated and transferred to pots with soil and placed in growth cabinets with different light intensities for five to eight weeks. One cabinet was the control and set to mimic the

glasshouse conditions as much as possible with a light intensity of 700 μmol m^{-2} s^{-1}. The other cabinet had a lower light intensity of 300 μmol m^{-2} s^{-1}.

9.2.2 Biomass measurement

For the hydroponic growth experiments, root and shoot tissues were harvested separately and dried in 65℃ oven for 72 hours. Root and shoot dry weight then be measured and the total dry weight was calculated. For the soil growth experiment, the above-ground tissue was collected and dry weights were determined. Relative dry weight was calculated as the biomass for each line in each treatment relative to the same lines in control treatments. Relative biomass and relative SE values were calculated as described in **Chapter 2**.

9.3 Results

9.3.1 Biomass accumulation under a high salt treatment

Previous results indicated that *OsALMT1* expression was affected by various abiotic stresses including salt and osmotic stress as well as by certain hormones. This is consistent with the hypothesis that *OsALMT1* helps regulate cellular osmolality and charge balance. To test this hypothesis longer-term growth experiments in 100 mM NaCl were performed with transgenic plants with altered *OsALMT1* expression. The water potential of wheat roots is estimated to be -0.5 to -0.7 MPa (see **Chapter 10**) and for rice it is approximately -0.5 MPa (Maki Katsuhara, unpublished). The 100 mM NaCl treatment would decrease the water potential of the nutrient solution to approximately -0.46 MPa (see Appendix **Table S1**) which is close to the water potential for the rice roots – at least initially. This treatment reduced biomass of the null lines by approximately 60% compared to control treatment. The two homozygous lines overexpressing *OsALMT1* accumulated less biomass both under control and salt treatments compared to their null lines (**Figure 9.1 a**). The homozygous line OE2-18 showed significantly less biomass under salt condition relative to its relative null line OE 2-8 indicating it was more

sensitive to this treatment than the null (**Figure 9.1 b**). The second over-expressing line tested, OE5-5, showed the same trend but the differences were smaller and not significant (**Figure 9.1**). No differences were detected in the relative biomass of the two RNAi lines compared to their null sister lines in this salt treatment (**Figure 9.1**). Note that due to restricted cabinet space the experiments with the over-expressing lines were conducted at a different time from the experiments with the RNAi lines which explains why the nulls were not more similar.

9.3.2 Biomass accumulation under a high mannitol treatment

Similar to the salt treatment, the 50 mM mannitol treatment reduced biomass of the null lines by approximately 50% of the control treatment (**Figure 9.2**). The two homozygous lines overexpressing *OsALMT1* tended to show lower relative biomass in mannitol compared to their null lines (**Figure 9.2 b**) but the differences were not significant. No differences were detected in the relative biomass of the two RNAi lines compared to their respective null sister lines either (**Figure 9.2 b**).

9.3.3 Biomass accumulation under a low Cl^- treatment

Transgenic lines and nulls were grown for four weeks in solutions containing "high" and "low" Cl^- concentrations of 502.7 µM and 2.7 µM, respectively (**Table 6.1**). The low Cl^- treatment decreased biomass of null lines by ~40% compared to the high Cl^- controls (**Figure 9.3**). For the two lines overexpressing *OsALMT1*, OE5-5 and OE2-18, relative biomass (low Cl^-/high Cl^-) was approximately 68% which was higher than relative biomass of the two null lines which were 53% and 58%. Although showing a consistent trend these differences between the overexpressing and nulls lines were not significant (**Figure 9.3 b**). Biomass changes for the two RNAi lines gave the opposite trend with both homozygous lines (R24-15 and R58-1) showing smaller relative biomasses compared with their corresponding null lines (**Figure 9.3 b**). This difference was significant for R58-1 but not for R24-15. These results indicate that reducing *OsALMT1* expression tends to decrease the capacity of rice to grow in conditions when availability of the major inorganic anion, Cl^-, is restricted. Lines overexpressing *OsALMT1* showed

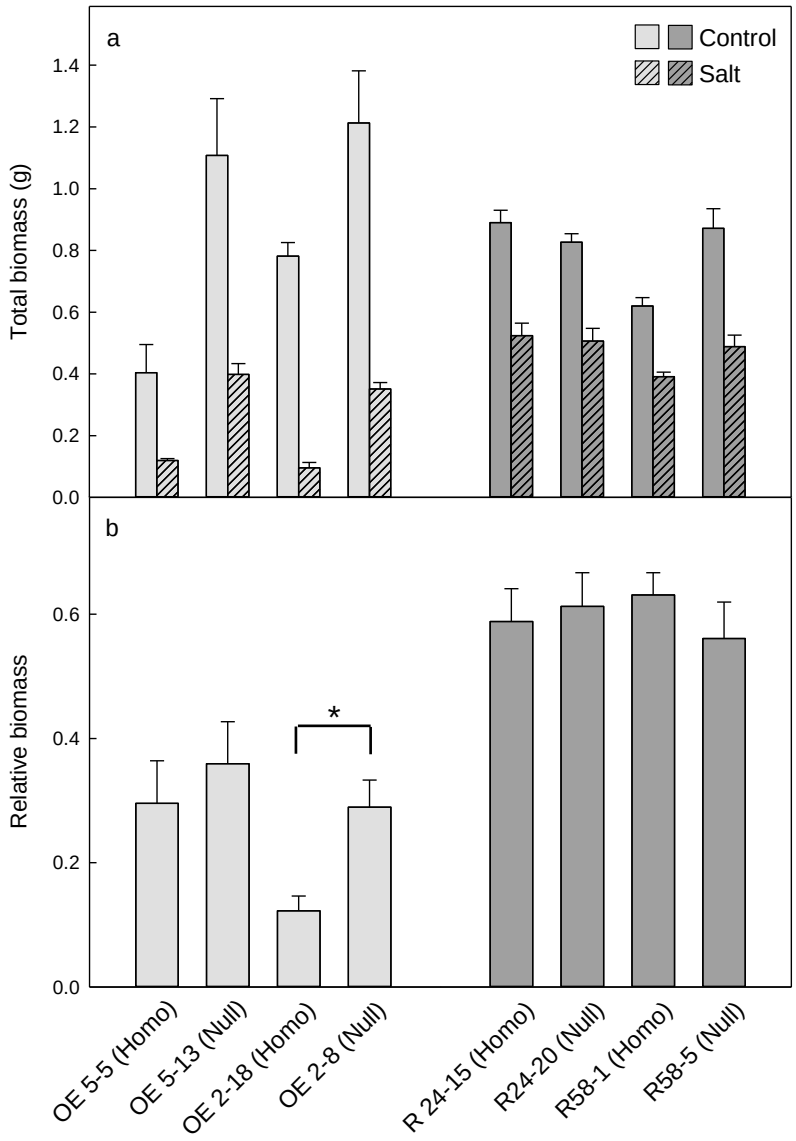

Figure 9.1 Total plant biomass and relative biomass under a salt treatment

Total plant biomass (a) and relative biomass (b) after four weeks growth with salt stress. Lines include two homozygous lines over-expressing *OsALMT1*, two RNAi lines with reduced expression and their respective null lines. Value represent average ± SE (n=4). Asterisks indicate significant differences (P=0.05) of the relative biomass between the transgenic lines and its corresponding null line using the method described in **Chapter 2**.

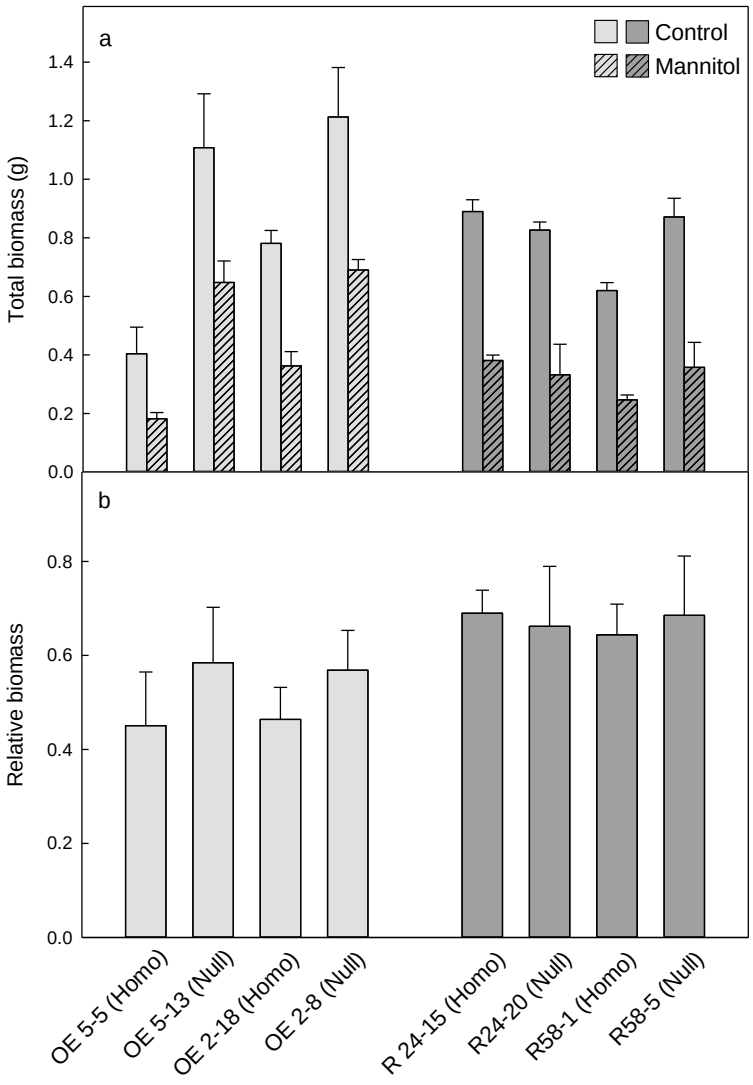

Figure 9.2 Total plant biomass and relative biomass under a high mannitol treatment

Total plant biomass (a) and relative biomass (b) after four weeks growth under high mannitol. Lines include two homozygous lines overexpressing *OsALMT1*, two RNAi lines with reduced expression and their respective null lines. Value represent average ± SE (n=4). Asterisks indicate significant differences (P=0.05) of the relative biomass between the transgenic lines and its corresponding null line using the method described in **Chapter 2**.

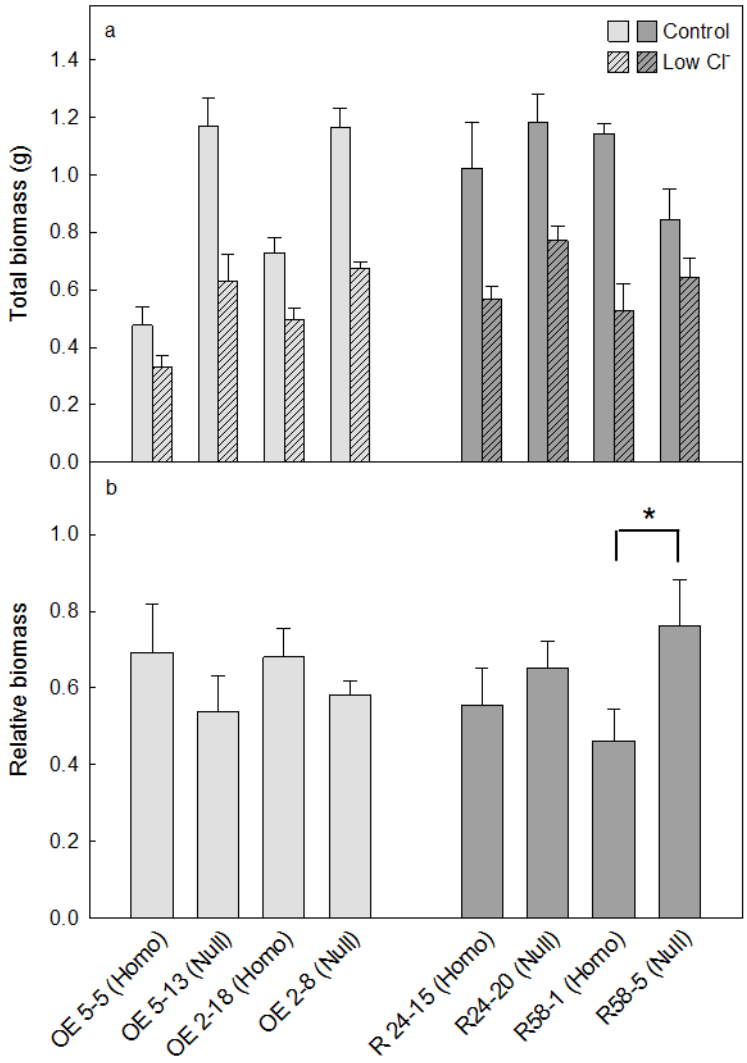

Figure 9.3 Total plant biomass and relative biomass in low Cl^-

Total plant biomass (a) and relative biomass (b) after four weeks growth with low Cl^-. Lines include two homozygous lines overexpressing *OsALMT1*, two RNAi lines with reduced expression and their respective null lines. Value represent average ± SE (n=5). Asterisks indicate significant differences (P=0.05) of the relative biomass between the transgenic lines and its corresponding null line using the method described in **Chapter 2**.

the opposite trend and grew better than nulls when Cl^- was restricted. These data are consistent with OsALMT1 providing an important transport pathway for organic anions during normal growth and especially when the availability of other inorganic anions is restricted.

9.3.4 Biomass under low light conditions

Transgenic lines and nulls were grown for eight weeks in a control or "high" light intensity (700 µmol m^{-2} s^{-1}) or a low light intensity (300 µmol m^{-2} s^{-1}). The low light treatment decreased biomass of the null lines by ~40% compared to the high light controls (**Figure 9.4 a**). Both lines overexpressing *OsALMT1* showed significantly larger decreases in biomass in low light compared to their nulls ($P_{0.05}$). Relative biomass of the homozygous OE2-18 and OE5-5 lines were 18% and 35% compared to their nulls of 63% and 77% respectively (**Figure 9.4 b**). Similarly, both RNAi lines with reduced *OsALMT1* expression (R24-15 an R58-1) also showed larger decreases in biomass in low light compared to their nulls ($P_{0.05}$) (**Figure 9.4 b**). This difference was significant ($P_{0.05}$) for both the R24-15 and R58-1 compared to their null lines R24-20 and R58-5. Therefore rice lines in which *OsALMT1* had been altered (increased or decreased) were more sensitive to low light conditions and accumulate less biomass than their null controls. Note that due to restricted cabinet space the experiments with the over-expressing lines were conducted at a different time from the experiments with the RNAi lines which explains why the nulls in these experiments were not the more similar to one another. However the important comparison is between the transgenic and their nulls.

9.3.5 Biomass accumulation during H_3BO_3 stress

Previous elemental analysis of grain showed two-fold higher B concentrations in grain of the transgenic lines over-expressing *OsALMT1* compared to nulls. Preliminary growth experiments showed that the biomass accumulation of WT plants was inhibited by 25% in 2.5 mM H_3BO_3 and by 48% in 5 mM H_3BO_3 (data not shown) Therefore growth of two transgenic lines overexpressing *OsALMT1* and two RNAi lines, along with nulls,

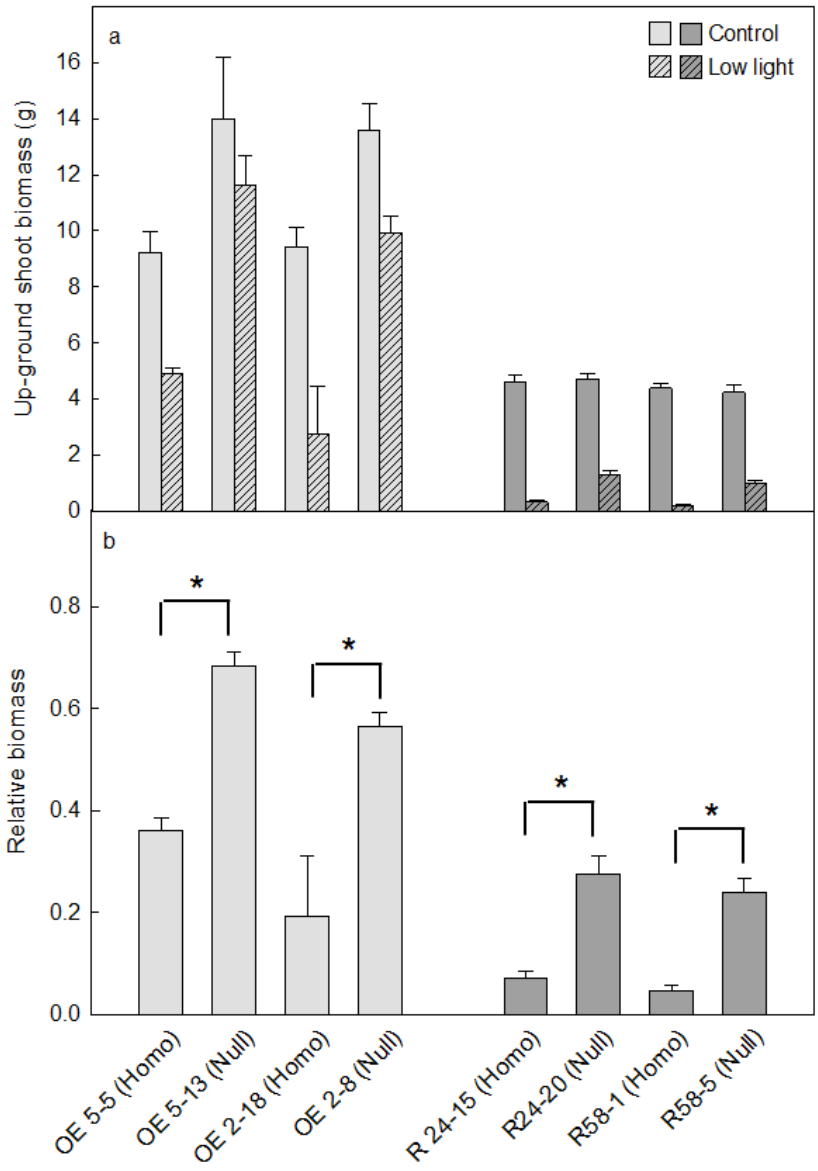

Figure 9.4 Shoot biomass and relative shoot biomass under low light

Total (a) and relative (b) biomass under low light stress was measured on two homozygous overexpression and RNAi lines as well as their null lines. The overexpression lines were harvested after eight weeks of treatment, the RNAi lines were harvested after four weeks of treatment. Value represent average ± SE (n=6). Asterisks indicate significant differences (P=0.05) of the relative biomass between the transgenic lines and its corresponding null line using the method described in **Chapter 2**.

was compared in nutrient solution containing 5 mM H_3BO_3. Shoot and root biomass for all plants decreased significantly in the high B treatment compared to controls (**Figure 9.5 a, c, and e**). Nevertheless the relative biomass of the shoots and roots were higher in lines overexpressing *OsALMT1* than the nulls indicating that they tended to be less sensitive to the high B treatment than their nulls. This difference was significant ($P_{0.05}$) for the OE5-5 and its null line for both root and shoot biomass. For the OE2-18 line only root biomass was significantly greater than its null (**Figure 9.5 b, d and f**). No differences in relative biomass were found for either of the RNAi lines compared to their nulls.

9.3.6 Biomass under $MnCl_2$ stress

Previous Chapters showed that Mn accumulation was sometimes greater in the leaves (**Chapter 7**) and grain (**Chapter 8**) of the transgenic lines overexpressing *OsALMT1* than their nulls. To test the sensitivity of these lines to higher Mn concentrations a longer-term growth experiment was performed over three weeks with control (1 µM Mn), 250 µM and 500 µM $MnCl_2$. In most null lines shoot growth was inhibited by 10 to 20% in 250 µM and 500 µM $MnCl_2$ and root growth was reduced by ~30% and 60% (**Figure 9.6**). In the two lines over-expressing *OsALMT1* the reduction in root and shoot biomass were larger. Relative biomass of the shoot and root as well as total biomass of the OE5-5 line, was significantly smaller than its null lines at 500 µM $MnCl_2$ (**Figure 9.6 b, d, f**). Similarly, relative biomass of the shoot biomass and total plant biomass of line OE2-18 was significantly smaller than it null line at 250 µM and 500 µM $MnCl_2$ but root biomass was significantly smaller at 500 µM $MnCl_2$ only. The two lines over-expressing *OsALMT1* also showed the brown spot phenotype on the leaves very clearly at both 250 µM and 500 µM $MnCl_2$ (**Figure 9.7 a,c**). By comparison the phenotype on leaves of the null lines, OE5-13 (null) and OE2-8 (null), was only mild even in 500 µM $MnCl_2$ (**Figure 9.7 b,d**).

Biomass changes in the two homozygous RNAi lines with reduced *OsALMT1* expression were not significantly different from their nulls (**Figure 9.6**). Furthermore they showed little or no symptoms on the leaves which was similar to the nulls of the over-expressing lines. These results indicate that overexpressing *OsALMT1* made the plants more

sensitive to Mn stress as measured by slower growth and a stronger phenotype of brown spots on the leaves.

9.4 Discussion

To investigate OsALMT1 function further longer-term growth experiments were performed with the transgenic plants in various treatments. These treatments were chosen largely on the results of the previous studies of expression analysis, malate efflux and observed phenotypes.

Despite showing large changes in *OsALMT1* expression during salt stress the changes in biomass accumulation of homozygous RNAi lines were no different to those occurring in their null lines. This indicates that reducing OsALMT1 expression to less than 20% of WT had no effect on plant responses to salt stress. By contrast increasing *OsALMT1* expression tended to make both transgenic lines more sensitive to salt stress but the relative biomass was only significantly different between OE2-18 and its null line OE2-8.

A similar pattern emerged for the mannitol treatment. No differences in relative biomass in the RNAi lines compared to nulls and only a trend for lower relative biomass in both lines overexpressing *OsALMT1*. Nevertheless this trend indicated that the over-expression lines tended to be more sensitive to osmotic stress whether from high salt or high mannitol treatments. Perhaps the continual loss of osmotically active malate ions from the root and shoot cells is a disadvantage when plants are experiencing osmotic stress. The salt treatment would potentially cause salt toxicity in addition to osmotic stress. The RNAi lines with only 10%-20% of WT expression could have maintained enough function under these treatments. A knock-out mutation could be more informative but this was not available for *OsALMT1* at the genetic resource centre when this project was started. Furthermore functional redundancy among the nine ALMT members in rice is possible.

Chapter 6 showed that a low Cl^- treatment had no effect on *OsALMT1* expression after 24 h but this might have been too short a period for the plant to experience symptoms of Cl^- deficiency. After several weeks in a hydroponic condition containing a low Cl^-

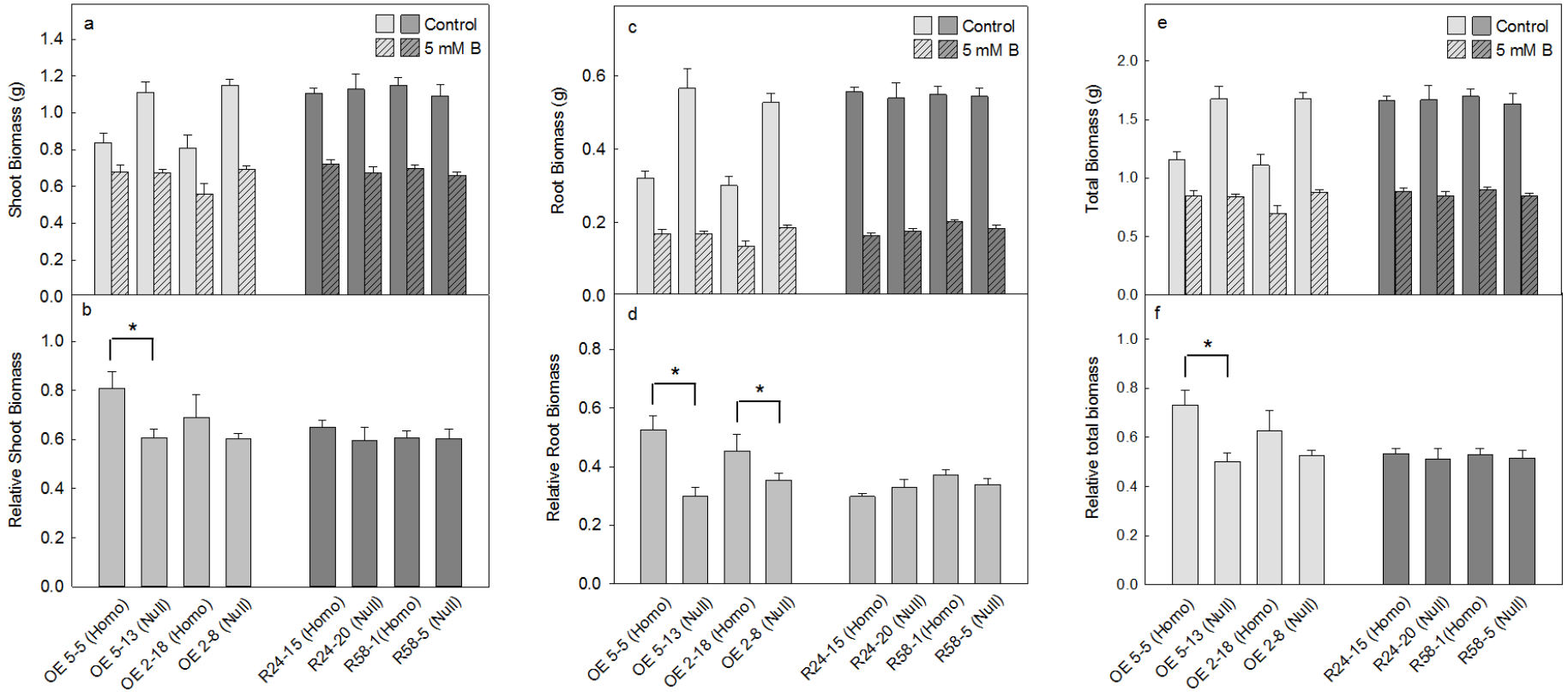

Figure 9.5 Shoot, root, total biomass and relative biomass of transgenic lines under a high H_3BO_3 treatment

(a) Shoot, (b) root and (c) total biomass under control (standard concentration in nutrient solution) and 5 mM H_3BO_3 treatments. Relative biomass was calculated by the ratio of biomass in the treatment compared to the controls. The seedlings were harvested after four weeks of growth. Value represent average ± SE (n=5). Asterisks indicate significant differences (P=0.05) in relative biomass between each transgenic line and its corresponding null line using the method described in **Chapter 2**.

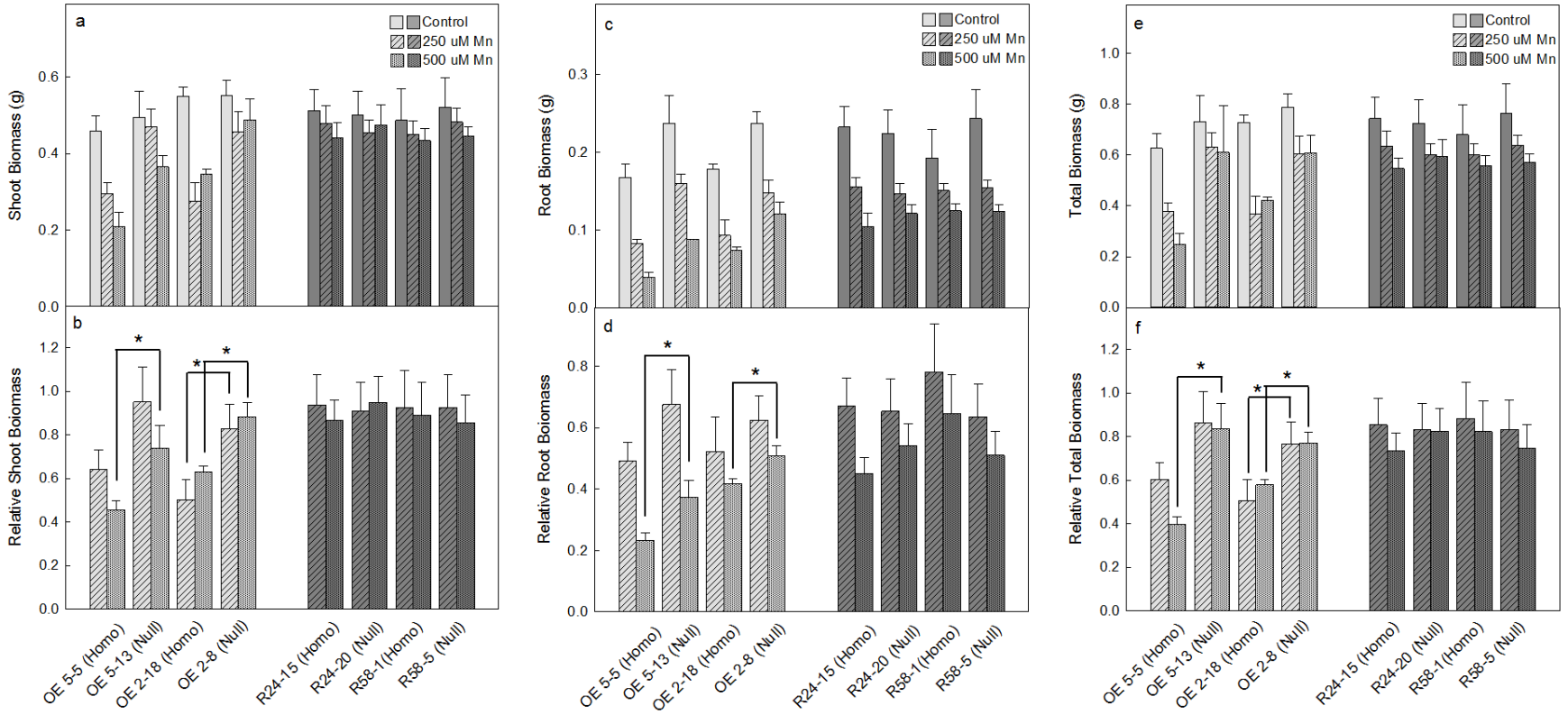

Figure 9.6 Shoot, root, total biomass and relative biomass of transgenic lines under a higher $MnCl_2$ treatments

(a) Shoot, (b) root and (c) total biomass under control (standard nutrient solution), 250 µM and 500 µM $MnCl_2$ treatments. Relative biomasses was calculated by the ratio of biomass in the treatment compared to the controls. The seedlings were harvested after four weeks of treatment. Value represent average ± SE (n=5). Asterisks indicate significant differences (P=0.05) of the relative biomass between the transgenic lines and its corresponding null line using the method described in **Chapter 2**.

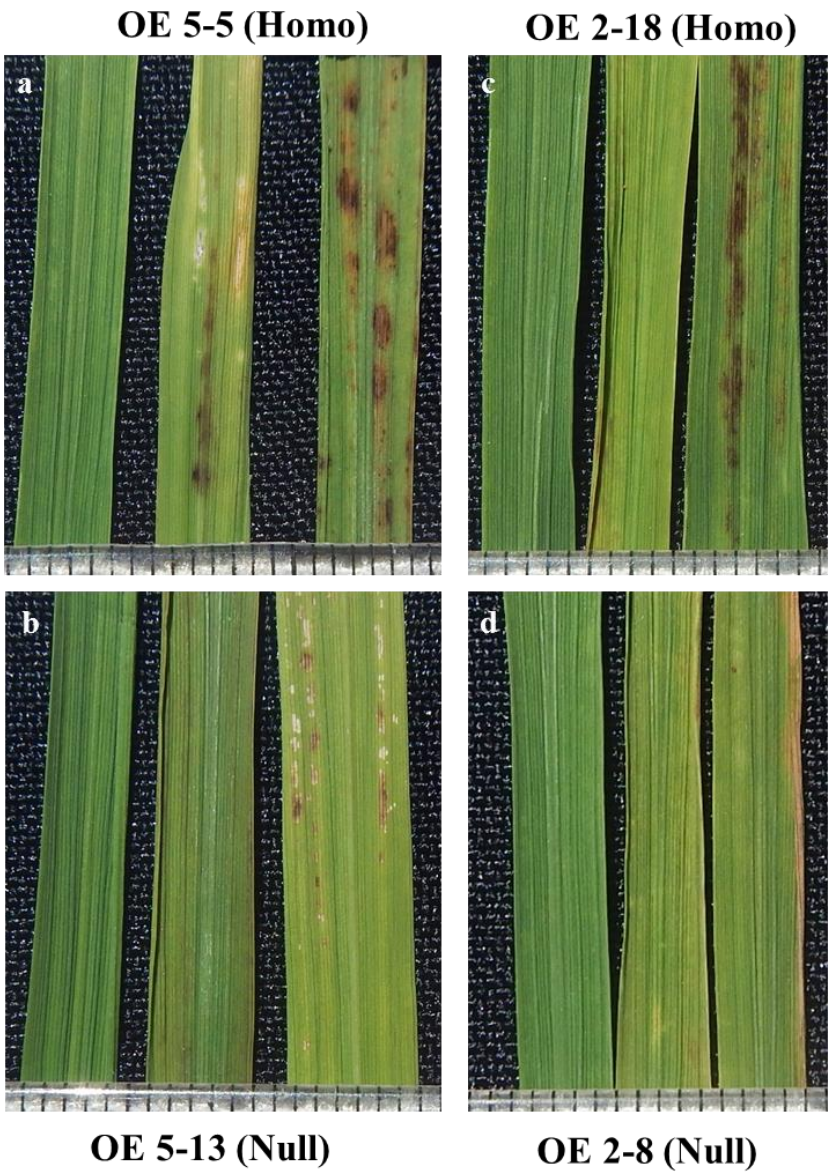

Figure 9.7 Leaf symptoms on rice lines in high Mn treatments

The leaves were collected from plants grown in control, 250 µM and 500 µM $MnCl_2$ treatments (left to right) after three weeks. (a) and (c) Two lines over-expressing *OsALMT1* (OE 5-5 and OE 2-18) and (c) and (d) their relative null lines (OE 5-13 and OE 2-8). Scale shows millimetres.

concentration, the biomass of all plants was significantly reduced. Interestingly, the growth of the transgenic lines with increased and decreased gene expression showed opposite trends. Lines with increased gene expression tended to be affected less by low Cl^- than their nulls whereas the RNAi lines tended to grow poorly compared to their nulls. Indeed, for one of the two RNAi lines, R58-1, relative biomass was significantly lower than its null line. The absence of a major inorganic anion like Cl^- from the hydroponic solution might increase the importance of organic anion movement for charge balance, osmotic adjustment and perhaps other functions. Reducing the expression of OsALMT1 therefore appears to compromise the ability of the plants to grow normally when other prevalent anions like Cl^- are less available. Increased expression of OsALMT1 could increase the capacity for malate (and fumarate) transport to partly compensate for reduced Cl^- availability. A even stronger phenotype might occur if NO_3^- availability is restricted at the same time as Cl^-.

Transgenic plants were also grown under a low light intensity because *OsALMT1* expression responded significantly to different light treatments (see **Chapter 6**). After an extended period of growth in low light, shoot biomass of both overexpressing lines and both RNAi lines were inhibited to a greater extent than their null sister lines. The relative biomass of each of the transgenic lines with higher and lower *OsALMT1* expression was significantly lower than their nulls. Therefore disturbing *OsALMT1* expression interferes with plant metabolism and growth in low light and suggests that OsALMT1 contributes in a fundamental way to carbon distribution and metabolism when photosynthesis is restricted. Further experiments are needed to determine whether increasing and decreasing *OsALMT1* expression affects growth and development via the same metabolic pathways or different pathways.

High B treatments were also tested because the transgenic lines overexpressing *OsALMT1* were previously shown to accumulate more B in leaves (see **Chapter 7**) and grain (see **Chapter 8**). The 5 mM H_3BO_3 treatment caused a ~50% decrease in total biomass in null plants. However both transgenic lines with increased *OsALMT1* expression grew better in 5 mM H_3BO_3 and showed a higher relative biomass for shoots and roots. Based on the previous results presented here showing the vascular localisation of OsALMT1 and the higher malate in xylem sap, we hypothesis that the malate in the xylem sap helps B transport from root to shoots and then loading in the grain. While B uptake in plants

appears to occur in the boric acid form via aquaporins, once in the cytosol the borate anion can be transported out of the cell via anion channels (e.g. BOR1 in rice, BOR1 in Arabidopsis and Bot1 in barley) (Nakagawa *et al.* 2007; Takano *et al.*, 2002; Sutton *et al*., 2007). This raises the possibility that OsALMT1 is permeable to borate anions and this is discussed in **Chapter 10**. More elemental analyses need to be done on the shoot and root tissues to confirm this idea.

Growth in high Mn concentrations were examined because previous results sometimes showed greater Mn accumulations in both leaf and grain tissues of transgenic lines with higher *OsALMT1* expression. Both overexpression lines were found to be more sensitive to Mn toxicity than their nulls and showed a stronger phenotype on the leaves (brown spots) which is commonly associated with Mn toxicity. These results are consisted with previous results. The higher malate concentrations in the xylem sap and malate efflux from the roots could be increasing Mn uptake and transport to shoots. These findings contrast with a recent report which concluded that that enhancing malate exudation from *Stylosanthes guianensis* roots (by increasing malate synthesis expression) conferred greater tolerance to Mn toxicity (Chen et al., 2015). Our results indicate that malate efflux does not necessarily to give tolerance to Mn because the transgenic rice lines with higher root malate efflux and higher malate concentrations in the xylem sap were more sensitive to Mn toxicity. Whether the biomass decrease is due to increased ability to accumulate Mn or increased sensitivity to oxidative stress which is related to higher Mn conditions need to be examined further.

These results demonstrated that several growth conditions affected the biomass accumulation of transgenic lines with increased *OsALMT1* expression and decreased expression. Lines with increased expression tended to be more sensitive to osmotic stress, low light and Mn toxicity and they tended to be more resistant to low Cl- treatments and to B toxicity. Transgenic lines with reduced *OsALMT1* expression were more sensitive when Cl^- availability is restricted and in conditions of low light.

9.5 References

Abdeeva I, Abdeev R, Bruskin S, Piruzian E (2012) Transgenic plants as a tool for plant functional genomics, Transgenic plants - Advances and limitations, PhD. Yelda Ozden Çift ģ (Ed.)

Belhaj K, Chaparro-Garcia A, Kamoun S, Nekrasov V (2013) Plant genome editing made easy: targeted mutagenesis in model and crop plants using the CRISPR/Cas system. Plant Methods 9: 1-10

Chen Z, Sun L, Liu P, Liu G, Tian J, Liao H (2015) Malate synthesis and secretion mediated by a manganese-enhanced malate dehydrogenase confers superior manganese tolerance in *Stylosanthes guianensis*. Plant Physiol 167: 176-188

Kondou Y, Higuchi M, Matsui M (2010) High-throughput characterization of plant gene functions by using gain-of-function technology. Annu Rev Plant Biol 61: 373-393

Nakagawa Y, Hanaoka H, Kobayashi M, Miyoshi K, Miwa K, Fujiwara T (2007) Cell-type specificity of the expression of Os *BOR1*, a rice efflux boron transporter gene, is regulated in response to boron availability for efficient boron uptake and xylem loading. Plant Cell 19: 2624-2635

Ostergaard L, Yanofsky MF (2004) Establishing gene function by mutagenesis in *Arabidopsis thaliana*. Plant J 39: 682-696

Pereira A (2000) A transgenic perspective on plant functional genomics. Transgenic Res 9: 245-260

Sutton T, Baumann U, Hayes J, Collins NC, Shi B-J, Schnurbusch T, Hay A, Mayo G, Pallotta M, Tester M, Langridge P (2007) Boron-toxicity tolerance in barley arising from efflux transporter amplification. Science 318: 1446-1449

Takano J, Noguchi K, Yasumori M, Kobayashi M, Gajdos Z, Miwa K, Hayashi H, Yoneyama T, Fujiwara T (2002) Arabidopsis boron transporter for xylem loading. Nature 420: 337-340

Chapter 10
General discussion and conclusions

10.1 General information on OsALMT1

This is the first study to characterise the molecular biology and functions of an *ALMT* gene in rice. From the nine *ALMT* members in rice, *OsALMT1* and *OsALMT2* were initially targeted because they sat together on a separate branch of a phylogenetic tree without any characterised member (**Figure 3.1**). The sequence of *OsALMT2* is highly similar with OsALMT1 but contains a premature stop codon in the coding region which is predicted to result in a truncation at the C-terminal end of about 200 amino acids. Experiments have previously shown that some truncations to the C-terminal region significantly inhibit transport activity of three other members of the family AtALMT1, TaALMT1, and AtALMT12 (Furuichi *et al.* 2010; Kobayashi *et al.* 2007; Mumm *et al.* 2013). No expression of *OsALMT2* could be detected in the roots or shoots but, even if it was expressed, the OsALMT2 protein may not function. By comparison, *OsALMT1* expression was easily detected in roots and shoots and a comprehensive description of *OsALMT1* biology was possible.

OsALMT1 was predicted to have the typical features of the family which, apart from the PF11744 domain, included six trans-membrane regions in the N-terminal half of the protein and a long hydrophobic C terminus (**Chapter 3**). We conclude that OsALMT1 localises to the plasma membrane where it facilitates malate export from the cytosol to the apoplast. This was established by generating transgenic lines expressing *OsALMT1* with a constitutive promoter. These transgenic lines showed a constitutive release of malate that was not detected in null segregate plants or WT plants. The rates of release were relatively high and comparable to efflux from the roots of Al-tolerant wheat plants (Delhaize *et al.* 1993; Ryan *et al.* 1995). These transgenic plants also released fumarate from their roots to a smaller extent. Whether OsALMT1 is also permeable to other anions, especially inorganic anions, can be resolved with electrophysiological measurements in the future.

Citrate efflux was also detected from roots of WT plants. Citrate efflux is known to contribute to Al resistance in rice although it is probably a minor mechanism (Yokosho *et al.* 2011). This trait is controlled by the *OsFRDL4* gene which encodes a MATE transporter. Al treatment induces the expression of *OsFRDL4* in roots and increases citrate release to the apoplast. The citrate efflux measured here from WT plants in control conditions is ~0.8 nmol seedling^{-1} h^{-1} which is equivalent to the ~600 nmol g DW^{-1} 24h^{-1} measured in the *osfrdl4* knock-out mutant treated with 50 μM Al treatment *(Yokosho et al.* 2011). In some experiments the citrate efflux from transgenic lines over-expressing *OsALMT1* was less than in the null lines which could reflect some competition for carbon to supply these two transporters (**Chapter 8**).

OsALMT1 gene is widely expressed in rice plants and especially in vascular tissues of roots and shoots, at the epidermis and root hairs, at the region of emerging lateral roots, in developing embryo and grain and in parts of the flower (**Chapter 5**). Vascular tissues include the xylem and phloem and associated companion cells and vascular parenchyma (Wilson 1966). The phloem is responsible for transporting photosynthetic products such as sugars from source to sink tissues, as well as proteins, organic anions and other organic molecules (van Dongen *et al.* 2003; Hijaz and Killiny 2014) and redistributing mobile nutrients out from senescing tissues (Bel and Hafke 2005; Pickard and Melcher 2005; Turgeon and Ayre 2005). The function of xylem in vascular plants is to transport water and water-soluble nutrients to the shoot with the transpiration stream. The translocation of certain minerals, micronutrients and even heavy metals (Fe, Mn, Si, Al, Ni, Cu and Zn), from roots to shoots and grain relies on organic compounds in the xylem sap (Durrett *et al.* 2007; Yokosho *et al.* 2009; Sasaki *et al.* 2011; Kramer *et al.* 1996). These compounds include citrate, quinate, histidine, nicotinamine, oxalate as well as malate. In the present study, transgenic rice lines over-expressing *OsALMT1* showed an almost two-fold higher malate concentration in the xylem sap which demonstrates that high expression of this anion channel can influence malate concentrations in the xylem and perhaps elsewhere (**Chapter 7**). The present study also showed that those same transgenic lines with higher *OsALMT1* expression sometimes had greater concentrations of several elements in grain and leaves. For instances increases in B concentrations were measured on several occasions but changes in Mn, Cu, Zn and Si were more variable. Increases in these elements, especially the metals, could be caused, in part, by the malate efflux from roots which enhances availability of these nutrients in the soil and, in part, by

higher malate concentrations in the xylem which increases transport to the shoots (**Chapter 7**).

The transgenic lines with high malate efflux from their roots were more resistant to Al^{3+} toxicity which is consistent with known mechanisms for Al resistance in plants (Delhaize *et al.* 2007; Ryan and Delhaize 2001) (**Chapter 8**). This does not mean that *OsALMT1* is necessary for conferring Al tolerance in WT plants. In fact that conclusion is unlikely for two reasons: rice is among the most Al^{3+}-resistant of all small-grain cereals and the mechanisms involved have been widely investigated with physiological and genetic approaches. Several genes have now been linked with resistance in rice, including *OsNRAT1* and *OsART1* and the MATE gene *OsFRDL4* mentioned above which facilitates citrate efflux, but none are from the ALMT family (Huang *et al.* 2012; Yokosho *et al.* 2011; Huang *et al.* 2009; Li *et al.* 2014; Ma *et al.* 2014). Although Al^{3+} treatment reduced malate efflux from roots of the over-expressing rice lines there must still be sufficient to enhance resistance.

10.2 Responses of *OsALMT1* expression to hormone treatments

OsALMT1 expression was significantly affected by the hormones ABA, IAA and SA but not by GA or methyl jasmonate (MeJA). ABA and IAA caused large decreases in expression in the roots after 6 and 24 h while SA increased expression in the roots. Furthermore IAA and SA increased expression four to six-fold in the shoots after 6 h. Some hormones inhibited malate efflux from the transgenic plants (**Chapter 8**). SA had the strongest response with a half maximal inhibition at ~50 μM SA. ABA and IAA reduced efflux by 50% at 100 μM but these experiments need to be repeated. Further experiments should examine the mechanisms of inhibition and particularly whether any direct interactions occur between these compounds and the OsALMT1 proteins.

Previous reports indicate that SA has the ability to change membrane properties and affect membrane potential and transport activity (Lurin C, *et al.*, 1996; Demidchik V, *et al*., 2002). Some studies have linked SA treatment with improved Al^{3+} resistance in Arabidopsis and *Cassia tora* perhaps by altering citrate efflux via MATE transporters (Liu *et al.* 2011; Yang *et al.* 2003). Al treatment inhibited the citrate efflux from

Arabidopsis roots and increased malate efflux via *AtALMT1* (Hoekenga *et al.* 2006). Citrate also reported to inhibit the AtALMT9-mediated malate currents by blocking the conduction pathway (Zhang *et al.* 2013). SA also reduced Al toxicity in *Coffea arabica* suspension cells by a different mechanism reportedly involving protein phosphorylation and signalling pathways (Muñoz-Sanchez *et al.* 2013). The links between SA and its effects on *OsALMT1* expression, malate efflux and citrate efflux need more investigation.

10.3 OsALMT1 and manganese

The transgenic lines over-expressing *OsALMT1* plants consistently developed a phenotype of brown spots on the leaves. This occurred in plants grown in soil and in standard hydroponic solutions with a low Mn concentration of 1 µM. This phenotype did not appear in any of the null lines, the RNAi lines or WT plants. The spots appeared first on the OE5-5 homozygous line and then on the OE2-18 and OE8-5 homozygous lines and so the severity of this phenotype was generally correlated with the level of *OsALMT1* expression. Necrotic brown spots are typical signs of Mn toxicity due to the damage oxidized Mn causes to proteins, lipids and phenolic compounds in the cell wall (Wissemeier and Horst 1991; Sasaki *et al.* 2011). Four results presented in this study are consistent with these symptoms being caused by Mn toxicity as detailed below: (i) The spots appeared on the older leaves first which is typical of Mn toxicity. The time of their appearance was variable and depended on the growth conditions. (ii) These symptoms developed more rapidly at higher temperatures and higher light intensities. The more rapid and more severe symptoms under higher light intensities is consistent with Mn accumulation since Mn toxicity in plants is associated with greater sensitivity to oxidative stress (González *et al.* 1998). (iii) Elemental analyses of the leaves and grain sometimes showed higher Mn concentrations in the transgenic lines with greater *OsALMT1* expression. There was not a strict correlation between the appearance of symptoms and total Mn concentrations in leaves. In some experiments the symptoms were visible in the over-expressing lines even though the measured Mn concentrations in leaves were similar to the null lines. This could be related to the distribution of Mn between the symplast and the apoplast. The preferential accumulation in the apoplast of leaves is associated with symptoms of Mn toxicity in rice rather than the total

concentration (Sasaki *et al.* 2011; see later). (iv) Transgenic lines over-expressing *OsALMT1* were significantly more sensitive to higher concentrations of Mn in the nutrient solution than the nulls. Therefore, increased *OsALMT1* expression may lead to the excessive accumulation or altered distribution of Mn and perhaps other metals in leaves. This hypothesis is explained further below following a brief summary of Mn nutrition in plants.

Mn is an essential micronutrient element in all plants. It has roles in photosynthesis, carbohydrate, lipid and lignin biosynthesis and as a cofactor in many enzymes (Marschner 2012). Mn is an important component of Mn superoxide dismutase (MnSOD), an antioxidant enzyme of mitochondria. Mn can exist in many oxidation states but the two common ones in cells are Mn^{2+} and Mn^{3+} (Marschner 2012). Mn uptake by plants also depends on soil pH as well as its mineralology and oxidation status. When soil pH is high (>7.5) Mn^{3+} dominates and this favours the formation of insoluble oxides (Rengel 2000; Marschner 2012). At lower soil pH (pH < 5.5) Mn^{2+} is more prevalent and this is absorbed most efficiently by plants (Marschner 2012).

Mn uptake and distribution involves uptake from the roots, loading in the xylem, movement to the shoot in the transpiration stream, and transport in the phloem for re-translocation. In rice these steps depend, in part, on transport proteins from the NRAMP and YSL families. In rice roots OsNRAMP5 localizes at the distal side of both exodermis and endodermis cells and is largely responsible for Mn uptake by roots (Sasaki *et al.* 2012). Free Mn ions can trigger oxidative stress so once in the cytosol Mn is chelated by compounds such as nicotianamine, phytosiderophores, phytate and carboxylic acids that reduce its potential to damage cells (Horst and Maier 1999; Pittman 2005; Fernando *et al.* 2010; Koike *et al.* 2004; Haydon and Cobbett 2007). These complexes can be distributed throughout the plant in the xylem or phloem, or stored in the apoplast and vacuole (Millaleo *et al.* 2010; Horst and Maier 1999). Previous studies showed that OsNRAMP5 is highly expressed in the vascular bundles of roots and shoots and especially in the parenchyma cells surrounding the xylem (Ishimaru *et al.* 2012). Reduced expression of *OsNRAMP5* in rice using RNAi techniques decreased Mn accumulation in the roots, and reduced Mn and Fe concentrations in shoots and xylem sap (Ishimaru *et al.* 2012). This indicates that OsNRAMP5 also plays an important role in the transport of Mn to the shoots (Yang *et al.* 2014). OsNRAMP3 is another transport protein from this family that

Figure 10.1 Model for the increased accumulation of Mn in transgenic lines overexpressing *OsALMT1*

The malate efflux from roots may increase the availability of Mn in soil and increases Mn uptake via the NRAMP5 transporter. Mn is transported into the xylem by a member of the YSL family (perhaps YSL2). The increased expression of OsALMT1 in the roots and shoots also raises the malate concentration in the xylem sap. This might help retain Mn in the apoplast perhaps by competing with nicotianamine or other compounds to chelate the Mn. This reduces Mn uptake into the symplast of leaves by the YSL6 transporter. Mn accumulates in the apoplast of the leaf tissue causing oxidative stress (especially in high light) which causes necrosis and the formation of brown spots. NA refers to nicotianamine.

is highly expressed in the vascular bundle and the node (a junction of vasculatures connecting leaves, stems and panicles). OsNRAMP3 appears to help regulate the remobilization of Mn as availability of this nutrient is restricted (Yamaji *et al.* 2013; Yang *et al.* 2013). Members of the YSL family are also involved in Mn translocation and homeostasis. For instance, OsYSL2 reportedly controls the loading of Mn^{2+}-nicotianamine to the phloem and the supply of Mn to developing grain (Koike *et al.* 2004).

In soils that favour Mn^{2+} formation such as acidic, poorly drained and reducing soils too much Mn uptake can occur and this can damage plants (Lynch and St.Clair 2004). Excess Mn can trigger oxidative stress, inhibit photosystem II and reduce the absorption of other essential elements (Ca, Mg, Fe, and P) (Marschner 2012). Plants suffer on several fronts and total biomass is generally reduced. Excess Mn accumulates in the vacuole and apoplast of mature leaves (Horst and Maier 1999; Hirschi *et al.* 2000; Schaaf *et al.* 2002). These tissues develop interveinal chlorosis and brown necrotic spots due to the accumulation of oxidized Mn and oxidized phenolic compounds in the apoplast (Fecht-Christoffers *et al.* 2003; Marschner 2012). OsYSL6 helps to reduce Mn toxicity when Mn accumulation is high because OsYSL6 transports the Mn^{2+}-nicotianamine complex from the apoplast to the symplast (Sasaki *et al.* 2011). In that study no differences were found in the total Mn concentrations between the leaves of *oysl6* knock-out mutants and WT rice plants. However the distribution of Mn within this tissue was different. The *oysl6* mutant line had higher Mn concentrations in the apoplast and lower concentrations in symplast than WT plants and it was the greater concentration of Mn in the apoplast that caused the brown spots associated with Mn toxicity (Sasaki *et al.* 2011).

As mentioned above, transgenic lines over-expressing *OsALMT1* sometimes accumulated higher concentrations of Mn in the leaves, and developed symptoms consistent with Mn toxicity - even at low external concentrations of Mn. Furthermore, growth experiments in **Chapter 9** found that these lines were more sensitive to higher concentrations of Mn than their nulls. The following model is proposed to explain the appearance of this phenotype in the transgenic lines over-expressing *OsALMT1*. Increasing *OsALMT1* expression increased malate efflux from roots and raised the malate concentration in the xylem sap. The higher malate in the xylem would compete with nicotianamine (and

perhaps other compounds) to form complexes with Mn. Accumulation of Mn in the leaf apoplast might occur because the Mn-malate complex cannot be unloaded from the xylem to the leaf cells by YSL transporters since they usually transport Mn: nicotianamine. High concentrations of Mn in the apoplast lead to oxidative stress, the accumulation of oxidized phenolic compounds and the development of necrotic spots (**Figure 10.1**). Further experiments are needed to test this idea by directly comparing the Mn concentrations in apoplast, symplast and xylem of the leaves of transgenic and null plants.

10.4 OsALMT1 and boron

Transgenic plants overexpressing *OsALMT1* sometimes showed higher concentrations of B in the leaves and grain. These transgenic lines were also less sensitive to B toxicity than their null lines and grew better in 250 μM and 500 μM boric acid (**Chapter 7 and 9**).

B is an essential plant nutrient required for normal cell wall structure. Most B in soils exists as boric acid (H_3BO_3) because it has a high pK_a of 9.2. Since boric acid is a small, neutral molecule it has a relatively high permeability through biological membranes. Therefore it was originally thought that B uptake by plants occurred by passive diffusion of this neutral species across the root cell membranes (Schnurbusch *et al.* 2010b). More recently it became clear that aquaporins are also important for boric acid uptake (Takano *et al.* 2006). For instance the aquaporin proteins AtNIP5;1 in Arabidopsis and HvNIP2;1 in barley are required for normal growth under B limiting conditions. The orthologue of these proteins in rice is OsNIP3;1 (Takano *et al.* 2006; Schnurbusch *et al.* 2010a; Hanaoka *et al.* 2014). Once in the cytosol, B forms complexes with sugars and glycoproteins and since the cytosolic pH is ~7.5 about 2% of the B exists as the borate anion ($(B(OH)_4^-$ or $H_4BO_4^-$).

B can be toxic to plants if taken up to excess. The potential toxicity of soils depends on their pH and mineralology but yield losses are likely in soils containing more than ~15 mg/kg B (Schnurbusch *et al.* 2010b). B is transported up to the shoots in the transpiration stream where it accumulates in the tip of mature leaves causing the tissue to become

chlorotic and die. Smaller root systems are also typical signs of B stress. Genotypic variation for B tolerance has been studied in many species and the tolerant plants appear to maintain lower concentrations of B inside their tissues. This is achieved by reducing B uptake via the aquaporin transporters and increasing B efflux back to the apoplast. The mechanism explaining tolerance was revealed when the first B-tolerance gene in plants was identified in barley (Reid 2007; Sutton *et al.* 2007). The gene, named *Bot1* (*Boron tolerance 1*), was orthologous to Arabidopsis *BOR1* which encodes an anion channel shown to load borate anions into the xylem, especially when B supply is restricted (Takano *et al.* 2006). Therefore Bot1 provides tolerance to barley by facilitating borate efflux from the root cells to the apoplast (Sutton *et al.* 2007; Schnurbusch *et al.* 2010a). The orthologue in rice is *OsBOR1* and this gene was found to be required for normal growth when B supply is restricted (Nakagawa *et al.* 2007). The knock-out mutant *osbor1* has reduced B concentrations in the shoots and in the xylem sap. Transcript of *OsBOR1* was detected in roots and shoots but levels were not affected by B supply. By contrast, OsBOR1 protein was only detected in roots during B deficiency indicating the levels of OsBOR1 protein, not transcript, is regulated by B supply from wildtype plants (Nakagawa *et al.* 2007).

The current study concluded that OsALMT1 is an anion channel which functions to transport malate out of the root cells and into the xylem. The greater B level in leaves and grain, and the improved tolerance of rice lines over-expressing *OsALMT1* to high B concentrations, raises the possibility that OsALMT1 is permeable to borate anions and mimics aspects of BOR1 function (**Figure 10.2**). As explained above, B uptake as boric acid would occur by passive diffusion over the root-cell membranes or through aquaporins down the concentration gradient. In the cytosol a small fraction exists as the borate anion which can be transported back to the apoplast or loaded into the xylem via BOR1 (Nakagawa *et al.* 2007), and possibly via OsALMT1 (**Figure 10.2**). When *OsALMT1* expression is increased in the transgenic plants, borate efflux would increase from all cells, including from the xylem parenchyma, which would increase B transport to the xylem. This explains the higher B concentration in shoots and grains of those transgenic plants. B concentrations in the shoots of the RNAi lines with reduced expression were the same as controls which indicates that the contribution of OsALMT1 to B accumulation in normal, low B, growth conditions is probably minor. Alternatively there could be some functional redundancy among the other RNAi lines. In transgenic

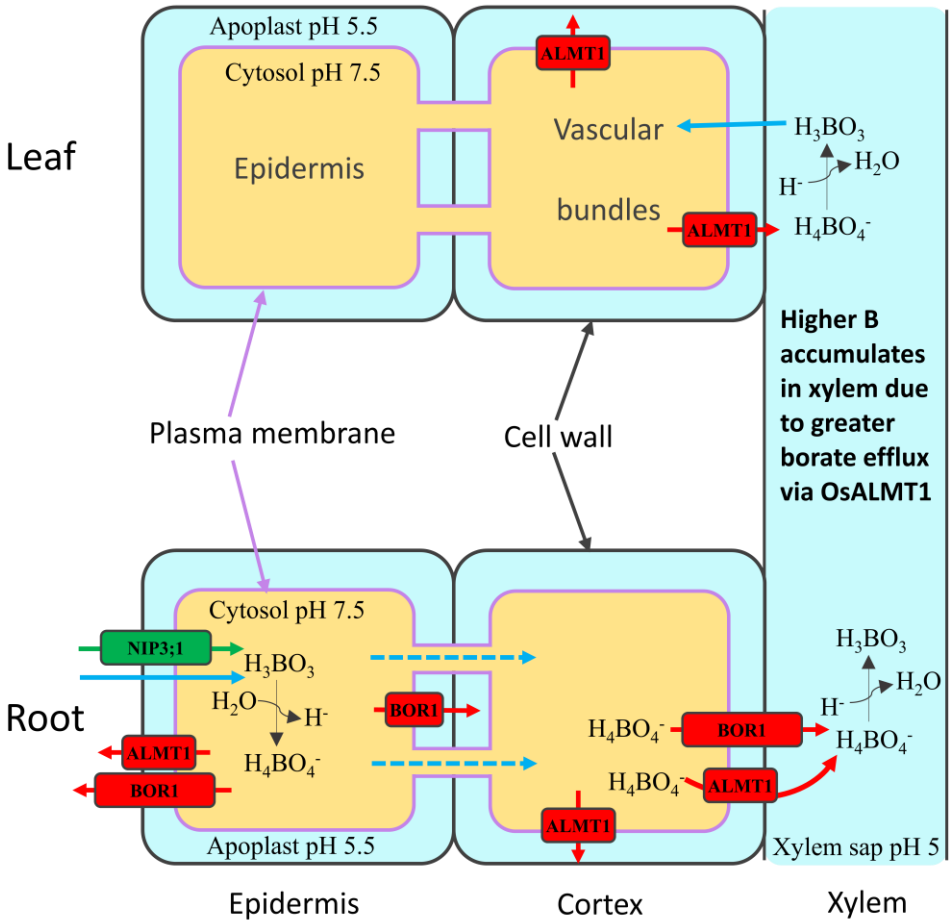

Figure 10.2 Model for how increased expression of OsALMT1 improves the tolerance of rice plants to toxic concentrations of B

This figure shows the direction of fluxes of B into and out of the roots when there is excessive B outside the root and explains why transgenic lines overexpressing *OsALMT1* are more tolerant of toxic concentration of B. The blue and green arrows represent passive diffusion of boric acid (H_3BO_3) across root cell membranes either through the membrane or via the aquaporin NIP3;1. The higher pH of the cytosol allow about 2% of the total B to form the borate anion ($H_4BO_4^-$) (pKa for B=9.24). The dashed arrows indicate flux through the plasmadesmata. Red arrows represent efflux of the borate anion through the BOR1 and OsALMT1 transporters. The $H_4BO_4^-$ anion can be loaded into xylem through BOR1 and OsALMT1. Greater OsALMT1 expression leads to more B release from the cytosol as borate and this provides tolerance from B toxicity. This figure includes only some of the likely transport processes and proteins involved in B transport from the soil to the leaves.

plants expressing high levels of *OsALMT1*, borate efflux from all cells would increase. Therefore borate loading to the xylem would be higher even in standard nutrient solution with low B concentrations. B accumulation would occur in the shoots and developing grain. However because the shoots also have high *OsALMT1* expression, the borate efflux from the leaf cells would also be higher and this would maintain a lower B concentrations in the symplast (as opposed to the apoplast). Maintaining a low B concentration in the symplast protects plants from B toxicity and explains why the transgenic lines with high *OsALMT1* expression accumulate B in the shoots and grow better in toxic concentrations of B (**Figure 9.5**).

10.5 OsALMT1 and water relations

Osmotic stress imposed on WT rice plants with salt, mannitol, PEG and by partial drying caused qualitatively similar changes in *OsALMT1* expression: reduced expression in leaves and increased expression in roots (**Chapter 6**). ABA is a hormone that regulates plant responses to various stress signals including osmotic stress and water stress. External applications of ABA affect the activity of antioxidant enzymes, guard cell function and transpiration rates (Naz and Khan 2014). It was expected that the responses of *OsALMT1* expression to ABA treatment would be similar to those induced by osmotic stress. This was not the case – in fact the trends were reversed. ABA strongly decreased expression in the roots and tended to increase expression in the shoots. Either the changes in expression during osmotic stress were not controlled by ABA or the concentrations of external ABA used in the experiments were too high and did not induce physiologically relevant changes in the cytosol. This is a real possibility because hormones can often have opposite effects depending on the concentration used. It is difficult to judge how the external application of hormones affects endogenous concentrations. Future work could examine the link between *OsALMT1* expression and hormones in more detail.

The following model provides an explanation for how the observed changes in *OsALMT1* expression in response to osmotic stress (high salt or mannitol, see **Chapter 6**) might assist rice plants adapt by either (i) altering malate transport and adjusting the concentrations of malate in the apoplast, or (ii) helping maintain electroneutrality as

other transport activities are triggered to decrease water potential in the root. Water moves from areas of higher water potential to areas of lower water potential. Water potential of the root tissue needs to be less than the water potential of the surrounding soil for uptake of water to occur. The high osmotic stress imposed by the salt and mannitol treatments etc. would reduce the water potential gradient between the root and nutrient solution which would decrease water uptake and transpiration. Therefore the plant needs to adjust its internal water potential to maintain water uptake. The changes in *OsALMT1* expression could assist this process either by changing water potential of the leaves or by maintaining electroneutrality while other transport events achieve this same outcome.

WT rice responded to osmotic stress by decreasing *OsALMT1* expression in the shoots which would reduce malate release from those cells to the apoplast, including the xylem (it is assumed the plants also closed their stomata to stop transpiration but this was not measured). Decreasing *OsALMT1* expression in the shoots would reduce the concentration of osmotically active compounds in the apoplast of that tissue and help maintain a water potential gradient from the apoplast and xylem to the leaf cells. Therefore water would move more easily out of the xylem to the xylem parenchyma and help keep the shoots hydrated.

Rice plants also responded to osmotic stress by increasing *OsALMT1* expression in the roots. Since *OsALMT1* expression in roots is especially strong in the xylem parenchyma the higher malate release from root cells to the xylem (and apoplast in general) may decrease water potential in the xylem. Malate can be continuously generated (within reason) through the tricarboxylic acid cycle or PEP carboxylase of those cells so malate can continue to be produced and released. The accumulation of malate and other osmotically active compounds in the xylem would decrease the water potential there and help maintain a water potential gradient from the soil/environment to the xylem (**Figure 10.3**). This hypothesis is consistent with the findings of Patonnier et al (1999) who found that malate and mannitol concentration in the xylem sap of ash trees (*Fraxinus excelsior*) increased during the onset of drought stress.

In transgenic lines with constitutively high *OsALMT1* expression the ability to modulate malate transport in the shoot and roots is compromised. This could explain why transgenic lines over-expressing *OsALMT1* tended to be more sensitive to osmotic stress

than null plants. They accumulated less biomass in control conditions compared to their nulls but performed even more poorly than the nulls when grown in either 100 mM NaCl or 50 mM mannitol. While the data from those growth experiments were significant for only one of the transgenic lines in the salt treatment (**Figure 9.1b**), the trends were consistent for all lines in both treatments. Those results indicate that OsALMT1 could contribute to the osmoregulation of rice, especially during periods of high osmotic stress, by regulating the concentrations of osmotically active malate ions in different tissues and by helping maintain electroneutrality as other transport processes are triggered in response to osmotic stress. Further work should monitor the changes in malate concentrations in the root and shoot tissues and in the xylem sap during osmotic stress. Interestingly, the RNAi lines with reduced *OsALMT1* expression showed no obvious affects on growth in control conditions or during osmotic stress (**Chapter 9**). This might be due to redundancy with other transporters performing comparable roles to OsALMT1 or by other mechanisms compensating for the reduced activity of OsALMT1.

10.6 OsALMT1 and electroneutrality

The loading and unloading of photosynthetic assimilates from cells, the transport of minerals and secondary metabolites across cell membranes for any other purpose are often electrogenic. This means they result in the net movement of charge from one side of the membrane to the other. These charges need to be balanced otherwise the membrane becomes hyperpolarised or hypopolarised, both of which are potentially damaging and unsustainable. To achieve this either an equal but opposite charge moves in the same direction or an equal charge moves in the opposite direction. The finding that *OsALMT1* is widely expressed throughout rice plants, including the vascular tissues, emerging lateral roots and developing grain, raises the possibility that OsALMT1 contributes to the maintenance of electroneutrality by regulating the movement of organic anions such as malate. It was considered likely that restricting the availability of a major inorganic anion like Cl^- might increase the importance of organic anions for charge balance and osmotic adjustment. To test this idea the expression of *OsALMT1* was measured after 6 and 24 h in a Cl^- free treatment. No changes in expression were detected but this may have been too short a period - especially since nitrate was still present in the

nutrition solution (**Chapter 6**). Therefore longer-term growth experiments were performed in a low-Cl^- solution. This treatment inhibited biomass accumulation in all lines. The results indicated that transgenic lines with higher *OsALMT1* expression tended to perform better than their null lines while the RNAi lines with reduced expression tended to perform worse than their nulls (**Chapter 9.3**). These differences were significant for one of the RNAi lines only, but the trends were quite consistent. Therefore decreasing *OsALMT1* expression tended to compromise the ability of rice plants to grow with restricted Cl^- availability perhaps because those plants were less able to maintain electroneutrality. By contrast, increasing *OsALMT1* expression could partly compensate for Cl^- deficiency and lead to better plant growth perhaps because the increased capacity for malate transport was able to compensate for the lack of Cl^-. The relative importance of malate transport for maintaining electroneutrality might be even more accentuated if similar growth experiments were performed but with restricted Cl^- and NO_3^-.

10.7 OsALMT1 and light

Several results showed a link between OsALMT1 function and light treatments as follows: (i) Several *cis*-elements related to light responses were found within the promoter region of *OsALMT1,* (ii) *OsALMT1* expression in WT plants changed in with light treatments (**Chapter 3**): A 24 h treatment in continual darkness decreased *OsALMT1* expression in leaves slightly but increased expression five-fold in the roots. Continual light increased expression in shoots by 10-fold (**Chapter 6**), (iii) Malate efflux from transgenic lines over-expressing *OsALMT1* increased with higher light intensity (**Chapter 8.5**), (iv) Transgenic lines with altered *OsALMT1* expression (higher or lower) grew poorly at low light intensity (**Chapter 9.4**). Those differences were significant for all lines tested and indicated that OsALMT1 function is important to plant growth in low light conditions. It is easy to imagine how transgenic lines with increased *OsALMT1* expression might suffer at low light because the constant release of malate (and other organic anions) from their roots would be an extra drain on fixed carbon. It is more difficult to reason why the RNAi lines with reduced expression are also compromised by low light. Low light would reduce photosynthesis which could restrict fixed carbon supply and generally reduce plant energy levels. In these conditions the transporters that

move carbon molecules over membranes and redistribute all forms of carbon throughout the plant could be more important. When the expression of OsALMT1 is disturbed in any way in plants, up-regulated or down-regulated, their ability to cope with the low light growth conditions is adversely affected. Normal OsALMT1 function is critical for plants to grow well in low light environments.

10.8 Conclusion

In conclusion, OsALMT1 is an anion channel that is permeable to malate, fumarate and perhaps borate. It localizes to the plasma membrane and is highly expressed in the vascular tissues and meristems and many other plant tissues. *OsALMT1* expression is responsive to light, osmotic and ionic stresses as well as certain hormones. Transgenic lines with greater *OsALMT1* expression tended to be more sensitive to osmotic stress, low light intensity and Mn toxicity and tended to be more resistant to restricted Cl^- availability and to toxic concentrations of B. Transgenic lines with reduced *OsALMT1* expression were more sensitive to restricted Cl^- availability and to low light. I propose that OsALMT1 facilities anion transport across cell membranes and that this process contributes to multiple functions in rice probably involving osmotic adjustment and the maintenance of electroneutrality.

10.9 Future directions

This study analysed the sub-cellular localisation, tissue specific localisation of OsALMT1, expression patterns of *OsALMT1* under various stresses and hormones, and generated transgenic lines with altered *OsALMT1* expression to investigate gene function. However, the work has raised more questions than it has answered and there are many more areas for further research in the future. Some obvious areas that would be interesting to persue further include the following:

- Transport studies in *Xenopus* oocytes to determine the relative permeability of OsALMT1 to anions and to confirm its predicted permeability to borate.

- Confirm the localisation of OsALMT1 to the plasma membrane with antibody techniques

- Photosynthetic analysis of the transgenic lines and nulls since the lines with higher and lower *OsALMT1* expression grew poorly in low light conditions

- Determine the distribution of Mn between the apoplast and symplast of the leaves and whether it is different in the transgenic and null lines

- Measure the reactive oxygen species in the leaves and compare their concentrations in the over-expressing and null lines

- Measure the Mn and B concentrations in the xylem sap compare their concentrations in the transgenic and null lines

- Investigate the mechanism of salicylic acid inhibition of OsALMT1 transport activity to determine whether this involves a direct interaction

- Investigate the effect of changing OsALMT1 expression on the expression of other genes (especially Mn and B transporters etc)

- Perform a metabolomic analysis on the transgenic and null lines to see how changing the expression of *OsALMT1* alters cellular metabolites.

- Investigate further the interactions of OsALMT1 and gamma amino butryic acid (GABA). A study published late in this project indicated that ALMTs can function as GABA receptors in plants (see **Chapter 8**). The expected inhibition of OsALMT1 activity by GABA and muscimol was not observed in this study but this interaction should be investigated again in oocytes. It remains possible that interactions between GABA and OsALMT1 are central to many of the observations reported here – especially responses to various stresses.

10.10 References:

Bel AJEv, Hafke JB (2005) 2 - Physiochemical determinants of phloem transport. In: Zwieniecki NMHA (ed) Vascular Transport in Plants. Academic Press, Burlington, 19-44

Delhaize E, Gruber BD, Ryan PR (2007) The roles of organic anion permeases in aluminium resistance and mineral nutrition. FEBS Lett 581: 2255-2262

Delhaize E, Ryan PR, Randall PJ (1993) Aluminum Tolerance in Wheat (*Triticum aestivum* L.). Plant Physiol 103: 695-720

Demidchik V, Shabala SN, Coutts KB, Tester MA, Davies JM Tester and Julia M. Davies (2002) Free oxygen radicals regulate plasma membrane Ca^{2+}-and K^{+}-permeable channels in plant root cells. J Cell Sci 116: 81-88

Durrett TP, Gassmann W, Rogers EE (2007) The FRD3-mediated efflux of citrate into the root vasculature is necessary for efficient iron translocation. Plant Physiol 144: 197-205

Fecht-Christoffers MM, Braun H-P, Lemaitre-Guillier C, VanDorsselaer A, Horst WJ (2003) Effect of manganese toxicity on the proteome of the leaf apoplast in cowpea. Plant Physiol 133: 1935-1946

Fernando DR, Mizuno T, Woodrow IE, Baker AJM, Collins RN (2010) Characterization of foliar manganese (Mn) in Mn (hyper)accumulators using X-ray absorption spectroscopy. New Phytol 188: 1014-1027

Furuichi T, Sasaki T, Tsuchiya Y, Ryan PR, Delhaize E, Yamamoto Y (2010) An extracellular hydrophilic carboxy-terminal domain regulates the activity of TaALMT1, the aluminum-activated malate transport protein of wheat. Plant J 64: 47-55

González A, Steffen KL, Lynch JP (1998) Light and excess manganese : implications for oxidative stress in common bean. Plant Physiol 118: 493-504

Hanaoka H, Uraguchi S, Takano J, Tanaka M, Fujiwara T (2014) OsNIP3;1, a rice boric acid channel, regulates boron distribution and is essential for growth under boron-deficient conditions. Plant J 78: 890-902

Haydon MJ, Cobbett CS (2007) Transporters of ligands for essential metal ions in plants. New Phytol 174: 499-506

Hijaz F, Killiny N (2014) Collection and chemical composition of phloem sap from *Citrus sinensis* L. Osbeck (sweet orange). PloS One 9: e101830

Hirschi KD, Korenkov VD, Wilganowski NL, Wagner GJ (2000) Expression of Arabidopsis *CAX2* in Tobacco. altered metal accumulation and increased manganese tolerance. Plant Physiol 124: 125-134

Hoekenga OA, Maron LG, Pineros MA, Cancado GMA, Shaff J, Kobayashi Y, Ryan PR, Dong B, Delhaize E, Sasaki T, Matsumoto H, Yamamoto Y, Koyama H, Kochian LV (2006) *AtALMT1*, which encodes a malate transporter, is identified as one of several genes critical for aluminum tolerance in *Arabidopsis*. PNAS 103: 9738-9743

Horst W, Maier P (1999) Compartmentation of manganese in the vacuoles and in the apoplast of leaves in relation to genotypic manganese leaf-tissue tolerance in *Vigna*

Unguiculata (L.) Walp. In: Gissel-Nielsen G, Jensen A (eds) Plant Nutrition-Molecular Biology and Genetics. Springer Netherlands, 223-234

Huang CF, Yamaji N, Chen Z, Ma JF (2012) A tonoplast-localized half-size ABC transporter is required for internal detoxification of aluminum in rice. Plant J 69: 857-867

Huang CF, Yamaji N, Mitani N, Yano M, Nagamura Y, Ma JF (2009) A bacterial-type ABC transporter is involved in aluminum tolerance in rice. Plant Cell 21: 655-667

Ishimaru Y, Takahashi R, Bashir K, Shimo H, Senoura T, Sugimoto K, Ono K, Yano M, Ishikawa S, Arao T, Nakanishi H, Nishizawa NK (2012) Characterizing the role of rice NRAMP5 in Manganese, Iron and Cadmium transport. Sci Rep 2: 286

Kobayashi Y, Hoekenga OA, Itoh H, Nakashima M, Saito S, Shaff JE, Maron LG, Pineros MA, Kochian LV, Koyama H (2007) Characterization of *AtALMT1* expression in aluminum-inducible malate release and its role for rhizotoxic stress tolerance in arabidopsis. Plant Physiol 145: 843-852

Koike S, Inoue H, Mizuno D, Takahashi M, Nakanishi H, Mori S, Nishizawa NK (2004) OsYSL2 is a rice metal-nicotianamine transporter that is regulated by iron and expressed in the phloem. Plant J 39: 415-424

Kramer U, Cotter-Howells JD, Charnock JM, Baker AJM, Smith JAC (1996) Free histidine as a metal chelator in plants that accumulate nickel. Nature 379: 635-638

Li JY, Liu J, Dong D, Jia X, McCouch SR, Kochian LV (2014) Natural variation underlies alterations in Nramp aluminum transporter (*NRAT1*) expression and function that play a key role in rice aluminum tolerance. PNAS 111: 6503-6508

Liu N, You J, Shi W, Liu W, Yang Z (2011) Salicylic acid involved in the process of aluminum induced citrate exudation in *Glycine max* L. Plant Soil 352: 85-97

Lynch JP, St.Clair SB (2004) Mineral stress: the missing link in understanding how global climate change will affect plants in real world soils. Field Crops Res 90: 101-115

Lurin C, Geelen D, Barbier-Brygoo H, Guern J, Maurel C (1996) Cloning and functional expression of a plant voltage-dependent chloride channel. Plant Cell 8: 701-711

Ma JF, Chen ZC, Shen RF (2014) Molecular mechanisms of Al tolerance in gramineous plants. Plant Soil 381: 1-12

Marschner H (2012) Marschner's mineral nutrition of higher plants. Marschner's Mineral Nutrition of Higher Plants (Third Edition):vii

Millaleo R, Reyes- Diaz M, Ivanov AG, Mora ML, Alberdi M (2010) Manganese as essential and toxic element for plants: transport, accumulation and resistance mechanisms. J Soil Sci Plant Nut 10: 470-481

Mumm P, Imes D, Martinoia E, Al-Rasheid KA, Geiger D, Marten I, Hedrich R (2013) C-terminus-mediated voltage gating of Arabidopsis guard cell anion channel QUAC1. Mol plant 6: 1550-1563

Muñoz-Sanchez JA, Chan-May A, Cab-Guillén Y, Hernández-Sotomayor SMT (2013) Effect of salicylic acid on the attenuation of aluminum toxicity in *Coffea arabica* L.

suspension cells: A possible protein phosphorylation signaling pathway. J Inorg Biochem 128: 188-195

Nakagawa Y, Hanaoka H, Kobayashi M, Miyoshi K, Miwa K, Fujiwara T (2007) Cell-type specificity of the expression of Os *BOR1*, a rice efflux boron transporter gene, is regulated in response to boron availability for efficient boron uptake and xylem loading. Plant Cell 19: 2624-2635

Naz H, Khan N (2014) Role of abscisic acid and water stress on the activities of antioxidant enzymes in Wheat. Cur Res J Bio Sci 6: 168-172

Patonnier MP, Peltier JP, Marigo G (1999) Drought-induced increase in xylem malate and mannitol concentrations and closure of *Fraxinus excelsior* L. stomata. J Exp Bot 50: 1223-1229

Pickard WF, Melcher PJ (2005) 1 - Perspectives on the biophysics of xylem transport. In: Zwieniecki NMHA (ed) Vascular Transport in Plants. Academic Press, Burlington, 3-18

Pittman JK (2005) Managing the manganese: molecular mechanisms of manganese transport and homeostasis. New Phytol 167: 733-742

Reid R (2007) Identification of Boron transporter genes likely to be responsible for tolerance to boron toxicity in Wheat and Barley. Plant Cell Physiol 48: 1673-1678

Rengel Z (2000) Manganese uptake and transport in plants. Metal Ions Biol Syst 37: 57-87

Ryan P, Delhaize E, Randall P (1995) Characterisation of Al-stimulated efflux of malate from the apices of Al-tolerant wheat roots. Planta 196: 103-110

Ryan PR, Delhaize E (2001) Function and mechanism of organic anion exudation from plant roots. Annu Rev Plant Physiol 52: 527-560

Sasaki A, Yamaji N, Xia J, Ma JF (2011) OsYSL6 is involved in the detoxification of excess manganese in rice. Plant Physiol 157: 1832-1840

Sasaki A, Yamaji N, Yokosho K, Ma JF (2012) Nramp5 is a major transporter responsible for manganese and cadmium uptake in rice. Plant Cell 24: 2155-2167

Schaaf G, Catoni E, Fitz M, Schwacke R, Schneider A, von Wirén N, Frommer WB (2002) A putative role for the vacuolar calcium/manganese proton antiporter AtCAX2 in heavy metal detoxification. Plant Biology 4: 612-618

Schnurbusch T, Hayes J, Hrmova M, Baumann U, Ramesh SA, Tyerman SD, Langridge P, Sutton T (2010a) Boron toxicity tolerance in Barley through reduced expression of the multifunctional aquaporin *HvNIP2;1*. Plant Physiol 153: 1706-1715

Schnurbusch T, Hayes J, Sutton T (2010b) Boron toxicity tolerance in wheat and barley: Australian perspectives. Breeding Sci 60: 297-304

Sutton T, Baumann U, Hayes J, Collins NC, Shi B-J, Schnurbusch T, Hay A, Mayo G, Pallotta M, Tester M, Langridge P (2007) Boron-toxicity tolerance in barley arising from efflux transporter amplification. Science 318: 1446-1449

Takano J, Wada M, Ludewig U, Schaaf G, von Wiren N, Fujiwara T (2006) The Arabidopsis major intrinsic protein NIP5;1 is essential for efficient boron uptake and plant development under boron limitation. Plant Cell 18: 1498-1509

Turgeon R, Ayre BG (2005) 3 - Pathways and mechanisms of phloem loading. In: Zwieniecki NMHA (ed) Vascular Transport in Plants. Academic Press, Burlington, 45-67

van Dongen JT, Schurr U, Pfister M, Geigenberger P (2003) Phloem metabolism and function have to cope with low internal oxygen. Plant Physiol 131: 1529-1543

Wilson K (1966) Esau,K - Vascular differentiation in plants. Nature 212: 343-344

Wissemeier AH, Horst WJ (1991) Simplified methods for screening Cowpea cultivars for manganese leaf-tissue tolerance. Crop Sci 31: 435-439

Yamaji N, Sasaki A, Xia JX, Yokosho K, Ma JF (2013) A node-based switch for preferential distribution of manganese in rice. Nat commun 4: 2442

Yang M, Zhang W, Dong H, Zhang Y, Lv K, Wang D, Lian X (2013) OsNRAMP3 is a vascular bundles-specific manganese transporter that is responsible for manganese distribution in rice. PloS One 8: e83990

Yang M, Zhang Y, Zhang L, Hu J, Zhang X, Lu K, Dong H, Wang D, Zhao FJ, Huang CF, Lian X (2014) OsNRAMP5 contributes to manganese translocation and distribution in rice shoots. J Exp Bot 65: 4849-4861

Yang ZM, Wang J, Wang SH, Xu LL (2003) Salicylic acid-induced aluminum tolerance by modulation of citrate efflux from roots of *Cassia tora* L. Planta 217: 168-174

Yokosho K, Yamaji N, Ma JF (2011) An Al-inducible MATE gene is involved in external detoxification of Al in rice. Plant J 68: 1061-1069

Yokosho K, Yamaji N, Ueno D, Mitani N, Ma JF (2009) OsFRDL1 is a citrate transporter required for efficient translocation of iron in rice. Plant Physiol 149: 297-305

Zhang J, Baetz U, Krugel U, Martinoia E, De Angeli A (2013) Identification of a probable pore-forming domain in the multimeric vacuolar anion channel AtALMT9. Plant Physiol 163: 830-843

Table S1 Physical Properties of NaCl

The osmotic pressure of NaCl was described by (Lange *et al.*, 2013).

NaCl

Molality (mmol kg^{-1})	Molarity[a] (20° C) (mmol l^{-1})	Freezing[a] point depression	Conductivity[a] at 20° C $\times 10^{-4}$ (mho m^{-1})	Osmotic[b] coefficient (ϕ) at 25° C	Osmotic pressure			
					Freezing[c] point (mosmol kg^{-1})	25° C[d] (mosmol kg^{-1})	(bar)	(MPa)
100	100	0.35	0.97	0.9324	188	186	4.61	0.46
200	199	0.69	1.83	0.9245	371	370	9.17	0.92
300	298	1.02	2.64	0.9215	549	553	13.14	1.31
400	397	1.36	3.38	0.9203	732	736	18.25	1.83
500	495	1.70	4.16	0.9209	915	921	22.83	2.28
600	593	2.03	4.90	0.9230	1,093	1,108	27.47	2.75
700	690	2.37	5.64	0.9257	1,276	1,296	32.13	3.21
800	787	2.71	6.32	0.9288	1,459	1,486	36.84	3.68
900	884	3.05	6.97	0.9320	1,642	1,678	41.60	4.16
1,000	980	3.40	7.63	0.9355	1,830	1,871	46.38	4.64
2,000	1,923	6.95	13.06	0.9833	3,730	3,933	97.50	9.75
3,000	2,828	10.81	17.77	1.0453	5,818	6,272	155.48	15.55
4,000	3,694	15.15	20.37	1.1158	8,154	8,926	221.28	22.13
5,000	4,524	20.10	21.55	1.1916	10,818	11,916	295.40	29.54

Table S2 Physical Properties of Mannitol

The osmotic pressure of Mannitol was described by Richard James (CSIRO) by personal contact.

Mannitol

Molarity (M)	(mM)	Os/kg	**Osmotic pressure** (bars)	(MPa)
0.027	27	0.028	-0.70	-0.07
0.055	55	0.055	-1.37	-0.14
0.083	83	0.084	-2.09	-0.21
0.110	110	0.112	-2.79	-0.28
0.138	138	0.141	-3.51	-0.35
0.166	166	0.170	-4.23	-0.42
0.194	194	0.200	-4.98	-0.50
0.222	222	0.230	-5.73	-0.57
0.251	251	0.260	-6.47	-0.65
0.279	279	0.290	-7.22	-0.72
0.307	307	0.321	-7.99	-0.80
0.336	336	0.353	-8.79	-0.88
0.364	364	0.384	-9.56	-0.96
0.393	393	0.416	-10.36	-1.04
0.422	422	0.449	-11.18	-1.12
0.451	451	0.482	-12.00	-1.20
0.480	480	0.515	-12.82	-1.28
0.509	509	0.549	-13.67	-1.37

Table S3 Nutrient solution for low Cl^- treatment

	Reagent	Final Concentration (μM)
	Normal	
Macro nutrients	KNO_3	250
	$CaCl_2$	250
	NH_4NO_3	250
	$MgSO_4$	75
	KH_2PO_4	10
Fe	EDTA:Fe	0.4
Micro nutrients	H_3BO_3	5.5
	$MnCl_2$	1
	$ZnCl_2$	0.175
	CuCl2	0.1
	Low Cl^-	
Macro nutrients	K_2SO_4	1000
	$CaSO_4$	250
	$(NH_4)_2SO_4$	100
	$MgSO_4$	75
	KH_2PO_4	10
Fe	EDTA:Fe	0.4
MES	MES	5000
Micro nutrients	H_3BO_3	5.5
	$MnCl_2$	1
	$ZnCl_2$	0.175
	CuCl2	0.1

Table S4 Elemental analysis of T2 rice leaf

Mineral concentrations in one month old leaves from one transgenic lines over-expressing *OsALMT1* OE5-5 and one RNAi lines with reduced OsALMT1 expression R58-1 and their relative null sister lines were measured with inductively coupled plasma mass spectrometry (ICP) analysis. Data show the average concentration of three individual plants with standard error (SE, n=3). The raw data for each element from the transgenic lines were compared to its null sister line and differences ($P<0.05$) indicated by an asterisk.

	OE5-5 (Homo)	OE5-13 (Null)	R58-1 (Homo)	R58-5 (Null)
B (mg/kg)	35.80±7.64	25.50±1.71	9.97±0.81*	24.70±4.67
Ca (%)	0.28±0.09	0.26±0.01	0.25±0.03*	0.64±0.10
Cd (mg/kg)	0.14±0.11	0.06±0.03	0.28±0.19	0.57±0.26
Co (mg/kg)	0.02±0.03	0.11±0.03	0.18±0.36	0.28±0.08
Cr (mg/kg)	0.66±0.08*	0.42±0.07	0.92±0.51	0.48±0.03
Cu (mg/kg)	10.66±0.44*	8.59±0.50	13.73±1.43	13.55±2.03
Fe (mg/kg)	71.03±3.62*	48.27±1.77	88.30±10.48	77.67±8.47
K (%)	1.98±0.06	1.76±0.04	2.46±0.13	2.49±0.05
Mg (%)	0.26±0.04	0.20±0.01	0.37±0.04	0.49±0.04
Mn (mg/kg)	252.33±67.67	268.67±24.83	290.67±51.24*	507.67±23.25
Mo (mg/kg)	5.42±0.52	4.15±0.16	6.87±1.30	8.57±0.94
Na (%)	0.02±0.01	0.03±0.00	0.00±0.00	0.03±0.01
P (%)	0.27±0.01	0.27±0.01	0.87±0.11	1.12±0.16
S (%)	0.24±0.01	0.17±0.01	0.29±0.02	0.32±0.03
Si (mg/kg)	1156.33±106.21	969.00±46.77	1170.00±41.63	1350.00±115.91
Ti (mg/kg)	2.19±0.41	1.06±0.06	0.81±0.33	0.77±0.09
Zn (mg/kg)	42.73±6.87	27.93±1.78	54.23±5.51	44.77±9.89

Table S5 Elemental analysis of T3 rice seed

T3 grain mineral concentrations were measured from two homozygous transgenic lines over-expressing *OsALMT1* (OE5-5 and OE2-18) and two RNAi lines (R24-15 and R58-1) and their relative null sister lines. Data show the average concentration of three individual plants with standard error (SE, n=3). The raw data for each element from the transgenic lines were compared to its null sister line and differences ($P<0.05$) indicated by an asterisk.

	B (mg/kg)	Ca (%)	Cu (mg/kg)	Fe (mg/kg)	K (%)	Mg (%)	Mn (mg/kg)	P (%)	S (%)	Si (mg/kg)	Zn (mg/kg)
OE5-5 (Homo)	5.46±1.02*	0.02±0.00	10.12±0.47*	22.37±5.70	0.52±0.02	0.16±0.00	32.10±2.85*	0.45±0.01*	0.14±0.01	170.67±31.16	41.37±4.07*
OE5-13 (Null)	2.37±0.25	0.02±0.00	7.06±0.17	13.30±1.10	0.54±0.07	0.12±0.01	16.27±0.75	0.36±0.02	0.12±0.00	150.33±22.34	26.67±3.81
OE2-18 (Homo)	1.94±0.35*	0.02±0.00	6.33±0.88	16.53±1.83	0.58±0.05	0.15±0.01	20.67±1.43	0.44±0.03	0.14±0.01	237.33±11.67*	31.83±3.01
OR2-8 (Null)	1.02±0.13	0.02±0.01	6.24±0.47	14.80±0.70	0.50±0.03	0.14±0.00	21.10±3.56	0.39±0.01	0.12±0.00	149.00±15.01	28.07±1.31
R24-15 (Homo)	0.17±0.05	0.02±0.00	4.67±0.28	8.69±0.35	0.26±0.01	0.11±0.00	26.53±2.13	0.29±0.01	0.09±0.00	109.83±23.24	28.17±0.50
R24-20 (Null)	0.26±0.06	0.02±0.01	5.07±0.81	13.42±3.83	0.30±0.04	0.11±0.00	30.30±3.09	0.28±0.02	0.10±0.02	101.00±4.51	28.57±0.83
R58-1 (Homo)	4.76±0.93	0.08±0.01	5.07±0.74	11.06±1.51	0.31±0.02	0.13±0.01	22.60±1.07	0.34±0.02	0.34±0.02	115.50±20.46	32.67±3.08
R58-5 (Null)	2.26±0.14	0.08±0.01	4.64±0.29	8.69±0.95	0.31±0.01	0.12±0.00	22.23±0.66	0.32±0.00	0.32±0.00	117.50±11.32	32.50±2.59